



REPORT DOCUMENTATION PAGE				
1a. REPORT SECURITY CLASSIFICATION <b>Unclassified</b>		1b. RESTRICTIVE MARKINGS		
2a. SECURITY CLASSIFICATION AUTHORITY		3. DISTRIBUTION / AVAILABILITY OF REPORT Approved for public release; distribution unlimited.		
2b. DECLASSIFICATION / DOWNGRADING SCHEDULE				
4. PERFORMING ORGANIZATION REPORT NUMBER(S)		5. MONITORING ORGANIZATION REPORT NUMBER(S)		
6a. NAME OF PERFORMING ORGANIZATION <b>New York University</b>	6b. OFFICE SYMBOL (if applicable)	7a. NAME OF MONITORING ORGANIZATION <b>Air Force Office of Scientific Research</b>		
6c. ADDRESS (City, State, and ZIP Code) <b>Department of Physics and Psychology 4 Washington Place, New York, NY 10003</b>		7b. ADDRESS (City, State, and ZIP Code) <b>Building 410 Bolling AFB, DC 20332-6558</b>		
8a. NAME OF FUNDING / SPONSORING ORGANIZATION <b>AFOSR</b>	8b. OFFICE SYMBOL (if applicable) <b>NL</b>	9. PROCURMENT INSTRUMENT IDENTIFICATION NUMBER <b>F49620-88-K-0004</b>		
8c. ADDRESS (City, State, and ZIP Code) <b>Building 410 Bolling AFB, DC 20332</b>		10. SOURCE OF FUNDING NUMBERS		
		PROGRAM ELEMENT NO. <b>G1102F</b>	PROJECT NO. <b>2313</b>	TASK NO. <b>A4</b>
		WORK UNIT ACCESSION NO.		
11. TITLE (Include Security Classification) <b>Attention, Imagery and Memory: A Neuromagnetic Investigation</b>				
12. PERSONAL AUTHOR(S) <b>Lloyd Kaufman and Samuel J. Williamson</b>				
13a. TYPE OF REPORT <b>Final</b>	13b. TIME COVERED <b>FROM 88-03-01 TO 91-09-30</b>	14. DATE OF REPORT (Year, Month, Day) <b>91-10-14</b>	15. PAGE COUNT <b>71</b>	
16. SUPPLEMENTARY NOTATION				
17. COSATI CODES			18. SUBJECT TERMS (Continue on reverse if necessary and identify by block number)	
FIELD	GROUP	SUB-GROUP	<b>Cognition, spontaneous brains rhythms, alpha rhythm, mental imagery, cortical activity, visual spatial attention, auditory sensory memory</b>	
19. ABSTRACT (Continue on reverse if necessary and identify by block number)				
<p>The techniques of magnetic source imaging (MSI) have been applied to studies of three important aspects of human cognition: (1) An investigation of the effects of selective spatial attention on information processing within the human visual cortex for stimuli of constant luminance have revealed that early response components from 120 to 180 ms latency provide evidence for such effects, but amplitude enhancements for later components are probably related to pattern recognition and task-relevant stimulus discrimination; (2) A study of the relationship between the performance of a cognitive task such as visual imagery, or silent rhyming, and the suppression of spontaneous cortical rhythms reveals that the location, onset time, and duration of suppression are task specific and correlate with measures of performance; (3) The first characterization of the functional attributes of neuronal activity in human auditory association cortex provides evidence that cortical activation traces in primary and association areas can be accurately characterized by distinct lifetimes, which typically amount to several seconds, and that these "sensory memories" characterize specific physical attributes of sounds.</p>				
20. DISTRIBUTION / AVAILABILITY OF ABSTRACT <input checked="" type="checkbox"/> UNCLASSIFIED/UNLIMITED <input type="checkbox"/> SAME AS RPT <input type="checkbox"/> DTIC USERS			21. ABSTRACT SECURITY CLASSIFICATION <b>Unclassified</b>	
22a. NAME OF RESPONSIBLE INDIVIDUAL <b>Dr. Alfred Freely</b>		22b. TELEPHONE (Include Area Code) <b>(202)767-5024</b>	22c. OFFICE SYMBOL <b>NL</b>	

Contents

1 Introduction 3

2 Objectives 3

3 Status of the Research Effort 4

    3.1 Highlights of the Results . . . . . 4

4 Publications 7

5 Personnel 9

    5.1 Faculty . . . . . 9

    5.2 Collaborating Faculty . . . . . 9

    5.3 Research Scientists . . . . . 9

    5.4 Collaborating Researchers . . . . . 9

    5.5 Graduate Research Assistants . . . . . 9

    5.6 Undergraduate Students . . . . . 9

    5.7 High School Students . . . . . 10

    5.8 Degrees Awarded . . . . . 10

6 Interactions with Other Groups 11

    6.1 7th International Conference on Biomagnetism . . . . . 11

    6.2 Relations with AAMRL at WPAFB . . . . . 11

    6.3 Invited Talks given by Members of the Laboratory . . . . . 11

    6.4 Contributed Presentations . . . . . 15

7 Inventions and Patent Disclosures 17

8 Major Publications 17

Accession For	
NTIS GRA&I	<input checked="" type="checkbox"/>
DTIC TAB	<input type="checkbox"/>
Unannounced	<input type="checkbox"/>
Justification	
By	
Distribution/	
Availability Codes	
Dist	Avail and/or Special
A-1	



## 1 Introduction

This report, which is submitted in accord with the requirements of Contract No. F49620-88-K-0004 between AFOSR and New York University, summarizes the scientific progress made during the term of grant support, from 1 March 1988 to 30 September 1991. The emphasis in this research is to develop and apply new applications of magnetic source imaging (MSI) to improve our understanding of cognitive functions of the human brain.

## 2 Objectives

The overall theme of this research is to exploit the advantages of magnetic source imaging to elucidate the physiological basis for human cognitive functions. By measuring the pattern of magnetic field across the scalp with superconducting detectors, it is possible to determine the positions within the head where the active neuronal sources lie. By comparison with magnetic resonance images of the brain, the corresponding anatomical regions of the brain can be identified, and this provides information as to the general function of that activity.

Specifically, three main areas of research were successfully completed: (1) An investigation of neuronal activity within the primary visual area of the brain in response to visual patterns, to determine which stages of information processing are influenced by a person's attention to a specific area of the visual field. Stimuli of constant luminance presented in various positions of the visual field produced early response components with 120 to 180 ms latencies whose characteristics indicate the influence of spatial attention; but amplitude enhancements for later components are probably related to pattern recognition and task-relevant stimulus discrimination. (2) A study of spontaneous rhythms of the brain revealed that suppression occurs in specific areas of the brain when a person relies on these areas to carry out certain cognitive tasks. Suppression over the visual areas of the brain at the back of the head were discovered during visual imagery, when comparing a visual form with others previously seen. Moreover, the duration of suppression was found to be a significant measure of how long the person takes to complete the comparison. Complementary studies revealed that suppression takes place over the side of the head when a person is in the process of seeking a word that rhymes with a non-imageable word displayed on a screen. These findings demonstrate that suppression is not a generalized attention affect but takes place locally at specific times when an area of the brain becomes involved. Thus, an extension of these studies may well be employed to identify differing cognitive strategies that individuals employ when engaged in complex mental tasks. (3) A novel characterization of the functional properties of the auditory areas of the brain was made possible by the identification and localization of neuronal activity in the association cortex. For the first time, the lifetime could be measured for the retention of the pattern of synaptic connections that are established within the cortex when a sound is presented. This duration of "sensory memory" in primary auditory cortex is about 2 sec, but in association cortex it is several seconds longer. These lifetimes vary markedly across individuals and therefore may well become useful as a measure of sensory performance.

In addition to these principal research goals, numerous supplementary studies were carried out to support these studies. The main highlights of all these results are summarized in the following section.

### 3 Status of the Research Effort

The main goals outlined in the original research proposal have been achieved. These are summarized by a listing of the highlights of our research findings. References cited here are listed in the Publications section that follows.

#### 3.1 Highlights of the Results

This research program has accomplished the following objectives:

- Provided the first demonstration that 3mm accuracy can be achieved consistently in locating neuronal activity in sensory cortex by the techniques of magnetic source imaging (Yamamoto et al. 1988). This study evaluated the performance of a 14-sensor system and the method of defining a head-based coordinate system introduced by the Principal Investigators.
- Discovered that spontaneous activity within the alpha bandwidth is suppressed over the occipital and parietal scalp when a subject is engaged in mental imagery. For a task in which the subject must determine whether an abstract figure just seen was a member of a memory set of figures recently seen, the duration of suppression was found to be comparable to the reaction time (Schwartz et al. 1989). This suggests that the duration of suppression may be a measure of cognitive processing time.
- Obtained the first evidence that visual cortex participates in the process of mental imagery. Extensive magnetic measurements over the parietal and occipital scalp show that the percentage suppression of alpha rhythm varies with position and is greatest near the midline (Kaufman et al. 1989B). Magnetic fields in this area arise from neuronal activity within the longitudinal fissure, *viz.* the visual cortex.
- Established that the distribution of alpha power over the posterior scalp differs significantly from that of beta power (16-24 Hz) in the three subjects that were studied. For two of the subjects there was poorly correlated, and for one (who had alpha power levels commensurate with his beta power levels) the alpha power could account for only about 20% of the variance in the beta power. This proves for the first time that beta has largely independent neural generators and that these fast rhythms cannot be construed as the residual activity of desynchronized alpha generators (Kaufman et al. 1990).
- Obtained the first evidence that the strongest sources of human alpha rhythm are found in the parieto-occipital sulcus (Williamson et al. 1989D). Using a pair of 7-sensor probes placed over the right and left hemispheres, data were obtained on 2 subjects that clearly place the equivalent current dipole sources within the sulcus. Moreover, the strength (moment) of the current dipoles that best account for the sources of successive spindles have nearly the same strength, suggesting that the cortical excitations are a unitary process. We have called these excitations "alphons" (Williamson et al. 1989B).
- Discovered a source of spontaneous rhythmic activity in the temporal area of the brain. This activity in the alpha band was found to be suppressed when a subject engages in silent

rhyming (Kaufman et al. 1989). Significantly, when a subject is to find a rhyme to a word presented visually, the onset of suppression over the visual area of the brain commences with the presentation but the onset over the temporal area is delayed by about 100 ms. Therefore, alpha suppression does not reflect a generalized attentional effect but rather the selective engagement of specific regions of the brain that participate in the cognitive task. Moreover, the reappearance of temporal alpha rhythm correlates with the time that the subject indicates a rhyme was found.

- Studied by computer simulations the patterns of spontaneous activity within primary visual cortex that may account for alpha suppression using a cruciform model. Instantaneous and averaged field power patterns across the occipital scalp were computed when patches of cortical activity become desynchronized. Suppression of the extracranial field power could not be attributed to "desynchronization" but could be understood if the cortical activity weakens within the patches. The spatial distribution across the scalp of power suppression reflects the underlying cortical anatomy. The fact that modulation of spontaneous activity of specific parts of the brain may be detected and localized on the basis of external field measurements raise the exciting possibility that the magnetoencephalogram can be used in functional brain imaging similar to PET (Kaufman et al. 1991).
- Investigated the effect of interstimulus interval (ISI) on the amplitude of the 100-ms component of the auditory response evoked by the onset of a tone burst stimulus. This followed up a study by Hari et al. (*Electroenceph. Clin. Neurophysiol.* 54: 561-569, 1982) that showed the amplitude for the magnetic component (N100m) increases with ISI until the ISI reaches the range of 4 to 8 sec and thereafter remains stable. However, the amplitude of the electric component (N100) indicated by the scalp potential continues to increase for ISIs as long as 16 sec. Our first attempt to study this effect in 1988 yielded inconsistent results and no publication was forthcoming. A second attempt was made in 1990, and it produced the following successful results.
- Identified a response to auditory stimuli in the auditory association cortex that has both 100 ms and 180 ms components (Lü et al. 1991B). We named these the "latent" components (denoted L100m and L180m), since they are strong only when the ISI is long, if stimuli are presented at constant ISI. Comprehensive investigations revealed that association cortex exhibits strong habituation effects. With extensive maps of the field pattern over the left and right temporal areas the positions of 100 ms and 180 ms components were established for the first time in both primary and association cortices.
- Established for the first time that the strength of neuronal activation traces established in primary and association auditory cortices in response to a tone burst stimulus can be accurately characterized by individual lifetimes (Lü and Williamson 1991). The lifetime in primary cortex is typically about 3 sec and in association cortex about 5 sec. These can be considered the durations of a "sensory memory" in each cortex. The corresponding lifetimes are identical in left and right hemispheres of a given subject, but they vary considerably across subjects. Neuromagnetic measurements provide an accurate measure of these lifetimes.

- Established for the first time that the feature of a stimulus that habituates a response in primary auditory cortex differs from the feature that habituates a response in association cortex (Lü et al. 1991B). For the former, the N100m component for the onset of a tone is habituated by the offset of the previous tone stimulus. It logically follows, and was established by measurements, that the 100-ms component following the offset of a tone is habituated by the preceding response to the onset of that same tone. By contrast, the response in association cortex is habituated only by the onset of the preceding tone.
  
- Completed a pilot study of responses in visual cortex to luminance and chrominance stimuli in collaboration with Dr. Olli V. Lounasmaa, Professor of the Academy of Finland, who is director of the neuromagnetism program at the Low Temperature Laboratory of the Helsinki University of Technology (HUT). Careful measurements with a 5-sensor probe suggested that in one subject the responses were at slightly different locations in the primary visual cortex (Krauskopf et al. 1989). However the difference was not statistically significant. A follow-up study conducted with the 24-sensor system at HUT also showed no significant differences for components having latencies as long as 180 ms (Klemic et al. 1991).
  
- Completed a study of spatial visual attention for stimuli of constant luminance begun under AFOSR support for the University Research Initiative. Under conditions when the subject did not have to deal with a high work load, the first indication of neuronal attentional effects in visual cortex were established for latencies between 120 and 180 ms using behavioral AOC procedures (Luber et al. 1989). Amplitude enhancements were also observed for later components, but they are probably related to pattern recognition and task-relevant stimulus discrimination. Marked differences across certain individuals were found from an AOC analysis that may well be reflected in physiological differences revealed by the neuromagnetic measurements. However, of particular interest, is our observation that certain subjects when performing under high work load displayed differences for earlier components. This is a novel finding, and a manuscript is being prepared for publication (Luber et al. 1991).
  
- Obtained the first realistic estimate for the spatial extent of cortical activity that is responsible for evoked responses in human sensory cortex. An analysis of published data on current source-density measurements in cat visual cortex and monkey somatosensory cortex showed that the current dipole moment per square millimeter of cortical area is the same for long-latency components at moments of peak activity, to within a factor of 2 (Lü and Williamson 1991). The value is 50 nA·m per mm<sup>2</sup>. Since a common range for dipole moments is 2 to 20 nA·m, the typical cortical area ranges from 40 to 400 mm<sup>2</sup>. Thus, activity across cortex is larger than a macrocolumn but considerably smaller than the total area for auditory, somatosensory, or visual responses.

Details of these studies are provided by the reprints and preprints that are included as the final section of this report.

## 4 Publications

This section contains a chronological list of publications in technical journals.

### References

- [1] T. Yamamoto, S. J. Williamson, L. Kaufman, C. Nicholson, and R. Llinás. Magnetic localization of neuronal activity in the human brain. *Proc. Natl. Acad. Sci. USA*, 85:8732-8736, 1988.
- [2] S. J. Williamson, M. Hoke, G. Stroink, and M. Kotani, editors. *Advances in Biomagnetism*. Plenum, New York, 1989. 771 pages.
- [3] B. J. Schwartz, C. Salustri, L. Kaufman, and S. J. Williamson. Alpha suppression related to a cognitive task. In S. J. Williamson, M. Hoke, G. Stroink, and M. Kotani, editors, *Advances in Biomagnetism*, pages 237-240, Plenum, New York, 1989.
- [4] L. Kaufman, M. Glanzer, Y. M. Cycowicz, and S. J. Williamson. Visualizing and rhyming cause differences in alpha suppression. In S. J. Williamson, M. Hoke, G. Stroink, and M. Kotani, editors, *Advances in Biomagnetism*, pages 241-244, Plenum, New York, 1989.
- [5] J. Krauskopf, G. Klemic, O. V. Lounasmaa, D. Travis, L. Kaufman, and S. J. Williamson. Neuromagnetic measurements of visual responses to chromaticity and luminance. In S. J. Williamson, M. Hoke, G. Stroink, and M. Kotani, editors, *Advances in Biomagnetism*, pages 209-212, Plenum, New York, 1989.
- [6] B. Luber, L. Kaufman, and S. J. Williamson. Brain activity related to spatial visual attention. In S. J. Williamson, M. Hoke, G. Stroink, and M. Kotani, editors, *Advances in Biomagnetism*, pages 213-216, Plenum, New York, 1989.
- [7] S. J. Williamson, J.-Z. Wang, and R. J. Ilmoniemi. Method for locating sources of human alpha activity. In S. J. Williamson, M. Hoke, G. Stroink, and M. Kotani, editors, *Advances in Biomagnetism*, pages 257-260, Plenum, New York, 1989.
- [8] S.J. Williamson and L. Kaufman. Theory of neuroelectric and neuromagnetic fields. In F. Grandori, H. Hoke, and G.L. Romani, editors, *Auditory Electric and Magnetic Fields*, pages 1-39, Karger, Basel, 1989.
- [9] L. Kaufman and S. J. Williamson. Neuromagnetic localization of neuronal activity in visual and extra-visual cortex. In B. Cohen, editor, *Vision and the Brain*, pages 271-287, Raven Press, New York, 1990.
- [10] S. J. Williamson and L. Kaufman. Theory of neuroelectric and neuromagnetic fields. In F. Grandori, H. Hoke, and G. L. Romani, editors, *Auditory Evoked Magnetic Fields and Electric Potentials*, pages 1-39, Karger, Basel, 1990.

- [11] L. Kaufman and S. J. Williamson. Responses to steady-state auditory stimulation. In F. Grandori, H. Hoke, and G. L. Romani, editors, *Auditory Evoked Magnetic Fields and Electric Potentials*, pages 283–312, Karger, Basel, 1990.
- [12] L. Kaufman, B. Schwartz, C. Salustri, and S.J. Williamson. Modulation of spontaneous brain activity during mental imagery. *J. Cognitive Neuroscience*, 2:124–132, 1990.
- [13] S. J. Williamson and L. Kaufman. Evolution of neuromagnetic topographic mapping. *Brain Topology*, 3:113–127, 1990.
- [14] Z.-L. Lü and S.J. Williamson. Spatial extent of coherent sensory-evoked cortical activity. *Exp. Brain Res.*, 84:411–416, 1991.
- [15] L. Kaufman, J. Kaufman, and J.Z. Wang. On cortical folds and neuromagnetic fields. *Electroenceph. Clin. Neurophysiol.*, 79:211–226, 1991.
- [16] Z.-L. Lü, S.J. Williamson, and L. Kaufman. Human auditory primary and association cortex have differing lifetimes for activation traces. submitted for publication., 1991.
- [17] S.J. Williamson and L. Kaufman. Neuromagnetic studies of sensory functions and mental imagery. In C.H.M. Brunia, G. Mulder, and M. Verbaten, editors, *Event-Related Brain Research*, chapter Suppl. 42, page in press, Elsevier, Amsterdam, 1991.
- [18] S.J. Williamson, Z.-L. Lü, and L. Kaufman. Advantages and disadvantages of magnetic source imaging. *Brain Topography*, in press, 1991.
- [19] S.J. Williamson. MEG versus EEG localization test. *Ann. Neurology*, 30:222, 1991.
- [20] S.J. Williamson. Biomagnetism, medical aspects. In G.L. Trigg, editor, *Encyclopedia of Applied Physics*, pages 453–471, VCH Publishers, New York, 1991.
- [21] L. Kaufman, S. Curtis, J.Z. Wang, and S.J. Williamson. Changes in cortical activity when subjects scan memory for tones. *Electroenceph. Clin. Neurophysiol.*, in press, 1991.
- [22] L. Kaufman and S.J. Williamson. Neuromagnetic studies of sensory functions and mental imagery. page in press, 1991.

## **5 Personnel**

### **5.1 Faculty**

Lloyd Kaufman, Ph.D., Professor of Psychology and Neural Science; Adjunct Professor of Physiology and Biophysics.

Samuel J. Williamson, Sc.D., University Professor of Physics, Neural Science, Physiology and Biophysics.

### **5.2 Collaborating Faculty**

Murray Glanzer, Ph.D., Department of Psychology

John Krauskopf, Ph.D., Center for Neural Science

Rodolfo Llinás, M.D., Ph.D., Professor and Chair, Department of Physiology and Biophysics

Olli V. Lounasmaa, Ph.D., Professor of the Academy of Finland, Low Temperature Laboratory, Helsinki University of Technology

### **5.3 Research Scientists**

Sarah Curtis, Ph.D., Assistant Research Scientist (Psychology)

Barry Schwartz, Ph.D., Assistant Research Scientist (Psychology)

Jia-Zhu Wang, Ph.D., Associate Research Scientist (Physics)

### **5.4 Collaborating Researchers**

Risto J. Ilmoniemi, Ph.D., Low Temperature Laboratory, Helsinki University of Technology, Espoo, Finland (Physics)

James Kaufman, Ph.D., I.B.M. Research Laboratory, Almaden, California

Christoph Michel, Ph.D., EEG Laboratory, Department of Neurology, University Hospital, Zürich, Switzerland (Physics)

Carlo Salustri, Ph.D., Istituto di Elettronica dello Stato Solido (CNR), Rome, Italy (Physics)

David Travis, Ph.D., Department of Psychology, NYU.

Tomoyo Yamamoto, M.D., Ph.D., Kyushu University, Japan (Otolaryngology)

### **5.5 Graduate Research Assistants**

Gladys Klemic, M.S. student, Department of Physics

Daniel Karron, Ph.D. student, Department of Applied Science

Zhong-Lin Lü, Ph.D. student, Department of Physics

Bruce Luber, Ph.D. student, Department of Psychology

### **5.6 Undergraduate Students**

Robert Kalimi, Department of Biology, research project, 1990.

Divya Chander, Harvard University, Hughes Summer Scholar Research Project, 1991.

Elena Vitale, New York University, Hughes Summer Scholar Research Project, 1991.

### **5.7 High School Students**

Michael Gat, Stuyvesant High School, Semi-Finalist in the Westinghouse Science Talent Search for a project in Neuromagnetism, 1990.

### **5.8 Degrees Awarded**

Robert Kalimi, B.A. in Biology, Biology Honor's Thesis: "Characterization of Noise in Neuromagnetism", June, 1990.

Gladys Klemic, M.S. in Physics, "Neuromagnetism: New Techniques and Applications", January, 1990.

Bruce Luber, Ph.D. in Psychology, "Neuromagnetic Effects of Visual Spatial Attention in Discrimination Tasks", expected in Fall, 1991.

## 6 Interactions with Other Groups

### 6.1 7th International Conference on Biomagnetism

The Principal Investigators were Co-Chairs of the 7th International Conference on Biomagnetism, which was held at New York University August 13-19, 1989. They also organized a day-long series of tutorials for the day preceding the start of the conference, to provide newcomers with an introduction to the fundamentals of biomagnetic measurements and the information that can be obtained from magnetic studies of biological systems. The conference attracted 400 participants. The proceedings were published by Plenum Press as a 771 page book edited by S.J. Williamson, M. Hoke, G. Stroink, and M. Kotani.

### 6.2 Relations with AAMRL at WPAFB

Professor Kaufman has interacted on several occasions with the neuromagnetism group under Dr. Glenn Wilson at Wright Patterson Air Force Base. This has included making trips to consult for the group and sharing information on recent research advances.

### 6.3 Invited Talks given by Members of the Laboratory

- 8 Mar 1988 *Neuromagnetic Studies of Neural Ensembles*, Biophysics Seminar, AT&T Bell Laboratories, Murray Hill, New Jersey.
- 9 Mar *Magnetic Studies of Neural Populations*, Colloquium, Department of Physics, Lehman College, City University of New York.
- 6 Apr *Coherent Activity of Neural Populations*, Opening Plenary Session, Conference on Neural Networks for Computing, Snowbird, Utah.
- 20 Apr *Neuromagnetism: A New Window on the Brain*, Evening Lecture, U.S. Coast Guard Academy, New London, Connecticut.
- 29 Apr *Neuromagnetic Functional Imaging*, Symposium on Recent Advances in Physics in Medicine, The Radiological and Medical Physics Society of New York, Memorial Sloan-Kettering Cancer Center, New York, New York.
- 14 Jun *SQUID Biomagnetic Measurements - Present and Future*, Presentation for Agency (M.I.T.I.) and National Electrotechnical Laboratory, Tokyo, Japan.
- 16 Jun *Biomagnetism*, Colloquium at Tokyo Denki University, Tokyo, Japan.
- 22 Jun *Recent Developments in Neuromagnetism*, Tohoku - Shinkei - Konwakai: Tohoku Neurology Seminar, Tohoku University School of Medicine, Sendai, Japan.
- 24 Jun *Functional Organization of Human Sensory Cortex Revealed Magnetically*, Seminar, National Electrotechnical Laboratory, Tsukuba, Japan.
- 6 Jul *Champs magnétiques associés à des courants nerveux*, Dixième Conférence Internationale "De la Physique Théorique à la Biologie", Versailles, France, 4-8 July.
- 11 Jul *Neuromagnetic Studies of Sensory and Cognitive Functions of the Brain*, Sonderkolloquium der Neurologischen Universitätsklinik Erlangen, Erlangen, Federal Republic of Germany.

- 12 Jul *Frontiers in the New Science of Biomagnetism*, Sondersitzung der Physikalisch-Medizinischen Sozietät Erlangen, Erlangen, Federal Republic of Germany.
- 15 Jul *Role of Magnetoencephalography in the Localization of Human Cortical Sensory Areas*, Symposium on Topographic Mapping of Brain Function, American Academy of Clinical Neurophysiology, 14-16 July, Boston, Massachusetts.
- 5 Oct *Neuromagnetism: A Bridge Between Physiology and Perception*, Seminar in the Low Temperature Laboratory, Helsinki University of Technology, Espoo, Finland.
- 18 Oct *The Biophysical Basis of Magnetoencephalography*, MEG Evening Seminars at the annual American Epilepsy Society Meeting, sponsored by Biomagnetic Technologies Inc., San Francisco, California.
- 21 Nov *Neuromagnetism: A Bridge Between Physiology and Perception*, Department of Physics Colloquium, Brown University, Providence, Rhode Island.
- 15 Dec *Magnetism of the Brain*, Seminar on Physics of the Brain organized for the National Association of Science Writers and the American Institute of Physics, New York, New York.
- 17 Jan 1989 *Magnetism of the Brain*, Seminar on Physics of the Brain, National Association of Science Writers and the American Institute of Physics, San Francisco, California.
- 31 Jan *Neuromagnetism: A Bridge between Physiology and Perception*, Western, Eastern and Alpine EEG Conference, Park City, Utah.
- 1 May *Magnetism and the Brain*, Seminar on Physics and the Brain, American Institute of Physics, D.C. Science Writer's Association, and the National Association of Science Writers, Washington, DC.
- 5 May *Neuromagnetism: A Bridge Physics Provides from Physiology to Perception*, Solid State Seminar, Departments of Applied Physics, Chemical Engineering, Electrical Engineering, and Mechanical Engineering, Yale University, New Haven, Connecticut.
- 29 May *Neuromagnetic Studies of Sensory Functions and Mental Imagery*, Plenary Session, EPIC IX - Ninth International Conference on Event Related Potentials of the Brain, Noordwijk, The Netherlands, May 28-June 3.
- 9 Sept *Intracranial Localization by Magnetoencephalography*, Advanced Workshop on Topographic EEG and EP Analysis, International Society for Brain Electromagnetic Topography, St. Vincent, Val d'Aosta, Italy, Sept 7 - 11.
- 15 Sept *Effect of Memory Scanning and Imagery on the Brain's Magnetic Field*, Colloquium, IBM Research Center, Almaden, California.
- 27 Sept *Magnetic Studies of the Brain - from Physiology to Cognition*, Physical Science Seminar, Bellcore Corporation, Red Bank, New Jersey.
- 9 Nov *Measurements of Magnetic Fields from Living Tissues*, New Horizons in Physics Lecture Series, The College at New Paltz/SUNY, New Paltz, New York.
- 6 Dec *Biophysical Basis of MEG*, Clinical Advances in Magnetoencephalography (MEG), American Epilepsy Society Satellite Symposium, Boston, Massachusetts.

- 7 Dec *Localization of Brain Function by Neuromagnetic Techniques*, Department of Medical Physics Seminar, Memorial Sloan Kettering Cancer Center, New York City.
- 8 Jan 1990 *Neuromagnetic Investigations of Human Sensory Systems*, Biophysics Seminar, University of Rio de Janeiro, Rio de Janeiro, Brazil.
- 11,12 Jan Four lectures: *Introduction to Biomagnetism; Biosusceptometry; Biomagnetic Source Modeling; and Neuromagnetism*. The First University of São Paulo Biophysics-Medical Physics Workshop for South America: New Trends in Chemical, Biological, and Medical Physics Research. Ribeirão Preto, SP, Brazil.
- 25 Jan *Magnetic Fields of the Brain*, Annual Meeting of the American Physical Society and American Association of Physics Teachers, Atlanta, Georgia.
- 7 Feb *Neuromagnetic Studies: From Physiology to Cognition*, Colloquium, Department of Physics, City College of the City University of New York, New York City.
- 8 Feb *Magnetic Localization of Human Brain Functions*, Biophysics Section of the New York Academy of Sciences, New York City.
- 29 Mar *Neuromagnetism*, Colloquium, Department of Physics, Polytechnic University, Brooklyn.
- 31 Mar *Magnetic Characterization of Brain Function – Epilepsy Today, Alzheimer's and Schizophrenia Tomorrow*, Plenary Session, Medical Alumni Day, New York University School of Medicine, New York, NY.
- 6 Apr *Effects of Memory Scanning on the Brain's Magnetic Field*, Society of Experimental Psychologists, Columbia University, New York, NY.
- 20 Apr *Advances in Superconducting Biomagnetic Instrumentation*, Seminar, Superconducting Technology, Inc., Santa Barbara, California.
- 21 Apr *Bioelectricity and Biomagnetism in the Central Nervous System*, Workshop on Bioelectricity and Biomagnetism in Clinical Medicine: What is it, Where is it going, is it practical and affordable?, Little Company of Mary Hospital, Torrance, California.
- 4 May *Neuromagnetic Localization of Sensory and Cognitive Functions*, Third Swiss EEG-EP Mapping Meeting, Department of Neurology, University Hospital, Zürich, Switzerland. May 4-5.
- 23 May *Neuromagnetism: A Bridge that Physics Provides between Physiology and Cognition*, Seminar, Department of Physics, Universidade de Lisboa, Portugal.
- 1 June *Recent Advances in Neuromagnetism*, Seminar, Center for Neuromagnetism, Veterans Administration Hospital, Albuquerque, New Mexico.
- 4 June *Advances in Cognitive Studies with Neuromagnetic Techniques*, Seminar, Neuromagnetism Laboratory, Life Sciences Division, Los Alamos National Laboratory, Los Alamos, New Mexico.
- 7 Sept *Magnetic Investigations of Higher Levels of Brain Function*, Colloquium, Department of Electronics, Kyushu University, Fukuoka, Japan.
- 13 Sept *Evolution of Neuromagnetic Topographic Mapping*, Invited Special Lecture, First International Congress on Brain Electromagnetic Topography, Osaka, Japan.

- 26 Sept *Principles of Neuromagnetism*, Course on Magnetism in Clinical Neurophysiology, Annual Meeting of the American Electroencephalographic Society, Houston, Texas.
- 10 Oct *Neuromagnetism: A Bridge between Physiology and Cognition*, Colloquium, Department of Physics and Astronomy, Rutgers the State University of New Jersey, Piscataway, New Jersey.
- 12 Oct *Magnetic Source Imaging: Capabilities and Prospects for Neuromagnetism*, Seminar, Mayo Clinic, Rochester, Minnesota.
- 16 Nov *Neuromagnetic Insight into Human Brain Functions from Physiology to Cognition*, Seminar, Department of Physiology and Biophysics, University of Washington, Seattle, Washington.
- 17 Nov *Magnetic Methods for Determining the Functional Organization of Human Auditory Cortex*, Special Invited Talk, American Speech-Language-Hearing Association 1990 Annual Convention, Seattle, Washington.
- 30 Nov *Neuromagnetic Studies of Human Sensory and Cognitive Brain Functions*, Colloquium, Department of Physics, Columbia University, New York City.
- 5 Dec *Parallels in the Functional Organization of Sensory Cortex: Humans and Animals*, Seminar, Institute of Animal Behavior, Rutgers the State University of New Jersey, Newark, New Jersey.
- 19 Dec *Neuromagnetic Studies of the Human Brain with SQUID Sensors: From Physiology to Cognition*, Seminar, Medical Research Department, Brookhaven National Laboratory, Upton, New York.
- 8 Feb 1991 *Magnetic Techniques for Mapping Spatial Organization of Sensory and Cognitive Function of the Human Brain*. Recent Advances in Neuroscience at New York University, Symposium in association with the Fidia Foundation exhibit *The Enchanted Loom: The Discovery of the Brain*, New York University Medical Center.
- 13 Mar *Advances in Superconducting Instrumentation for Neuromagnetism: Extending our View from Physiology to Cognition*. IEEE Engineering in Medicine and Biology Society, New York Metropolitan Area Division, Rockefeller University.
- 15 Mar *Towards Forming Functional Images of the Brain*. Society of Experimental Psychologists, University of California, Los Angeles, California.
- 19 Mar *Functional Organization of the Human Brain Determined Magnetically*. Symposium of the Division of Biological Physics entitled "Neuromagnetism - From the Microscopic to Macroscopic", American Physical Society Meeting, Cincinnati, Ohio, March 18-22.
- 21 May *Magnetic Source Imaging*. Lead Speaker for Technology Applications Symposium: Technology Requirements for Biomedical Imaging, sponsored by Georgetown University Medical Center, American Medical Association, and Strategic Defense Initiative of Department of Defense, Washington, DC., May 21-22.
- 29 May *Magnetic Source Imaging of Human Cortical Activity*. Neurons, Vision, and Cognition. An International Symposium at New York University, New York City, May 28 - June 1.
- 4 Aug *Advantages and Limitations of Magnetic Source Imaging*. 3rd Congress of the International Society for Brain Electromagnetic Topography, Toronto, Canada, July 29 - August 1.
- 18 Aug *From Benchmark to Discovery: An Historical Perspective*. Plenary Address, 8th International Conference on Biomagnetism, Münster, Germany, August 18-24, 1991.

**6.4 Contributed Presentations****1988**

*Tonotopic organization of the human auditory cortex utilizing a multi-channel SQUID system*

T. Yamamoto, W. Hostetler, S.J. Williamson, and R. Llinás

18th Annual Meeting of the Society for Neuroscience, Toronto, Ontario, Canada, November 13-18, 1988.

**1989**

*Alpha Suppression Related to a Cognitive Task*

B.J. Schwartz, C. Salustri, L. Kaufman, and S.J. Williamson

7th International Conference on Biomagnetism, August, 1989, New York City.

*Differences in Alpha Suppression by Visualizing and Rhyming*

L. Kaufman, Y. Cycowicz, and S.J. Williamson

7th International Conference on Biomagnetism, August, 1989, New York City.

*Neuromagnetic Measurements of Visual Responses to Chromaticity and Luminance*

J. Krauskopf, G. Klemic, O.V. Lounasmaa, D. Travis, L. Kaufman, and S.J. Williamson

7th International Conference on Biomagnetism, August, 1989, New York City.

*Brain Activity Related to Spatial Visual Attention*

B. Luber, L. Kaufman, and S.J. Williamson

7th International Conference on Biomagnetism, August, 1989, New York City.

*Method for Locating Sources of Human Alpha Activity*

S.J. Williamson, J.-Z. Wang, and R.J. Ilmoniemi

7th International Conference on Biomagnetism, August, 1989, New York City.

*Distributed Sequential Activity of the Human Brain Detected Magnetically by CryoSQUIDS*

G.A. Klemic, D.S. Buchanan, and S.J. Williamson

7th International Conference on Biomagnetism, August, 1989, New York City.

**1990**

*Neuronal Sources of Human Alpha Rhythm*

S.J. Williamson and J.Z. Wang

March Meeting of the American Physical Society, Bulletin of the American Physical Society 35: 499 (1990).

*Spatial Extent of Coherent Sensory-Evoked Cortical Activity*

Z.-L. Lü and S.J. Williamson

Society for Neuroscience 20th Annual Meeting, St. Louis, MO, Oct. 28 - Nov. 2 (1990).

**1991**

*Neuronal Sources of Human Alpha Rhythm.*

S.J. Williamson and J.Z. Wang

Twenty-fourth Annual Winter Conference on Brain Research  
Vail, Colorado, January 26 - February 2, 1991

*Recent Advances in Neuroscience at New York University*, Symposium in association with the Fidia Foundation exhibit "The Enchanted Loom: The Discovery of the Brain", 8-10 February, 1991.

*Spatial extent of coherent sensory-evoked cortical activity.*  
Z. Lü and S.J. Williamson

*Auditory attention and the neuromagnetic field*  
S.T. Curtis, L. Kaufman, and S.J. Williamson.

*Do Verbal and Imaging Tasks Have Differing Effect on Cortical Activity?*  
Y.M. Cycowicz, L. Kaufman, M. Glanzer, and S.J. Williamson.

*An Effect of Memory Scanning on Spontaneous Cortical Activity*  
L. Kaufman, S.T. Curtis, J.-Z. Wang, and S.J. Williamson.

*Magnetic localization of sources of human alpha rhythm.*  
Z. Lü, J.-Z. Wang, and S.J. Williamson.

*Changes in Cortical Activity When Subjects Scan Memory for Tones*  
L. Kaufman, S. Curtis, J.-Z. Wang, and S.J. Williamson  
7th International Conference on Biomagnetism, August, 1991, Münster, Germany.

*Neuronal Sources of Human Parieto-Occipital Alpha Rhythm*  
Z.-L. Lü, J.Z. Wang, and S.J. Williamson  
7th International Conference on Biomagnetism, August, 1991, Münster, Germany.

## **7 Inventions and Patent Disclosures**

This program of research was not directed toward producing inventions. Several innovative techniques for registering magnetic resonance images and magnetic source images were developed, but that was under the sponsorship of AFOSR-90-0221 grant entitled "Cognition and the Brain". None of these were considered by the Office of Industrial Liaison of New York University to be patentable.

## **8 Major Publications**

This section contains preprints and reprints of representative publications describing the results of this research program. A major publication on spatial visual attention is in preparation and will be submitted separately as a Technical Report. The following articles are:

Alpha Suppression Related to a Cognitive Task

Modulation of Spontaneous Brain Activity during Mental Imagery

Visualizing and Rhyming Cause Differences in Alpha Suppression

Method for Locating Sources of Human Alpha Activity

On Cortical Folds and Neuromagnetic Fields

Spatial Extent of Coherent Sensory-evoked Cortical Activity

Human Auditory Primary and Association Cortex Have Differing Lifetimes for Activation Traces

Brain Activity Related to Spatial Visual Attention

Magnetic Localization of Neuronal Activity in the Human Brain

Changes in Cortical Activity when Subjects Scan Memory for Tones

*Advances in Biomagnetism*

S.J. Williamson, M. Hoke, G. Stroink, and M. Kotani, Editors  
Plenum Press, New York  
Pages 237 - 240

ALPHA SUPPRESSION RELATED TO A COGNITIVE TASK

Barry J. Schwartz, Carlo Salustri\*, Lloyd Kaufman, S. J. Williamson

Neuromagnetism Laboratory  
Departments of Psychology and Physics and Center for Neural Science  
4 Washington Place, New York University, New York, NY 10003

INTRODUCTION

Is the visual cortex involved in manipulating mental images as well as visual stimuli? This question may now be amenable to a direct test.

When subjects are in a resting but alert state, alpha activity (8-12 Hz) predominates in the spontaneous EEG. It has been reported (Kaufman and Locker, 1970; Pfurtscheller, et al., 1977, 1987) that alpha activity diminishes coinciding with presentation of visual stimuli and that the duration of this alpha suppression is much longer than that of the classic evoked response. In this paper we report that MEG activity during a visual memory task shows a dramatic amplitude reduction in the alpha range lasting 500 to 2000 msec, following which the amplitude recovers despite continuous visual fixation on the display.

Recent evidence argues against the general idea that alpha arises from simultaneously active "generators" that become desynchronized during arousal, causing partial self-cancellation of their fields. Microelectrode studies using dogs (Lopes Da Silva and van Leeuwen, 1978) suggest that alpha originates in small areas of visual cortex and spreads over relatively short distances. Recent magnetoencephalography (MEG) studies (Chapman, et al., 1984; Ilmoniemi, et al., 1988) showed that alpha spindles have multiple sources in occipital and perhaps in parietal areas.

The accuracy provided by MEG for localizing neuronal activity in sensory cortex (Yamamoto, et al, 1988) suggests that alpha suppression can be localized specifically to visual cortex. To test this hypothesis we used a combination of two classic paradigms: Sternberg's memory matching task (Sternberg, 1969) and Shepard's mental rotation task (Shepard and Metzler, 1971). Both tasks require a search of memory for representations of visual images, and performance in each case is indexed by systematic differences in choice reaction time (RT). We observed alpha suppression and averaged responses. In this paper we present data from one 41 year old male subject. These results are similar to those obtained with 6 other subjects. Data analysis from other subjects will be described in detail in subsequent publications.

METHODS

The subject, seated on a chair in a magnetically shielded room, maintained fixation on a small cross and viewed a sequence of three irregular polygon shapes on a dark background in the lower right quadrant of his visual field. Each shape was seen outlined in white for 1 sec followed by a 0.3 sec dark interval; 3.0 sec after the disappearance of the last image a fourth "probe" shape was presented for only 0.1 sec. In one block of trials ("choice reaction time", CRT) the subject pressed one of two buttons after seeing the probe, indicating whether it belonged in the memory set or was new. In a second block of trials ("simple reaction time", SRT) the subject simply had to press one

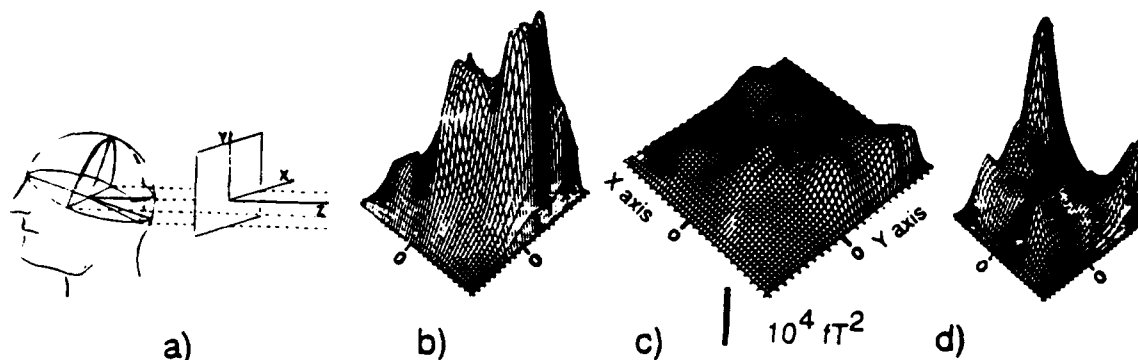


Fig. 2. (a) Distribution of average alpha power across the posterior scalp portrayed by an azimuthal equal distance projection. Equal distances across the surface of a spherical representation of the head from the center of projection map onto equal distances across a flat plane. The x-axis corresponds to a horizontal line normal to the midline, the y-axis to a vertical parallel to the midline. (b) Distribution of average *baseline alpha*, defined as the average alpha power observed within a 200 msec interval 100 msec prior to presentation of the visual probe in the CRT condition. (c) Distribution of alpha power averaged over a 100 msec interval centered on the moment of maximum suppression. The locations of the midlines are indicated by the short lines in these graphs. (d) Distribution of the ratio of residual to baseline alpha, which defines the *relative alpha suppression*.

To characterize the suppression of alpha activity during mental *imagery*, the magnitude of average alpha power was plotted as a function of position over the posterior scalp (Fig. 2 a-d). The average power within a 2 sec interval 200 msec prior to presentation of the probe stimulus represents the *baseline*, which has a peak in the right hemisphere about 5 cm above the inion and 5 cm to the right of the midline. It is important to note that the distribution changes during maximum suppression, with overall reduction in activity most pronounced in the vicinity of the midline. Figure 2d represents the proportional change in alpha power, or the ratio of b) to c) at each location over the scalp. If the suppression of alpha were global and uniform, this surface would be flat. Instead, the relative suppression is greatest in a band about the midline above the inion and below the vertex. The pattern of relative suppression is consistent with changes of limited extent and near the surface of visual cortex.

The temporal pattern of alpha suppression for SRT and CRT tasks is very similar for seven subjects, with individual differences in reaction time and mean duration of suppression. Interestingly, there are large and stable individual differences in the magnitude of power in alpha among subjects, differences which remain constant over the months involved in our observations. There are also individual differences in local patterns of alpha distribution for the three subjects whose fields have been extensively mapped. Individual differences in the strength and distribution of alpha cannot be attributed to differences in skull thickness (Leissner, Lindholm, and Petersen, 1970), since thickness of the skull has a negligible effect on magnetic fields. Instead, they must be attributed to underlying brain anatomy and neural function.

When alpha is suppressed, beta activity (16-24 Hz) does not show an increase, contrary to some predictions. In fact, there is a correlated *decrease* in beta power during alpha suppression. The distribution of beta power across the scalp is not the same as that of the alpha band. For this subject, BS, one percent of the of variance in the beta distributions could be accounted for by the alpha distributions. Partly independent neuronal populations must be responsible for spontaneous activity in these two bandwidths, although both populations exhibit suppression when subjects search visual memory.

button as soon as he saw the probe shape. In this task, the subject still had to attend to the whole sequence of visual shapes in order to know which one required a response. Each block consisted of a sequence of 30 trials.

The component of the magnetic field normal to the subject's head was recorded over posterior and parietal areas at 65 different locations by means of a 5-channel SQUID-based Neuromagnetometer (Williamson, et al., 1983; Buchanan, et al., 1988) The outputs of the SQUIDS were bandpassed between 0.1 - 50 Hz. Each recording epoch lasted 7 sec, 3 sec prior to and 4 sec following the onset of the (100 msec) visual probe.

Visual evoked potentials were extracted after digitally filtering the MEG between 1 and 20 Hz and then averaging over the 30 recording epochs. Alpha activity was isolated by filtering each epoch of data between 8 and 12 Hz, and computing the variance across the 30 trials in each block as a function of time for each SQUID channel. This variance is the mean square field (power), which excludes the average evoked response. Temporal changes in this variance are due to changes in amplitude, not to coherence across the epochs. An examination of single trial data shows that alpha activity (filtered from 8 to 12 Hz) is not time-locked stimulus onset.

## RESULTS

Our results show that MEG power in the alpha band undergoes a systematic reduction during the performance of visual memory-search tasks. Alpha power for CRT trials is sharply suppressed for about 1500 msec. For SRT trials, suppression lasts for about 500 msec, beginning at the time of probe stimulus onset. Both tasks require subjects to attend to all visual stimuli. The duration of evoked responses for both tasks are typical of sensory evoked responses, on the order of 100 msec. Alpha suppression and RT's, on the other hand, are on the order of 500 msec to 1500 msec.

The RT for the SRT task coincides with the minimum of its alpha power curve, about 500 msec after the onset of the probe. Suppression of alpha power for CRT trials is significantly longer in duration. At 1200 msec after stimulus onset, the alpha power is half way through its recovery back to its *baseline* level. RT for the CRT task occurs during its recovery phase (Figure 1). The longer duration of the suppression in the CRT task is consistent with the interpretation that the visual cortex is engaged during a search of memory.

The distribution of alpha power over the scalp prior to and following the suppression is quite similar, showing a correlation of 0.81 over 65 measured positions ( $p < 0.001$ ). There is less of a similarity in distribution over the scalp during the time maximum suppression.

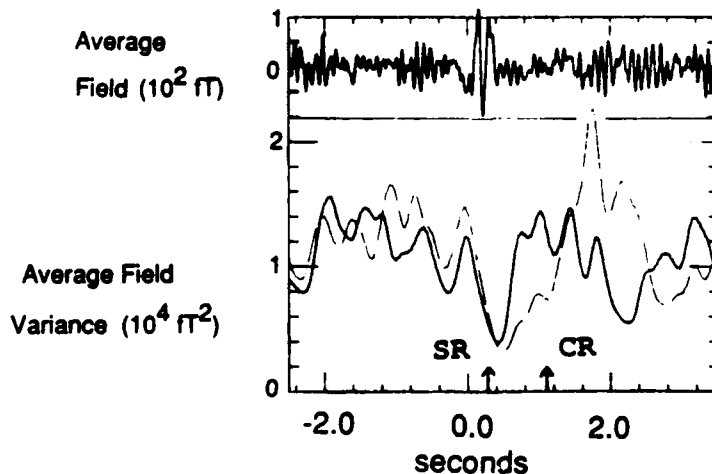


Fig. 1. A representative plot of variance across epochs. The darker trace is the SR condition, the lighter trace is the CR condition. Reaction times are indicated by arrows. An averaged evoked response is shown for comparison of its time span. This evoked field is a grand average of 10 groups of 30 trials for all 5 sensors, as it was impossible to obtain a sharply defined evoked field averaging only 30 trials.

## CONCLUSIONS

These data support the hypothesis that power within the alpha and beta bands is systematically reduced during the performance of a mental task involving the matching of memories of visual images. The source of this reduction appears to be in the visual cortex, a finding that is consistent with local cerebral blood flow studies (Roland and Frieberg, 1985).

Although the field pattern of alpha appears to be suppressed over a widespread area on the occipital scalp, a more local pattern of suppression is clearly superimposed on it. Functionally, this suppression is correlated not merely with visual attention, but more specifically with the task of visual memory search, since its duration varies with task and also correlates with RT. We believe the above procedure will prove useful for direct tests of hypotheses about the roles of various areas of the brain during different types of mental acts.

## ACKNOWLEDGEMENTS

Supported in part by Air Force Office of Scientific Research Grants F49620-88-K-0004 and F49620-86-C-0131. C. Salustri is partially supported by Associazione Italiana Ricerche Neurologiche (ARIN).

\* Permanent address: Istituto di Elettronica dello Stato Solido (CNR), via Cineto Romano 42, I-00156 Rome, Italy.

We thank Arthur Robinson and John P. Snyder for advice about azimuthal equal distance projections, and Jia Zhu Wang and Irene Martin for assistance with software development.

## REFERENCES

- Buchanan, D.S., Paulson, D., and Williamson, S.J. (1987). Instrumentation for clinical applications of neuromagnetism. In: Fast, R.W., Ed., *Advances in Cryogenic Engineering* Vol. 33, Plenum Press, New York, pp. 97 - 106.
- Chapman, R.M., Ilmoniemi, R.J., Barbanera, S., and Romani, G.L. (1984). Selective localization of alpha brain activity with neuromagnetic measurements. *Electroenceph. clin. Neurophysiol.* 58, 569-572.
- Costa Ribeiro, P., Williamson, S.J., and Kaufman, L. (1988). SQUID arrays for simultaneous magnetic measurements: calibration and source localization performance. *IEEE Trans. Biomed. Engr.* BME-35, 551 - 560.
- Kaufman, L. and Locker, Y. (1970). Sensory modulation of the EEG. *Proc. 78th Annual Conv. Amer. Psychol. Assoc.*, 179-180.
- Leissner P., Lindholm, L.-E. and Petersen, I. (1970). Alpha amplitude dependence on skull thickness as measured by ultrasound technique. *Electroenceph. and clin. Neurophysiol.*, 29, 392-399
- Lopes Da Silva, F.H. and van Leeuwen, S. (1978). The cortical alpha rhythm in dog: The depth and surface profile of phase. in *Architectonics of the Cerebral Cortex*, M.A.B. Brazier and H. Petsche, Eds. (Raven Press, New York, 1978), pp. 319-333.
- Pfurtscheller, G. (1988). Mapping of event-related desynchronization and type of derivation *Electroenceph. clin. Neurophysiol* 70, 190-193.
- Pfurtscheller, G. and Aranibar, A. (1977). Event-related desynchronization detected by power measurements of scalp EEG. *Electroenceph. clin. Neurophysiol* 42, 138-146.
- Roland, P.E. and Frieberg, L. (1985). Localization of cortical areas activated by thinking. *J. Neurophysiol.* 53, 1219-1243.
- Shepard, R.N. and Metzler, J. (1971). Mental rotation of three dimensional objects. *Science*, 220, 632-634.
- Sternberg, S. (1969). Memory scanning: mental processes revealed by reaction time experiments. *Amer. Scientist*, 57, 421-457.

# Modulation of Spontaneous Brain Activity during Mental Imagery

L. Kaufman, B. Schwartz, C. Salustri,\* and S. J. Williamson

Departments of Psychology and Physics,  
and Center for Neural Science  
New York University

## Abstract

■ Magnetic measurements of average power of human alpha and beta activity over the occipital and parietal areas of the scalp reveal spatially selective suppression of the activity of the occipital cortex when abstract figures are briefly presented visually and subjects simply indicate that they saw the figure. However, the duration of the suppression increases markedly when subjects must indicate whether or not they had previously seen the figure. The reaction time is similarly prolonged during the search of visual memory, and is commensurate with the duration of selective suppression of brain activity. It is also demonstrated that alpha activity is not replaced by beta activity during this suppression, but that power in the beta band is also diminished during memory search. Low correlations between

the scalp distributions of power in the beta and alpha bands indicate that partly different neuronal populations give rise to activity of these different frequency bands. Since magnetic fields are negligibly affected by intervening bone tissues, dramatic asymmetries in the distribution of alpha activity across the scalps of individuals and the differences in distribution between individuals cannot be ascribed to differences in skull thickness but are due instead to differences in underlying brain anatomy or function. Nevertheless, a common pattern of suppression of alpha activity is observed across subjects during well-controlled cognitive tasks. This implies that the visual system is involved in mental imagery. ■

## INTRODUCTION

Spindles of alpha activity (8–14 Hz) encountered in the ongoing EEG of resting though wakeful subjects tend to be inhibited ("blocked") when subjects open their eyes and attend to visual objects. It has been suggested that blocked alpha activity is "replaced" by "desynchronized" low-voltage fast beta activity (14–24 Hz). Andersen and Andersson (1968) proposed that alpha waves result from driving of cortical neurons by cells of the thalamus having their own rhythmic outputs. Nonspecific output from the ascending reticular formation (Maruzzi and Magoun 1949) may serve to inhibit thalamic relay neurons and, indirectly, the cortical pyramidal cells that are the proximate generators of alpha waves. Thus, activation of the cortex, in the sense of an increased probability of response to external stimulation, is presumed to be reflected in a widespread desynchronization of EEG activity, which is mediated by the brainstem reticular formation (Steriade 1981).

Blockage is often described as "desynchronization," which presumes that alpha arises from simultaneously active "generators" that become desynchronized during

arousal, causing partial self-cancellation of their fields. As already indicated, this desynchronization is widely attributed to nonspecific arousal, but there is evidence also for sensory-specific thalamic effects on cortical alpha sources (Sakakura 1968).

The theory that thalamic pacemakers (Andersen and Andersson 1968) control alpha activity is viewed as incomplete. Alpha rhythms are now ascribed to oscillating circuits in which single cells may act as either resonators or oscillators (Jahnsen and Llinás 1985), as well as to thalamocortical interactions (van Rotterdam et al. 1982). Questions have also been raised about the degree of coherence of alpha activity across the cortex. It is commonly believed that the "synchronized" activity is widespread across large areas of cortex. However, microelectrode studies suggest that alpha originates in small areas of the visual cortex and spreads over relatively short distances, with very loose coupling between the small alpha-generating areas (Lopes da Silva and van Leeuwen, 1978), a finding that is inconsistent with the notion of coherence over large cortical regions.

Recent magnetoencephalographic (MEG) studies suggest that alpha consists of sequences of spindles, some overlapping temporally, which originate at multiple sources in occipital and parietal areas (Chapman et al. 1984; Vvdensky et al. 1986), with each spindle having a

\*Permanent address: Istituto di Elettronica dello Stato Solido (CNR), via Cineto Romano 42, I-00156 Rome, Italy.

different source configuration (Ilmoniemi et al. 1988). These microelectrode and MEG results suggest that blockage may actually occur on a more localized basis than had previously been thought, and that desynchronization may not play a prominent role in its occurrence.

Although it is clear from the foregoing that the spontaneous activity of the brain is as yet incompletely understood, it has long been suspected that it is affected by cognitive processes. For example, Slatter (1960) presented evidence associating alpha blockage with mental imagery. Blockage may also be induced by visual attention. Other cognitive processes may also affect alpha activity. Pfurtscheller and Aranabar (1977) observed a reduction in power (mean square voltage) in the 8–14 Hz band of the EEG subsequent to flexion of the thumb. This phenomenon, which was labeled "event related desynchronization" (ERD), was observed to be stronger with active electrodes over both parietal areas rather than over the contralateral central area, so it is not possible to determine from the data whether such a voluntary motor act is associated with a change in activity arising in somatosensory or motor cortex. More recently, Pfurtscheller and his colleagues (Pfurtscheller 1988; Klimesch et al. 1988) mapped the ERD in the form of two-dimensional topographic displays to determine how alpha power varies over the scalp, depending on the mental task. When subjects were ignorant of whether a word or a numerical stimulus was to be presented on a given trial, the parietal and occipital regions seemed to become more active, as reflected in a larger ERD. However, with prior knowledge of the stimulus there was significantly more activity over the central region. Klimesch et al. (1988) suggest on the basis of such measures that the occipital regions play an important role in memory, as exemplified in a reading task, but also assert that attentiveness rather than memory-related processes is the predominant contributing factor.

We have applied the reference free method of MEG to study alpha blockage and its relation to mental imagery. Our goal was to exploit the precision of MEG source localization (Yamamoto et al. 1988) and avoid the ambiguities encountered by Pfurtscheller et al. (1988) and Pfurtscheller (1988) in interpreting EEG data. Our reasoning was as follows: Assuming that the sources of alpha activity are very loosely coupled so that the underlying activity is largely incoherent (Lopes da Silva and van Leeuwen 1978), and that blockage may be induced by activity in specific sensory areas, then it may be possible to monitor changes in different bands of spontaneous brain activity originating in the visual cortex while subjects manipulate mental representations of visual objects. This would enable us to test the conjecture that the machinery of the visual system is actually involved in mental imagery (Sternberg 1966, 1969; Shepard and Metzler 1971; Kosslyn 1983). A negative finding could be interpreted as consistent with the alternative view that the visual system is not involved in mental imagery, and

the performance of such tasks could depend, *inter alia*, on the use of propositional knowledge about the objects whose "mental images" are putatively being compared (Pylyshyn 1981).

## RESULTS

We report that alpha activity is locally suppressed during a task involving matching of mental images, indicating that visual cortex is involved. The term "suppression" rather than "blockage" is used in this paper because we deal simply with a reduction in power of the MEG within the classic band of alpha activity, and not necessarily with the reduced probability of spindling normally associated with so-called blockage. Furthermore, the results to be described raise some serious questions about long-held assumptions implicit in the use of the term "desynchronization," so the more neutral term "suppression" is better suited to our purposes. As described in more detail in the Methods section, to examine the effect of mental imagery on the *spontaneous* activity of the brain we measured changes in power within several different bands of the MEG, both subsequent to visual presentation of an abstract shape and while subjects scanned their memories for previously seen shapes. Before measuring MEG power, components of the MEG that are time locked to the stimulus were removed so that our measure reflected time-dependent changes in levels of spontaneous activity and not the classic sensory-evoked response. The resulting smoothed envelope of MEG power over time remained in-step with the visual stimulus, even though the individual oscillations were not time locked to the stimulus.

This study combined elements of both the Sternberg (1966) and Shepard (Shepard and Metzler 1971; Shepard and Cooper 1982) paradigms. A sequence of random polygon shapes was presented for the subject to remember and compare with a subsequently presented "probe" shape. Subjects followed one of two different sets of instructions. One instruction, the *Simple Reaction Task* (SRT), required pressing a button as soon as possible after seeing the probe, whether or not the probe had been a member of the memory set. The second instruction, the *Choice Reaction Task* (CRT), required pressing a button if the probe matched one of the members of the original "memory set" or a different button if it did not match. Reaction time (RT) was measured on all trials.

Alpha power for CRT and SRT trials (Figure 1) is sharply suppressed after presentation of each probe and quickly recovers for the SRT trials. However, suppression is prolonged following the probe for the CRT trials. Similarly, choice RTs for the probes were significantly longer than simple RTs. Average simple and choice RTs obtained during the trials are shown on the alpha power plots as arrows with error bars. In the SRT trials the average RT nearly coincides with the time at which alpha power reaches its minimum. However, the choice RTs

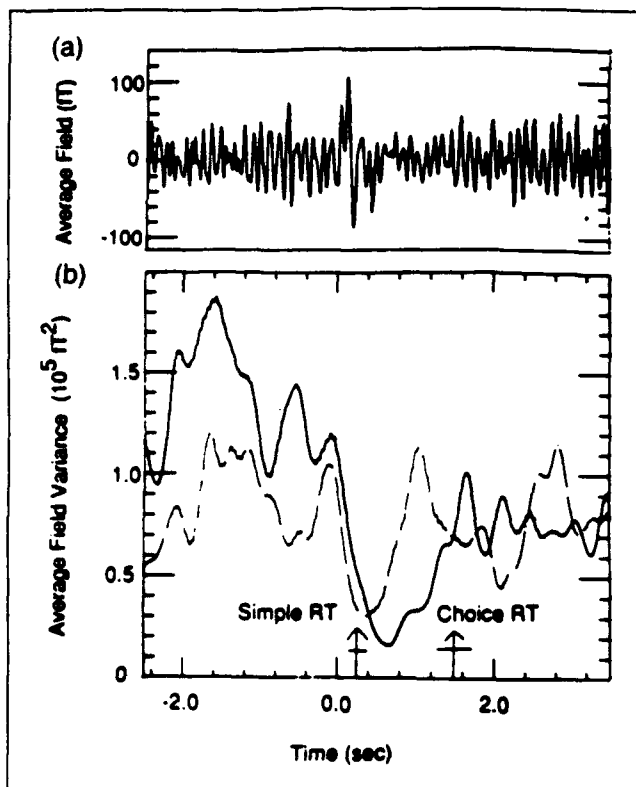


**Figure 1.** (a) A grand average of several average evoked responses associated with presentations of probe stimuli in the choice RT task and recorded within a bandwidth of 1–20 Hz from several occipital positions of subject LK. The duration of this AEF is measured in milliseconds. This AEF is of slightly larger amplitude than the comparable AEF obtained in the simple RT task, and nearly 100 msec longer in duration. It is to be contrasted with the modulation of activity in the alpha band, which is portrayed in (b). (b) The dashed trace (simple RT task) and the solid trace (choice RT task) represent variances about average brain activity within an 8–12 Hz band recorded at one place external to the scalp of subject LK. The power is expressed in femtoesla squared ( $fT^2$ ). The abrupt drop in power in the SRT trace at the time of presentation of the probe (0 on the x axis) is of much shorter duration than that of the suppression in the CRT, while the subject searches visual memory. The mean RTs associated with each of these traces are represented by arrows with error bars representing 1 standard deviation.

tended to occur well into the recovery phase of the alpha power, indicating that subjects were comparing the previously seen probe stimulus to the memory set throughout the period of suppression in alpha power. Table 1 shows mean RTs and standard deviations computed from several hundred trials for each of three subjects. It also shows the mean durations of suppression of alpha activity and its variability across several blocks of trials for each of the subjects. It is clear that for all subjects the RT in the Simple Reaction Task was always much shorter than the duration of suppression. However, in the Choice Reaction Task, the RT does not differ significantly from the duration of suppression. In every case, the duration of suppression in the choice task is about twice that of the simple task.

A conventional visually evoked field (VEF) is also shown in Figure 1. As more than 30 trials were needed to obtain a relatively noise-free version of the VEF, it represents an average of responses time locked to the onset of shape presentation averaged across data at several different positions over the scalp. The duration of the VEF is much shorter than either the suppression in power or the RT. There is, however, a consistent difference in amplitudes of VEFs obtained under CRT and SRT conditions, with the former having a larger amplitude and somewhat longer duration ( $\sim 100$  msec) than the latter. The difference in duration is far smaller than the difference in RT. This is similar to the result of Farah et al. (Farah 1988; Farah et al. 1988). In their experiment subjects either formed an image of a letter before presentation of a target letter, or they were instructed not to form such an image. When the image that was formed was the same as that of the target letter, the amplitude of the 173 msec component of the average visually evoked potential (VEP) was larger than when the imaged letter was different from the presented letter, and also of greater amplitude than the response to a letter prior to which no image was formed. Farah's effect is widely distributed over parietal and occipital electrodes but the limited number of electrodes makes it impossible to determine the degree to which the evoked response of interest arises from a particular region of the brain.

To test for the existence of local suppression of brain activity in the alpha band while processing a mental *image*, i.e., matching the mental representation of a form to members of a memory set, the magnitude of average alpha power within a 2 sec interval 200 msec prior to presentation of the probe was plotted as a function of position over the posterior scalp, as projected onto a plane (Figure 2a). The magnitude of this *baseline alpha* differs among subjects (Figure 2b). Subject LK exhibits very strong alpha over his left hemisphere, and significantly weaker activity over the right hemisphere. Subject BS has somewhat higher levels over right hemisphere, and the average alpha power of subject CS is about two orders of magnitude less than that of LK, and one order of magnitude less than that of BS. Such individual differences in the strength and distribution of alpha cannot be attributed to differences in skull thickness (Leissner et al. 1970), as the thickness of the skull has a negligible effect on magnetic fields. Differences and asymmetries in underlying brain anatomy and functional neural states must be the main causes of the observed differences.

Despite these individual differences, the two regions of greatest baseline alpha on either side of the midline for LK and BS (Figure 2c) overlap the positions of field extrema associated with the VEF. As the center of a line connecting these field extrema determines the position of an underlying equivalent current dipole source (Williamson and Kaufman 1981), neuronal activity lies near the longitudinal fissure with the current predominantly parallel to the fissure. However, because of the asym-

**Table 1.** Reaction Times and Duration of Alpha Suppression for Two Tasks.<sup>a</sup>

Subject	Reaction Time (msec)			Alpha Suppression (msec)		
	Mean	SD	N	Mean	SD	N
BS						
Choice task	1186.7	431.2	323	900	275.4	7
Simple task	365.8	158.3	288	428.6	85.9	7
CS						
Choice task	852.2	261.4	354	845.0	251.0	12
Simple task	237.7	100.2	353	427.0	90.5	12
LK						
Choice task	1389.9	363.3	207	1114.3	114.4	7
Simple task	248.6	135.0	230	600.0	28.9	7

<sup>a</sup>Each alpha suppression duration was determined as the time spanning the two half-amplitude points between downward-going and upward-going parts on the alpha-power-vs-time-plots, which were derived for a run of 30 trials, with each 30-trial run representing a different probe position. The *N* represents the number of separate measurement runs for which recovery could be measured. Reaction times on each trial are averaged, excluding those for which there was no response.

metry in the pattern, it is likely that several different sources of various orientations contribute to the observed field. The distribution of baseline alpha obtained from subject CS is far more complicated than for the other two subjects, suggesting contributions from a complex array of sources in the longitudinal, calcarine, and parietooccipital fissures.

During the period of suppression (Figure 2d), the *residual alpha* clearly exhibits an approximately dipolar pattern for subjects LK and BS. During maximum suppression the locations of the extrema of LK are about 6 cm above the inion and 3 or 4 cm to either side of the midline, which places the source of the residual neuronal alpha activity in the visual cortex near the longitudinal fissure. The peak alpha activity over BS's right hemisphere is about 5 cm above inion and 5 cm to the right of the midline. There are several peaks over the left hemisphere about 4 cm to the left of the midline and as high as 7 cm above the inion. The depth of an equivalent current dipole source that accounts for most of LK's pattern is approximately 4.0 cm beneath the scalp. It should be noted that such shallow depths virtually preclude the possibility that the neural tissue giving rise to the observed pattern is a large sheet of cortical tissue. The reason is that a source that is large relative to its distance from the scalp will result in a very wide separation between the field extrema at the scalp, and this field configuration mimics that which would be produced by a very deep dipolar source (Maclin 1983). Thus, the relatively shallow depth is consistent with activity of a confined region of visual cortex. Assuming a separation of about 9 cm between the extrema for subject BS, the depth of the source would be about 4.5 cm. Of course, the distribution for subject CS is clearly extremely com-

plicated, probably because of the relatively weak level of his alpha activity, and extraneous brain "noise" may well predominate in his pattern. We ran CS as extensively as the other two subjects because we were aware that the results were atypical. We have now conducted similar experiments with at least 11 other subjects, and none of them displays such weak alpha activity which, in CS's case, is virtually indistinguishable from the level of his beta activity. Despite this, at some places about his scalp the suppression effect was very clear, and as shown in Table 1, the durations of suppression under the CRT and SRT conditions, and his RTs as well, are quite similar to the other two subjects.

Figure 2d shows the distribution of the ratio of residual to baseline alpha power. This *relative residual alpha* is weakest about the midline about 6 cm above the inion for subjects LK and BS. Therefore, the greatest relative suppression for both subjects is located approximately over the visual cortex, indicating that sources in the visual cortex are most markedly affected. As already indicated, the distribution of the change is not so clear for subject CS, perhaps because the overall level of baseline alpha was extremely low. However, in the time series of power such as those shown in Figure 1, CS exhibited essentially the same type of suppression of alpha during the CRT and SRT tasks as the other subjects.

Plots similar to those of the baseline alpha (Figure 2b) were constructed for alpha power averaged over the interval 2500–2700 msec after presentation of the probe. The spatial variation of this *recovered alpha* is highly correlated with the plots of baseline alpha. The coefficients of correlation of two-dimensional distributions of data points between these late measures and the baseline measures are 0.98 for LK, 0.81 for BS, and 0.80 for CS.

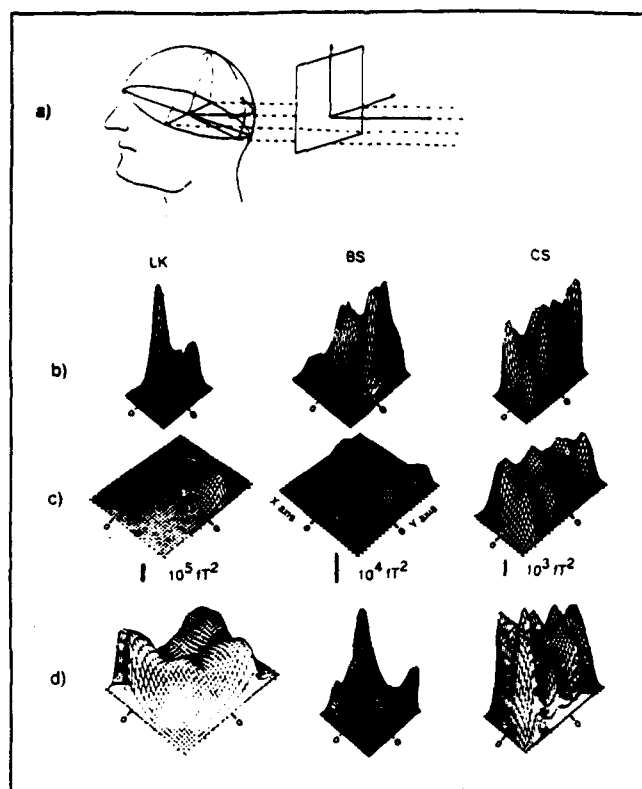


**Figure 2.** (a) Distribution of average alpha power across the posterior scalp is portrayed by an azimuthal equal distance projection, in which equal distances across the surface of the sphere from the center of projection are mapped onto equal distances across a flat surface. The  $x$  axis of this plane corresponds to a horizontal line through the inion, while the  $y$  axis is the vertical parallel to the midline. (b) Distribution for three subjects of average *baseline alpha*, defined as the average alpha power observed within a 200 msec interval 100 msec prior to presentation of the visual probe in the CRT task. The peak power for LK is about 6 cm above the inion and  $r$  4 cm to the left of midline. The peak power for BS is about the same distance above the inion and 3–4 cm to the right of midline. (c) Distribution of alpha power averaged over a 100 msec interval centered on the moment of maximum suppression, illustrated in Figure 1, defined as the *residual alpha*. The locations of the midlines are indicated by the short lines in these graphs. (d) Distribution of the ratio of residual to baseline alpha, which defines the *relative residual alpha*.

These are all significant at better than the 0.001 level and provide evidence that the initial and final distributions of alpha power are largely the same throughout the experiment.

It is sometimes taken for granted that when alpha is blocked it is replaced by beta activity (14–24 Hz) because of a presumed increase in brain “activation,” which is associated with “desynchronization.” There is no direct evidence for these assumptions, and Pfurtscheller et al. (1988) have already observed ERD associated with beta as well as with alpha rhythms. We reinforce this observation, since we were unable to detect any increase in beta in the bandwidth 16–24 Hz during suppression of alpha. In fact, there is a correlated decrease in power

within the beta band. This is illustrated in Figure 3a, where, despite its relatively low power, the beta band exhibits a suppression effect that coincides in time with that observed in the alpha band.

We examined distributions of beta activity over the same time periods that were used in analyzing the alpha data shown in Figure 2. These beta distributions are shown in Figure 3b and c. Coefficients of correlation were computed between the spatial distributions of the alpha and beta baselines (Figures 2b and 3b), and it was found that only a small percentage of the variance in the beta distributions can be accounted for by the alpha distributions of two of our subjects (29% for LK, 1% for BS). However, 60% of the variance in CS’s baseline beta distribution could be accounted for by his alpha distribution. It is noteworthy that the overall level of his beta activity nearly equalled the level of his alpha activity, a fact that distinguishes CS from all of our other subjects. In any event, at least partly independent neuronal populations must be responsible for spontaneous activity in these two bandwidths, but both populations are affected when subjects search visual memory. This is exemplified by the residual beta distribution (Figure 3c), which shows a reduction in beta power during the time of matching the probe to the members of the memory set, and by the relative residual beta distribution (Figure 3d), which shows that the suppression of beta is focused on an area over and around the midline. Again, this distribution is quite unlike the relative residual alpha distribution obtained from the same subjects at the same time.

To demonstrate that the prolonged suppression of the occipital spontaneous MEG when subjects search visual memory is specific to the task of mental imagery it is necessary to show that other kinds of mental work, e.g., scanning nonvisual memory, do not produce the same effects. Therefore, a control study was carried out with subjects instructed to determine if a probe word was or was not a member of a set of three previously seen words, or, alternatively, respond as quickly as possible with a button press regardless of whether the probe had been a member of the memory set. The words were selected from a list of abstract words that were used in another experiment (Kaufman et al. 1990). These words are rated low in imaginability. They were selected for this control experiment to minimize the possibility that subjects would try to form images of objects when rehearsing the words for identification after the probe word is presented. The numbers of items and the times of presentation were identical to the shape experiment. However, the boldface letters had a substantially larger stroke width than the widths of the lines forming the polygons of the shape experiment, and were subjectively much brighter. Also, we did not attempt to map the field patterns about the subject’s heads but simply went back to positions on the heads of our original three subjects that we had previously identified as places where the suppression effect is easily detected.

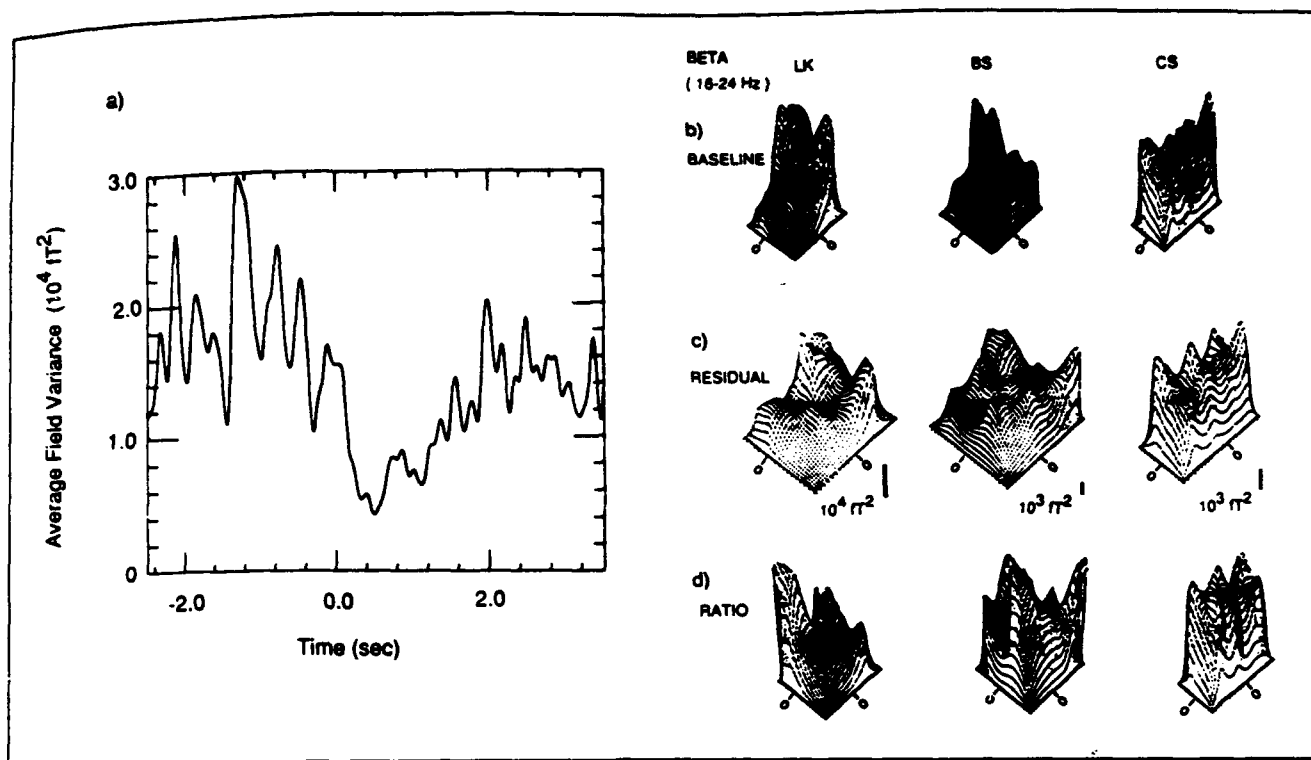


**Figure 3.** (a) The solid trace is representative of the variation in power of activity in the beta (16–24 Hz) band before and after presentation of the probe for subject LK. Note that the average power is more than an order of magnitude less than that found in the alpha band with this same subject (Figure 1b), and that the time course of the suppression is the same. (b) Distribution for three subjects of average *baseline beta* derived from filtering the MEG (16–24 Hz) over the same period of time as that used to obtain the similar plot of *baseline alpha* (Figure 2b). The correlation with the corresponding alpha distribution is quite low for LK and BS (see text). (c) Distributions of *residual beta* derived from data obtained at the same time as the distributions of *residual alpha* shown in Figure 2c. (d) Distributions of *relative residual beta* computed from the preceding two distributions. Note the maximum suppression in the region over the midlines of subject LK and BS.

The central finding of this control experiment is that the durations of suppression in both the SRT and CRT conditions were identical for all three subjects. However, the RTs in these two conditions were similar to those observed in the form experiment, i.e., the choice RT was about twice as long as the simple RT. Therefore, even though subjects engage in similar amounts of processing of the items in both experiments, the difference in processing of visual forms is related to the suppression of occipital MEG activity, while processing linguistic items is not related to differences in occipital alpha.

It may be worth noting that Kaufman et al. (1990) found that forming mental images of objects represented by words results in a period of suppression of occipital alpha that is more than twice the period of suppression found when subjects scan memory to find words that rhyme with the same or similar words.

These data support the notion that power within the alpha and beta bands is systematically reduced during the performance of a mental task involving the matching of memories of visual images. The source of this reduction appears to be in the visual cortex, a finding that is consistent with local cerebral blood flow studies (Roland and Friberg 1985). This effect depends on the mental load presented by the task, as indicated by its correspon-

dence with the RT. It cannot be attributed solely to visual attention, since visual attention is paid to the display throughout the entire time course of both the SRT and CRT tasks and there is a similar effect of selectively attended to items in our control condition, but it does not produce a differential effect on suppression duration. We conclude that areas of visual cortex are involved in this process of matching mental images.

## METHODS

The three subjects studied in detail were all males. LK (the only left-hander) was 62, BS 41, and CS 37 years of age. All had normal vision for the viewing distance to the stimuli.

The stimuli were generated by an Amiga 1000 computer and projected through a port in a magnetically shielded room by means of an Elektrohome video projector. The image was formed on a screen and reflected by a series of mirrors to be viewed by a subject sitting in a kneeling stool looking down into a mirror. This exposed the occipital and parietal areas of the subject's head so that a five-channel magnetic field sensing system (Williamson et al. 1984) could be placed near the scalp. The five detection coils of the neuromagnetometer are

arranged in the pattern of a cross, with the outer four positioned on a circle of 4 cm diameter. The array is placed near the scalp so the axes of the coils are nearly perpendicular to its surface. A specialized system (*Probe Position Indicator*, Biomagnetic Technologies, Inc., San Diego) was employed to determine the positions of the detection coils with respect to the head prior to and after each run to ensure that the head had not moved. Yamamoto et al. (1988) found that these positions could be reliably determined with an accuracy of better than 3 mm.

The subject was given 30 trials involving the SRT task, and then 30 trials involving the CRT task. This was repeated in sequence with the sensors moved to new locations until the field had been measured at 45–65 different positions in the posterior portion of the scalp, ranging from occipital through parietal areas. Each detection coil is connected to a sensor incorporating a SQUID (Superconducting QUantum Interference Device), and the voltage provided by each SQUID system is bandpassed (0.1–50 Hz) by analog filters and recorded in a computer. The average visually evoked field time locked to the stimulus onset was determined for each 30 trial run, within a bandwidth of 1–20 Hz. A similar average evoked response was obtained within the bandwidth 8–12 Hz, and the variance (which is a measure of mean square field) about this average was computed for each 30 epoch trial and smoothed by a low-pass filter at 8 Hz to determine how the average spontaneous alpha power varied with time across the epoch. A similar procedure was carried out for signals in the bandwidth 16–24 Hz to provide average spontaneous beta power. Fluctuations in power over the duration of the averaging epoch cannot be attributed to changes in coherence of the activity, but are due exclusively to changes in its amplitude, even though this activity is not time locked to the stimulus.

This method differs from that used by Pfurtscheller and his colleagues in that they simply computed the squared value of activity in the alpha band (8–13 Hz) without first removing activity time locked to the stimulus. Actually, the method we employed is based on one developed by Kaufman and Price (1967) for use with very high-frequency EEG activity, and by Kaufman and Locker (1970) who applied it to alpha-band EEG activity. In effect, Kaufman and Locker computed the variance about the mean response and used this as a measure of alpha power.

The stimulus polygons were presented as white lines against a dark background. The angular subtense of the longest segment of each of these forms did not exceed 3.5°. Three forms were presented sequentially below and to the right of fixation (about 0.5° obliquely downward from the center of a fixation cross) for 1 sec each and separated by 0.3 sec. One second after the last of the polygons, the color of the fixation cross changed from white to red, warning the subject to maintain fixation.

Two seconds later the "probe" was presented in the same place for only 100 msec.

After a response deadline of 4 sec, a tone of high pitch or of low pitch was presented to inform the subject if the probe had been a member of the previously seen set, or if it had not. Three seconds later the entire process was repeated, using a set of forms drawn at random from a total population of 12 such forms.

## DISCUSSION

An interesting property of the power measurement is that, in principle, it does not require synchronization of its neuronal sources. This differs from the averaged evoked response, which depends on the activity of its neuronal sources being time locked to some external event, e.g., a physical stimulus. We compared the phases of the alpha activity within and across single epochs and could find no signs of systematic changes in coherence within each time series, i.e., there was no evidence of a shift from synchrony to asynchrony within epochs that was time locked to the presentation of the probe. This is illustrated in Table 2, which gives the coefficients of correlation among the alpha carrier of the modulation observed in single epochs obtained at four different times. As shown in the table, these carriers are not at all correlated, and therefore their phases are independent of the onset of the probe stimulus.

Since the change in average amplitude of signals from a set of independent generators would be revealed in power measurements even when the frequency and phase of the activity of each neuronal generator are randomly related to those of the other, the measure is also immune to differences in neuronal source orientations. However, it is possible that the modulated alpha activity picked up at scalp positions that are near each other is due to the activity of locally coherent neuronal generators. To test for this we computed coefficients of correlation among the five simultaneously recorded epochs sensed by the five channels of our magnetometer. The correlation matrix is shown in Table 3. It is clear that pick-up coils with center-to-center separations of 2 cm do detect significantly coherent activity since the correlation among such coils is about 0.7. However, for more widely spaced coils, the correlation falls off precipitously. It should be noted that the recordings on which these correlations are based were made from a position where the modulation effect was very strong.

Synchronized activity from physically opposed sources would tend to be self-cancelling. However, independently oscillating neurons would give rise to alpha activity that would increase as some function of the number of neuronal sources, even if they were oriented in different directions. The magnitudes of the effects we have observed are sufficient to raise questions about the notion that alpha activity is due to the synchronization of neuronal generators, and that suppression is due to de-

**Table 2.** Correlation Matrix for Five Consecutive 7-sec Long Epochs of Data from the Same Run and Location Sensed by One MEG Probe Channel<sup>a</sup>

Correlation Matrix 8–12 Hz Data					
Epoch 1	1.0000				
Epoch 2	-0.0203	1.0000			
Epoch 3	-0.1454	0.2506	1.0000		
Epoch 4	-0.1079	-0.0284	0.0235	1.0000	
Epoch 5	-0.1532	-0.0688	-0.1829	-0.0002	1.0000
Epoch #	Epoch 1	Epoch 2	Epoch 3	Epoch 4	Epoch 5

<sup>a</sup>None of these correlations reaches significance.

**Table 3.** Correlations among 36-sec Long Epochs Measured Concurrently by Each of Five Channels<sup>a</sup>

Correlation Matrix 8–12 Hz Data across Channels					
Channel 09	1.0000				
Channel 10	0.8169	1.0000			
Channel 11	0.7616	0.6794	1.0000		
Channel 12	0.8636	0.5502	0.6730	1.0000	
Channel 13	0.8473	0.7708	0.4724	0.7491	1.0000
Channel #	09	10	11	12	13

<sup>a</sup>Data are filtered from 8–12 Hz. The pick-up coils of the channels are 1.7 cm in diameter and are separated from each other by a center-to-center distance of 2 cm. These coils are arranged in a cross-like configuration, with channel 09 at the center and the others labeled consecutively in the clockwise direction.

synchronization. Macroscopic desynchronization alone would simply not affect the magnitude of suppression revealed by the MEG, since the power measurement is itself immune to such desynchronization. Of course, this does not rule out a role in the generation of alpha for synchronized activity of neurons in close proximity to each other. But large scale coherence is obviously no longer a viable concept.

It is also interesting to note that we did not observe any systematic changes in power in the band of MEG activity below 7 Hz, while both the alpha and beta bands did display the effect. This raises some interesting questions for future research. More specifically, it may be presumed that there is a significant amount of neuronal activity associated with the scanning of visual memory. However, while that scanning is going on we report a diminution of spontaneous MEG activity, and do not see any sign of a temporally commensurate VEF. It may well be that extremely slowly changing fields, outside the bandwidth of our filters, accompany the action potentials related to the processing of information during the scanning of visual memory. We suggest that this is a suitable subject for further exploration.

Still another problem for future research concerns the role of general arousal and attention versus that of spe-

cific mental processes in affecting the level of spontaneous brain activity. It is known that general arousal may block alpha, but a maintained state of arousal does not lead to sustained blockage, since, as we have shown, the level of alpha activity is modulated over time when a mental process intervenes. Perhaps *changes* in arousal state are related to transient changes in brain activity, which reflect the brain's *readiness* to act, while steady states of arousal have less of an effect. This could well produce modulation of alpha such as we have observed, but it should be observed more widely over the scalp. Clearly, we must determine if experiments similar to those described here, but conducted in other sense modalities, produce different distributions of suppression.

#### Acknowledgments

Supported in part by Air Force Office of Scientific Research Grants F49620-88-K-0004 and F49620-86-C-0131. C. Salustri is partially supported by Associazione Italiana Ricerche Neurologiche (ARIN). We thank Arthur Robinson and John P. Snyder for advice about azimuthal equal distance projections, Jia Zhu Wang and Irene Martin for assistance with software development, and Samuel Feldman and Risto Ilmoniemi for advice about alpha rhythms.

## REFERENCES

- Andersen, P. & Andersson, S. A. (1968). *Physiological Basis of Alpha Rhythm*. New York: Appleton-Century-Crofts.
- Chapman, R. M., Ilmoniemi, R. J., Barbanera, S., & Romani, G. L. (1984). Selective localization of alpha from brain activity with neuromagnetic measurements. *Electroencephalography and Clinical Neurophysiology*, *58*, 569-572.
- Farah, M. (1988). Is visual imagery really visual? Overlooked evidence from neuropsychology. *Psychological Review*, *95*, 307-317.
- Farah, M., Perronnet, F., Weisberg, L. L., & Perrin, F. (1988). Electrophysiological evidence for shared representational medium for visual images and visual percepts. *Journal of Experimental Psychology: General*, *117*, 248-257.
- Ilmoniemi, R. J., Williamson, S. J., & Hostetler, W. E. (1988). New method for the study of spontaneous brain activity. In K. Atsumi, M. Kotani, S. Ueno, T. Katila, & S. J. Williamson (Eds.), *Biomagnetism '87*. Tokyo: Tokyo Denki Univ. Press, 182-184.
- Jahnsen, H. & Llinás, R. (1985). Ionic basis for electroresponsiveness and oscillatory properties of guinea-pig thalamic neurons in vitro. *Journal of Physiology (London)*, *349*, 227-247.
- Kaufman L. & Locker, Y. (1970). Sensory modulation of the EEG. *Proceedings of the American Psychological Association, 75th Meeting*, pp. 179-180.
- Kaufman, L. & Price, R. (1967). The detection of cortical spike activity at the human scalp. *IEEE Transactions of Biomedical Engineering, BME-14*, 84-90.
- Kaufman, L., Glanzer, M., Cycowicz, Y., & Williamson, S. J. (1990). Visualizing and rhyming cause differences in alpha suppression. In S. J. Williamson, G. Stroink, & M. Kotani (Eds.), *Proceedings of the 7th International Conference on Biomagnetism*. NY: Plenum, 241-244.
- Klimesch, W., Pfurtscheller, G. & Muhl, W. (1988). Mapping and long-term memory: The temporal and topographical pattern of cortical activation. In G. Pfurtscheller & F. H. Lopes da Silva (Eds.), *Functional Brain Imaging*. Toronto: Hans Huber, 131-142.
- Kosslyn, S. N. (1983). *Ghosts in the Mind's Machine*. New York: Norton.
- Leissner, P., Lindholm, L.-E., & Petersen, I. (1970) *Electroencephalography and Clinical Neurophysiology*, *29*, 392-399.
- Lopes da Silva, F. H. & van Leeuwen, S. (1978). The cortical alpha rhythm in dog: The depth and surface profile in phase. In M. A. B. Brazier & H. Petsche (Eds.), *Architectonics of the Cerebral Cortex*. New York: Raven Press, 319-333.
- Maclin, E. (1983). Unpublished Ph.D. dissertation, New York University.
- Maruzzi, G. & Magoun, H. W. (1949). Brain stem reticular formation and activation of the EEG. *Electroencephalography and Clinical Neurophysiology*, *1*, 455-473.
- Pfurtscheller, G. & Aranabar, A. (1977). Event-related cortical desynchronization detected by power measurements of scalp EEG. *Electroencephalography and Clinical Neurophysiology*, *42*, 817-826.
- Pfurtscheller, G. (1988). Mapping of event related desynchronization and type of derivation. (1988). *Electroencephalography and Clinical Neurophysiology*, *70*, 190-193.
- Pfurtscheller, G., Steffan, J., & Maresch, H. (1988). ERD-mapping and functional topography—temporal and spatial aspects. (1988). In G. Pfurtscheller & F. H. Lopes da Silva (Eds.), *Functional Brain Imaging*. Toronto: Hans Huber, 117-130.
- Pylshyn, Z. W. (1981). The imagery debate: Analogue media versus tacit knowledge. *Psychological Review*, *88*, 16-45.
- Roland, P. E. & Frieberg, L. (1985). Localization of cortical areas activated by thinking. *Journal of Neurophysiology*, *53*, 1219-1243.
- Sakakura, H. (1968). Spontaneous and evoked unitary activities of cat lateral geniculate neurons in sleep and wakefulness. *Japanese Journal of Physiology*, *18*, 23-42.
- Shepard, R. N. & Metzler, J. (1971). Mental rotation of three-dimensional objects. *Science*, *171*, 701-703.
- Shepard, R. N. & Cooper, L. A. (1982). *Mental Images and Their Transformations*. Cambridge, MA: MIT Press.
- Slatter, K. H. (1960). Alpha rhythms and mental imagery. *Electroencephalography and Clinical Neurophysiology*, *12*, 851-859.
- Steriade, M. (1981). Mechanisms underlying cortical activation: Neuronal organization and properties of the midbrain reticular core and intralaminar thalamic nuclei. In O. Pompeiano & C. Ajmone-Marsan (Eds.), *Brain Mechanisms of Perceptual Awareness and Purposeful Behavior*. New York: Raven Press, 327-377.
- Sternberg, S. (1966). High speed scanning in human memory. *Science*, *153*, 652-654.
- Sternberg, S. (1969). Memory scanning: Mental processes revealed by reaction time experiments. *American Scientist*, *57*, 421-457.
- van Rotterdam, A., Lopes da Silva, F. H., van den Ende, J., Viergever, M. A., & Hermans, A. J. (1982). A model of the spatial-temporal characteristics of the alpha rhythm. *Bulletin of Mathematical Biology*, *44*, 283-305.
- Vvedensky, V. L., Ilmoniemi, R. J., & Kajola, M. S. (1986). Study of the alpha rhythm with a SQUID magnetometer. *Medical & Biological Engineering & Computing*, *23*, 11-12.
- Williamson, S. J. & Kaufman, L. (1981). Magnetic fields of the cerebral cortex. In S. N. Erné, H. D. Hahlbohm, & H. Lubbig (Eds.), *Biomagnetism*. Berlin: Walter de Gruyter, 353-402.
- Williamson, S. J., Pelizzone, M., Okada, Y., Kaufman, L., Crum, D. B., & Marsden, J. R. (1984). Five channel SQUID installation for unshielded neuromagnetic measurements. In H. Weinberg, G. Stroink, & T. Katila (Eds.), *Biomagnetism: Applications and Theory*. New York: Pergamon, 46-51.
- Yamamoto, T., Williamson, S. J., Kaufman, L., Nicholson, C., & Llinás, R. (1988). Magnetic localization of neuronal activity in the human brain. *Proceedings of the Academy of Sciences USA*, *85*, 8732-8736.

VISUALIZING AND RHYMING CAUSE DIFFERENCES IN ALPHA SUPPRESSION

L. Kaufman, M. Glanzer,\* Y.M. Cycowicz, and S.J. Williamson

Neuromagnetism Laboratory,  
Departments of Psychology and Physics and Center for Neural Science  
\*Department of Psychology  
4 Washington Place, New York University, New York, NY 10003, U.S.A.

INTRODUCTION

The alpha rhythm of the EEG is strongest over the occipital region, and the visual cortex is apparently a major contributor (Chapman et al., 1984; Vvdensky et al., 1987; Williamson, et al., 1989). Since behavioral evidence suggests that the visual cortex may also be involved in mental imagery (cf. Shepard and Metzler, 1971), we set out to determine if forming mental images produces changes in the occipital alpha rhythms of the MEG. It has been demonstrated that scanning memory for visual forms causes changes in alpha activity originating in visual cortex (Kaufman, Schwartz, Salustri, and Williamson, 1989). However, this study did not control for a possible effect of mental effort *per se*, since scanning visual memory was compared only with a condition in which subjects merely responded as soon as they saw a visual form. To prove that changes in alpha accompanying the processing of visual images is due to such processing and not to mental effort, it is necessary also to provide a non-visual cognitive task that is approximately as difficult as that of forming mental images.

There are precedents for this type of experiment. For example, visual imagery is accompanied by changes in occipital alpha activity of the EEG (Golla, et al., 1943), but performance of a language-related task does not have so apparent an effect (Slater, 1960). However, the use of non-visual tasks, e.g., memorization and classifying words, may affect the alpha activity (Pfurtschuller, 1988), so it is unclear that changes in alpha activity provides an unambiguous indication of processes entailing mental imagery.

Farah (1988) presented words to subjects who responded either by forming mental images of objects represented by the words, or by simply reading them. This did result in a difference in amplitudes of the occipital event related potentials elicited by the words, but the number of electrodes used in this study was not sufficient to permit identification of the location of the sources of the potential changes.

Using cerebral blood flow (CBF) techniques, Roland and Friberg (1985) found extensive activation of posterior regions of the brain during mental imagery, but no increase in CBF when subjects did mental arithmetic or engaged in a cognitive task entailing the scanning of memory to determine if tones had been previously heard. Since suppression of alpha originating in the occipital cortex accompanies the search of visual memory (Kaufman, et al. 1989), we sought in this experiment directly to compare the effects of forming mental images of objects represented by words with those of finding words in memory that rhyme the same visual presented words. The hypothesis tested is that forming rhymes of visually presented words will affect alpha suppression differently than does forming a mental image.

## METHODS

Our word stimuli were drawn from a large population of words composed of words that represent easily imaged objects and also abstract words which subjects find difficult to respond to by forming images. On each trial subjects saw 24 sequentially presented words. These were constructed from the master list and were composed either of all imageable words or half imageable words and half abstract words. The latter were used in trials where subjects had to search their memories and find words that rhymed with the presented words. Alternatively, when viewing all imageable words subjects were instructed to form mental images of the objects represented by the words. Since only 12 of the 24 words used in the rhyming task were imageable, subjects were exposed to twice as many rhyming trials as imaging trials. By combining 12 responses (corresponding to 12 imageable words) from each of two rhyming trials, we were able to determine if imageable words produce different responses under the two different conditions. Subjects pressed a button to indicate when they had either formed an image or found a rhyme. Finally, subjects were also shown lists of 24 nonsense words to which they responded by pressing a button as soon as they were seen. Comparing the reaction times (RTs) in the imaging and rhyming task permits assessment of the relative difficulties of the two tasks as compared to the simpler control task of merely observing the appearance of a nonsense word.

The word stimuli were generated by an Amiga 100 computer and projected by an Electrohome video projector onto a screen in a magnetically shielded room. Subjects inside the room maintained fixation on a point on the screen which was reflected by mirrors to the subject. The words were presented 7 sec apart for 200 msec each.

Subjects were seated on a kneeling stool and leaned forward with their heads on a vacuum cast while they looked downward into a mirror to see the screen. A probe containing a 5-sensor SQUID-based Neuromagnetometer<sup>®</sup> (Biomagnetic Technologies, inc.) was placed at the occipital area of the scalp over the right or left hemisphere near the region where alpha rhythm is strongest. The five detection coils detected the field at five different places normal to the posterior portion of the head.

With the coils placed near the scalp the subject performed the rhyming task for two blocks of stimuli, then they performed the imaging task, and finally, the control task both for only one block of stimuli. Measurements of the MEG were recorded for 6 seconds for each word stimulus, beginning 2 seconds before the stimulus appeared and extending 4 seconds afterwards. This was followed by one more second with no recording to provide a total interstimulus interval of 7 seconds. The outputs of all five channels of the SQUID electronics were bandpass filtered from 0.1-50 Hz and then applied to an HP 9000 model 350 computer for analysis. Also, RTs corresponding to the time of button press were stored for each trial, and then averaged later within each experimental condition.

All epochs were digitally bandpassed from 8 to 12 Hz before computing the average response and the variances about the averages. The variance represents brain activity that is not coherently related to the presentation of the visual stimulus. The variance is actually the power (mean square field) of the spontaneous activity in the alpha band. Thus we will use the term 'alpha power' to describe the results.

Four young adult subjects, two female and two male, served in this experiment.

## RESULTS

Figure 1 shows alpha power as a function of time for the three conditions: imaging task with imageable words, rhyming task with imageable and non-imageable words, and control task with the nonsense words. The suppression of alpha in all cases started at the time of word presentation. In general, there is a short-lived (about 0.5 sec) suppression of alpha under all conditions. However, this initial suppression effect is supplemented, in the imaging condition only, by an additional period (about 1 sec) of suppression. The initial effect may be related to a shift in generalized arousal level, while the supplementary suppression probably reflects the role of visual cortex in forming images. Although rhyming is also a cognitive act, there is no suppression of occipital alpha other than described here as the initial suppression effect. This same effect is present in the control condition.

The foregoing results are generally true for all four subjects. However, there were strong individual differences in the average magnitude of alpha activity across subjects as well as positions at which the field was measured. The latter differences among probe recording positions over the occipital scalp reflected both differences in alpha power as a function of probe position, and also

differences in the magnitude of suppression, which was strongest in the vicinity of the midlines of all subjects. The difference in the magnitude of the suppression between positions is related to the distance between the detection coil and the "source" whose activity is suppressed when subjects form images. It is evident that RTs for the imaging and rhyming tasks are essentially the same for all subjects, while the RT for the control task is about one half of the for the other two tasks. This is offered as evidence for the approximately equal difficulty of the rhyming and imaging tasks.

Mean Reaction Time (sec)

Subject	Imaging	Rhyming	Control
STF	0.958	1.740	0.686
LS	1.490	0.876	0.575
JB	1.176	1.177	0.582
BOR	1.085	1.139	0.663

Since the duration of suppression in the rhyming task is short as compared with that for the imaging task, and that the RT is comparable to that of the imaging task, it is clear that changes in occipital alpha reflect only the effects of imaging, and do not reflect the language-related rhyming task. Assuming that both rhyming and imaging require about the same amount of attentional effort, we also conclude that the prolonged suppression of alpha during imaging is not due to changing levels of attention.

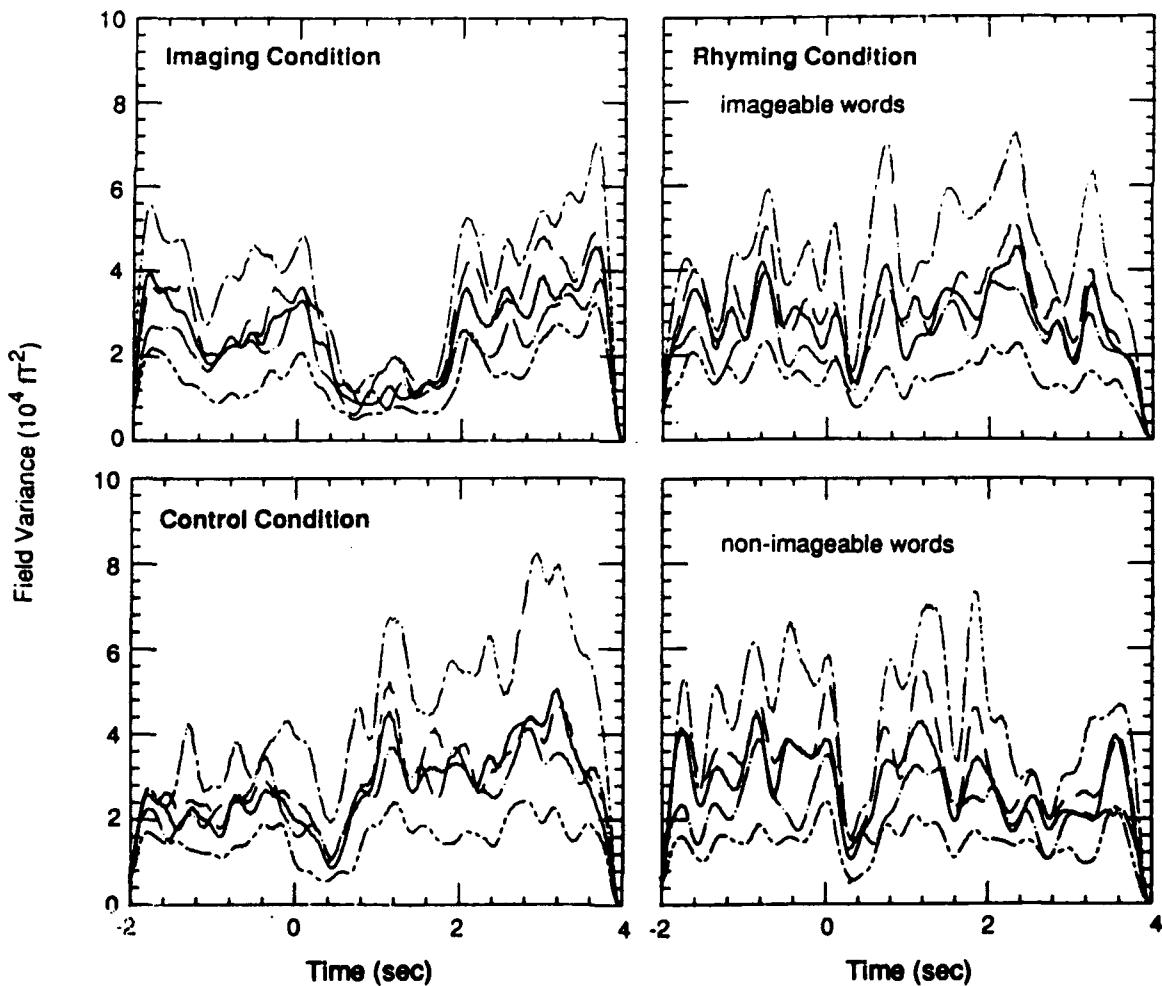


Fig. 1. Alpha power of subject LS for the three conditions. The five curves in each condition represent the five sensors. At time zero the word stimuli appears on the screen.

## CONCLUSIONS

We have found that power within the alpha band is reduced when subjects form mental images. Since Kaufman et al. (1989) showed that activity of sources in visual cortex is suppressed when visual memory is scanned, it is possible that visual cortex is also affected during the imagery task of the present study. Two different processes are apparently involved. These are the so-called *initial effect*, and the subsequent prolonged suppression associated with imagery. The initial effect appears to be a general process, since it accompanies all tasks, but the second order prolonged effect may be modality specific.

We also conclude that alpha suppression is not due to attentional differences since we assume that in both cases, imaging and rhyming, the subject has to attend in order to perform the tasks. The fact that prolonged suppression occurs only for imaging tasks is consistent with the conjecture, which we are now testing, that language related tasks have effects similar to that describe for imagery here, but occurring elsewhere in the brain.

## ACKNOWLEDGEMENTS

We thank B. Schwartz for his assistance with this project. This research is supported in part by Air Force Office of Scientific Research Grants F49620-88-K-004 and F49620-86-C-0131.

## REFERENCES

- Chapman, R.M., Ilmoniemi, R., Barbanera, S., and Romani, G.L. (1984). Selective localization of alpha from brain activity with neuromagnetic measurements. *Electroenceph. clin. Neurophysiol.* 58, 569 - 572.
- Fara, M.J. (1988). Is visual imagery really visual? Overlooked evidence from neuropsychology. *Psychological Review* vol 95: 307-317
- Golla, F., Hutton, E.L., and Gray Walter, W.G. (1943). The objective study of mental imagery. I. Physiological concomitants. *J. Mental Sci.* 75, 216-223.
- Kaufman L., Schwartz B., Salustri C., Williamson S.J. (1989). Modulation of spontaneous brain activity during mental imagery. *submitted for publication.*
- Pfurtscheller, G. Steffean, J. Naresch, H. (1988). ERD mapping and functional topography: Temporal and spatial aspects. In: Pfurtscheller, G. and Lopes da Silva, F.H., Ed., *Functional Brain Imaging*, Hans Huber Publishers, pp. 117-130.
- Roland, P.E. and Frieberg, L. (1985). Localization of cortical areas activated by thinking. *J. of Neurophysiology*, 53, 1219-1243.
- Shepard, R.N., and Meltzer, J. (1971). Mental rotation of three-dimensional objects. *Science*, 171, 701-703
- Slatter, K.H. (1960). Alpha rhythm and mental imagery. *Electroenceph. clin. Neurophysiol.* 12, 851-859.
- Vvedensky V.L., Guntovoy, K.G., Ilmoniemi R.J., and Kajola M. (1987). Determination of the sources of the magnetic alpha rhythm of man. *Human physiology* 13, 934-939 [in Russian].
- Williamson, S.J., Wang, J-Z., and Ilmoniemi, R.J. (1989). Method for Locating Sources of Human Alpha Activity. This conference.

*Advances in Biomagnetism*

S.J. Williamson, M. Hoke, G. Stroink, and M. Kotani, Editors  
Plenum Press, New York  
Pages 257 - 260

## METHOD FOR LOCATING SOURCES OF HUMAN ALPHA ACTIVITY

S.J. Williamson, J.-Z. Wang, and R.J. Ilmoniemi\*

Neuromagnetism Laboratory, Departments of Physics and Psychology and  
Center for Neural Science, New York University, New York, NY 10003, U.S.A.

\*Low Temperature Laboratory, Helsinki University of Technology  
02150 Espoo, Finland

## INTRODUCTION

Alpha activity is commonly defined as electrical fluctuations between 8 and 13 Hz that can be detected on the occipital scalp and are attenuated by visual stimuli. While projections from brain stem play a role in its generation (c.f. Steriade and Llinás, 1988), evidence for the cortical origin of these electrical signals has been obtained from studies of potentials at various depths within the cortex of animals. Lopes da Silva and van Leeuwen (1978) suggest that alpha sources originate in different epicenters from which activity spreads across cortex in several directions. Previous magnetic studies on humans of the covariance between the EEG and magnetic recordings with a single sensor indicate sources deep within the occipital lobe (Carelli et al., 1983). Studies with a four-sensor system (Vvedensky, Ilmoniemi, and Kajola, 1986) indicate that there are time series of the rhythm lasting for typically 1 sec during which the oscillation period is constant. We call these time series *spindles*, whether or not occurring in the sleeping state. Ilmoniemi, Williamson, and Hostetler (1988) using a 14-sensor system found that the magnetic field pattern during a spindle appears relatively stable, indicating that its source is a specific configuration of neurons. Moreover, an analysis of the time-invariant spatial pattern based on a 14-dimensional signal space indicates it is possible to distinguish between most of the sources of the observed spindles. In other words, the human alpha rhythm represented by the spindles is generated by a large number, or possibly a continuum, of different source configurations. We introduce the term *alphon* for the neuronal excitation producing a spindle. The purpose of the present study is to develop a technique to determine the locations in the human brain of alphas and to characterize the orientation and strength of their equivalent current dipole moments.

## METHODS

Two dewars, each containing seven dc-SQUID sensors (Biomagnetic Technologies, inc.) were positioned over the left and right occipital areas to record magnetic activity. The detection coils were second-order gradiometers with 1.5-cm diameter and 4-cm baseline, and the sensor noise level was about 20 fT/ $\sqrt{\text{Hz}}$  for most channels, while one or two exhibited noise as high as 50 fT/ $\sqrt{\text{Hz}}$ . Individual sensors were calibrated with a relative accuracy of better than 1%. With the subject prone and alert, recordings within the bandwidth 0.5-50 Hz were made for 16-sec epochs of spontaneous activity with eyes closed. The total level of instrument and subject noise was determined with eyes open. Data were digitally filtered in the bandwidth 8-13 Hz, and a computer routine was used to spot those segments of the time-series where the rms amplitude within the middle 12 seconds of the epoch significantly exceeds the noise level.

A spindle was defined by a time-series where signals in all the sensors are coherent and can be attributed to a single source. The criteria were: (1) the peak rms amplitude averaged across 14 sensors exceeds 500 fT; (2) this mean amplitude across sensors exceeds 200 fT for at least 3 oscillations before and after the peak; (3) the period between zero crossings is stable to within 5% throughout the duration; and (4) field polarity reverses between the two probes, to ensure that the source lies somewhere between them. To ensure accuracy in locating each alphon, it was important to achieve a high signal-to-noise ratio, because only a small area of the field pattern is measured. By positioning the probes so that field extrema of the individual spindles are close by, the source positions in three dimensions can be determined without need to move the dewars. The accuracy of this "fixed position" technique when probes are placed directly over the extrema has been analyzed by Costa Ribeiro et al. (1988) who considered the cases of a single probe with 5 or 7 sensors and two probes with 7 sensors each. However, this is the ideal situation, since determining the positions and fields of the two extrema is sufficient to determine all 5 dipole parameters (Williamson and Kaufman 1981). If both extrema are not within the areas of the probes, accuracy in location greatly diminishes. Therefore it was essential to maximize the signal-to-noise ratio, and so the best estimate for the mean amplitudes of each spindle was obtained from elements of the covariance matrix computed across the time-series of the spindle.

Positions and orientations of individual sensors relative to a head-based cartesian coordinate system was determined by the Probe Position Indicator (PPI) method (Buchanan et al. 1987). This system is indexed to the periauricular points and nasion, with the origin placed midway between the former. This method, together with data from the 14-sensor system, has been shown to provide 3-mm accuracy in determining the location of a current dipole at a depth of about 4 cm in a conducting sphere, model head, and human auditory cortex (Yamamoto et al., 1988). The set of 14 mean values for each spindle was used to determine the location of the current dipole best representing its source, using a minimum chi-square criterion. The subject's head was modeled as a sphere, whose center of curvature was determined by digitizing the shape of the occipital and parietal areas of the scalp using PPI and determining the least-squares fit with a sphere. Preliminary studies indicated that strongest spindle amplitudes were detected with the probes placed over right and left occipital scalp, about 4-8 cm above the inion and displaced symmetrically by about 6-8 cm to left and right of the midline. Signals were generally very weak directly over the midline or farther than 9 cm to either side of the midline, in agreement with measures of relative covariance (Carelli et al., 1983; Chapman et al., 1984). Strong alpha rhythm generally exhibited field extrema of opposite polarity over left and right hemisphere, indicating that the corresponding alphons lie near the midline. Each alphon was modeled by a current dipole, so its center of activity could be characterized by 5 parameters specifying location, orientation in the plane tangent to the sphere, and strength.

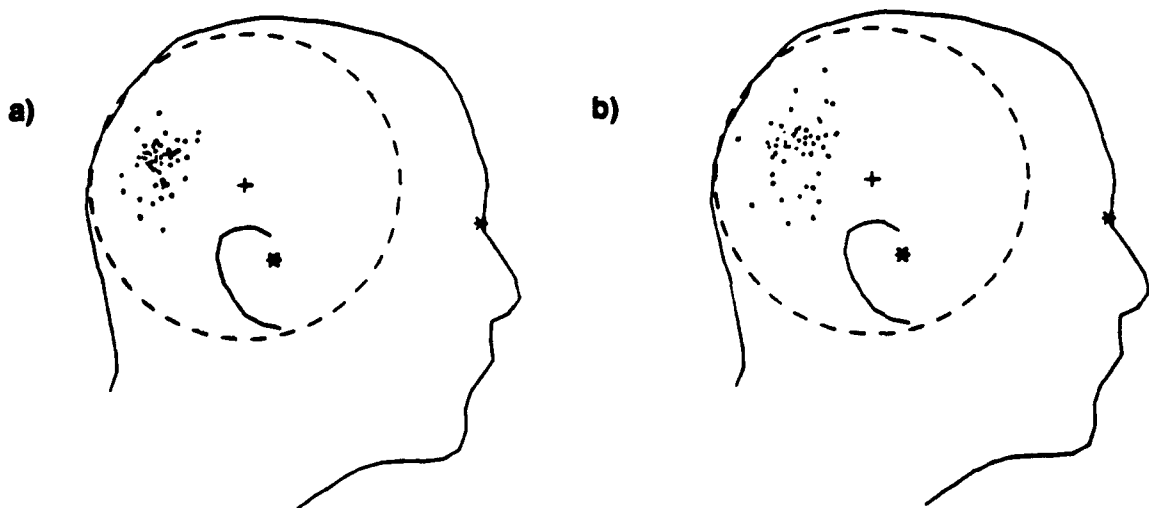


Fig. 1. Sagittal view of deduced alphon positions for those producing spindles with (a) one field extremum lying within the area of a probe and (b) neither extremum lying within the area of a probe. Nasion and periauricular points: \* ; center of sphere model for posterior head: +; subject: S.

We found that the variety of alphas for a given subject was so diverse that very few of the spindles provided extrema that simultaneously appeared within the areas of the two probes. This remained true when the probes were placed at various asymmetrical positions over left and right hemispheres with one further from the inion or midline than the other. The deduced positions for a set of about 100 alphas of a subject are shown in Fig. 1, where those providing an extremum within the area of one probe (a) are compared with a nearly equal number whose extrema lie outside (b). The greater scatter in the latter case is due in part by less accuracy in localization. The uncertainty in position (95% confidence) for the former case is typically about 0.8 cm in radial position and 1.3 cm in distance above the midline. Most alphas lie within 2 cm of the midline. Similar results were obtained for a second subject. Measurements over many days produced on the average 1-2 spindles meeting the criteria during each 12-second analysis period. These source positions are in a tighter cluster and lie much shallower than the average positions estimated on the basis of relative covariance measurements (Carelli et al., 1983; Chapman et al., 1984). Visual inspection of our time-series showed on the order of 5 times more spindle features that did not meet our present criteria for defining a spindle.

The deduced dipole orientations were generally within 30 deg of the longitudinal fissure (Fig. 2a). When probes were placed on either side of the midline so the line joining them makes an angle of 45 deg with the midline, spindles could not be detected. This justifies our primary reliance on data obtained with the probes placed above the inion at the same distances, or at distances differing by no more than 5 cm. Since extracranial magnetic fields arise from intracellular currents, the source of the field most likely is an aligned population of cortical neurons. The most conspicuous preferentially aligned population is that of the pyramidal cells. In this case the orientation of the current dipoles indicates that alphas are largely confined to the floor and/or ceiling of the calcarine fissure, which is aligned approximately perpendicular to the longitudinal fissure. The few dipoles tipped as much as 20 deg may well have contributions from neurons in the longitudinal fissure as well. We cannot rule out the possibility that alphas also occur within the parietal-occipital fissure. Indeed, the fact that many are located rather high above the inion suggests this to be the case.

The remaining parameter of interest is alphon strength. Fig. 2b illustrates the distribution of current dipole moment for about 100 alphas. A remarkable feature is that all of the alphas have similar strengths, with a typical rms moment of about 40 nA-m. The cutoff of the distribution at low strengths may be influenced in part by our minimum-field criterion for identifying a spindle. This effect merits additional study, but in any event the narrowness of the distribution argues that the alphon is a characteristic excitation, involving about the same number of neurons no matter where it occurs. The deduced alphon strength is sensitive to the choice for the center of curvature of the sphere modeling the posterior head. If the midpoint between the periauricular points is used

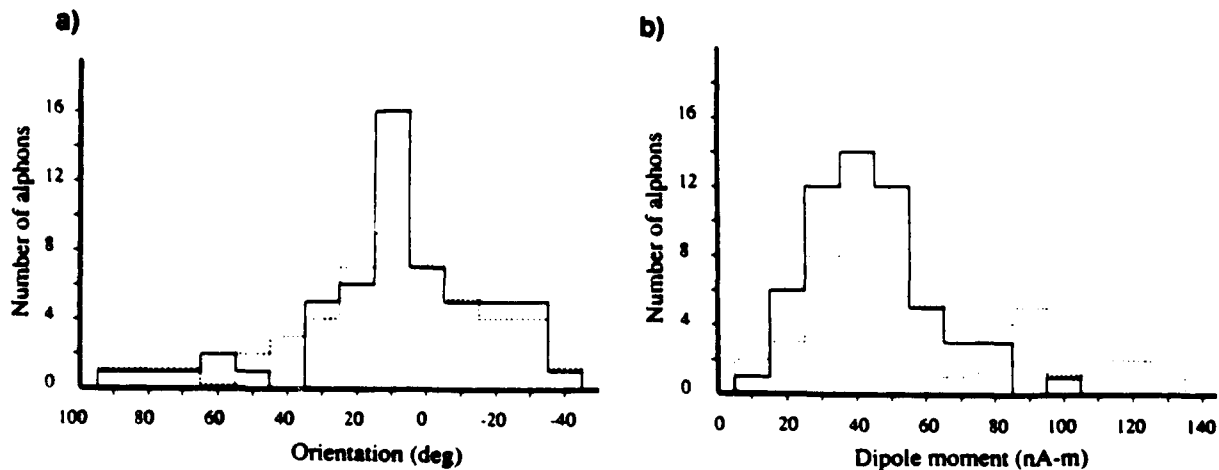


Fig. 2. a) Distribution of alphon orientation in the tangent plane, with positive angles measured clockwise from the inion-vertex line. b) Distribution of alphon strength. Solid curves describe about 50 alphas where an extremum lies within the area of a probe, dashed curve about 50 where an extremum does not. Subject: S.

instead, the amplitude decreases to about 20 nA·m.

An alphon strength of 40 nA·m is only an order of magnitude stronger than a typical sensory evoked response. Considering estimates for postsynaptic currents in pyramidal cells, an area of cortex of only a few square millimeters, corresponding to  $10^5$  coherently active pyramidal cells, is required to account for an alphon. This area is considerably smaller than deduced on the basis of the cited relative covariance measurements, but is consistent with electrophysiological studies (Lopes da Silva and van Leeuwen, 1978).

## CONCLUSION

The picture that emerges from this work is that magnetic alpha rhythm arises from many discrete sources oscillating one after another, and occasionally overlapping temporally. Alphons giving rise to the observed activity are clustered near the midline, extending to a depth of several centimeters. Dipole orientations are nearly parallel to the longitudinal fissure indicating that the underlying neuronal activity is largely confined to cortical areas within calcarine fissure or perhaps parietal-occipital fissure. Deduced source strengths are consistent with each alphon extending across only a few square millimeters of cortical area.

## ACKNOWLEDGEMENTS

We thank Dr. D.S. Buchanan for calibrating the sensors, P. Fusco for technical help, and L. Kaufman and D. Brenner for helpful discussions. The work was supported in part by Air Force Office of Scientific Research Grants F49620-86-C-0131 and F49620-88-K-00004.

## REFERENCES

- Buchanan, D.S., Paulson, D., and Williamson, S.J., 1987, Instrumentation for clinical applications of neuromagnetism, in: *Advances in Cryogenic Engineering, Vol. 33*, Fast, R.W., Ed., Plenum Press, New York, pp. 97-106.
- Carelli, P., Foglietti, V., Modena, I., and Romani, G.L., 1983, Magnetic study of the spontaneous brain activity of normal subjects, *Il Nuovo Cimento* 2D, 538-546.
- Chapman, R.M., Ilmoniemi, R.J., Barbanera, S., and Romani, G.L., 1984, *Electroenceph. clin. Neurophysiol.* 58, 569-572.
- Costa Ribeiro, P., Williamson, S.J., and Kaufman, L., 1988, SQUID arrays for simultaneous magnetic measurements: calibration and source localization performance. *IEEE Trans. Biomed. Engr.* BME-35, 551-560.
- Ilmoniemi, R.J., Williamson, S.J., and Hostetler, W.E., 1988, New Method for the study of spontaneous brain activity, in: *Biomagnetism '87*, Atsumi, K., Kotani, M., Ueno, S., Katila, T., and Williamson, S.J., Eds., Tokyo Denki University Press, pp. 182-185.
- Lopes da Silva, F.H., and Storm van Leeuwen, W., 1978, The cortical alpha rhythm in dog: the depth and surface profile of phase, in: *Architectonics of the Cerebral Cortex*, Brazier, M.A.B., and Petsche, H., Eds., Raven Press, New York, pp. 319-333.
- Steriade, M., and Llinás, R.R., 1988, The functional states of the thalamus and the associated neuronal interplay, *Physiol. Revs.* 68, 649-742.
- van Rotterdam, A., Lopes da Silva, F.H., van den Ende, J. Viergever, M.A., and Hermans, A.J., 1982, A model for the spatial-temporal characteristics of the alpha rhythm, *Bull. Math. Biol.* 44, 283-305.
- Vvedensky, V.L., Ilmoniemi, R.J., and Kajola, M.L., 1986, Study of the alpha rhythm with a 4-channel SQUID magnetometer, *Med. & Biol. Eng. & Computing* 23, Suppl. Part 1, 11-12.
- Williamson, S.J., and Kaufman, L., 1981, Evoked cortical magnetic fields, in: *Biomagnetism*, Erné, S.N., Hahlbohm, H.-D., and Lübbig, H., Eds. de Gruyter, Berlin, pp. 353-402.
- Yamamoto, T., Williamson, S.J., Kaufman, L., Nicholson, C., and Llinás, R., 1988, Magnetic localization of neuronal activity in the human brain, *Proc. Natl. Acad. Sci. USA* 85, 8732 - 8736.

EEG 90130

## On cortical folds and neuromagnetic fields

Lloyd Kaufman<sup>a</sup>, James H. Kaufman<sup>b,\*</sup> and Jia-Zhu Wang<sup>a</sup>

<sup>a</sup> New York University and <sup>b</sup> IBM Research, 14-1 Watson Research Center, New York, NY (U.S.A.)

(Accepted for publication: 11 January 1991)

**Summary** A folded cortical source of neuromagnetic fields, similar in configuration to the visual cortex, was simulated. Cortical activity was modelled by different distributions of independent current dipoles. The map of the summed fields of the dipoles of this cruciform model changed, depending upon the statistical distribution of the electrical activity of the dipoles and its geometry. Arrays of dipoles of random orientations and strengths produced field patterns that could be interpreted as due to moving neural currents, although the geometry of the neural tissue remained unchanged and the average activity remained approximately constant. The field topography at any instant was apparently unrelated to the depth or orientation of the underlying structure, thus raising questions about how to interpret topographic MEG and EEG displays. Furthermore, asynchronous activity (defined as independent directions and magnitudes of activity of the dipoles) did not result in less field power than when the dipoles were synchronized, i.e., when the direction of current flow was correlated across all of the dipoles within the cruciform structure. Therefore, in this model 'alpha blockage' cannot be mimicked by desynchronization.

More generally, for the cruciform or any other symmetrically folded and active cortical sheet, 'blockage' cannot be attributed to desynchronization. The same is true for the EEG except that smooth unfolded sheets of radially oriented dipoles would result in enhancement of voltage due to synchronization. Such radial dipoles do not contribute to the MEG.

Blockage was simulated by reducing the amount of activity within different portions of the synchronized cruciform model. This resulted in a dramatic increase in the net field because attenuation broke the symmetry of the synchronized cruciform structure. With asynchronous dipoles populating the structure, the attenuation of the same portion of the structure had no easily discerned effect on the net field. However, maps of average field power were consistently related to the position of the region of attenuated activity. The locations of regions of attenuated activity were determined by taking the difference between the mean square field pattern obtained when all portions of the cruciform structure were active and the pattern obtained when a portion of the structure was relatively inactive. When activity of the same portions were incremented rather than attenuated, the resulting plot of average power was essentially the same as that of the attenuated portion derived by taking these differences between power distributions.

The major conclusions are that the concepts of synchronization and desynchronization have no explanatory power unless the physical conditions under which they occur are specified precisely. Also, we explain why changes in spontaneous activity of cortex associated with changes in cognitive states cannot be detected simply by averaging event-related brain activity. However, averaging field power (as opposed to field) does recover task-related *modulation* of brain activity. The fact that modulation of the spontaneous activity of specific parts of the brain may be detected and localized on the basis of external field measurements raises the exciting possibility that MEG can be used in functional brain imaging similar to PET.

**Key words:** Magnetoencephalography; Dipole; Synchronization; Field power

The position, orientation and strength of a neural generator of extracranial magnetic fields can often be determined even when the electrical properties of the head are totally ignored. This capability of magnetoencephalography (MEG) is realizable when neural generators are modeled as *current dipoles*. Using the same basic model, when electroencephalographic (EEG) data are used to compute the location of a neural generator, it is extremely important that the electrical properties of the head be taken into account (Fender 1987).

To illustrate the efficacy with which sources may be located using MEG data, consider the experiments by Weinberg et al. (1986) and by Yamamoto et al. (1988) in which a small current source was placed within a plastic skull filled with a conducting solution. Using MEG measures, in both experiments this current dipole was located with a 3-dimensional accuracy of about 3 mm. This is the same accuracy Yamamoto et al. obtained when the source was placed within a simple plastic sphere, thus demonstrating that irregularities in skull shape may have little effect when using the MEG for source localization. Yamamoto et al. also located the equivalent current dipole source of the magnetic counterpart to the N100 component of the auditory evoked potential within 3 mm of the center of the cortical layer forming the floor of the lateral sulcus

\* Now at IBM Almaden Research Center, San Jose, CA, U.S.A.

Correspondence to: Dr. L. Kaufman, Dept. of Psychology and Neural Science, New York University, 6 Washington Place, New York, NY 10003 (U.S.A.).

near Heschl's gyrus, suggesting that the same accuracy holds even in the presence of the complicated electrical milieu of active neural tissue. Baumann et al. (1989) attained an accuracy of better than 5 mm in a similar experiment, and Rose et al. (1989) report similar accuracies in locating current dipoles implanted in the inferior frontal region of a patient's brain. Barth et al. (1986) found that the accuracy with which such a source can be located in the skull of a cadaver is largely unaffected when its electrical environment is drastically altered as, for example, by making a large hole in the skull. By contrast, such localized inhomogeneities within the medium surrounding active neural tissue have an extremely strong effect on locating sources of EEG activity (Nunez 1981).

The evidence for the relative efficacy of source localization using the MEG is from experiments and analyses in which the 'source' can be well represented by a single equivalent current dipole, e.g., a clump of simultaneously active neurons of small extent relative to the distance at which its field is measured. In this paper we shall show that there are instances in which it is necessary to consider effects of convoluted source configurations, even when they are relatively small, as their field patterns strongly depend upon their geometry, and also the states of the individual oscillators at any instant of time.

In practice, the use of the single current dipole model appears to work very well in accounting for unitary components of evoked responses. It is also useful in theoretical problems, e.g., where the neural generator is modeled as a line composed of current dipoles lying end-to-end (Wikswa and Roth 1988), or as a uniform sheet of simultaneously active current dipoles (Cuffin 1978; Okada 1985; Nunez 1986). Where such sources are at a relatively large distance from the sensing coil, the spatial frequency content of their extracranial fields is indistinguishable from that which would be produced by a single equivalent current dipole. As Wikswa and Roth (1988) point out, with sensing elements close to such sources it is possible to obtain information about their physical dimensions. However, this is relevant only when the sensing element is in close physical proximity to the exposed brain, which is not germane to the problems dealt with here.

The present work was motivated by the fact that the cortex is a highly convoluted structure in which current flowing within neurons of opposed walls of its folds may exhibit many different spatio-temporal patterns. As we shall see, this can result in time-varying field patterns that may be interpreted incorrectly as being due to rotating and moving patterns of neural currents within the cortex. Thus, changes in field patterns (and patterns of potentials too) can arise over time because of changes in the distribution of activity within a popu-

lation of neurons, and this will also depend upon the geometry of the source configuration. These and related phenomena have profound implications for interpreting changes in brain activity conventionally attributed to *synchronization* and *desynchronization*, states that are often presumed to underly alpha production and its blockage. It also has implications for understanding other phenomena observable in the now widely used topographic displays of the EEG (Duffy 1986, 1988; Lehmann 1987), as well as the MEG, although topographic displays of the real-time MEG have yet to be employed.

### The equivalent current dipole model

To understand the problems associated with extended and convoluted cortical sources of neuromagnetic fields, it is important to be acquainted with the basic premises underlying most conventional methods of 'source localization,' which is ostensibly one of the more valuable aspects of the MEG. Therefore, we begin with a brief review of the methods and assumptions typically used in locating an equivalent current dipole source of external neuromagnetic fields. These methods are similar in part to those employed even earlier in the EEG literature.

In deducing sources of the EEG, the head is often modeled as a set of 3 concentric shells surrounding a sphere containing a current dipole (cf., Nunez 1981). The current dipole may be taken to represent a cluster of elongated neuronal processes (dendrites) in which current is flowing. The 3 concentric layers of different conductivities stand for the scalp, skull, and cerebrospinal fluid, which pose barriers of different resistance to the flow of volume currents that arise at one end of the dipole and flow throughout the intracranial space to return at the other end. It is necessary to employ a head model composed of several such layers because their different conductivities affect the flow of the volume currents as they pass through the intervening tissues represented by the layers (cf., Fender 1987). However, as Grynszpan and Geselowitz (1973) demonstrated, radial variations in conductivity within a sphere do not affect the magnetic field as it emerges from and reenters the outer shell. Hence, there is no benefit to be gained by employing a multilayered sphere, as opposed to a single sphere, when using the distribution of the component of the magnetic field radial to the surface of the sphere in determining the location, orientation, and strength of a current dipole within the sphere. This is one reason why the MEG lends itself to the use of simpler models than those needed when deducing source location from EEG data.

Since the simple sphere model is adequate to illustrate the principles of source localization, and also to

demonstrate the possible ambiguities that result from the use of more complicated source configurations, this paper deals only with the single sphere head model<sup>1</sup>.

Radially oriented current dipoles, including dipoles that lie at the center of a sphere, produce no external magnetic field. This is predicted from the general finding of Baule and McFee (1963) that there is no external field for a conducting body of axial symmetry if a current dipole is oriented axially. The field associated with the volume currents would exactly cancel the equal and opposite tangential field associated with the current dipole itself. Therefore, only tangential current dipoles (including dipole components tangential to the surface of the sphere) are sources of external fields. Based on this, it is widely assumed that the predominant sources of the extracranial field are neurons normal to the cortical surface within the sulci of the brain, while those oriented normal to gyri contribute relatively little, as they are largely radial in orientation with respect to the surface of the scalp. However, both the radially and tangentially oriented dipoles contribute to the EEG.

Fig. 1 shows a current dipole within a conducting medium. The volume currents are drawn as thin lines emerging from one end of the dipole and converging on the other end. If the dipole were contained in a sphere filled with a conducting solution, the volume currents would not contribute to the radial field external to the sphere. The reason for this is quite simple. Although the volume currents are confined by the inner surface of the low-conductivity sphere and therefore produce a magnetic field, this field is parallel to the outer surface of the scalp (Williamson and Kaufman 1987). Therefore, the radial component of the field is due solely to the current dipole itself. Our problem is to determine from external measures of the field the position of the dipole within the sphere in 3 dimensions, its orientation, and its strength (the so-called *current dipole moment*,  $|\vec{Q}|$ ).

The field of the current dipole tangential to the surface of the sphere in which it is contained encircles the dipole and emerges from the surface of the sphere in one region as it reenters the sphere's surface in another region. The direction of the field at any point in space outside the sphere may be represented by two components. One, the tangential component, predominates when the field is measured directly over the

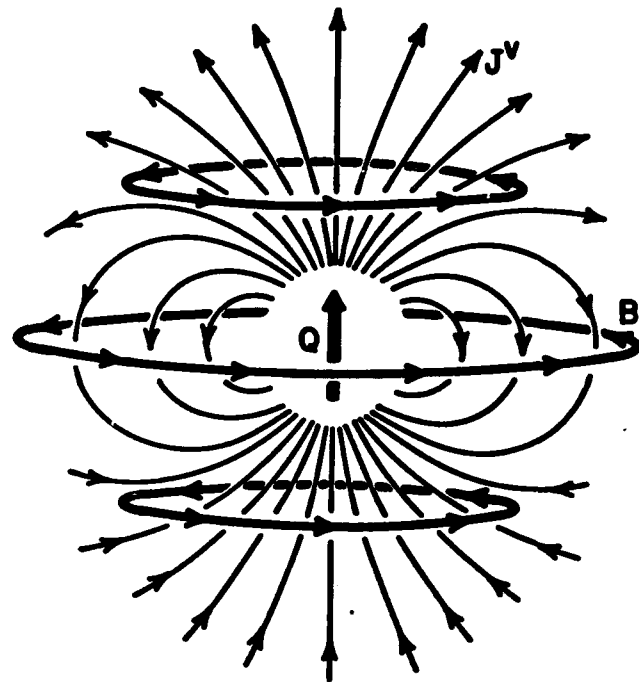


Fig. 1. A current dipole in a conducting medium. The magnetic field ( $B$ ) is due solely to the current dipole, with the volume currents (thin lines) making no contribution to the field.

dipole, and the other, the radial component, predominates where the field emerges from or reenters the surface of the sphere.

In practice it is customary to measure only the radial component of the field. There are 2 reasons for this. First, it is more convenient to place a pickup coil parallel to the scalp. Second, the tangential component may be contaminated by secondary sources. Therefore, this paper shall focus on the radial component of the field, which is the quantity measured in real MEG experiments.

When the dipole is deeper within the sphere, the places where the radial components are at their maximum are farther apart than when the dipole is relatively shallow. As described in Williamson and Kaufman (1981), the depth of a current dipole beneath the surface of a sphere is simply related to the angular separation of the radii from the sphere's center to the two points at which the radial field has maximum strength (the *field extrema*).

Let us now consider a single current dipole. By computer it is straightforward to find an exact numerical solution for its field at the surface of a sphere. In this example (Fig. 2a) the dipole is 6 cm away from the center of a 10 cm radius sphere. The values of the field, which are 'measured' at 841 points on the surface of the sphere, are projected onto a plane. The plane itself is placed at right angles to the radius between the sphere's center and the dipole and is tangential to the sphere itself. Fig. 2b shows the actual isofield contour

<sup>1</sup> More realistic head shapes are currently being used in place of spheres (Hämäläinen and Sarvas 1987; Meijs et al. 1987; Ducla-Soares et al. 1988). However, a sphere fitted to the local inner contours of the skull above the source and filled with a uniform conducting medium (Hari and Ilmoniemi 1986) is adequate for localization of equivalent current dipole sources with an accuracy of a few millimeters. Furthermore, using representations of actual head shapes rather than spheres as head models in this paper would only obscure its main message.

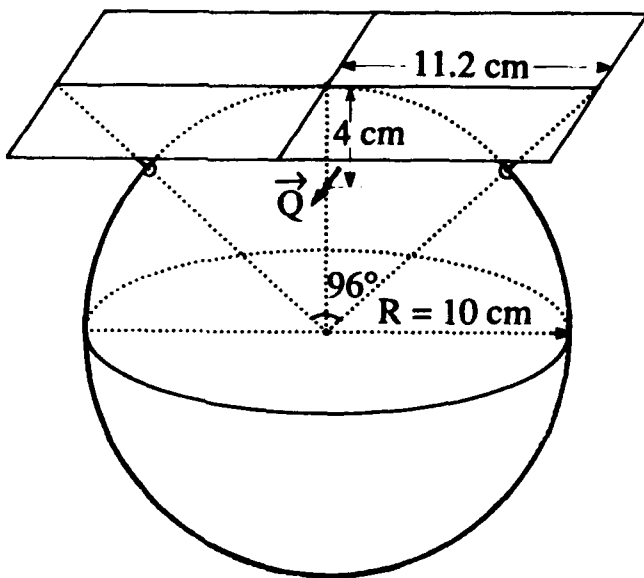
map. The 0,0 coordinate is directly over the dipole, and the field extrema are the centers of the innermost isofield contour lines. The precise values of these lines are arbitrary and depend upon the current dipole moment. Following the prescription of Williamson and Kaufman (1981), we can easily tell that this dipole ( $|\vec{Q}| = 1$ ) is located 4 cm beneath the surface and is exactly between the field extrema.

In practice one cannot measure the field at a very large number of positions simultaneously. Although magnetic field measuring systems composed of 37 independent sensors have recently become available, they are not yet widely used. It is more common for investigators to make large numbers of sequential measurements, generally using systems composed of one or a few independent channels. In fact, the widespread use of sequential measurements rather than many simultaneous measurements may well have led to the emphasis on single current dipole models, as it is not possible to determine the ever changing field pattern associated with the spontaneous activity of the brain from sequential measurements.

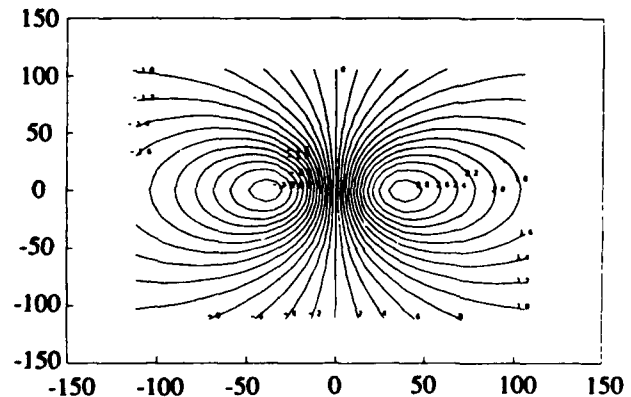
As a practical matter, the use of a few sensors to map the field of a single dipolar source entails accepting a number of important assumptions. The first is that the current dipole moment remains constant over the time required to measure the field at a sufficiently large number of points. The second is that the source

of the field also remains constant in position and orientation. Third, contributions of other sources to the measured field are of little or no consequence once their effects have been taken into account, i.e., there is no interaction between background activity and event-related (evoked) activity. In the case of sensory evoked responses, their fields are averaged over several stimulus presentations, and then the sensor is moved to another location, where the entire procedure is repeated. After a sufficiently large number of observations have been made at many different positions, the average values obtained at each time after presentation of the stimulus and at each position are used to generate field maps. This process discriminates against the unrelated fields associated with the presumably independent spontaneous activity of the brain and favors the field associated with the putative source of the response evoked by the sensory stimulus. The resulting field map is then fit to an ideal map (similar to Fig. 2b) that would be produced by a single equivalent dipole. The position, orientation and strength of the hypothetical dipole that produced the ideal map is then adjusted until a statistically justifiable fit to the actual data is achieved.

The equivalent current dipole source computed in this manner is considered to be a solution to the so-called *inverse problem*. However, caution is needed in interpreting this solution as it can be shown that



(a)



(b)

Fig. 2. a: schematic of current dipole 4 cm from surface of 10 cm radius sphere. The radial component of the field at the surface is projected onto a  $22.4 \times 22.4$  cm square area placed tangential to the sphere, with its center directly over the dipole. b: the isofield contour plot based on computing the field of the unit dipole in 'a' at  $29 \times 29$  points at the surface of the sphere. The contours represent relative field strength in arbitrary units.

there is no unique solution to the inverse problem, i.e., a large number of different source configurations could account for any particular isofield contour map. However, if the inverse problem is constrained by means of a priori assumptions so that only a limited number of solutions are possible, then there may indeed be a unique solution to the constrained problem. Such a solution, however, is really a hypothesis requiring independent information for its confirmation (Scherg 1990).

### Cruciform source configuration

Up to this point we have assumed that the field of interest is generated by a small region of tissue that becomes active at a particular time after some stimulating event. The 'small region' is presumed to be composed of similarly oriented and concurrently active neurons and can therefore be represented by a current dipole. Ongoing spontaneous activity tends to mask the event-related activity, but averaging improves the signal-to-noise ratio so that the field of the generator affected by the stimulus can be mapped and a statistically significant solution to the inverse problem may be found. However, logically speaking, this is not the only way in which to envision the 'source.'

In attempting to explore how the detailed shape of the brain influences the field pattern generated by extended sources, we next employ a source configuration based on the cruciform model of the visual cortex (Fig. 3a). With a dipole for every square millimeter of surface within the fissures of the model, we have a complex cortical fold containing 1386 dipoles. Each dipole may be thought of as a hypercolumn of neurons oriented normal to the surface of the cortex within the

fissures of the model. The opposed walls of the simulated longitudinal and calcarine fissures are separated from each other by 4 mm. All fissures are 2 cm deep and, normal to the radius passing through the center of the structure, 1 cm wide and 1 cm high. As shown in Fig. 3b, the cortical surface farthest from the center of the sphere is 3 cm away from the sphere's surface (the scalp). The model extends 2 cm deep, so its innermost elements are 5 cm from the center of the 10 cm radius sphere.

### Computing the field

The field of a point current dipole varies inversely with the square of the distance between the point at which the field is measured and the current dipole. This relation is given in equation 1.

$$\vec{B}_r = \frac{\mu_0}{4\pi} \frac{\vec{Q} \times (\vec{r} - \vec{r}_0)}{|\vec{r} - \vec{r}_0|^3} \quad (1)$$

where  $\vec{B}$  = the field at a point  $\vec{r}$  in space,  $\vec{r}_0$  = the vector from the center of the sphere to the dipole,  $\vec{Q}$  = the current dipole moment, and  $\mu_0$  = the permeability of free space. Since we are interested in only the radial field external to a sphere, the normal component of  $\vec{B}$  ( $B_n$ ) is simply the dot product

$$B_n = \vec{B} \cdot \frac{\vec{r}}{|\vec{r}|}$$

By superposition (cf., Jackson 1975), we can solve the field of each of the 1386 sources separately and add the resulting vectors computed at  $29 \times 29 = 841$  points on the sphere's surface. We then calculate the radial component ( $B_n$ ) of each field vector, which is the physical quantity measured in MEG experiments, on a spherical surface whose projection tangential to the 'scalp' is  $22.4 \times 22.4$  cm, as illustrated in Fig. 2a. The center of this projection is directly over the radius of the sphere passing through the geometrical center of the cruciform model.

### Simulating an evoked response

To test the implementation of the model described above, we simulated an evoked response due to the activation of a portion of its dipole population. To conduct this test it was necessary that we be even more specific about the assumptions related to the nature of the activity underlying *evoked responses*. Therefore, we assumed that all the dipoles comprising a 1 cm deep portion of one quadrant (the shaded areas of Fig. 4) were oriented in the same direction. In separate simulations two different 1 cm deep portions of one quadrant were used. One of these regions was the outer half of the quadrant (Fig. 4a), which was therefore bounded by an outer border 3 cm from the surface and an inner border 4 cm from the surface of the sphere. The other

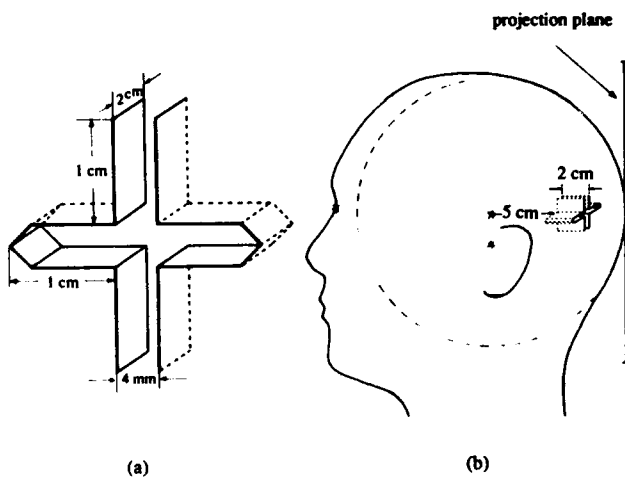


Fig. 3. a: representation of the cruciform structure which is populated with a total of 1386 current dipoles ( $1/\text{mm}^2$ ). b: location of the cruciform structure within a spherical model of a head. The structure extends from 3 to 5 cm away from the surface of the 10 cm radius sphere.

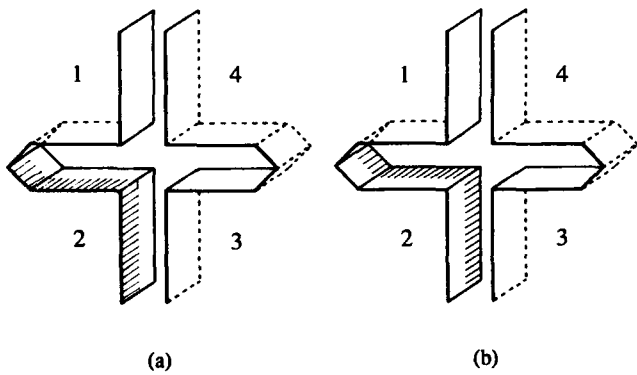


Fig. 4. Simulating an evoked response. The shaded portions of the cruciform structure contained dipoles that were all oriented in the same direction, while all of the other 1386 dipoles had random orientations. a: the boundaries of the shaded portion nearest the surface. The outermost boundary is 3 cm deep, while the boundary farthest from the surface is 4 cm deep (6 cm from the sphere's center). b: the deeper (shaded) portion of the same quadrant, with boundaries 4 and 5 cm away from the surface.

portion (Fig. 4b) was delimited by borders 4 cm and 5 cm deep. The directions of all of the other dipoles in the model were randomized. The dipole moments of both the synchronized (same direction) dipoles in the small portion and the larger asynchronous (random directions) remainder of the structure were random-

ized and, on average, the level of activity per unit area of the two regions was about the same. This simulates a situation where neurons of an array of dipoles within a portion of sensory cortex are made to respond synchronously to a stimulus (but not increase in level of activity after stimulation as it might be presumed to do in the case of evoked neuronal activity), while the larger unaffected portion continues to exhibit random asynchronous activity, but at the same average level per unit area. To mimic changes in the field pattern with time, the orientations of these dipoles (inward toward the brain or outward toward the surface) and moments were changed. One hundred different patterns were generated, and the average of all patterns was computed. Thus, we were able to test the model and determine if it is possible to accurately locate the center of gravity of the array of synchronously active dipoles regardless of the effects of dipoles comprising its surroundings.

Fig. 5 contains samples of the individual field patterns prior to averaging (representing the external field at an instant of time), as well as two average field patterns. The instantaneous patterns are asymmetrical (multipolar) and may be quite different from each other, e.g., their field extrema are at different places, depending upon the sets of random numbers describ-

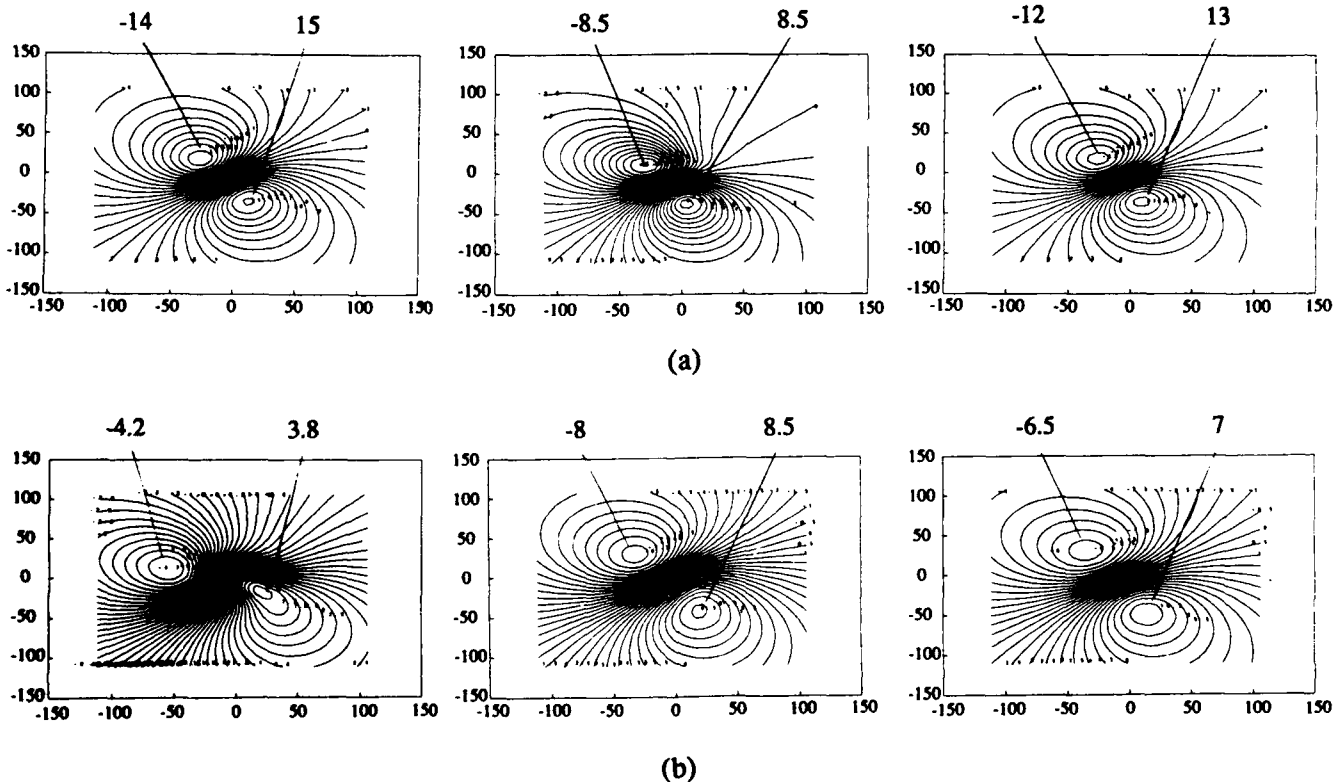


Fig. 5. a: the two isofield contour patterns on the left are samples of the fields (instantaneous fields) obtained when the shallow shaded region 'a' of Fig. 4a contained aligned (synchronized) dipoles. The plot on the right is the average of 100 such samples and it exhibits a dipolar pattern centered directly over the shallow shaded region and slightly displaced from the center of the cruciform structure. b: the lowermost left-hand instantaneous isofield contour patterns were generated with deeper shaded region of Fig. 4b. Note the greater separation between the field extrema of the average plot of this series. It corresponds to the greater depth of b relative to a.

ing the dipole moments. This difference is especially pronounced between the two left-hand patterns of the lower row in the figure and they illustrate the claim in the introduction that field patterns obtained at any 'instant of time' can differ from those obtained at other instants of time. However, as a result of the averaging process, the features that change from one distribution of dipole moments to another tend to be self-cancelling, while invariant features not visible in the individual plots are relatively enhanced. For this reason the two averaged isofield contour plots in Fig. 5 are apparently dipolar in character. Note that the extrema obtained with the deeper synchronized portion are clearly further apart than are those obtained with the more shallow synchronized portion. Also note that the point lying midway between the two extrema in each of the averaged plots is offset from the center to a position directly above the center of the synchronized quadrant.

If the invariant features are attributable to the activity of a synchronously active subset of the dipoles, then the depth of an equivalent current dipole representing that subset should be approximated by the geometric mean of the depths of the innermost and outermost boundaries of the region it occupies. This follows from the fact that field strength varies inversely with the square of the distance to its source, so the fields of dipoles near the outermost boundary of the region should be more strongly represented in the field at the surface than those of dipoles near the deepest boundary.

In this numerical simulation small deviations from this geometrical mean are to be expected because it is an approximation, and because of the presence of sampling imbalances in the sets of random numbers. These geometric means are 3.45 cm for the shallow (Fig. 4a), and 4.47 cm for the deeper (Fig. 4b) synchronized portions of the cruciform structure. Calculating the depths of the equivalent current dipoles from the angular separations of the average extrema on the surface of the sphere gives values of 3.53 cm and 4.49 cm for these same two portions, respectively. Similar values were obtained in replications of the simulation, but with two different quadrants of the model.

This example illustrates how the single equivalent dipole model may be used to determine the location of the center of gravity of an extended set of dipoles and sets the stage for consideration of more complicated dipole arrays.

## Results

### *Synchronous versus asynchronous activity*

As shown in the previous example, field patterns associated with random current dipole moments vary

widely, depending upon the distribution of dipole moments within the array. In the face of such variability, it is difficult if not impossible to interpret any individual pattern as being due to activity within a particular structure. However, when a small region of synchronized activity is present, a stable pattern emerges after averaging, and this pattern is clearly related to the location and orientation of the underlying synchronized sources within the cruciform structure. This suggests that it is worthwhile to explore further the differences and similarities between effects of synchronous and asynchronous activity.

In many textbooks synchronization is described as a basis for alpha activity and the slow EEG waves occurring during sleep, while desynchronization is presumed to be the proximate 'cause' of alpha blockage and the relatively fast activity associated with arousal (cf., Sheperd 1988). These same terms are widely used with the same sense in the literature (cf., Pfurtscheller and Aranibar 1977; but see Hobson and Steriade 1986 for cautionary language). To simulate synchronization in the context of the cruciform structure, all of the dipoles in its walls were oriented in the same direction, e.g., all were directed inward from the surface of the cortex (Fig. 6a). However, the magnitudes of these dipoles differed randomly from one position to the next, and the pattern of random values was changed to discover how different distributions of dipole magnitudes affect the field pattern outside the sphere.

It should be noted that the term *synchronization* need not imply that the direction of current flow is the same for *all* of the columns represented by the dipoles, as assumed here. Alternatively, synchronization of activity could be limited to one or more small cortical regions or patches, as in the example of the evoked response described above. Also, synchronization could mean that several patches, located at various distances from each other, are more or less loosely coupled to each other, and the level of correlation of activity between the patches could be related to the distance between them. Internally synchronized patches may oscillate independently of each other. In fact, Lopes da Silva and Storm van Leeuwen (1978) demonstrated that alpha band activity across the surface of the dog's visual cortex exhibits coherence (synchronization) over distances no greater than a few millimeters. Based on this finding, it is apparent that widespread coherence of alpha activity detected at the scalp is not matched by similar spatial coherence among columns across the cortex. Instead, the summed activity of a number of largely independent generators oscillating at frequencies within the alpha band may well produce what is often described as circulating and moving 'coherent' patterns of alpha activity in the EEG. Because of the finding of Lopes da Silva and Storm van Leeuwen, we chose to use a model in which there is no synchronized

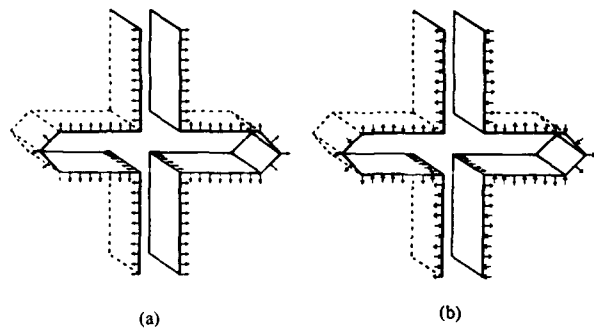


Fig. 6. a: simulating synchronization which, in this case, is defined as having all of the dipoles oriented in the same directions relative to the surface of the cruciform structure, i.e., all dipole moments range from 0 to +1. b: simulating asynchrony of the dipoles. All have randomly chosen directions as well as magnitudes, i.e., their moments range from -1 to +1.

activity outside the 1 mm area assigned to a given dipole to produce our asynchronous model. This mimics a situation in which 1 mm square areas of cortex oscillate at alpha (or other) frequencies independently of each other (Fig. 6b).

More concretely, assume that on average the cells of a hypercolumn are active with a somewhat variable frequency of, say, between 8 and 13 Hz, but the average frequency and phase of the hypercolumn are independent of that of the other columns. Therefore, at any instant of time the net current within one column may differ in direction and magnitude from that of any other column. To represent this hypothetical situation we selected a random value from -1 to +1 to represent the net current of any of the 1386 columns. The net external field resulting from the superposition of the fields associated with each of these sources is computed. To represent the state of the cortex at different times, the simulation was run a number of times applying different initial seeds to the random number generator. Each initial random seed is associated with a different list of random numbers, and the patterns were generated by assigning these numbers to the dipoles in the array, beginning at different places in the list. For each pattern, the average amount of activity in each wall of the model was approximately the same, thus enabling us to directly test the idea that

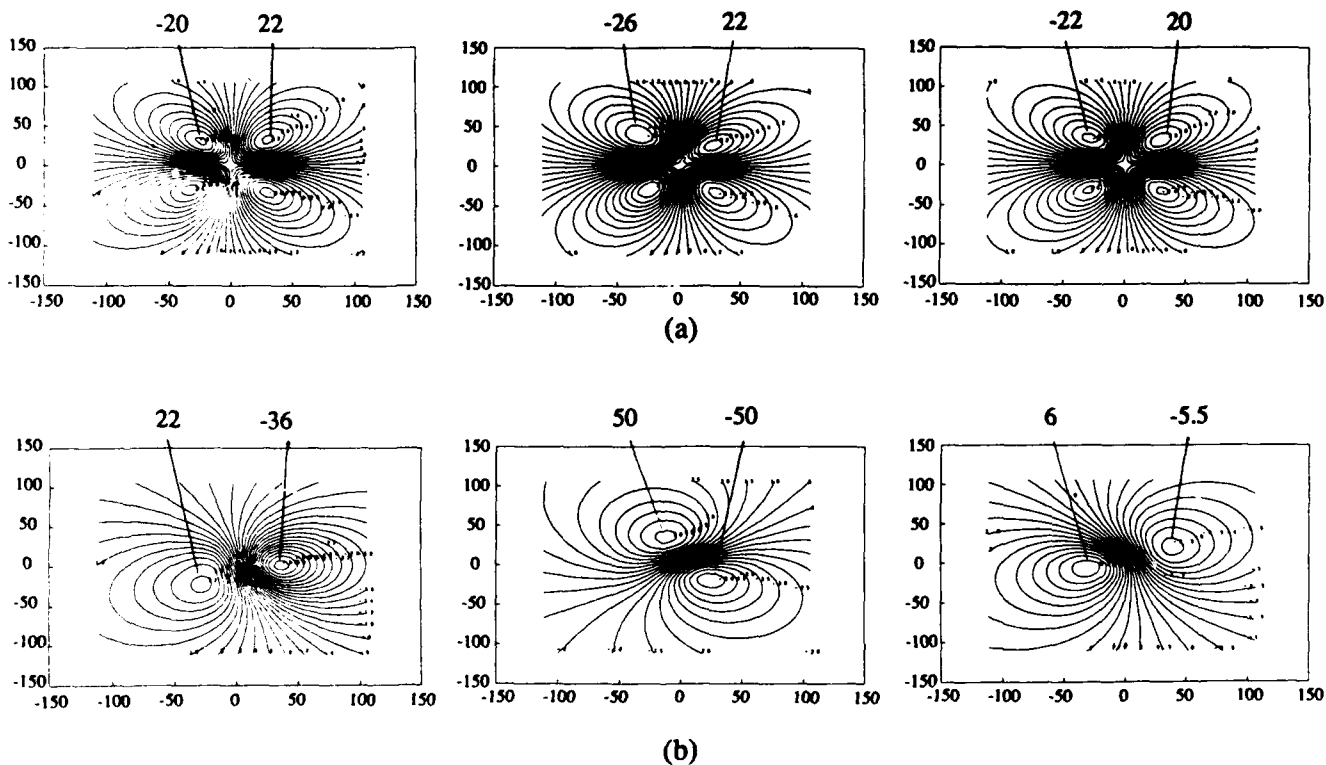


Fig. 7. a: the two left-hand field patterns were produced by synchronized dipoles with randomly different magnitudes. The similarities among individual patterns are evident despite this randomness and become even more salient in an average of 100 such patterns, which is predominantly quadrupolar in appearance, as shown on the upper right. The numerals above each pattern are the relative field values at the extrema. These are about the same in the instantaneous patterns on the left, and also in the average pattern on the right. b: field patterns of lower row are associated with asynchronous dipoles. Note the differences among the individual isofield contour patterns on the left. The field strengths at the two extrema on the far left are similar to those of the synchronized patterns represented in row a. In the middle pattern of this row we see field extrema that are about twice as strong as in the other instantaneous patterns. Moreover, the field extrema are in different locations. The average of 100 patterns on the right exhibits a much weaker residual pattern, because these changes in field pattern geometry from one instant to another tend to be self-cancelling.

differences in the statistics of the dipoles rather than their net energy will affect the distribution of the external fields.

Fig. 7a contains representative field patterns generated by the synchronized dipoles where only current magnitudes were randomized. Despite obvious differences among the patterns they all seem to share some common features. Synchronization results in remarkably stable patterns regardless of changes in the moments of the dipoles. In fact, averaging across a large number of different patterns for each of 3 initial seeds results in the generation of very similar multipolar patterns, where each of them contains four extrema.

Let us now contrast this with the field patterns obtained using arrays of asynchronous dipoles, those

generated by selecting a value of  $-1$  to  $+1$  to represent the current of any one of the 1386 dipoles (Fig. 7b). The individual patterns obtained for different random arrays are generally quite different from each other. Although the centers of these patterns are located more or less directly over the radius passing through the center of the cruciform structure, the asymmetric extrema found in most patterns seem to rotate around that center. From one field pattern to another, extrema of opposite signs (emerging or reentering) often appear at overlapping positions in otherwise similar patterns. In fact, the extremely low field strength in the averaged patterns shown in Fig. 7b is due to the fact that fields of opposed sign tend to cancel each other in generating the average plot. These

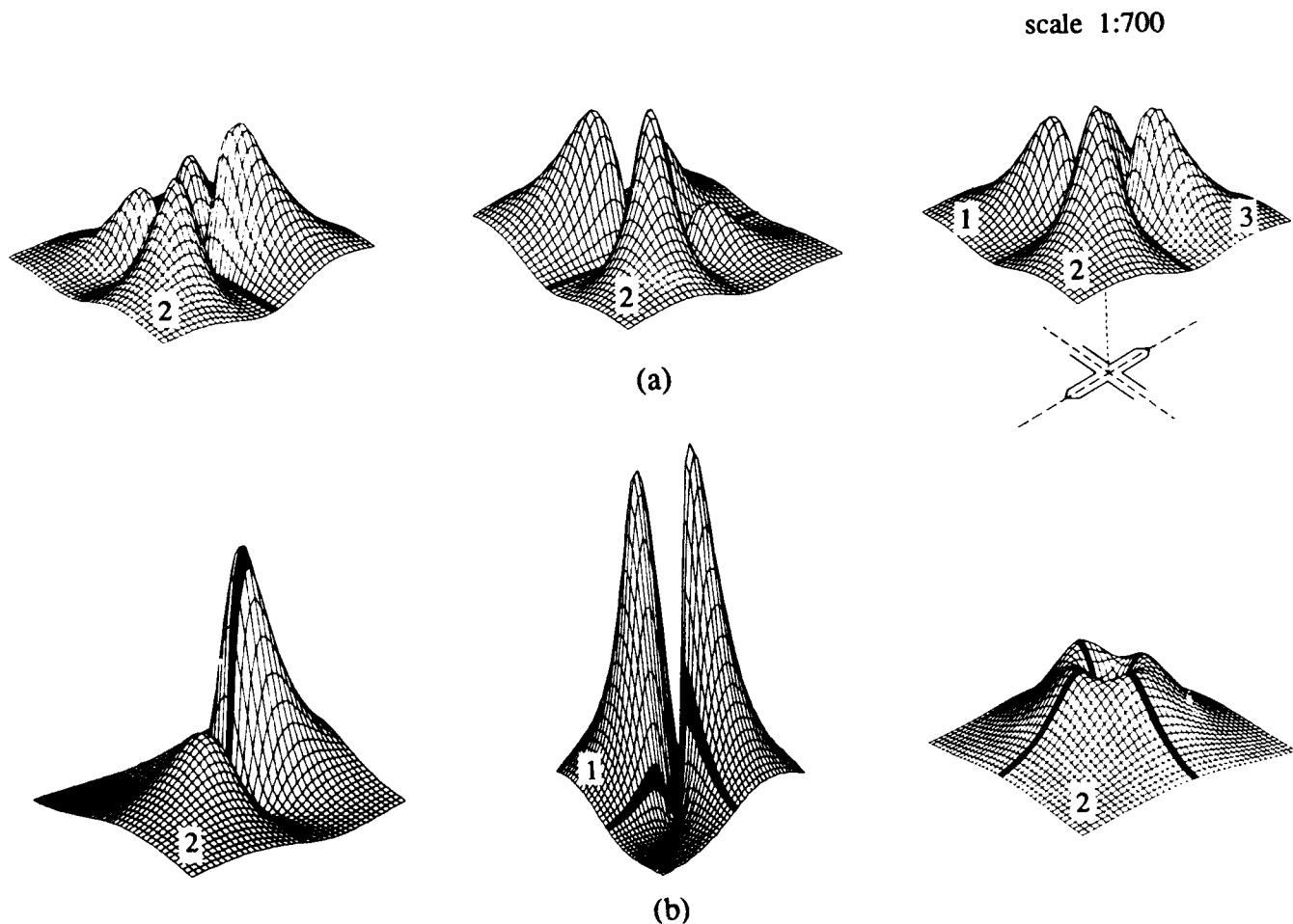


Fig. 8. Field power patterns corresponding to field patterns of Fig. 7. Power is in arbitrary units and the scale of the z-axes of all plots represents relative power. a: synchronous arrays of dipoles were used to produce the upper left-hand set of patterns and, on the right, an average of 100 such patterns – the *mean square field* (note the consistent 4-lobed structure). b: asynchronous arrays of dipoles were used to produce the lower left-hand patterns, with the mean square field of 100 such patterns on lower right. Note that the lobes in the asynchronous mean square field pattern on the right have similar power to those of the synchronous mean square field. By contrast, the related average field pattern of the lower row of contour plots of Fig. 7 tends toward the residual noise level. The numerals 3, 2 and 1 stand for quadrants of the underlying cruciform structure, which is depicted in Fig. 4. The structure is inserted under the power plot on the upper right. It is drawn about  $3\times$  its size relative to the size of the plane on which power is projected. The center of the structure is directly beneath the center of the power plot. It is important to recognize that this structure is very small in spatial extent as compared to the spatial extent of the field power patterns depicted in this and other figures.

average field values are clearly weaker than those obtained with synchronized dipole arrays.

The differences between the average fields obtained with synchronous and asynchronous arrays do not demonstrate that desynchronization (shifting from synchrony to asynchrony) leads to weaker fields. Note in Fig. 7 that the peak values of the instantaneous fields associated with the synchronized array of dipoles have arbitrary values of 20 to  $-26$  units of field, while those associated with the desynchronized array of dipoles range from 22 to  $-50$  units in the same scale. In fact, while the averaged field patterns generated by desynchronized arrays of dipoles must be much weaker than those generated by synchronized dipoles, the instantaneous (non-averaged) patterns of both types may be equally strong and, in some instances, the patterns associated with desynchronization may even be stronger. This is made quite obvious when *field power* is averaged rather than field, albeit with the loss of information as to the direction of the field.

Field power is simply the square of the field. Fig. 8 contains several samples of individual field power plots similar to the isofield patterns of Fig. 7 but presented as 3-dimensional graphs. All graphs in this figure are drawn to the same arbitrary scale. (In this case 1:700 is the scale of the z-axis where 1 unit along the z-axis is equal to 700 units of field.) Thus, in each graph the z-axis is proportional to field power, and the other two axes represent distances in mm in the 2-dimensional plane onto which the original field data were projected. It is obvious from the lowermost left-hand graphs that at any instant of time the locations of the regions of greatest power (strongest radial field regardless of its direction) are quite variable, depending upon the specific array of desynchronized dipoles. The regions of greatest power tend to circulate about the center of the graph from one instantaneous plot to the next. However, a plot of average power (*mean square field*) reveals invariant features not present in single plots based upon particular distributions of dipole moments.

Fig. 8 contains mean square field plots based on averaging 100 different power patterns for both the synchronized and desynchronized conditions. In both plots the maximum powers are of the same order of magnitude, although there are differences in their topographies. Nevertheless, as demonstrated here, in this model desynchronization per se does not necessarily result in less power than is encountered where the underlying dipoles are synchronized with each other, and, in instantaneous plots, may even result in more power.

It should be noted that random noise unrelated to the contributions of the underlying dipole population would necessarily contribute to mean square power plots. However, on average such contributions would

shift the baseline of the plot, and not distort the spatial modulation of the field power, which is related to the underlying geometry of the source configuration.

#### *Suppression of activity*

Kaufman et al. (1990) demonstrated that there is a marked suppression of occipital MEG alpha activity when subjects search their memories to determine if a briefly presented form was or was not a member of a previously seen set of forms. The duration of this suppression is commensurate with the time to press a button indicating completion of the search. When subjects do not search memory but merely press a button as soon as possible after seeing the test form, then the suppression is of a much shorter duration, as is the reaction time. This effect was most pronounced over the midline in the occipital region and probably occurred in visual cortex. The beta rhythm was also found to exhibit suppression, but its scalp distribution differed from that of the alpha, suggesting that at least partially different neuronal populations underlie these two bands of MEG activity. This work suggests that alpha and beta activity may be suppressed within relatively localized regions of cortex, but up to now no method for locating the sites of the suppression has been available. We now extend some of the previously developed concepts to demonstrate one method for locating cortical areas where activity has been blocked or suppressed.

In what follows we define blockage as the suppression or attenuation of activity of a subset of dipoles comprising the cruciform structure. Where the dipole activity is synchronous, i.e., all dipoles have the same directions, then locating the site of suppression is actually straightforward. For example, when the activity of all of the aligned dipoles of one quadrant is attenuated by a factor of 10, the quadrupolar appearance of the power plot is changed to an asymmetric multipolar pattern with only 2 extrema observed. As illustrated in Fig. 9, these patterns are systematically related to the positions of the suppressed quadrants.

In view of their extremely unbiological stability, these patterns have only one noteworthy attribute. As shown in Fig. 9, the powers at the two extrema where one quadrant is suppressed are actually much greater than the powers at any of the 4 extrema where all quadrants are active, implying that more means less. (Note that the scale of Fig. 9 is 1:20,000 as compared to only 1:700 in Fig. 8.) However, the apparent paradox is easily resolved since the geometry of the cruciform structure requires that all synchronized dipoles on opposite walls cause quadrupolar and higher order multipolar terms to dominate the field. However, with one quadrant suppressed, symmetry is broken and a dipolar term emerges which makes a much stronger and necessarily dominant contribution to the overall pattern. It is

scale 1:20000

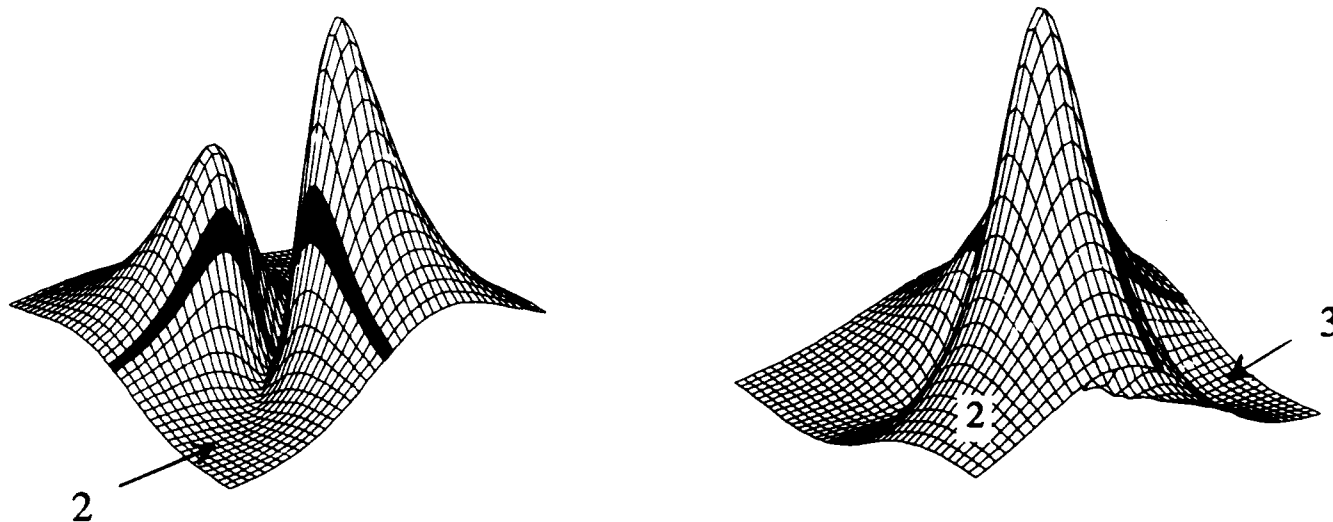


Fig. 9. The same random arrays of *synchronized* dipoles, used to generate the power plots depicted in Fig. 8, were used here but with activity of dipoles of one quadrant of the cruciform structure attenuated. The plot on the left was generated with quadrant 2 (see Fig. 4) of the cruciform structure attenuated by a factor of 10 and the plot on the right with quadrant 3 attenuated. The resulting mean square field patterns have only two lobes and not four, and markedly greater power (the scale is 1:20,000 as opposed to 1:700 in Fig. 8). This is a result of the breaking of symmetry, which permits a strong dipolar term to emerge.

generally true that symmetrically folded arrays of synchronous dipoles produce weaker field patterns than the same arrays with broken symmetry. This is a major reason for insisting that an explanation of alpha blockage in terms of desynchronization must be justified by taking the geometry of the assumed source configuration into account.

The field patterns associated with asynchronous generators are less obviously affected by suppression of different regions within the folded cortex. As illustrated in Fig. 10, the plots of power based on any set of random numbers differs from those generated with another set of random numbers. To introduce suppression the amplitudes of the dipoles of 1 of the 4 quadrants of the model were attenuated by a factor of ten<sup>2</sup>. The result of this for two of the quadrants is illustrated in Fig. 10. Several single power plots reveal no systematic relation to the suppressed quadrant. However, the mean square fields do differ from those obtained with all 4 quadrants equally active.

As shown in the right-hand plot of Fig. 8b, with all 4 quadrants active the circular region of greatest power in the mean square field plot has 4 relatively shallow

peaks, although only 2 peaks of much greater power are present in the 2 'instantaneous' traces on the left. As shown in Fig. 10, despite the presence of a suppressed quadrant, 2 peaks of varying power are present in the instantaneous plots, but there is no obvious way in which these differ from the instantaneous plots of Fig. 8b. However, the right-hand mean square field plots of Fig. 10 have only 3 peaks when 1 quadrant is suppressed, and, as we have seen, there are 4 peaks when all quadrants are active. Nevertheless, the visual differences between the patterns are slight and interpretations are possibly affected by subjective judgment. However, an objective method for identifying the suppressed region and determining its depth is possible.

According to the superposition principle, the net field at a point in space is the linear sum of the fields of all of the contributing generators at that point. Therefore, the contribution of any portion of the cruciform structure to the total field is equal to the difference between the total field and the field generated by the portion whose level of activity is suppressed. For example, suppression of activity of one quadrant of the total structure would result in a net field pattern that differs from the pattern that arises from the activity of the total pattern prior to suppression. Hence, the pattern derived by taking the difference between the pattern measured during suppression and that prior to suppression would reveal the contribution of the sup-

<sup>2</sup> In each pair of runs (quadrant suppressed and quadrant not suppressed), the same random seed was passed to the random number generator, but the magnitudes alone were reduced for the designated subset of dipoles.

pressed portion. Of course, this is not strictly true when corresponding differences between mean square field patterns (as opposed to field per se) are taken. In fact, the difference between the mean square field patterns obtained with all quadrants active and with one quadrant suppressed contains cross-terms in the vector products of the fields originating from each of the two sets of dipoles. However, if the moments of well separated sources are uncorrelated as compared with adjacent sources (as they are in this case), the contributions of the cross-products to the difference between mean square fields tend to be zero because of averaging. We have verified this in the present simulation by taking differences between individual field patterns with all quadrants active and with one quadrant suppressed, squaring the difference patterns and then averaging them. Resulting patterns are virtually indistinguishable from those derived simply by taking differences between the corresponding mean square field plots, which are shown here.

As we have seen, the reason for emphasizing field power is that averaging the field can result in cancella-

tion of information contained in the individual patterns included in the average. Field power, however, is additive. This makes it possible to ignore changes in the sign of the field and, other than the sign of the field, preserves much of the information present within single patterns when mean square field is computed. This includes information related to specific regions with suppressed activity. Therefore, to determine the position and depth of a suppressed quadrant, we subtract the mean square field obtained with the suppressed quadrant from the mean square field obtained with all quadrants active, as shown in Fig. 11.

The power difference plots in Fig. 11 were obtained with 3 different suppressed quadrants. The locations of these quadrants in the underlying model are indicated in the figure. It is to be noted that the difference plots are approximately U-shaped, with two prominent power peaks on the U. The minimum on these surfaces is located directly above the suppressed quadrant. This gives the lateral position of the suppressed quadrant. Assuming a uniform density of dipole moments within the suppressed quadrant, its depth should be 3.87 cm,

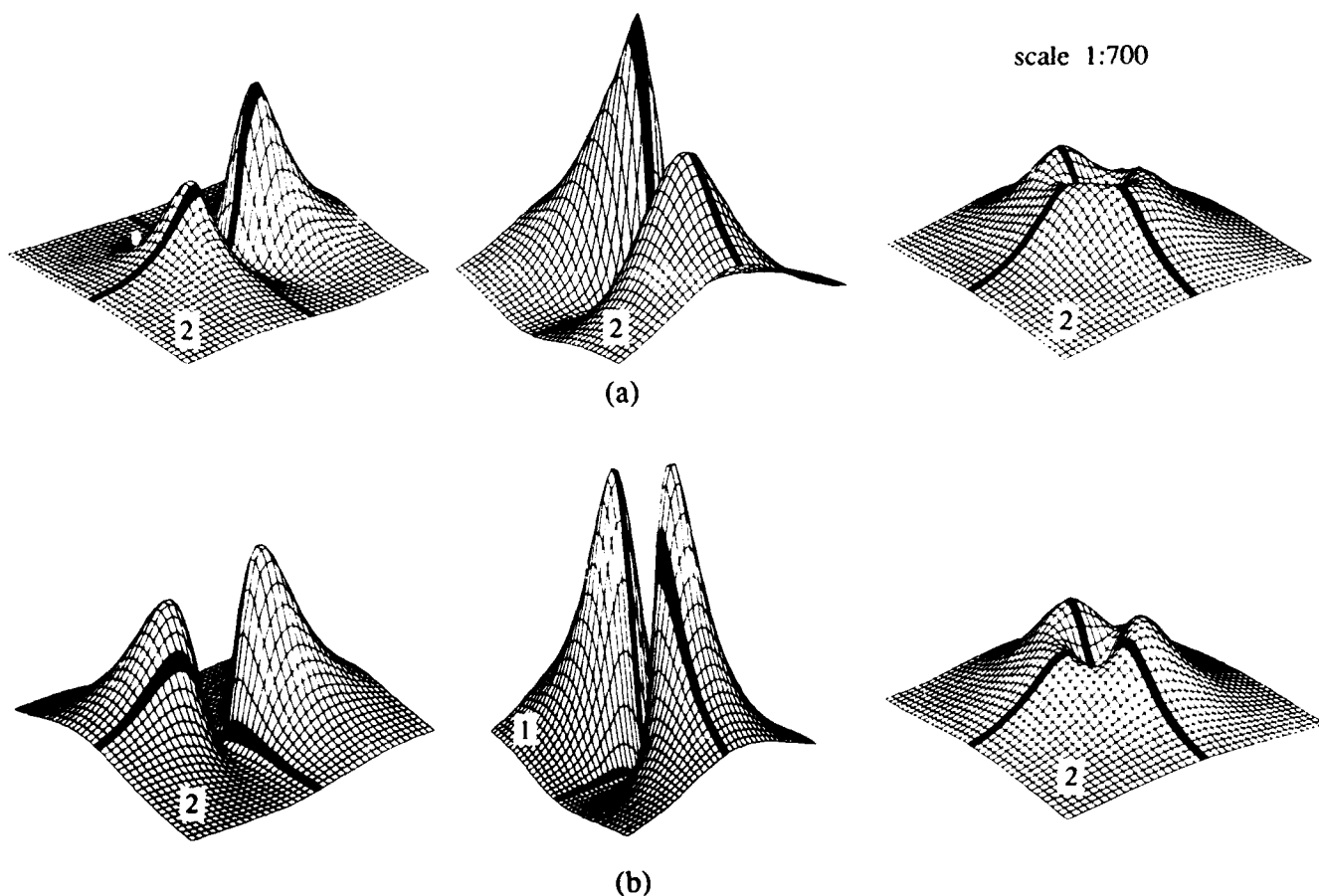


Fig. 10. a: the two power plots on the left were obtained with asynchronous generators and with activity of quadrant 2 attenuated by a factor of 10. The right-hand plot is an average of 100 such plots of instantaneous power. b: similar instantaneous and averaged power plots, but with activity of quadrant 3 attenuated by a factor of 10. The darkened cells are directly over the projections of the fissures in the cruciform structure of Fig. 4. The instantaneous patterns are highly variable, but mean square fields (on right) do differ from each other, but it is difficult to decide which quadrant is suppressed.

scale 1:100

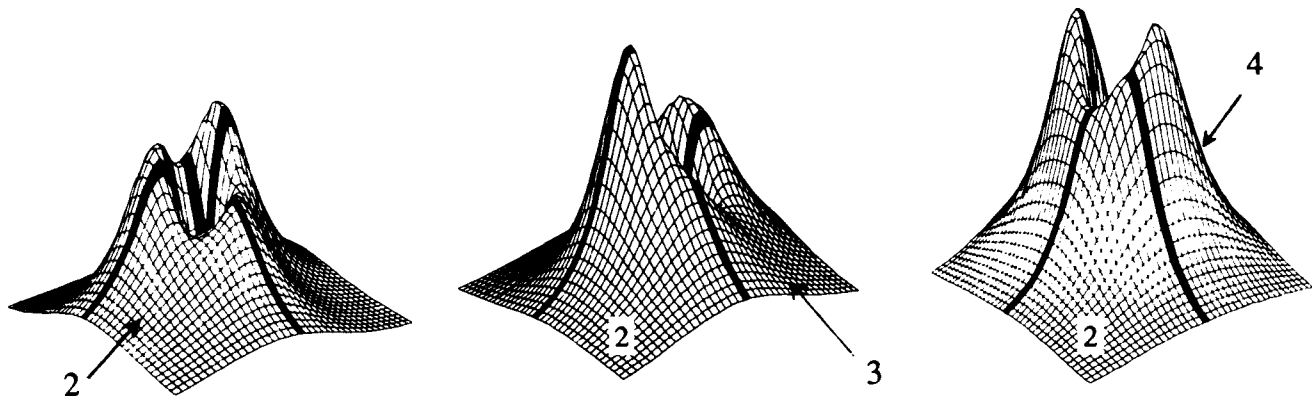
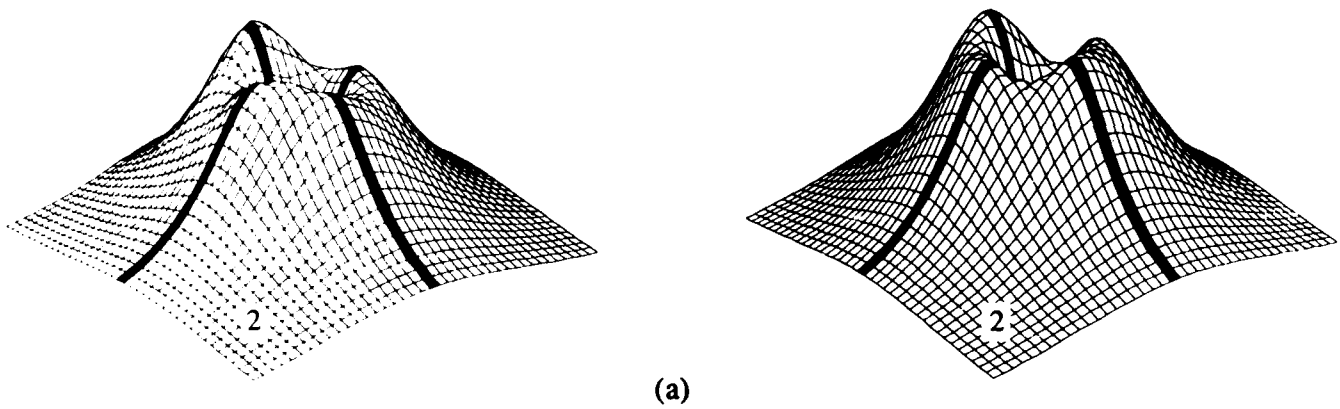


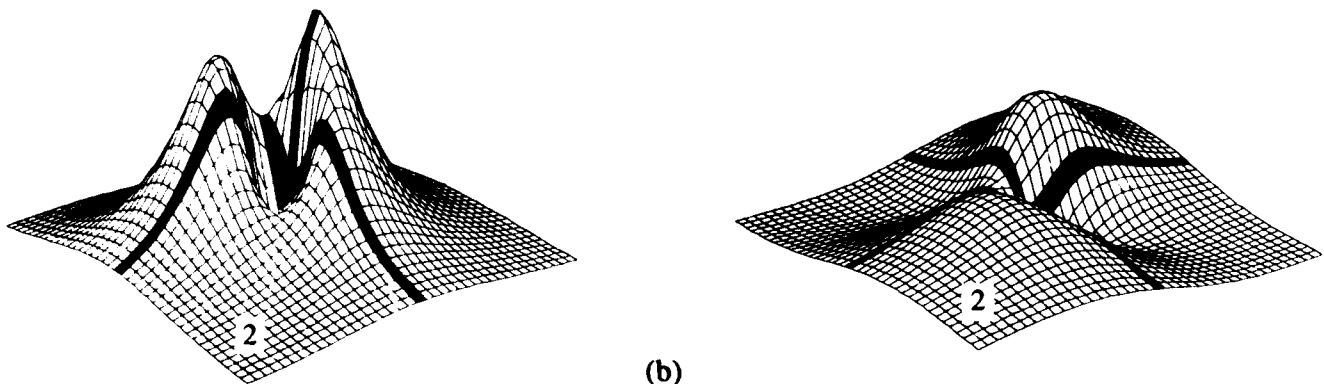
Fig. 11. Subtraction of mean square field with one quadrant attenuated (as in Fig. 10) from mean square field with 4 quadrants equally active (Fig. 8b). The 3 'difference patterns' were obtained with quadrants 2, 3 and 4 attenuated. Patterns differ, depending upon which quadrant is attenuated. The angular separations between prominent two lobes in each plot give the depth of the suppressed quadrant. The minima between the two extrema in each pattern are slightly offset from the centers and located over the attenuated quadrant which, as shown in Fig. 8, is small relative to the spatial extent of the projection plane.

scale 1:500



(a)

scale 1:100



(b)

Fig. 12. a: two mean square patterns obtained with, from left to right, the shallow (Fig. 4a) and deep (Fig. 4b) portions of one quadrant attenuated. b: differences between the mean square plots with all quadrants active and mean square plots with shallow portion (on left) and deeper portion (on right) of one quadrant suppressed. Note the wider separation between the two lobes in the latter pattern. This angular separation gives the depth of the relatively inactive portion of the structure.

since its most shallow boundary is 3 cm, and its most distal boundary 5 cm from the surface. By measuring the angular distances between the maxima in all three graphs we find the depth to be 3.17, 3.43, and 3.49 cm from the surface for quadrants 2, 3, and 4, respectively.

To use this same procedure in locating still smaller suppressed regions of the structure, the level of activity of a 1 cm deep portion of one quadrant, rather than the entire quadrant, was attenuated. This was either the portion of the quadrant closest to the surface of the sphere or the one closest to the center of the sphere (Fig. 4). Does suppression at different depths differentially affect the external field pattern?

Fig. 12 gives the results for suppression of the shallow and deep portions of but one of the quadrants. Replication with the other quadrants gave essentially the same results. The difference plots reveal that the net power associated with the deeper structure is less than that attributable to the shallower structure, as is to be expected. Moreover, there is an easily discerned difference in the separations of the extrema in the two power difference plots. The extrema associated with the deeper structure are more widely separated and of lower magnitude. It is to be noted that these differences in power and in space between extrema are related to a relatively inactive portion of cortex, and

not to a relatively more active portion of cortex, as in the case of evoked responses.

#### *Increments in magnitude of asynchronous activity*

The flexibility permitted by this type of model makes it possible to envision possible but as yet unobserved phenomena. For example, modelling an evoked response required some arbitrary assumptions. These were that the background activity is at least as strong as the evoked activity, and that it changes over time at every point of the structure. This assumption required us to adopt the asynchronous model of background activity. Since the evoked response was not allowed to contribute a spatially changing pattern to the overall field, we opted to model it as a synchronized region. Afterwards the solution to recovery of the evoked response and determining the location of its generator was relatively simple and conventional. Averaging field alone recovers the source. However, this also allowed us to think about other possible kinds of stimulus-related activity. For example, it is possible that a sensory stimulus simply results in an increase in the amount of activity within a region of cortex, without altering its statistics. In this case, both the background and the affected area could be composed of randomly oriented dipoles of random magnitudes, but the average activity

scale 1:10000

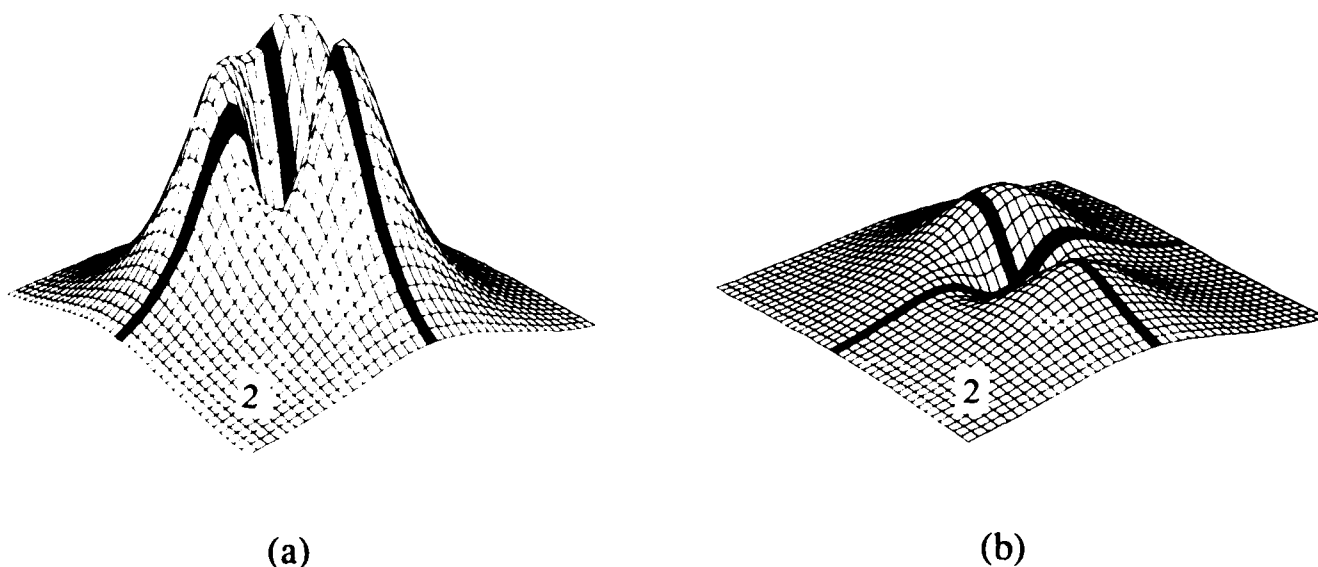


Fig. 13. Mean square field plots with a shallow quadrant (quadrant 2) of asynchronous activity incremented (Fig. 4a), and a deeper portion of the same quadrant of asynchronous activity (Fig. 4b), also incremented. The pattern on the left reveals less widely separated extrema than the one on the right, and these separations correspond to the depths of the affected asynchronous quadrant portions. The minima between the extrema lie over the incremented quadrants, which is offset slightly from the intersection of the dark stripes representing the central fissures of the cruciform structure. Therefore, field power measures permit localization of regions of incremented, as well as decremented, regions of asynchronous activity.

within the affected area would be greater than it was prior to the hypothetical stimulus. Simply averaging the field patterns would not reveal such a response or its source.

As shown in Fig. 13, the incremented activity of a 1 cm deep portion of one quadrant of the overall array of asynchronous generators can be detected, provided that power is averaged. As demonstrated in Fig. 7, when the dipoles are asynchronous, the average field pattern converges toward a residual noise level, and this would be true even if the net activity of a portion of a subset of the asynchronous dipoles were less active than the other members of the set. Furthermore, after averaging power the depth of the active region can be computed simply by measuring the angular separation between the extrema and using the standard formula. Averaging field rather than power could not produce such consistent results.

### Conclusions

The major conclusions are that synchronization and desynchronization are not particularly useful explanatory concepts with regard to alpha blockage and related phenomena. The only way in which they can be useful is if these concepts are employed within the framework of a specific theory incorporating the geometry of the underlying cortex as well as the distribution of activity within it. For example, if the underlying cortex is assumed to be parallel to the scalp, then alignment of all its dipole sources so that they pointed either inward or outward would produce strong potentials at the surface. However, if some of the radially oriented dipoles were directed outwards and others inwards, the potentials would be much weaker. This is because aligned and radially oriented dipoles across a uniform surface can be modelled as a single dipole. However, with the radially oriented dipoles pointing either inward or outward at random, the higher multipole terms predominate. Therefore, the potentials would be weaker. However, it must be noted that in the case of a spherical head model, these radially oriented dipoles could not produce external magnetic fields, although they would produce potentials. As a result, switching from synchrony to asynchrony in this specific model would mimic alpha blockage. But it could only do so in the EEG and not the MEG because there would be no external magnetic field. Any more or less realistic MEG models would not be composed of radially oriented dipoles but of tangential dipoles, and these are more numerous in sulci. As we have seen, tangential dipoles within symmetrically folded sheets of cortex could not exhibit blockage in the MEG as a result of desynchronization. Yet alpha blockage is easily seen in real-time MEG recordings.

By extension, it seems likely that desynchronization is also inapplicable to the EEG, provided of course that neurons in fissures make a substantially greater contribution to the EEG than do radially oriented neurons in gyri. To claim otherwise, and to hold that alpha blockage is not caused by a reduction in level of activity of single units, we would be required to argue that alpha blockage in the EEG is caused by desynchronization, while alpha blockage in the MEG is caused by synchronization, an apparently absurd conclusion.

Another related conclusion is that while the single equivalent current dipole model is quite useful in dealing with circumscribed and synchronized regions of cortical activity, it does not do full justice to problems related to the intricate geometry of cortical folds and the statistics of the activities of the generators of the fields. In this case simple field measurements may not be informative, especially since averaging may not reveal the evolution of field patterns over time. However, power measurements do permit time averaging of samples of MEG, and these may reveal invariant spatio-temporal properties. These invariant properties may be related to mental states of subjects as well as the types of stimuli employed. Thus, when subjects engage in some mental tasks and suppression or enhancement of the spontaneous activity of different regions of the brain does occur, then taking differences in field power patterns can make it possible to locate and identify the affected regions.

In principle, the brain may be affected in different ways by sensory stimuli or by mental operations associated with them. Yet not all of the states of the brain may be revealed by straightforward signal averaging. For example, the mere increase or decrease in the level of synchronous activity of a region of the brain could be revealed by averaging MEG activity time-locked to the stimulus. However, if the affected region is asynchronously active it will not contribute to the average response, although it could contribute to mean square field patterns and differences among them. This is consistent with observations that average levels of the 'noise' of some regions of the brain do change in step with evoked responses of the EEG (Kaufman and Price 1967; Kaufman and Locker 1970; Pfurtscheller 1988). If it can be verified in practical situations that both decrements and increments in this background activity may now be traced to specific brain regions, then it would raise the tantalizing possibility of performing genuine functional brain imaging using the MEG to complement similar efforts involving PET.

This work was partially supported by Air Force Office of Scientific Research Grants Nos. AFOSR-90-0221 and F49620-88-K-0004 (L. Kaufman, principal investigator) and by IBM.

We thank Samuel J. Williamson, Yoshio C. Okada, James Moeller and 3 anonymous referees for their careful and critical reading of this paper.

## References

- Barth, P.S., Beatty, J., Broffman, J. and Sutherling, W. Magnetic localization of a dipolar current source implanted in a sphere and a human cranium. *Electroenceph. clin. Neurophysiol.* 63: 260-273.
- Baule, G.M. and McFee, R. Detection of the magnetic field of the heart. *Am. Heart J.*, 1963, 66: 95-96.
- Baumann, S., Rogers, R., Papanicolaou, A. and Saydjari, C. Replicability for localization of the P1, N1 and P2 components of the auditory evoked response in an unselected group of subjects. In: S.I. Williamson, M. Hoke, G. Stroink and M. Kotani (Eds.), *Advances in Biomagnetism*. Plenum Press, New York, 1989: 101-104.
- Costa-Ribeira, P., Williamson, S.J. and Kaufman, L. Method for calibrating a SQUID neuromagnetometer array for locating neural sources in the brain with minimal data. *IEEE Trans. Biomed. Eng.*, 1988, 35: 551.
- Cuffin, B.N. On the use of electric and magnetic data to determine electric sources in a volume conductor. *Ann. Biomed. Eng.*, 1978, 6: 173-193.
- Ducla-Soares, E., Rose, D. and Sato, S. Volume current effects in magnetoencephalography. *Phys. Med. Biol.*, 1988, 33, Suppl. 1: 33.
- Duffy, F.H. *Topographic Mapping of Brain Electrical Activity*. Butterworth, Boston, MA, 1986.
- Duffy, F.H. Clinical use of brain electrical activity mapping. In: G. Pfurtscheller and F.H. Lopes da Silva (Eds.), *Functional Brain Imaging*, Hans Huber, Toronto, 1988: 149-160.
- Fender, D.H. Source localization of brain electrical activity. In: A.S. Gevins and A. Rémond (Eds.), *Handbook of Electroencephalography and Clinical Neurophysiology. Vol. 1. Methods of Analysis of Brain Electrical and Magnetic Signals*. Elsevier, Amsterdam, 1987: 355-399.
- Grynspan, F. and Geselowitz, D.B. Model studies of the magneto-cardiogram. *Biophys. J.*, 1973, 13: 911-925.
- Hämäläinen, M. and Sarvas, J. Feasibility of the homogeneous head model in the interpretation of neuromagnetic data. *Phys. Med. Biol.*, 1987, 32: 91-97.
- Hari, R. and Ilmoniemi, R. Cerebral magnetic fields. *Crit. Rev. Biomed. Eng.*, 1986, 14: 93-126.
- Hobson, J.A. and Steriade, M. Neuronal basis of behavioral state control. In: V.B. Mountcastle, F. Bloom and S.R. Geiger (Eds.), *The Nervous System. Handbook of Physiology, Vol. 4*. American Physiological Society, Bethesda, MD, 1986: 701-823.
- Jackson, D. *Classical Electrodynamics*, 2nd Edition. Wiley, New York, 1975.
- Kaufman, L. and Locker, Y. Sensory modulation of the EEG. *Proc. Am. Psychol. Ass.*, 75th Meeting, 1970: 179-180.
- Kaufman, L. and Price, R. The detection of cortical spike activity at the human scalp. *IEEE Trans. Biomed. Eng.*, 1967, BME-14: 84-90.
- Kaufman, L., Schwartz, B.J., Salustri, C. and Williamson, S.J. Modulation of spontaneous activity during mental imagery. *J. Cogn. Neurosci.*, 1990, 2: 124-132.
- Klimesch, W., Pfurtscheller, G. and Mohl, W. Mapping and long-term memory: the temporal and topographical pattern of cortical activation. In: G. Pfurtscheller and F.H. Lopes da Silva (Eds.), *Functional Brain Imaging*. Hans Huber, Toronto, 1988: 131-142.
- Lehmann, D. Principles of spatial analysis. In: A.S. Gevins and A. Rémond (Eds.), *Handbook of Electroencephalography and Clinical Neurophysiology. Vol. 1. Methods of Analysis of Brain Electrical and Magnetic Signals*. Elsevier, Amsterdam, 1987: 309-354.
- Lopes da Silva, F.H. and Storm van Leeuwen, W. The cortical alpha rhythm in dog: the depth and surface profile and phase. In: M.A.B. Brazier and H. Petsche (Eds.), *Architecture of Cerebral Cortex*. Raven Press, New York, 1978: 319-333.
- Meijs, J.W.F., Bosch, F.G.C., Peters, M.J. and Lopes da Silva, F.H. On the magnetic field distribution generated by a dipolar current source situated in a realistically shaped compartment model of the head. *Electroenceph. clin. Neurophysiol.*, 1987, 66: 286-298.
- Nunez, P. *Electric Fields of the Brain*. Oxford Univ. Press, New York, 1981.
- Nunez, P.L. The brain's magnetic field: some effects of multiple sources on localization methods. *Electroenceph. clin. Neurophysiol.*, 1986, 63: 75-82.
- Okada, Y. Discrimination of localized and distributed current dipole sources and localized single and multipole sources. In: H. Weinberg, G. Stroink and T. Katila (Eds.), *Biomagnetism: Applications and Theory*. Pergamon Press, New York, 1985: 266-272.
- Pfurtscheller, G. Mapping of event related desynchronization and type of derivation. *Electroenceph. clin. Neurophysiol.*, 1988, 70: 190-193.
- Pfurtscheller, G. and Aranibar, A. Event-related cortical desynchronization detected by power measurements of scalp EEG. *Electroenceph. clin. Neurophysiol.*, 1977, 42: 817-826.
- Pfurtscheller, G., Steffan, J. and Maresch, H. ERD-mapping and functional topography - temporal and spatial aspects. In: G. Pfurtscheller and F.H. Lopes da Silva (Eds.), *Functional Brain Imaging*. Hans Huber, Toronto, 1988: 117-130.
- Romani, G.L., Williamson, S.J. and Kaufman, L. Tonotopic organization of the human auditory cortex. *Science*, 1982, 216: 1339-1340.
- Rose, D.F., Sato, S. and Ducla-Soares, E. Subdural electrode as a dipole source for MEG. *Electroenceph. clin. Neurophysiol.*, 1989, 72: 86-90.
- Scherg, M. Fundamentals of dipole source potential analysis. In: F. Grandori, M. Hoke and G.L. Romani (Eds.), *Auditory Evoked Magnetic Fields and Electric Potentials*. Karger, Basel, 1990: 40-69.
- Shepherd, G.M. *Neurobiology*. Oxford University Press, New York, 1988.
- Weinberg, H., Brickett, P., Coolsma, F. and Baff, M. Magnetic localization of intracranial dipoles: simulation with a physical model. *Electroenceph. clin. Neurophysiol.*, 1986, 64: 159-170.
- Wikswow, Jr., J.P. and Roth, B.J. Magnetic determination of a single cortical current source: a theoretical analysis. *Electroenceph. clin. Neurophysiol.*, 1988, 69: 266-276.
- Williamson, S.J. and Kaufman, L. Evoked cortical magnetic fields. In: S.N. Erné, H.-D. Hahlbohm and H. Lubbig (Eds.), *Biomagnetism*. Walter de Gruyter, Berlin, 1981: 353-402.
- Williamson, S.J. and Kaufman, L. Analysis of neuromagnetic signals. In: A.S. Gevins and A. Rémond (Eds.), *Handbook of Electroencephalography and Clinical Neurophysiology. Vol. 1. Methods of Analysis of Brain Electrical and Magnetic Signals*. Elsevier, Amsterdam, 1987: 405-444.
- Yamamoto, T., Williamson, S.J., Kaufman, L., Nicholson, C. and Llinás, R. Magnetic localization of neuronal activity in the human brain. *Proc. Nat. Acad. Sci. (U.S.A.)*, 1988, 85: 8732-8736.

## Spatial extent of coherent sensory-evoked cortical activity

H.-L. Lü and S.J. Williamson

Neuromagnetism Laboratory, Departments of Physics and Psychology, and Center for Neural Science, New York University, New York City, NY 10003, USA

Received March 21, 1990 / Accepted July 16, 1990

**Summary.** Analysis of published values for the depth profile of evoked potentials in primary sensory cortex of cat and monkey provide a consistent estimate for the net current dipole moment per unit area of cortical surface. Comparison with values of the total current dipole moment obtained from neuromagnetic studies on human subjects indicates that coherent neuronal activity giving rise to long-latency sensory evoked components recorded in the human electroencephalogram or magnetoencephalogram extends over a cortical area that is typically 40–400 mm<sup>2</sup>.

**Key words:** Cerebral cortex – Current source-density – Sensory response – Extent of neuronal activity – Current dipole moment – Cat – Monkey

### Introduction

apid progress has been made in the past decade to exploit magnetic and electric techniques for the purpose of providing quantitative information on sensory-related activity of the human cortex. For instance, it is possible to present neuromagnetic techniques to locate the center of auditory-evoked long-latency activity in cerebral cortex with a consistent accuracy of 3 mm (Yamamoto et al. 1988). Comparison with mathematical representations of stimulus-related functional sequences, such as the tonotopic (Romani et al. 1982) and amplitude (Pantev et al. 1988) loci across auditory cortex, suggest that the precision is somewhat better. It is also possible to establish a quantitative measure for the strength of neuronal activity, by using a suitable model for the source. The simplest model is a current dipole whose magnetic field (or potential) pattern across the scalp best matches the measured pattern. The orientation of the model dipole when representing evoked activity of auditory, somatosensory,

or visual areas is generally perpendicular to the cortical surface, implying that the current it represents likely arises from currents of pyramidal cells.

However, at noise levels encountered in typical magnetic measurements, it is not possible to differentiate between magnetic field patterns generated by cortical sources of different spatial extent of activity unless the spread of activity is at least comparable to the distance to the nearest sensor – typically several centimeters (Okada 1985). The extent of cortical involvement is an important issue when considering possible models for neural networks that would account for observed signals. Consider that the just-noticeable difference for pitch in human auditory studies corresponds to a shift of the center of activity by ~10  $\mu$ m along the tonotopic axis, and the just-noticeable difference for loudness to a shift of ~100  $\mu$ m along the (approximately orthogonal) amplitude axis. Then if cortical response strengths were determined experimentally to correspond to an active cortical area on the order of 1 cm<sup>2</sup>, it would be unrealistic to interpret the psychophysical measures as reflecting a columnar organization, with activity limited to the column of best frequency and amplitude. Instead, neuronal populations responding to distinguishable frequencies or intensities must be largely overlapping across cortex.

As a first step toward determining the spatial extent of evoked cortical activity, we have utilized data on current source-density analyses in the somatosensory cortex of macaque monkey to determine the corresponding current-dipole moment that characterizes the activity underlying 1 mm<sup>2</sup> of cortical surface during moments of peak activity. A similar analysis was carried out with published data on visual cortex of the cat. The close correspondence in results prompts us to report these values as a first step toward establishing a quantitative relationship in higher mammals between physiological activity of sensory cortex and macroscopic measures provided by the electroencephalogram (EEG) and magnetoencephalogram (MEG). We also suggest that this measure of cortical activity may well characterize human sensory functions as well.

Offprint requests to: S.J. Williamson (address see above)

## Method

We have analyzed electric potential data obtained by other researchers who employed arrays of microelectrodes extending through the depth of sensory cortex of two animal species – the cat and macaque monkey. For latencies of peak response we compute the net current-dipole moment per square millimeter of cortical surface area. Comparing this with observed values for the total current-dipole moment obtained from neuromagnetic studies of human subjects, we estimate the corresponding area of human cortex that overlies the observed coherent neuronal responses. An earlier study by Okada (Okada 1989) of the neuromagnetic field evoked by electrical stimulation of cells in a slice of turtle cerebellum *in vitro* provides an example where excellent quantitative agreement with only 20% discrepancy is obtained between intracortical potential measurements and the external magnetic field strength on the basis of present theory.

As material we have chosen recent electrophysiological studies of sensory evoked activity of cerebral cortex that characterize with comparatively fine resolution the current source density (CSD) at various depths. The data are those of Mitzdorf (1987) for visual cortex of cat, Mitzdorf and Singer (1979) for visual cortex of macaque monkey, and Cauller and Kulics (1990) for somatosensory cortex of macaque monkey. We shall describe our method by reference to the data of Mitzdorf (1987) obtained in penetrations through visual areas 17 and 18 in cat, which are representative of many close inspections of several thousand CSD profiles. Several stimuli were employed. One was a double reversal of a grating with spatial frequency of 0.5 cycle/deg, presentation time of 100 ms, and

interstimulus interval of 1200 ms. Figure 1a illustrates the depth dependence of the observed field potentials at long latencies recorded at 150  $\mu\text{m}$  intervals within area 17. The corresponding depth profile of the current source-density is shown in Figure 1b. These traces represent the density of current appearing in the extracellular space from the intracellular medium at the indicated depth, as given by the negative of the second derivative of the variation of extracellular potential with depth (Mitzdorf 1987). The methodology of current source-density analysis has been described elsewhere (e.g., Nicholson and Freeman 1975) and will not be reviewed here.

For simple geometries, the predominant source of extracranial magnetic field is the *intracellular* current, as evidenced by the relative polarities of sensory evoked potentials and magnetic fields (Hari et al. 1980) and studies of isolated nerve preparations (Wikswow et al. 1980, Swinney and Wikswow 1980, Plonsey 1981, Roth and Wikswow 1985). The intracellular current flows in the opposite direction to that of the extracellular current. Since the distribution of current source-density was nearly invariant parallel to the laminae, we computed the intracellular current per unit area of cortical surface flowing perpendicular to the laminae at each depth (illustrated in Fig. 1c) by reversing the sign of the current source density, integrating it from the most superficial electrode to the deepest electrode, and multiplying by the conductivity of the medium for translaminar current flow.<sup>1</sup> The net current-dipole moment-density, expressed as the current-dipole moment per square millimeter of

<sup>1</sup> We used the value  $0.5 \Omega^{-1} \text{m}^{-1}$  for the conductivity, which is established with an uncertainty of about  $\pm 15\%$  as reported by Hoeltzel and Dykes (1979)

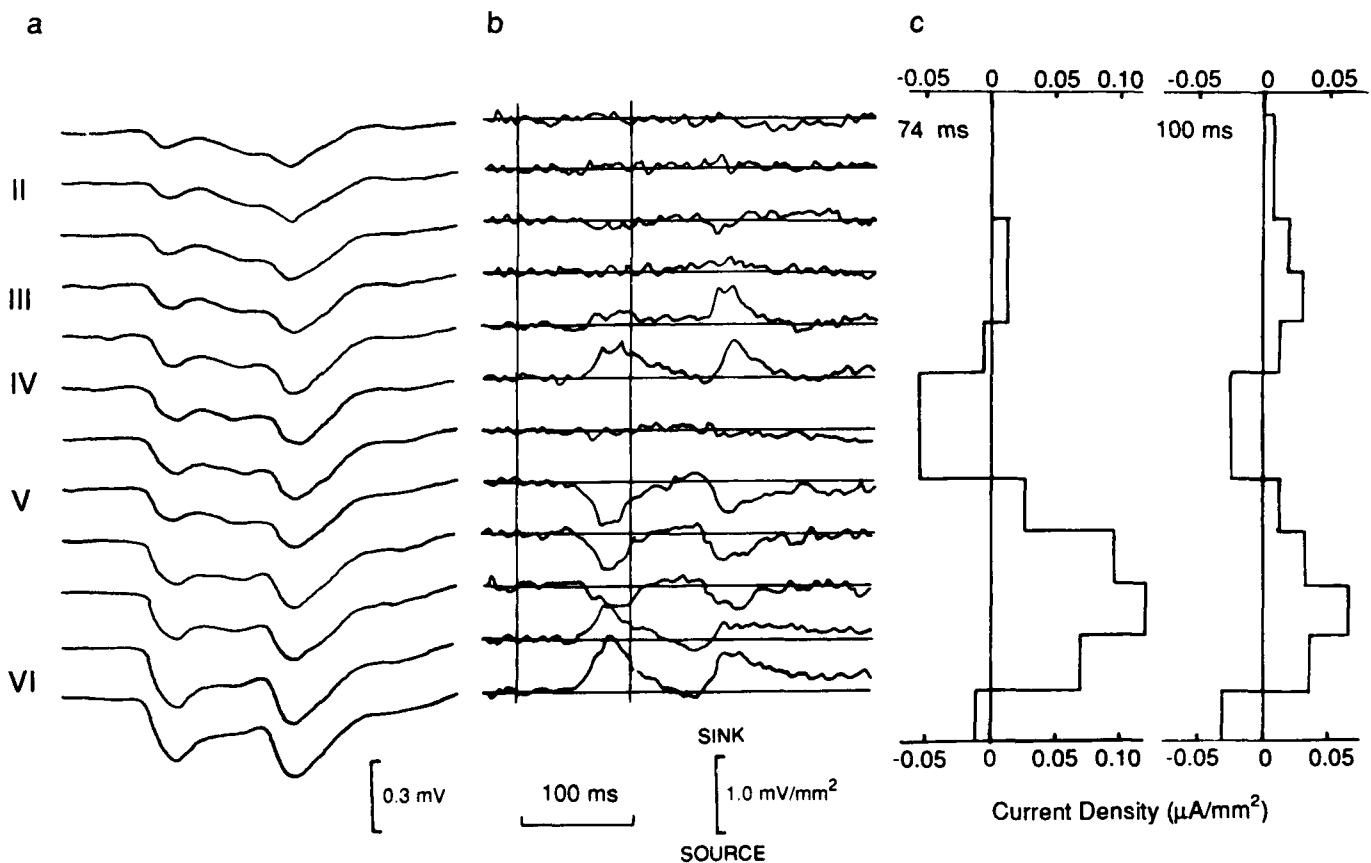


**Fig. 1.** a Field potential measurements shown for 150  $\mu\text{m}$  depth intervals in visual area 17 of cat in a cortical area responding to a double reversal of a grating, with receptive field within the central 3 deg, and b computed current source density profiles in the *extracellular* medium where sinks are indicated by upward deflection, with times of pattern reversal denoted by the two vertical lines

(adapted from Mitzdorf 1987). c Computed profile for the trans-laminar *intracellular* current density, averaged over 150  $\mu\text{m}$  depth intervals for responses at 74 and 100 ms. Integration of current source-density was from surface of cortex to depth, with positive sign indicating current directed toward the surface

cortical surface area, was obtained by integrating this intracellular current density over the same path. As a measure of control, we computed the total current entering the intracellular space and compared it with the total current that leaves, both per unit area of cortical surface. With ideal data and accurate analysis, the two would be equal. The ratio of their difference to the average of the two values is called the "current imbalance", and this value when expressed as a percentage serves as a measure of error in the procedure. Table 1 lists representative values in the third column. The effect of current imbalance on the deduced current-dipole moment-density is obtained by comparing the results of computing the values of the latter in two ways: integrating into the depth of cortex and by integrating from the bottom to the superficial layer. These respective values are shown in the fourth column.<sup>2</sup>

The effects of boundaries separating media of differing electrical conductivity may also contribute to the magnetic field outside the scalp. One such "secondary source" is where the pattern of intracellular current of a neuron is perturbed near the outer surface of its membrane. This has the effect of enhancing the field produced by the intracellular current and has been considered by Okada (1989) in studies of a slice of turtle cerebellum *in vitro*. As this effect appears to provide only a ~10% contribution to the observed field, it will be neglected in our future considerations. Another secondary source is the pial membrane covering the cortical surface. Because the electrical conductivity of cortex is less than that of cerebrospinal fluid outside the membrane, there is a net secondary current source distribution along the membrane pointing in the same direction as the cortical dipole moment. This effect may indeed be very large and produce a field that is comparable to that of intracellular currents, as evidenced by their studies of cerebellar tissue in a bath of physiological saline. However, for cortical sources in sulci and fissures this contribution will be cancelled by an oppositely directed secondary source in the facing sulcal wall (Huang et al. 1990) and therefore need not be considered further.

The present analysis will not distinguish between different cell populations in cortex that contribute to the dipole moment, for instance pyramidal cells of overlapping dendritic trees whose cell bodies lie in different cortical layers. In the following analysis we will consider only the total intracellular current at each depth of cortex. However, we should note that comparisons of extracranial magnetic fields with current source-density profiles during direct electrical stimulation of cortex of rat provide a means of identifying separate contributions (Barth and Sutherling 1988).

## Results

Three sets of current source-density measurements were analyzed. The first to be described are the data of Mitzdorf (1987) for visual areas 17 and 18 of cat. Data for visual area 17 shown in Fig. 1a display three strong components with latencies of about 76, 152, and 228 msec. The most likely reason for obtaining large non-zero values of current imbalance for two of these components, as well as for several other components given in Table 1, is that the array of electrode positions did not properly sample all neuronal sources or sinks, particularly in superficial layers. In addition, typical length constants describing the variation of intracellular current along dendritic branches into the depth of cortex are

A simpler procedure to determine the current-dipole moment-density from the depth dependence of the field potential is to compute the difference in potential between depth and surface and multiply it by the translaminar conductivity. However, this method does not provide a measure of the effect or inaccuracies, unlike the present procedure

about 100  $\mu\text{m}$ , which implies that electrode spacings greater than this will miss details in the transcortical potential profile. This problem is accentuated when the current source-density is computed by taking the second spatial derivative of the profile. Other complications may arise from the influence of efferent and afferent fibres on the local conductivity, but there is no gauge as yet for the magnitude of this effect.

Numerical values for the computed current-dipole moment-density are summarized in the right-hand column of Table 1 for a variety of responses of cat to visual grating stimuli. The units for current-dipole moment-density are expressed as picoampere-meter per square millimeter of cortical surface ( $\text{pA} \cdot \text{m}/\text{mm}^2$ ).

It is noteworthy that markedly greater current-dipole moment-densities may be obtained for direct electrical stimulation. We have analyzed data of Mitzdorf and Singer (1979) on the macaque monkey where electrical stimulation was applied to the optic chiasm. Table 2 shows that the corresponding current-dipole moment-

**Table 1.** Visually evoked responses in the visual cortex of cat. In the right-hand column, the first value for the current-dipole moment-density is obtained by integrating the deduced intracellular current from the most superficial electrode to the deepest and the second value by integrating in the opposite direction. Positive values indicate moment directed toward cortical surface. Analysis of data of Mitzdorf (1987)

Stimulus	Latency (ms)	Current imbalance (%)	Dipole moment per unit area ( $\text{pA} \cdot \text{m}/\text{mm}^2$ )	
			Downward	Upward
Movement of grating <sup>a</sup> (Area 17)	76	15	96	67
	152	32	-104	-48
	228	42	118	24
Movement of grating <sup>b</sup> (Area 17)	141	21	72	37
	193	24	57	38
	259	14	76	49
Double reversal of grating <sup>c</sup> (Area 17)	74	9	35	17
	100	28	-44	-12
	183	50	51	-51
Appearance of grating <sup>d</sup> (Area 18)	80	16	34	74
	100	-30	113	47
	160	17	75	26
	200	0	25	25
Appearance of grating <sup>e</sup> (Area 18)	100	-10	81	54
	500	25	140	62
	560	2	25	31

<sup>a</sup> Receptive field within the central 3 deg for movement (at 13 deg/s) of a rectangular grating (40 × 50 deg) with spatial frequency of 0.2 cycle/deg

<sup>b</sup> As in (a) but for a circular grating of 12 deg diameter

<sup>c</sup> Receptive field within the central 3 deg for double reversal, with 100 ms interval, of a grating with spatial frequency of 0.5 cycle/deg

<sup>d</sup> Receptive field 12 deg eccentric to appearance of a large-area grating (72 deg) of spatial frequency 0.1 cycle/deg at constant average luminance

<sup>e</sup> As in (d) but sparing a region of 22 deg in diameter around the receptive field

**Table 2.** Electrically evoked responses in visual cortex of monkey. Positive values indicate moment directed toward cortical surface. Analysis of data of Mitzdorf and Singer (1979)

Stimulus	Latency (ms)	Dipole moment per unit area (pA · m/mm <sup>2</sup> )
Electrical stimulation	10	400
	12	-140
	14	390

density for a short-latency response is typically about 10 times greater than those for natural stimuli characterized in Table 1. How much of this difference may be attributed to differences between short-latency and long-latency characteristics remains to be determined.

We have also analyzed current source-density studies for the monkey obtained in somatosensory studies by

Cauler and Kulics (1990). Measurements were reported for 200  $\mu\text{m}$  intervals into the depth of cortex at the crown of the postcentral gyrus of two awake monkeys, with special care to ensure that the penetrations were perpendicular to the pial surface (to within 13°). This location corresponds to the projection of hand representations in somatosensory areas 1 and 2. Responses to separate mechanical and electrical stimulation of the receptive field center of the palm or finger were recorded. Figure 2a, b illustrates responses to mechanical stimulation of finger IV. Using these data we computed the percentage current imbalance as described previously for cat, by comparing the difference between the total source and total sink of intracellular current with the average of their absolute values. These imbalances are shown as a percentage in Table 3. Similarly we computed the translaminar intracellular current per unit area of cortical surface, as illustrated in Fig. 3c. Integrating through cortex downward and then upward provides two measures for the

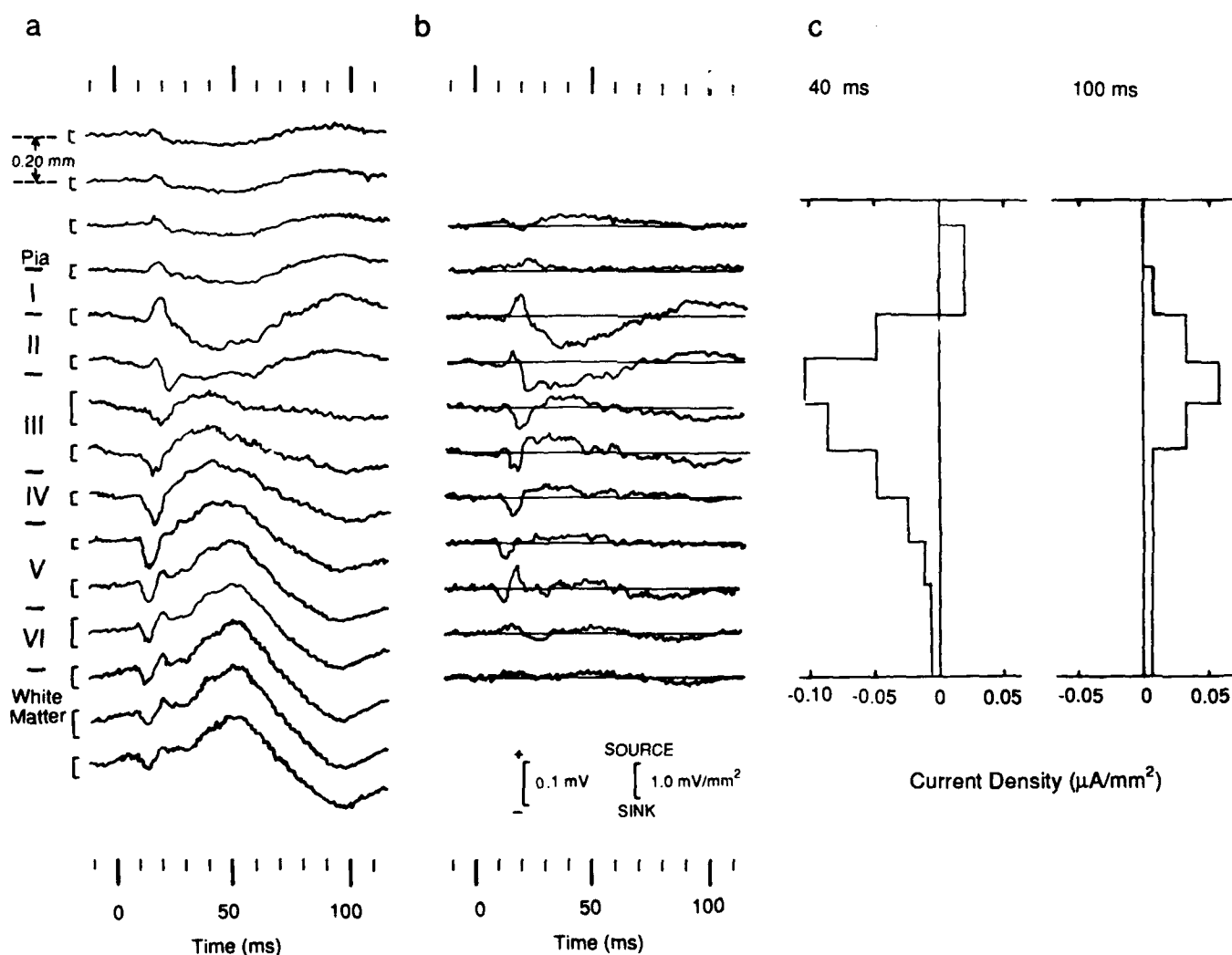


**Fig. 2.** a Field potential measurements at 200  $\mu\text{m}$  depth intervals in somatosensory area SI of monkey, in response to mechanical stimulation of the receptive field center of finger IV, and b computed current source density profiles in the extracellular medium with sinks indicated by downward deflection (adapted from Cauler and

Kulics 1990). c Computed profile for trans-laminar intracellular current density, for 40 and 100 ms latencies. Integration of current source-density was from surface of cortex to the depth, with positive sign indicating current directed toward the surface

**Table 3.** Somatosensory evoked responses in SI cortex of awake monkey. The first value for the dipole moment per unit area is obtained by integrating the deduced intracellular current from the most superficial electrode to the deepest and the second value by integrating in the opposite direction. Positive values indicate moment directed toward cortical surface. Analysis of data of Cauller and Kulics (1990)

Stimulus	Latency (ms)	Current imbalance (%)	Dipole moment per unit area ( $\text{pA} \cdot \text{m}/\text{mm}^2$ )	
			Downward	Upward
Electrocutaneous	40	33	-36	-100
Mulation of thenar	50	12	-63	-108
Pinence	100	17	30	91
Mechanical stimulation	40	17	-76	-121
receptive field center:	50	28	-74	-120
finger IV	100	10	36	22
Electrocutaneous	40	-8	-90	-74
Mulation of receptive	80	-40	20	45
field center:	100	40	-28	-54
of thumb				

Current-dipole moment-density as summarized in the right-hand column of Table 3.

### Discussion

The purpose of this analysis is to determine whether there is sufficient uniformity in the strength of sensory evoked, spatially coherent cortical activity in mammals to establish an estimate for a "typical" level of activity. Although the conclusions we shall draw are based on this limited set of data, the agreement we obtain across the two species and sensory modalities for long latency responses is sufficiently strong to suggest a more general applicability. A useful measure for activity is the current-dipole moment-density representing the integral of intracellular current through the thickness of cortex, per unit surface area. Variability in this measure may be expected, because the number of participating neurons could depend on the task required and also because response strength in sensory cortex, as measured by the total current dipole moment, is influenced by many factors such as attention (Curtis et al. 1988) and adaptation (Amamoto et al. 1988).

Nevertheless, it is remarkable that despite these considerations, the limitations in the accuracy of our analysis, and the fact that data from different species and sensory modalities were included, all of the estimates in Tables 1 and 2 lie within a factor of  $\sim 2$  of the value  $50 \text{ pA} \cdot \text{m}/\text{mm}^2$ . We obtain a more reliable gauge if we direct attention to those values that are established with the highest confidence, viz. to those where the current imbalance is less than 25%. Confining attention to these in Table 1, we take for each condition and latency the range of values computed by integrating upward and downward through cortex. Then the average of the magnitudes across conditions and latencies is  $53 \text{ pA} \cdot \text{m}/\text{mm}^2$

(S.D. = 28). This is remarkably close to the average obtained in the same way for the values in Table 3:  $66 \text{ pA} \cdot \text{m}/\text{mm}^2$  (S.D. = 33). We conclude that a representative value for natural stimuli at suprathreshold levels could be taken as  $50 \text{ pA} \cdot \text{m}/\text{mm}^2$  with an uncertainty of a factor of 2 above and below that value. Enhancement in strength by an order of magnitude is shown in Table 2 for short-latency responses to a stimulus that is not normally experienced, viz. electrical stimulation of white matter in the visual system of monkey.

We now argue that these values for long-latency responses may well be representative of sensory-evoked activity in human cerebral cortex, aside perhaps from the primary visual area. Our justification is the similarity of cell density for cat, macaque monkey, and human. Rockel et al. (1980) concluded that except for visual area 17 of primates there is a basic uniformity in cortical cell density across species. This conclusion was based on observations for a variety of species that about 110 neurons are found in a  $30\text{-}\mu\text{m}$ -wide by  $25\text{-}\mu\text{m}$ -length strip of cortex, from either motor, somatosensory, primary visual, frontal, parietal or temporal areas. About 75% of these cells are pyramidal cells. The only exception to the common neuron count of Rockel et al. occurred in the binocular region of area 17 in primates, where about 2.5 times more neurons were found than in other areas. The comparable level of evoked current-dipole moment-density that we deduce for macaque somatosensory cortex and cat visual areas 17 and 18 suggests further that the neuronal activity levels across these species are similar. We propose therefore that a typical value of  $50 \text{ pA} \cdot \text{m}/\text{mm}^2$  is appropriate for the current-dipole moment-density of long latency components in human cortex as well. The actual value may well be  $\sim 50\%$  greater than this estimate because of the greater thickness of human cortex. This comparative uniformity of cortical response across species may well be limited to stimuli well above threshold, where cortical response levels are insensitive to stimulus strength. When a stimulus is weakened, a level is reached where cortical response begins to decline, and the corresponding current-dipole moment-density may well be species and stimulus dependent. It is important to define these limits by future studies in other species, in primate visual areas where the cell density is higher, and in other sensory modalities. The prospect of establishing quantitative relationships between activity in animal preparations and non-invasive studies of humans should encourage continued development of current source-density techniques. In particular, attention must be devoted to solving the technical problems that appear in the present analysis as a large current imbalance between total intracellular sources and sinks for several temporal components.

Neuromagnetic studies of sensory evoked responses in human cortex reveal typical neuronal activity levels that correspond to a current-dipole moment in the range of  $2\text{--}20 \text{ nA} \cdot \text{m}$  for middle and long-latency responses (for a recent conference proceedings, see Williamson et al. 1989). For the current-dipole moment-density just cited, these values correspond to cortical activation extending over a surface area in the range  $40\text{--}400 \text{ mm}^2$ . A reason-

able estimate for the smallest detectible area is  $\sim 10 \text{ mm}^2$ , based on the weakest current dipole at a shallow depth that can be detected with the sensitivity of contemporary field sensors or electrodes. Since auditory, somatosensory, and visual cortical areas in human each comprise many square centimeters, MEG and EEG techniques are capable of monitoring comparatively confined cortical excitations.

However, even  $10 \text{ mm}^2$  is a much larger area than certain length scales of organization in human cortex. One example is the  $10 \mu\text{m} \times 100 \mu\text{m}$  module that would be required to provide a columnar mosaic across the tonotopic and amplitopic surface of human auditory cortex, if the centers of contiguous columns are spaced by dimensions that are characteristic of just-noticeable differences in pitch and loudness. An important implication of this finding is that neuronal activity in human auditory cortex evoked by the onset of a tone burst is largely overlapping for these close-lying but distinguishable attributes of the stimulus.

It is of some interest to consider the prospect that activity could be observed in such a small region as a macrocolumn of visual cortex, with the dimension of about  $800 \mu\text{m} \times 800 \mu\text{m}$  (Mountcastle 1979). Unfortunately, such an area could produce a current dipole moment that is an order of magnitude too weak to be detected by present magnetic techniques. While the continuing development of magnetic sensors for human studies may ultimately provide this sensitivity, the first success is more likely to come in animal studies where the detection coil can be placed much closer to the neuronal source (Wikswow et al. 1989). A miniaturized sensing system with the detector only 1.5 mm from the exposed cortical surface is expected to provide this advantage (Buchanan et al. 1989).

*Acknowledgements.* We thank U. Mitzdorf for providing helpful information on studies of the cat, and L.J. Cauller and A.T. Kulics for their data on monkey prior to publication. We acknowledge many helpful discussions with L. Kaufman, J.A. Movshon, and C. Nicholson. Research supported in part by Air Force Office of Scientific Research grants F49620-88-K-0004 and F49620-88-C-0131.

## References

- Barth D, Sutherling W (1988) Current source-density and neuro-magnetic analysis of the direct cortical response in rat cortex. *Brain Res* 450:280-294
- Buchanan DS, Crum DB, Cox D, Wikswow JP (1989) MicroSQUID: a close-spaced four channel magnetometer. In: Williamson SJ, Hoke M, Stroink G, Kotani M (eds) *Advances in biomagnetism*. Plenum, New York, pp 677-679
- Cauller LJ, Kulics AT (1991) The neural basis of the behaviorally relevant N1 component of the somatosensory-evoked potential in SI cortex of awake monkeys: evidence that backward cortical projections signal conscious touch sensation, submitted
- Curtis S, Kaufman L, Williamson SJ (1988) Divided attention revisited: selection based on location or pitch. In: Atsumi K, Kotani M, Ueno S, Katila T, Williamson SJ (eds) *Biomagnetism '87*. Tokyo Denki University Press, Tokyo, pp 138-141
- Hari R, Aittoniemi K, Järvinen M-L, Katila T, Varpula T (1980) Auditory evoked transient and sustained magnetic fields of the human brain. *Exp Brain Res* 40:237-240
- Hoeltzel PB, Dykes RW (1979) Conductivity in the somatosensory cortex of the cat: evidence for cortical anisotropy. *Brain Res* 177:61-82
- Huang J-C, Nicholson C, Okada Y (1990) Distortion of magnetic evoked fields and surface potentials by conductivity differences at boundaries in brain tissue. *Biophys J* (in press)
- Mitzdorf U, Singer W (1979) Excitatory synaptic ensemble properties in the visual cortex of the macaque monkey: a current source density analysis of electrically evoked potentials. *J Comp Neurol* 187:71-84
- Mitzdorf U (1987) Properties of the evoked potential generators: current source density analysis of visually evoked potentials in the cat cortex. *Int J Neurosci* 33:33-59
- Mountcastle V (1979) An organizing principle for cerebral function: the unit module and the distributed system. In: Schmidt FO, Worden FG (eds) *The neurosciences, fourth study program*. MIT Press, Cambridge, Ma, pp 21-42
- Nicholson C, Freeman JA (1975) Theory of current source-density analysis and determination of conductivity tensor for anuran cerebellum. *J Neurophysiol* 38:356-368
- Okada Y (1985) Discrimination of localized and extended current dipole sources and localized single and multiple sources. In: Weinberg H, Stroink G, Katila T (eds) *Biomagnetism: applications and theory*. Pergamon Press, New York, pp 266-272
- Okada Y (1989) Recent developments on the physiological basis of magnetoencephalography (MEG). In: Williamson SJ, Hoke M, Stroink G, Kotani M (eds) *Advances in biomagnetism*. Plenum, New York, pp 273-278
- Pantev C, Hoke M, Lütkenhöner B, Lehnertz K (1988) Influence of stimulus intensity on the location of the equivalent current dipole in the human auditory cortex. In: Atsumi K, Kotani M, Ueno S, Katila T, Williamson SJ (eds) *Biomagnetism '87*. Tokyo Denki University Press, Tokyo, pp 146-149
- Plonsey RW (1981) Generation of magnetic fields by the human body (theory). In: Erné SN, Hahlbohm H-D, Lübbig H (eds) *Biomagnetism*. Walter de Gruyter, Berlin, pp 177-205
- Rockel AJ, Hiorns RW, Powell TPS (1980) The basic uniformity in structure of the neocortex. *Brain* 103:221-244
- Romani GL, Williamson SJ, Kaufman L, Brenner D (1982) Characterization of the human auditory cortex by the neuro-magnetic method. *Exp Brain Res* 47:381-393
- Roth BJ, Wikswow JP Jr (1985) The magnetic field of a single axon: a comparison of theory and experiment. *Biophys J* 48:93-109
- Swinney KR, Wikswow JP Jr (1980) A calculation of the magnetic field of a nerve action potential. *Biophys J* 32:719-732
- Wikswow JP Jr, Barach JP, Freeman JA (1980) Magnetic field of a nerve impulse: first measurements. *Science* 208:53-55
- Wikswow JP, Friedman N, Kilroy AW, van Egeraat JM, Buchanan DS (1989) Preliminary measurements with MicroSQUID. In: Williamson SJ, Hoke M, Stroink G, Kotani M (eds) *Advances in biomagnetism*. Plenum, New York, pp 681-684
- Williamson SJ, Hoke M, Stroink G, Kotani M (eds) (1989) *Advances in biomagnetism*. Plenum, New York
- Yamamoto T, Williamson SJ, Kaufman L, Nicholson C, Llinás R (1988) Magnetic localization of neuronal activity in human brain. *Proc Natl Acad Sci USA* 85:8732-8736

**Human Auditory Primary and Association  
Cortex Have Differing Lifetimes For  
Activation Traces**

Zhong-Lin Lü, Samuel J. Williamson\* and Lloyd Kaufman

Neuromagnetism Laboratory,  
Departments of Physics and Psychology  
and Center for Neural Science

New York University

New York City, NY, 10003, U.S.A.

Telefax: 1-212-995-4011

August 29, 1991

\*To whom correspondence should be addressed.

## Summary:

The magnetic field pattern over the temporal area of the scalp 100 msec following the onset of a tone burst stimulus provides evidence for neuronal activity in auditory primary and association cortex that overlap in time. Habituation studies indicate that onset and offset features of a tone produce activation traces in primary cortex that are at least partially common, but only the onset produces an appreciable trace in association cortex. The characteristic time constant for the decay of the latter's activation trace is several seconds longer than for the former.

**Keywords:** Cortical activation trace — Event-related field (ERF) — Event-related potential (ERP) — Habituation — Interstimulus interval (ISI) — Magnetic source image (MSI)

Psychophysical studies of recognition memory for tone pitch provide evidence for a short-term component having a duration of about 2 - 5 sec <sup>24,5</sup>. Behavioral <sup>4</sup> and electrophysiological investigations <sup>22</sup> of auditory memory functions in animals provide evidence that similar short-term memory functions are served by sensory areas of cerebral cortex. We have exploited advantages of magnetic source imaging (MSI) to investigate the retention of stimulus-related information within areas of the primary and association auditory cortex. By measuring the accompanying magnetic field just outside the scalp it is possible to locate active populations of neuronal activity within the human brain <sup>2</sup>. Such studies of sensory areas have provided evidence for functional organizations that are similar to those observed in electrophysiological studies of animal models, such as a tonotopic sequence across primary auditory cortex <sup>19</sup>. We report studies of the 100-ms component of the event-related field for tone-burst stimuli that reveal contributions from primary and association auditory cortex that habituate to different physical aspects of the stimuli. The two areas have different characteristic time constants, which vary considerably across individual subjects. The duration of the activation trace for these components may well reflect the period of time over which an event remains available for processing by working (short-term) memory, although the neural residue of the event need not actually be processed.

Four right-handed adult volunteers served as subjects after providing informed consent. All of the studies were carried out within a magnetically shielded room with the subject comfortably reclined on his side. Bursts of a 1 kHz tone were presented by earphones with a constant interstimulus interval (ISI). They were generated by an Amiga 1000 computer and presented contralaterally via Etymotic Research type ER3-5A earphone, which produced no detectible magnetic artifact. The stimulus duration was 500 msec with a ramp of 12 msec for the onset and offset to enhance spectral purity. The intensity was estimated as 75 db SPL. The magnetic field associated with the response was measured by standard techniques <sup>31</sup> with a neuromagnetometer probe consisting of an array of 5 sensors <sup>29</sup>. With the probe placed at a measurement position over the scalp, the subject was presented with 200 epochs having a short ISI of 1.2 sec and then 100 epochs involving a long ISI of 6 sec. This was repeated in sequence with the probe moved to new locations until the field had been measured at 100-120 different positions over the lateral area of the scalp. The output signal of each sensor is bandpass filtered (0.1-100 Hz) and recorded by a computer. The average auditory evoked field time-locked to the stimulus onset was determined for each run, within a bandwidth of 0.5 to 20 Hz.

Isofield contours were computed to characterize the field pattern over the lateral scalp at a latency of 100 msec for two subjects, for both a short ISI condition of 1.2 sec and long ISI condition of 6 sec. Coordinates are specified in the PPN system <sup>27</sup>. The origin is midway between the periauricular points; the X-axis passes from the origin through the nasion; the z-axis is perpendicular to both X-axis and line between the periauricular points and passes from the origin dorsally to emerge near the vertex; and the Y-axis is perpendicular to both X- and Z-axes and passes from the origin outward through the left hemisphere near the ear canal.

In the short ISI condition (Fig. 1a), field extrema of opposite polarity were identified at the anterior temporal and parietal ends of the lateral sulcus, for all subjects. The field emerges from the scalp in the posterior region and enters in the anterior region, to encircle the neuronal source lying midway between. We denote this component as N100m, the

'm' indicating it is observed magnetically, and identify it with the classic 100-ms component of primary auditory cortex originating from neuronal activity on the superior temporal plane<sup>2,1,16</sup> The location and other parameters of the current dipole source best accounting for its field pattern for three representative subjects are listed in Table 1.

Figure 1b shows the contour map obtained at the moment of peak activity evoked by stimuli with the long ISI. Two features in this plot should be emphasized: (a) The pattern extends to the lower region of the plot near the ear canal where there is no evidence of the classic N100m component and where the latency at the moment of peak field is about 10 msec shorter than that of N100m; (b) The amplitude of the posterior extremum in the long ISI condition is much greater than that displayed at the anterior extremum. The field pattern can be explained if we assume that one field extremum of a second neuronal source overlaps that of N100m in the posterior region, and the other extremum lies near the ear. For convenience we shall refer to the contribution of this second source, which becomes significant only for long latencies with this paradigm, as the *latent* component and denote it by L100m. This terminology is based on the definition of latent as "not apparent but capable of being expressed".

Standard procedures were followed to locate the neuronal sources<sup>28</sup>. The head was modeled by a sphere of uniform conductivity, placed at the center of curvature that describes the inner surface of the skull extending over an area of 5 cm diameter overlying the source, as determined from MRIs<sup>12</sup>. With the position and orientation of the N100m dipole fixed, a subsequent 2-dipole fitting program was employed to deduce the L100m dipole. We assumed the N100m dipole's position and orientation remained unchanged and allowed the program to adjust only its strength and all 5 parameters of the L100m dipole. To obtain a second estimate for the parameters of both sources, the parameter values provided by the first fit were used as an initial estimate for the sources in a two-dipole fitting program, which adjusted the 10 parameters determining the positions and the orientations of both dipoles. The quality of the fit was gauged by computing the square of the correlation between the measured field at each position and the field predicted by the best fitting dipoles. The two procedures yielded results that differ in placement of each source by only 4 mm.

The current dipole parameters describing the individual N100m and L100m neuronal sources are listed in Table 1. Typically, the L100m dipole was found to lie about 2 cm inferior to that of the N100m dipole, as illustrated in the magnetic source images of Fig. 2. While dipole orientations and positions differ between hemispheres, their positions relative to cortical topography are similar. The location of N100m lies within primary auditory cortex, with intracellular current oriented perpendicular to the surface, as expected for post-synaptic responses of pyramidal cells. To our knowledge, neuronal activity giving rise to the L100m component has not previously been localized. Of the six candidate sources that may contribute to N100<sup>14</sup>, the closest to the L100m source is Tb of Wolpaw and Penry<sup>30</sup>. However, this was thought to be radially oriented, whereas the L100m clearly has a strong tangential component.

The more inferior location of L100m places it within the auditory association cortex<sup>15</sup>, with activity extending into the supratemporal sulcus. Using 50 pA·m/mm<sup>2</sup> as an estimation for the current dipole moment per unit area of cortical surface<sup>13</sup>, we deduce the areas of cortical involvement producing N100m and L100m as about 200 mm<sup>2</sup> and 100 mm<sup>2</sup>, respectively. If L100m has a strong radial component of intracellular current (not detected

magnetically) its total area of activity will exceed this estimate.

The field patterns for individual dipoles revealed a location on the scalp where the field has an appreciable contribution from only the N100m source (near the "-200" notation in Fig. 1b) and another location where it was produced by only the L100m source ("-100" in Fig. 1b). By placing the probe at one or the other location, the activity of an individual neuronal source could be monitored. In this way the ISI dependence of the strengths of N100m and L100m responses could be independently measured for the range of ISIs between 0.8 sec and 16 sec, for each subject.

It has long been known that the classic N100 of the event-related potential (ERP) measured at the vertex exhibits refractory properties, so that amplitudes diminish if stimuli are presented sufficiently soon after an identical preceding one<sup>17</sup>. However, these studies did not take account of the presence of L100m and so did not identify the separate contributions of responses having different habituation features. As illustrated in Fig. 3 for both hemispheres of 2 subjects, the amplitude of L100m reaches its asymptotic value at a much longer ISI than that of N100m. To obtain these data, several trials of from 50 to 200 stimuli each were presented with representative ISIs before each main recording session began, since animal studies<sup>25,6,7</sup> revealed that habituation can extend for many minutes or even hours. With this preparation of the subject, stable results could be obtained consistently, both within a session and across sessions on different days.

Weak responses obtained with short ISIs is a characteristic of habituation. This has been demonstrated in studies of animal models where electrodes were placed directly on the auditory cortex<sup>10,20,3,26</sup>. Subcortical as well as cortical processes play important roles in habituation, as recently summarized by Weinberger<sup>21</sup> although receptors do not<sup>11,23</sup>. Such a decrement in response for repeated stimulation is but one of four characteristics of habituation. The other three are increments in response to: presentation of a different stimulus to demonstrate that the response to standards is not a result of a change in the subject's general state (called here "elevated probe response"); presentation of the same stimulus following a period in which stimuli are withheld (spontaneous recovery); and presentation of the same stimulus following an inserted stimulus of a different type (dishabituation). Therefore, responses were recorded and separately averaged for a probe stimulus one octave higher, when inserted between every 5th standard stimulus presented with a 1 sec ISI. The probe stimuli evoked significantly higher averaged N100m and L100m responses than the preceding standards (elevated probe response). Moreover, the following standard evoked a stronger response than if the probe had not been present (dishabituation). If trains of tones presented with 1.0 sec ISI are separated by 5 sec of silence, the averaged responses to the first stimulus of each train is significantly higher than for the others (spontaneous recovery). Therefore, the weak responses characterized in Fig. 3 meet the traditional criteria to be classified as examples of habituation.

We find in all cases that the effect of ISI on response amplitudes can be described adequately by the expression  $A(1 - e^{-(t-t_0)/\tau})$ , where the amplitude  $A$ , time constant  $\tau$ , and time origin  $t_0$  are fitting parameters. We emphasize that the *shape* of the curve in each case is determined by a single parameter  $\tau$ . Table 2 summarizes the corresponding values of the time constants. Each subject's left and right hemisphere responses for a given component have essentially the same respective values. For a given subject,  $\tau$  is significantly shorter for N100m than L100m. However,  $\tau$  varies considerably across subjects, indicating marked

inter-subject differences in habituation characteristics.

Another important feature of the fitted curves shown in Fig. 3 is the difference in time origins  $t_0$  for N100m and L100m responses. The curves for L100m intersect the horizontal axis near the origin, which corresponds to the onset of the previous tone (The data are consistent with  $t_0 = 0$  being the intercept). By contrast, the curves for N100m have their intercepts at the offset of the previous tone. Fig. 3 shows that  $t_0$  is nearly equal to the tone duration. This difference in intercepts provides clear evidence that the N100m is primarily habituated by the offset of the preceding tone and L100m by the onset.

That the offset habituates the N100m onset to the following tone suggests there may be a reciprocal relationship, *viz.* that the onset of a tone habituates the offset response to the same tone. In support of this, Fig. 3 insets show how the offset amplitude increases with tone duration (with a fixed silent period of 500 ms separating tones). The dependence is identical to the increase in amplitude of the onset N100m with increasing ISI, for tones of short duration. The time constants differ by less than 0.3 sec for each subject.

One natural interpretation of the present results is to consider the difference between the maximum response at very long ISI and the observed response at any shorter ISI as a measure for the existing level of the neuronal activation trace that was established by responses to previous stimuli need not be further reactivated<sup>18</sup>. Our data indicate that an adequate empirical description of this difference has the form of a decaying exponential  $Ae^{(t-t_0)/\tau}$ , where  $(t - t_0)$  is the elapsed time since the last activation and the parameter  $\tau$  is the lifetime. When these notions are applied to the habituation characterized by our data, we may infer that decay of the cortical activation trace for L100m commences near the onset of the tone stimulus. This suggests that information processing in the corresponding region of association cortex emphasizes the initial features of the stimulus. By contrast, decay of the activation trace for N100m commences after the onset and again after the offset. This suggests that the activation trace associated with the offset N100m is similar to that for the onset N100m, and both are related to activity in primary cortex. Indeed, Hari *et al.*<sup>9</sup> have shown that both onset and offset N100m responses detected magnetically are in primary cortex, although the center of neuronal activity for the offset on the average is about 7 mm anterior to the onset.

The present study provides evidence that decay of the activation trace in each cortical area can be characterized empirically by a single lifetime for the class of stimuli employed. This is undoubtedly an oversimplification for describing the details of the relevant physiological processes, for  $\tau$  characterizes only the rate-limiting step. Moreover, it is reasonable to expect that the lifetime may well depend on certain physical aspects of a sound.

This research was supported in part by grants F49620-88-K-0004 and AFOSR-90-0221 from the Air Force Office of Scientific Research and by support from Silicon Graphics, Incorporated. We thank N. Chase for support in the MR studies, J. Stephenson for assistance in recording them, D. Karron for contributions in developing computer analyses of MR images, J.-Z. Wang for help with computer systems, E. Vitale for assistance with the experiments, and A. Fregly for helpful encouragement.

## References

- [1] Bak, C., Kofoed, B., Lebech, J., rmark, K. Sæ, and Elberling, C. Auditory evoked magnetic fields from the human brain. Source locatization in a single-dipole approximation. *Phys. Lett.*, 82A (1981) 57-60.
- [2] Brenner, D., Lipton, J., Kaufman, L., and Williamson, S. J. Somatically evoked magnetic fields of the human brain. *Science*, 199 (1978) 81-83.
- [3] Buchwald, J.S. and Humphrey, G.L. An analysis of habituation in the specific sensory systems. In Stellar, E. and Sprague, J.M., editors, *Progress in Physiological Psychology*, Academic Press, New York, 1973, pages 1-75.
- [4] Colombo, M., D'Amato, M.R., Rodman, H.R., and Gross, C.G. Auditory association cortex lesions impair auditory short-Term memory in monkeys. *Science*, 247 (1990) 336-338.
- [5] Crowder, R.G. *Principles of Learning and Memory*. Erlbaum, Hillsdale, 1976.
- [6] Gerken, G.M. and Neff, W.D. Experimental procedures affecting evoked responses recorded from auditory cortex. *Electroenceph. Clin. Neurophysiol.*, 15 (1963) 947-957.
- [7] Hall, R.D. Habituation of evoked potentials in the rat under conditions of behavioral control. *Electroenceph. Clin. Neurophysiol.*, 24 (1968) 155-165.
- [8] Hari, R., Aittoniemi, K., Järvinen, M.-L., Katila, T., and Varpula, T. Auditory evoked transient and sustained magnetic fields of the human brain: Localizaton of neural generators. *Exp. Brain Res.*, 40 (1980) 237-240.
- [9] Hari, R., Pelizzone, M., Mäkelä, J. P., Hällström, J., Leinonen, L., and Lounasmaa, O. V. Neuromagnetic responses of the human auditory cortex to On- and offsets of noise bursts. *Audiology*, 26 (1987) 31-43.
- [10] Horn, G. Physiological and psychological aspects of selective perception. In et al., D.S. Lehrman, editor, *Advances in the Study of Behavior*, Academic Press, New York, 1965, pages 155-216.
- [11] Horvath, R.S. Variability of cortical auditory response. *J. Neurophysiol.*, 32 (1969) 1056-1063.
- [12] Karron, D., Lü, Z.-L., and Williamson, S.J. submitted for publicatiou.
- [13] Lü, Z.-L. and Williamson, S.J. Spatial extent of coherent sensory-evoked cortical activity. *Exp. Brain Res.*, 84 (1991) 411-416.
- [14] Näätänen, R. and Picton, T. The N1 wave of the human electric and magnetic response to sound. *Psychophysiology*, 24 (1987) 375-425.
- [15] Pandya, D.N. and Seltzer, B. Association areas of the cerebral cortex. *TINS*, (1982) 386-390.

- [16] Pantev, C., Hoke, M., Lehnertz, K., Lütkenhöner, B., Anogianakis, G., and Wittkowski, W. Tonotopic organization of the human auditory cortex revealed by transient auditory evoked magnetic fields. *Electroenceph. Clin. Neurophysiol.*, 69 (1988) 160-170.
- [17] Picton, T. W., Hillyard, S. A., and Galambos, R. Habituation and attention in the auditory system. In Keidel, W. D. and Neff, W. D., editors, *Handbook of Sensory Physiology, Vol. 5. Auditory System. Clinical and Special Topics*, Springer-Verlag, Berlin, 1976, pages 343-389.
- [18] Picton, T. W., Woods, D. L., and Proulx, G. B. Human auditory sustained potentials I. The nature of the response. *Electroenceph. Clin. Neurophysiol.*, 45 (1978) 186-197.
- [19] Romani, G. L. and Fenici, R. Study of the human heart conduction system by the biomagnetic technique. In *Proc. U. S.-Italy Symposium on Methods of Noninvasive Diagnosis in Cardiovascular Disease*, Bethesda, MD, November 1982.
- [20] Thompson, R.F. and Spencer, W.A. Habituation: A model phenomenon for the study of neuronal substrates of behavior. *Psychol. Rev.*, 73 (1966) 16-43.
- [21] Weinberger, N.M., Ashe, J.H., Methenate, R., McKenna, T.M., Diamond, D.M., and Bakin, J. Retuning auditory cortex by learning: A preliminary model of receptive field plasticity. *Concepts in Neurosci.*, 1 (1990) 91-132.
- [22] Weinberger, N.M. and Diamond, D.M. Physiological plasticity in auditory cortex: rapid induction by learning. *Progress in Neurobiology*, 29 (1987) 1-55.
- [23] Westenberg, I.S., Paige, G., Golub, B., and Weinberger, N.M. Evoked potential decrements in auditory cortex. I. Discrete-Trial and continual stimulation. *Electroenceph. Clin. Neurophysiol.*, 40 (1976) 337-355.
- [24] Wickelgren, W.A. Associative strength theory of recognition memory for pitch. 6, (1969) 13-61.
- [25] Wickelgren, W.A. Auditory or articulatory coding in verbal short-term memory. *Psychol. Rev.*, 76 (1969) 232-235.
- [26] Wickelgren, W.O. Effect of acoustic habituation on click-evoked responses in cats. *J. Neurophysiol.*, 31 (1968) 777-785.
- [27] Williamson, S. J. and Kaufman, L. Advances in neuromagnetic instrumentation and studies of spontaneous brain activity. *Brain Topography*, 2 (1989) 129-139.
- [28] Williamson, S. J. and Kaufman, L. Analysis of neuromagnetic signals. In Gevins, A. S. and Rémond, A., editors, *Methods of Analysis of Brain Electrical and Magnetic Signals*, Elsevier, Amsterdam, 1987, pages 405-448.
- [29] Williamson, S. J., Pelizzone, M., Okada, Y., Kaufman, L., Crum, D. B., and Marsden, J. R. Magnetoencephalography with an array of SQUID sensors. In Collan, H., Berglund, P., and Krusius, M., editors, *ICEC10: Proc. Tenth International Cryogenic Engineering Conference*, Butterworth, Guildford, England, 1984, pages 339-348.

- [30] Wolpaw, J. R. and Penry, J. K. A temporal component of the auditory evoked response. *Electroenceph. Clin. Neurophysiol.*, 39 (1975) 609-620.
- [31] Yamamoto, T., Williamson, S. J., Kaufman, L., Nicholson, C., and Llinás, R. Magnetic localization of neuronal activity in the human brain. *Proc. Natl. Acad. Sci. USA*, 85 (1988) 8732-8736.

## Tables

Table 1: Parameters describing the location  $x, y, z$ , orientation  $\psi$ , and strength  $Q$  of the current dipole best accounting for the field pattern of the indicated response component.

Subject	Condition	$x(cm)$	$y(cm)$	$z(cm)$	$\psi(degree)$	$Q(nAm \cdot m)$
ZL(Left)	<i>N100m'</i>	-0.9	6.3	6.2	-140	3.3
	<i>N100m</i>	-0.4	6.5	6.4	-143	9.8
	<i>L100m</i>	-2.50	6.6	4.4	-111	2.8
ZL(Right)	<i>N100m'</i>	-0.3	-6.7	6.0	145	4.4
	<i>N100m</i>	-0.2	-7.2	6.2	151	7.3
	<i>L100m</i>	1.0	-6.0	4.2	114	9.1
SW(left)	<i>N100m'</i>	0.8	4.3	5.4	-122	11.4
	<i>N100m</i>	1.2	5.2	5.9	-122	11.4
	<i>L100m</i>	-1.9	6.7	4.2	-94	2.3
WS(left)	<i>N100m'</i>	0.4	6.9	5.9	-168	2.3
	<i>N100m</i>	-0.4	6.6	6.0	-170	6.8
	<i>L100m</i>	-1.8	5.4	4.5	-175	5.3

Table 2: Parameters for the expression  $A(1 - e^{(t-t_0)/\tau})$  that best fit the ISI dependence for the indicated onset response components and tone duration dependence for the offset component. Brackets indicate the durations, and parentheses indicate standard deviations.

Subject	Hemisphere	Condition	A (fT)	$t_0$ (sec)	$\tau$ (sec)
ZL	Left	L100m [0.5 sec]	126 (0.9)	-0.2 (0.4)	5.0 (0.9)
		N100m [0.5 sec]	185 (1.0)	0.2 (0.2)	3.5 (0.4)
		N100m [1.0 sec]	178 (0.4)	0.6 (0.2)	3.5 (0.4)
ZL	Right	L100m [0.5 sec]	155 (0.7)	0.0 (0.1)	5.2 (0.7)
		N100m [0.5 sec]	262 (0.4)	0.0 (0.2)	3.3 (0.3)
SW	Left	L100m [0.5 sec]	154 (0.5)	-0.4 (0.3)	3.9 (0.5)
		N100m [0.5 sec]	150 (0.8)	0.5 (0.1)	1.3 (0.2)
SW	Right	L100m [0.5 sec]	85 (1)	-0.4 (0.7)	3.8 (0.8)
		N100m [0.5 sec]	126 (0.4)	0.4 (0.2)	1.5 (0.3)
		N100m [1.0 sec]	126 (0.7)	1.0 (0.1)	1.3 (0.2)
		N100m [2.0 sec]	98 (0.8)	1.9 (0.2)	1.0 (0.2)

## Figure Caption

**Fig. 1.** Isofield contours for subject ZL characterizing the measured field pattern over the left hemisphere 100 ms following the onset of a tone burst stimulus. Arrows denote the direction of current dipole sources that account for each pattern, with their bases placed at the dipole's surface location. In the right panels, the upper arrow is the N100m source and the lower arrow is the L100m source. Insets illustrate response waveforms obtained at the indicated positions. Both waveforms also exhibit a 200 ms component.

**Fig. 2.** Deduced locations for neuronal sources that are responsible for N100m (upper arrow) and L100m (lower arrow), on sagittal MRIs of the left hemispheres of two subjects. Coordinates are expressed in the PPN system, with a distance of 1 cm between adjacent ticks on the axes. The base of each arrow indicates the respective positions, with the ellipse indicating the estimated range of uncertainty (95% confidence level), and the direction of each arrow specifies the flow of intracellular current. The N100m source lies within the lateral sulcus, and L100m source lies within 1 cm of the superior temporal sulcus.

**Fig. 3.** Response amplitudes *versus* ISI over left and right hemispheres for 2 subjects, for tones of 0.5 sec duration (N100m: squares; L100m: circles), 1.2 sec (N100m: triangles), and 2 sec (N100m: inverted triangles). Insets illustrates the dependence for the N100m offset response for tones of different duration indicated by the horizontal axis.

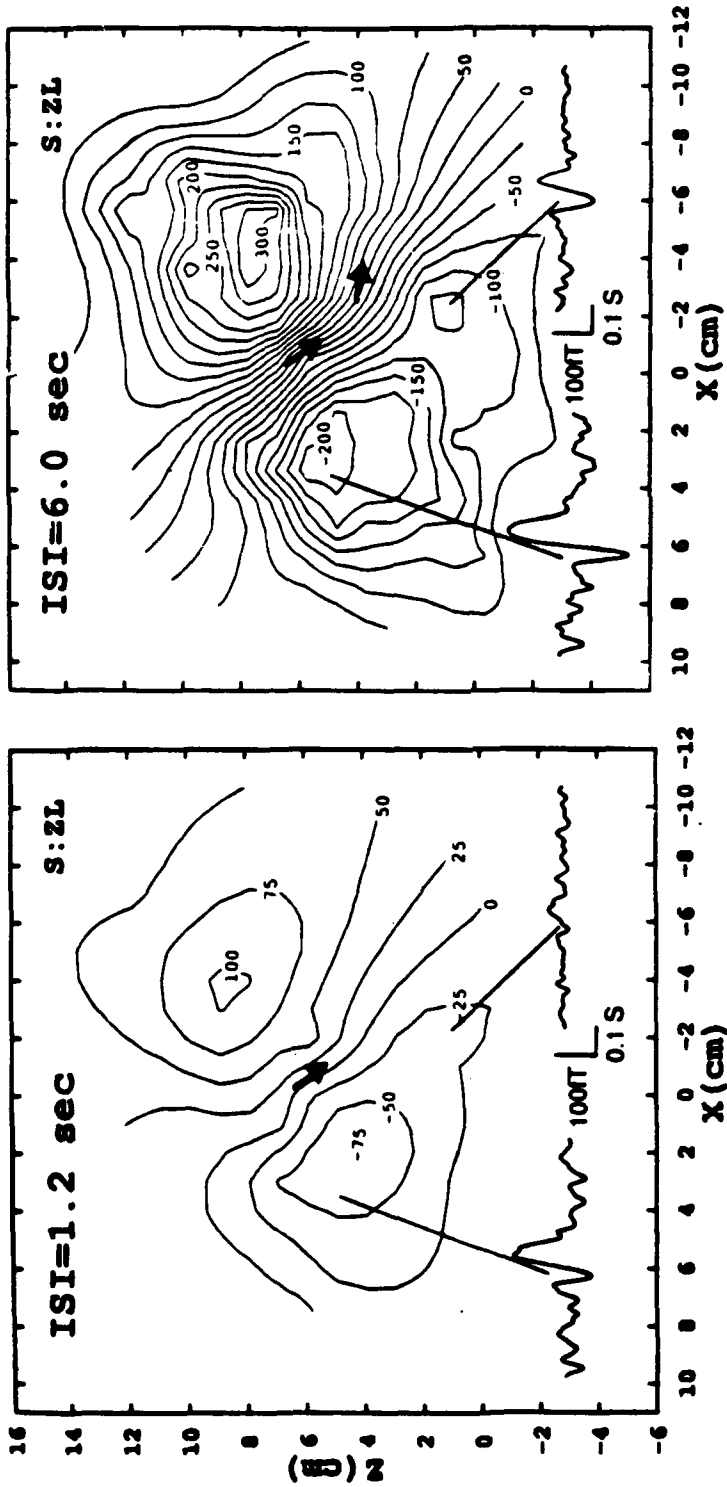
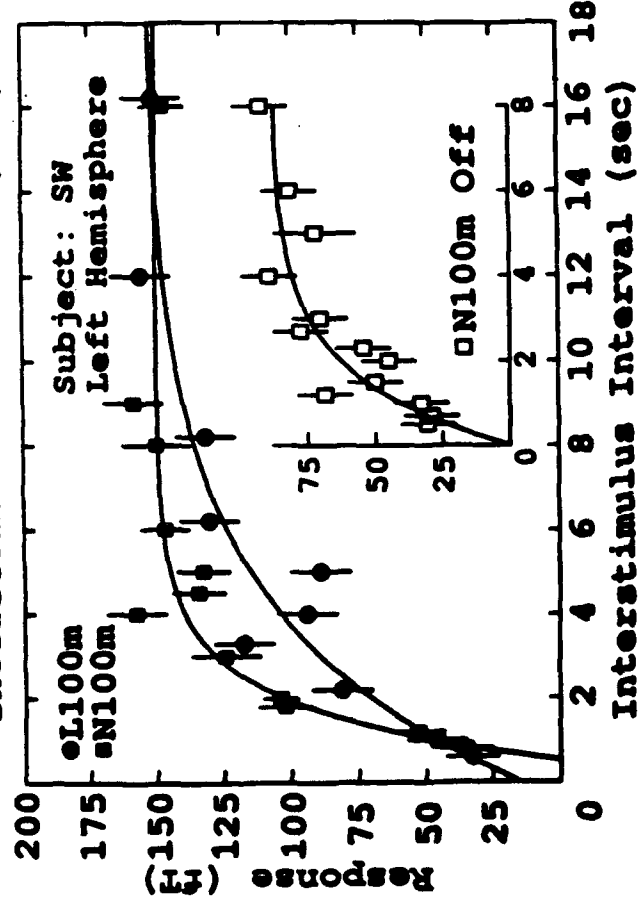
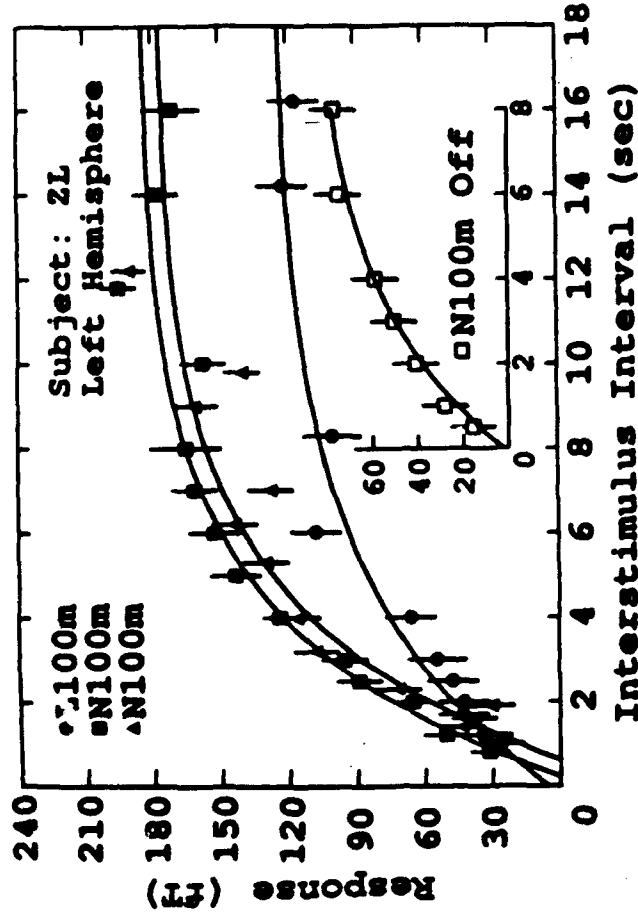
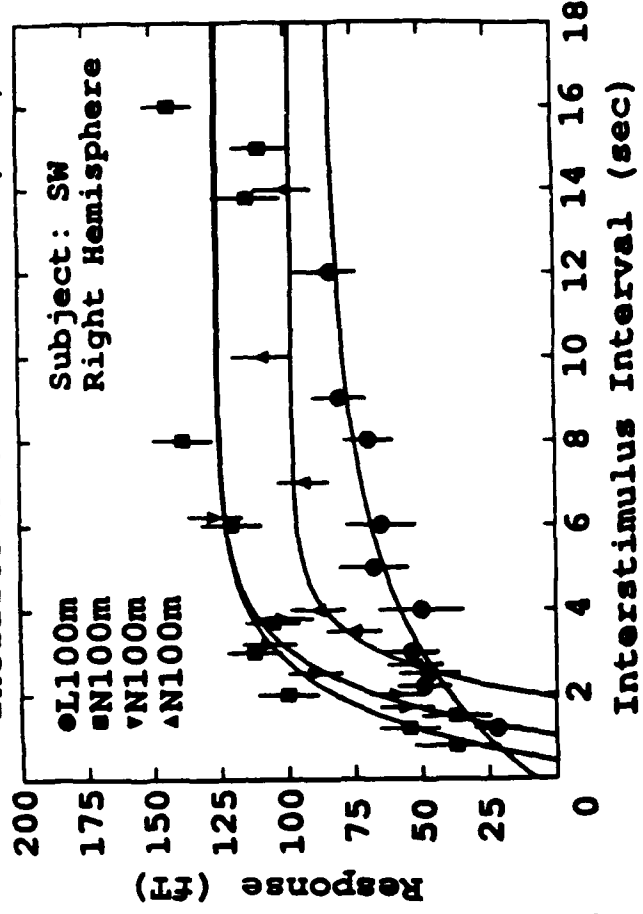
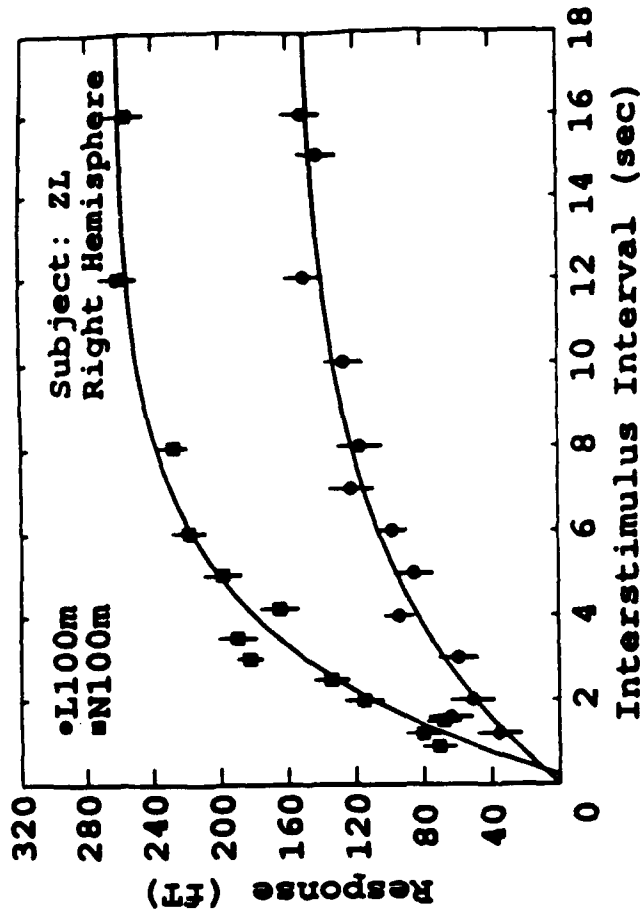


Fig. 1



*Advances in Biomagnetism*

S.J. Williamson, M. Hoke, G. Stroink, and M. Kotani, Editors  
Plenum Press, New York  
Pages 213 - 216

## BRAIN ACTIVITY RELATED TO SPATIAL VISUAL ATTENTION

B. Luber, L. Kaufman, and S.J. Williamson  
Neuromagnetism Laboratory  
Departments of Psychology and Physics and Center for Neural Science  
New York University, New York, NY 10003, U.S.A.

## INTRODUCTION

When attention is directed toward one location in the visual field, electrical potentials evoked by stimuli at that location are enhanced relative to when attention is directed elsewhere (Eason et al., 1969, VanVoorhis and Hillyard, 1977). This enhancement begins about 100 msec after stimulus onset, and components both positive and negative over the next 200 msec are affected. These results led Hillyard and Mangun (1986) to propose that attention modulates a mechanism at the thalamic level which gates neural activity along the pathway which includes the lateral geniculate nucleus in the thalamus and the striate cortex. However, Harter and Aine (1984) suggested that the modulation of ERP components by spatial attention is due to activity in a second visual pathway, following a route which passes through the superior colliculus in the midbrain, the pulvinar nucleus of the thalamus, and the parietal cortex. This proposal was based on anatomical and physiological research on cats and macaque monkeys. Conclusions drawn from ERP research about these theories can only be tentative, given that the poor spatial resolution of scalp electrode measurements often makes it difficult to determine the neural origins of effects of spatial attention on the activity of the brain. In this study, we made use of the high spatial and temporal resolution afforded by measuring the brain's magnetic field in locating the places where focused spatial attention modulates activity in the cerebral cortex.

## METHODS

Three paid right-handed subjects with normal vision, two female and one male, were employed in this experiment. A visual stimulus containing either 2 or 4 parallel vertical bars within a square field 1 deg on a side was presented in random sequence above the horizontal meridian, either 5 deg to the left or to the right of a central fixation point. The bars were alternating black and white, each slightly less than one order of magnitude below and above a background gray luminance of  $0.68 \text{ cd/m}^2$ . The 4-bar pattern had a 20% probability of occurrence. All bar patterns were presented for 34 msec with a random ISI of 1100 msec mean and 250 msec SD. Stimuli were generated using a Commodore Amiga computer, and projected into a magnetically-shielded room with an Electrohome color projection system. The subject was seated facing the projection screen and was instructed to maintain fixation on a small cross while attending to either the right or left field. Subjects depressed a button whenever the 4-bar pattern appeared in the field to which attention was being paid. Presentations continued until at least 100 stimuli had occurred on each side. This procedure was then repeated, with the subject instructed to attend to the stimuli in the other field.

Magnetic field measurements were made using a multisensor probe incorporating 5 SQUID-based second-order gradiometers, each having a 1.5 cm coil diameter and a 3.4 cm baseline between adjacent coils. The outputs of the SQUID electronics were bandpassed between 0.1-50 Hz and then sampled by an HP9000 Model 350 computer at a rate of 128/sec. Sampling began 100 msec before stimulus onset and continued over a 700 msec recording epoch. Recorded data were digitally filtered from 2-30 Hz, and recorded epochs were averaged selectively by stimulus location across

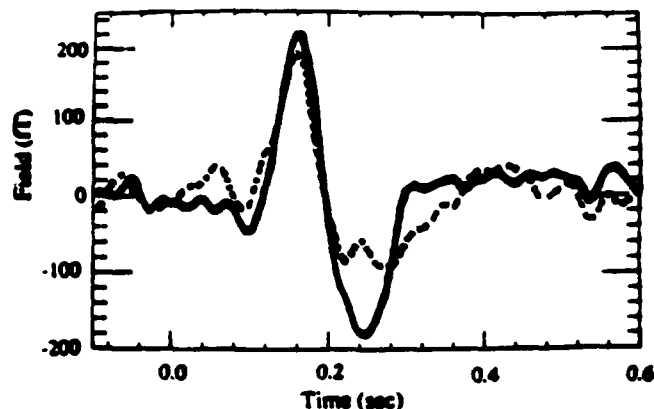


Fig. 1. Time courses of averaged responses to stimuli in the right visual field in attended (solid line) and unattended (dashed line) conditions, obtained over the occipital area of the scalp. Stimulus onset is at 0 seconds.

both 2 and 4 bar patterns. Reaction time and accuracy data were also recorded and analyzed.

Measurements were made over the entire posterior region of each subject's head. In the case of subject SS, recordings were made from 34 probe positions, resulting in 170 spatially separate measurements. For subjects BR and JV, 48 and 19 probe positions were used, providing measurements from 240 and 95 locations, respectively. Sensor positions and orientations relative to a head-based coordinate system were determined by the PPI system (Biomagnetic Technologies, Inc.).

Isofield contour maps were constructed in the following way. Magnetic field amplitudes at a selected instant in time were retrieved from the averaged data along with their associated sensor positions. Data from across the occipital and parietal regions of the scalp were transferred onto a two-dimensional surface using an azimuthal equal distance projection. According to this scheme, the midpoint between periauricular positions of the head was taken as the center of a sphere; and distances from this origin along any great circle were indicated by the same distances from the origin across the flat graph. These data were used by a program which performs Laplacian and spline interpolations and generated isofield contour maps.

## RESULTS

Typical time series of responses to the attended and unattended stimuli presented in the right visual field are shown in Figure 1 for subject SS. There is a strong resemblance between the field patterns and response strengths for both the attended and unattended stimuli until about 200 msec after the onset of the stimulus. Between 200 and 360 msec, the strength of response to the attended stimulus is strongly enhanced relative to the response to the unattended stimulus. This is a common feature of the difference in waveforms between attention conditions in all three subjects: early similarity in amplitude up to about 150 to 210 msec after stimulus onset, followed by increasingly marked differences in amplitude and, in some cases, component structure, over the next 150-200 msec.

Examples of contour maps are given in Figures 2 and 3. Figures 2a and 2b represent the field patterns 150 msec after stimulus onset for the attended-right and unattended-right location, respectively for subject SS. There is no significant difference between main features of the patterns. Overall pattern and field amplitudes reflect similar underlying neural activity at this latency. This is to be contrasted with Figures 2c and 2d, which represent the field for the same situation at a latency of 252 msec. At this time, field amplitudes in the attend case are much larger and contribute to a more well-defined structure than in the unattended condition.

Figure 3 presents data analogous to Figure 2, this time for subject BR's responses to stimuli in the left visual field. Field patterns at 173 msec latency are quite similar over attended and unattended conditions. At 228 msec, this situation changes, once again with field amplitudes in the attended case (3c) much larger than in the unattended (3d).

In Figures 2c-d and 3c-d it can be seen that the fields, while remaining strong, have become difficult to interpret in terms of a simple dipolar pattern. This is true of the field maps for all three

subjects over the 200-350 msec range. Strong peaks often emerge over parietal and temporal regions many centimeters from occipital locations where earlier peaks occurred. While it is difficult to interpret these field patterns in terms of dipolar sources, their widespread nature does suggest extrastriate neural activity. It is interesting to note that the time at which the field patterns begin to become increasingly complex appears to be quite similar to the onset latency of attention effects.

Further analyses revealed other properties of the spatial attention effect on neural activity. The data can be averaged not only by spatial position, but also by the identity of the stimulus as a target or a non-target. The resulting waveforms show no differences in responses until about 275 msec after stimulus onset. Neural activity modulated by spatial attention prior to this latency does not discriminate between target and non-target stimuli, implying that the effect is solely due to spatial location.

## CONCLUSIONS

Using a similar paradigm in the auditory domain (Curtis, Kaufman and Williamson, 1988), components with sources in the primary auditory cortex as early as 100 msec reveal strong effects of attention. Unlike that study, here attention did not strongly affect the neuromagnetic response to visual stimuli until about 150-210 msec after stimulus onset. This is well after at least the first component of cortical response has occurred. Furthermore, analyses of target/non-target stimuli imply that the manipulation of spatial location alone modulates responses at least until 275 msec. These results suggest that in this study mechanisms of spatial attention have their effect on cortical processing over a period of 100 msec or more, beginning only after that processing has been underway for as long as 100 msec. This result was not found by VanVoorhis and Hillyard (1977). In grand average waveforms over twelve subjects, they found that a similar manipulation of spatial attention resulted in the enhancement of ERP components as early as 100 msec after stimulus onset. One

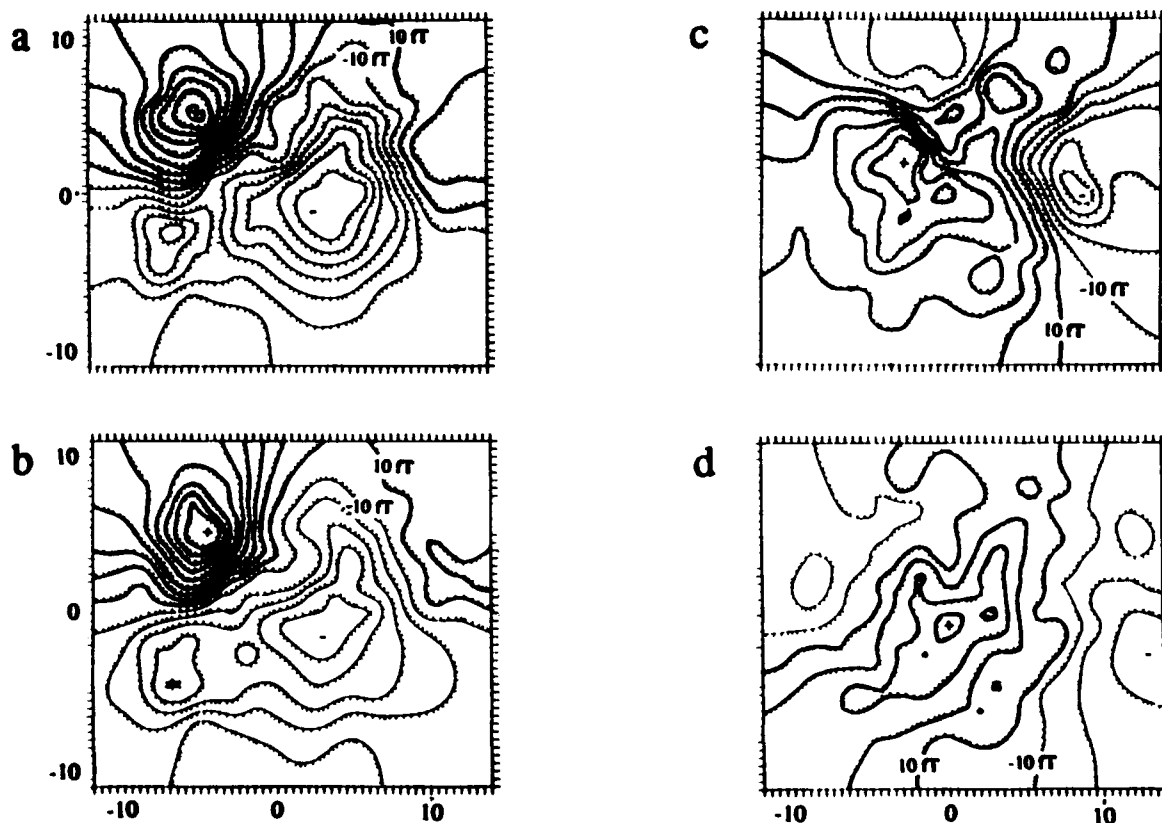


Fig. 2. Isofield contour maps over occipital area of subject SS for: 150 ms field pattern when (a) attended and (b) unattended; 252 ms field pattern when (c) attended and (d) unattended. The origin of each projection is approximately on the midline (which extends vertically along  $x=0$ ) of the scalp about 3 cm above the inion. Isofield contours are drawn in 20 fT increments and distances are in cm. An extremum of the emerging field is indicated by +.

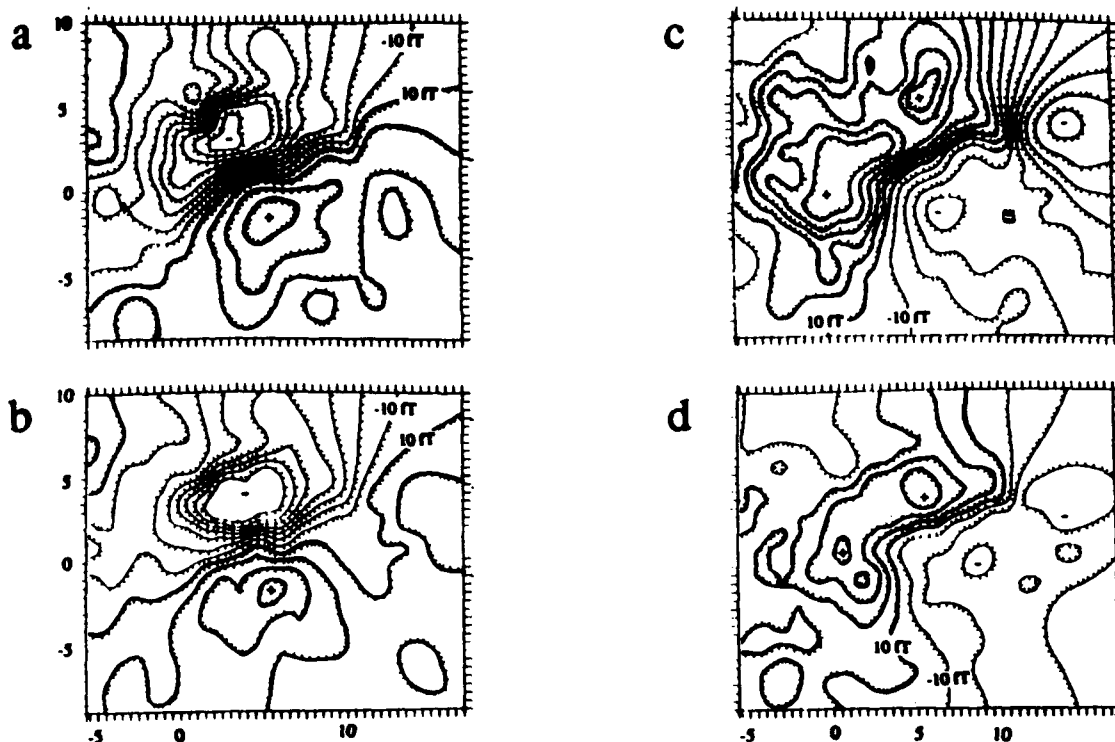


Fig. 3. Same as in Figure 2, for subject BR. Field patterns at 173 ms when (a) attended and (b) unattended; and at 228 ms when (c) attended and (d) unattended.

major difference in the two studies is that luminance increments were used in stimuli in the Van-Voorhis et al. research, while stimuli of approximately constant luminance were used in this study. Entoptic stray light from these increments could contaminate ERP data with unintended responses from other regions of the retina, including the fovea. We suggest the effect of this parameter requires further investigation. Of course, since scalp electrodes may be more sensitive to relatively distant sources than is the magnetic field measuring instrument, the early effects of attention may well be due to activity of sources far from the visual areas. Both alternatives need further study.

#### ACKNOWLEDGMENTS

We thank G. Sperling and B.J. Schwartz for helpful discussions. This research was supported in part by Air Force Office of Scientific Research Grants F49620-88-K-0004 and F49620-88-C-0131.

#### REFERENCES

- Curtis, S., Kaufman, L., and Williamson, S.J. (1988). Divided attention revisited: selection based on location or pitch. In: Atsumi, K., Kotani, M., Ueno, S., Katila, T., and Williamson, S.J., Eds., *Biomagnetism '87*. Tokyo Denki University Press, Tokyo, pp. 138-141.
- Eason, R., Harter, M., and White, C. (1969). Effects of attention and arousal on visually evoked cortical potentials and reaction time in man. *Physiology and Behavior* 4, 283-289
- Harter, R.H., and Aine, C.J. (1984). Brain mechanisms of visual selective attention. In: Parasuraman, R., and Davies, R., Eds., *Varieties of Attention*. Academic Press, New York, pp. 293-321.
- Hillyard, S.A., and Mangun, G.R. (1986). The neural basis of visual selective attention: A commentary on Harter and Aine. *Biological Psychology* 23, 265-279
- Van Voorhis, S., and Hillyard, S.A. (1977). Visual evoked potentials and selective attention to points in space. *Perception and Psychophysics* 22, 54-62.

# Magnetic localization of neuronal activity in the human brain

(neuromagnetism/cortical activity/superconductivity quantum interference device)

T. YAMAMOTO\*<sup>¶</sup>, S. J. WILLIAMSON\*<sup>†</sup>, L. KAUFMAN\*<sup>‡</sup>, C. NICHOLSON\*, AND R. LLINÁS\*<sup>§</sup>

\*Department of Physiology and Biophysics, New York University Medical Center, New York, NY 10016; and Departments of <sup>†</sup>Physics and <sup>‡</sup>Psychology, New York University Faculty of Arts and Sciences, New York, NY 10003

Contributed by R. Llinás, August 10, 1988

**ABSTRACT** The performance of a cryogenic system that monitors the extracranial magnetic field simultaneously at 14 positions over the scalp has been evaluated to determine the accuracy with which neuronal activity can be located within the human brain. Initially, measurements were implemented on two model systems, a lucite sphere filled with saline and a model skull. With a magnetic field strength similar to that of a human brain, the measurement and analysis procedures demonstrated a position accuracy better than 3 mm, for a current dipole 3 cm beneath the surface. Subsequently, measurements of the magnetic field pattern appearing 100 ms after the onset of an auditory tone-burst stimulus were obtained in three human subjects. The location of the current dipole representing intracellular ionic current in active neurons of the brain was determined, with 3-mm accuracy, to be within the cortex forming the floor of the Sylvian fissure of the individual subjects, corresponding closely to the Heschl gyrus as determined from magnetic resonance images. With the sensors placed at appropriate positions, the locations of neuronal sources for different tone frequencies could be obtained without moving the recording instrument. Adaptation of activity in human auditory cortex was shown to reveal long-term features with a paradigm that compared response amplitudes for three tones randomly presented.

Locating neuronal activity within the human brain by measuring the concomitant extracranial magnetic field pattern has been a laborious procedure with single-sensor instruments. Typically, 40 or more positions must be sequentially measured over the scalp, which may take as long as 6 hr to complete. The development of multisensor systems (1-4) made it possible to improve the efficiency of this process, an advance that is of considerable importance for both clinical and research applications. We have installed, at the New York University Medical Center, a commercially available 14-sensor system (Biomagnetic Technologies, San Diego, CA) representing state-of-the-art performance and have evaluated techniques to locate accurately the three-dimensional position of neuronal activity within the human brain (the 14-sensor system consists of two model 607 neuromagnetometers).

The effectiveness of these systems has been evaluated through measurements on two types of carefully designed physical models or "phantoms" (a lucite sphere and a plastic skull), both containing a conducting fluid in which an electrical current dipole was placed at a known position. Measurements were made with field strengths at physiological levels (500 fT); this is an important distinction between this and prior studies (5, 6). To determine the relevance of such localization to human measurements, we investigated the auditory-evoked magnetic field for tone bursts and compared the deduced locations of neural activity with the particular

anatomical features of each individual as revealed by magnetic resonance images (MRIs). We then implemented a procedure that permitted source localization without having to move the sensors, a method that greatly speeds the process and allows this technique to be routinely applicable to clinical research and diagnostics for the first time. To illustrate a use of this methodology, we studied an adaptation phenomenon and demonstrated that reduction of signal strength is not a consequence of the cortical shifting to a different location or position but is a modulation of amplitude of a given population of neurons.

We chose to study the auditory modality of human subjects because neuromagnetic measurements have revealed interesting spatial organizations of functions not previously observed in humans—e.g., tonotopic map (7, 8) and amplitopic map (9). There is considerable interest in determining whether these features can be identified with activity in the auditory cortex. Despite numerous electrical (10) and magnetic (11-17) experiments involving this modality, variations in the cortical anatomy across subjects have not yet been shown to affect these measures. It should be noted that localization of equivalent current dipole sources for interictal epileptiform activity based on neuromagnetic measures has agreed with the positions of large lesions seen in computerized tomography (CT) scans (18-20), but even in these cases there was no *a priori* knowledge that the activity should be associated with the particular area of the lesion.

Obtaining the position of a localized source from a field map across the scalp is conceptually simple if neuronal activity is sufficiently well confined to enable it to be modeled as an equivalent current dipole, representing the net orientation and strength of current. The methods for locating such a source have been summarized (21). The procedure is particularly simple when the head may be modeled by a conducting volume of special symmetry, such as a sphere where electrical conductivity depends only on the distance from the center. Since the magnetic field loops around the axis of the dipole, there is one region of the head where the field emerges and another where it enters. The source lies below the center of the pattern, and its depth is determined by the ratio of the distance between the two extrema of the radial field component and the radius of the head. The deeper the source, the greater the distance between field extrema. When the spherical model is applied to a human head the sphere is chosen to characterize the curvature of the inner surface of the skull overlying the approximate position of the dipole. The choice of this criterion was motivated by predictions of numerical modeling that only the conducting medium of the brain need be taken into account, for the currents that diffuse through the skull are too weak to affect appreciably the measured field (22). Moreover, the region of

Abbreviations: MRI, magnetic resonance image; PPI, probe position indicator; SQUID, superconducting quantum interference device.

<sup>¶</sup>To whom reprint requests should be addressed.

<sup>§</sup>Present address: Department of Otolaryngology, Faculty of Medicine, Kyushu University, Fukuoka, 812, Japan.

the skull directly over the source appears to provide the greatest effect on the external field pattern (23).

## METHODS AND RESULTS

**Magnetic Sensing System.** The neuromagnetic measuring system consists of (Fig. 1A) a magnetically shielded room to reduce the effect of ambient field noise and radio frequency signals, two cryogenic dewars holding liquid helium in which the magnetic sensors are suspended, gantries to support the dewars from the ceiling of the shielded room, a probe position indicator (PPI) consisting of a transmitter on each dewar and set of three receivers placed on a band about the subject's head to determine the position and orientation of the sensors with respect to the head, and a bed or chair for the subject. Each dewar contains a set of seven sensors whose detection coils (Fig. 1B) are oriented so they point to the approximate center of the subject's head. The bottom of each outer coil is mounted 2 cm from the axis of the center coil. Each detection coil has the geometry of a second-order gradiometer (three coaxial coils connected in series, the center coil having twice as many turns as the bottom and top coils, and wound in the opposite sense) to further reduce the effect of residual magnetic noise within the shielded room. The diameter of the detection coil is 1.5 cm, and the baselength between adjacent coils is 3.7 cm. The detection coil is coupled to a superconducting quantum interference device (SQUID) located higher in the dewar and the SQUID's response to a field is monitored by a set of room temperature electronics whose voltage output is proportional to the net magnetic flux threading the detection coil. The system, therefore, responds to signals within the bandwidth from dc to several kilohertz. A complement of amplifiers and bandpass filters process the signals from the set of 14 SQUIDs before recording on a computer. An additional four SQUIDs and detection coils are included in each dewar to further reduce field noise by adaptive filtering procedures, but they were not needed for the studies reported here.

**Head-Based Coordinate System.** All measurements were referred to a three-dimensional coordinate system based on the subject's periauricular points and nasion. The axes of this system are defined by touching these positions in turn with a stylus connected to the PPI. The origin of the head-based system is defined as the midpoint between the periauricular

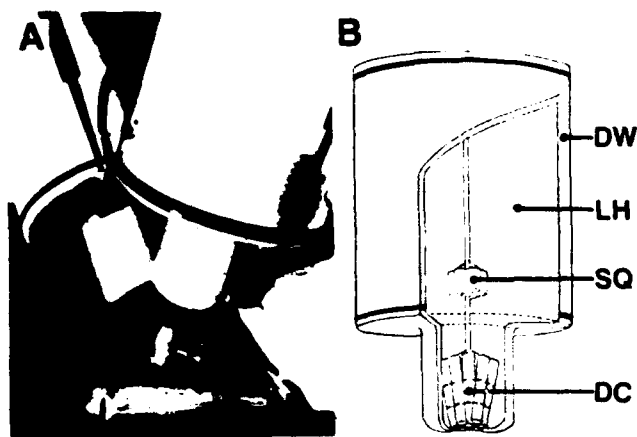


FIG. 1. (A) Neuromagnetic system located in a magnetically shielded room. Two dewars are suspended over the subject's head in the positions used to record activity of auditory cortex of the left hemisphere. (B) Each dewar (DW) contains liquid helium (LH), seven SQUIDs (SQ), and respective detection coils (DC). Detection coils are wound of superconducting wire and supported by an insulating mount so they all point to a position that is close to the center of the subject's head.

points. The  $x$  axis is defined as the line from the origin that passes through the nasion. The  $z$  axis is defined as the line passing upward from the origin in a direction that is perpendicular to the plane defined by the  $x$  axis and the line joining the periauricular points. Finally, the  $y$  axis is defined as the line passing out of the left side of the head from the origin, lying perpendicular to the  $x$  and  $z$  axes. All sensor measurement positions about the head are specified in this head-based system by the PPI.

**Model Sphere.** The first evaluation of this system was carried out through measurements of the field pattern from a current dipole placed within a spherical conductor (Fig. 2A). A Lucite sphere with an inner radius of 10.5 cm and a thickness of 2 mm was filled by a saline solution, and a hole through the bottom permitted an insulating rod to be inserted and held at various positions inside. Attached to the rod was a tightly twisted pair of insulated fine wires whose end segments formed the top of a "T" at the end of the rod, with tips exposed to permit current to flow into the solution. This provided a current dipole 5 mm long. The current ( $58 \text{ nA} \cdot \text{m}$ ) was sufficient to produce a peak field at the sphere's surface of about 500 fT. A Velcro band attached three PPI receivers to the sphere at widely separated noncolinear positions. The PPI stylus was touched to positions marked on the sphere representing the periauricular points and nasion, and these were recorded automatically to establish a head-based coordinate system. The two dewars were oriented at about  $30^\circ$  and  $45^\circ$  from the vertical so their sensors could monitor fields on opposite sides of the dipole. A sinusoidal current (10 Hz) was passed through the current dipole, and the corresponding magnetic field was averaged for 1000 periods. The bandwidth of recording was 1–50 Hz. After each measurement, the sphere was turned about a vertical axis so measurements could be made at another pair of positions. The PPI automatically computed the new positions of each sensor in head-based coordinates.

To obtain a qualitative appreciation of the field pattern, an isofield contour map was produced, with minimal smoothing defining the contours (Fig. 2B). The classic field pattern of a current dipole was obtained with a region of outward directed field and another of inward directed field on opposite sides of the dipole. Some irregularity in the contours came from the fact that not all of the sensors are oriented radially for each position. While this affected the smoothness of the contours, it did not affect the accuracy of the program that determines the location, orientation, and moment of the current dipole; since the program takes into account the actual orientation of the sensor with respect to the surface of the sphere.

This procedure was repeated 32 times over a 1-month period to determine the reproducibility of the method. The corresponding deduced positions of the dipole are compared in Fig. 2C with the actual position obtained from x-rays of the setup. All of the positions lie within 3 mm of the actual source position.

**Model Skull.** To confirm the above measurements by using a non-radially symmetric model, a similar procedure evaluated the accuracy of locating a current dipole within a model skull. The model consisted of a plastic skull whose eye sockets and lower edge were sealed to contain a saline solution. A current dipole was inserted upward from the base, to lie approximately 3 cm beneath the skull in the left posterior frontal area. The shape of the outer surface of the skull over a circular area with a radius of approximately 5 cm centered over the dipole was digitized with the PPI stylus. The position was determined by computer for the center of the best-fitting sphere to model the cranium. Magnetic measurement procedures were similar to those for the sphere just described, except that the individual dewars were moved from one place to another to record field values. Approximately 63 sensor positions were recorded in a session. This

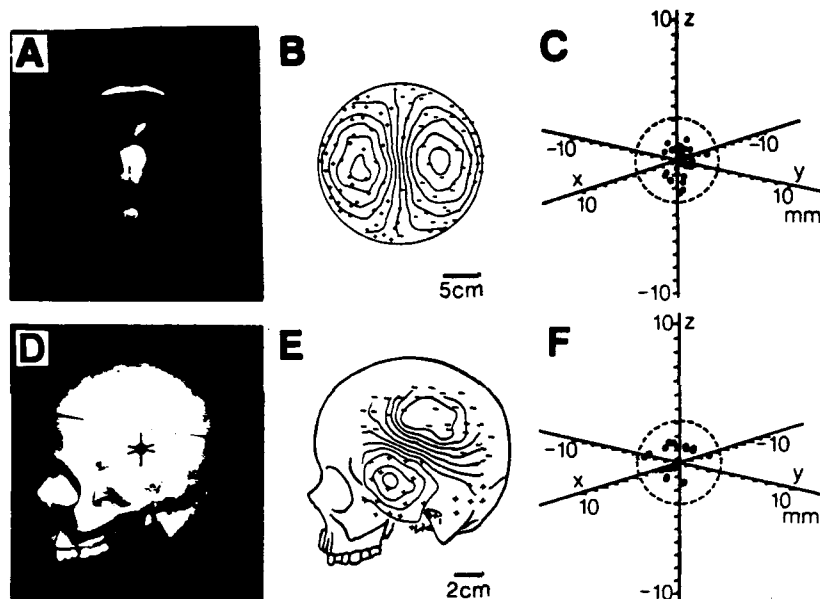


FIG. 2. (A) Lucite sphere with current dipole supported by a rod inside it. (B) Isofield contours at 100-fT intervals obtained from field values measured at locations denoted by + (field entering the surface) and - (field emerging from the surface). (C) Corresponding deduced locations of the current dipole for 32 sets of measurements, with the origin denoting the actual location of the dipole. (D) Plastic model skull with an indication of the position above a current dipole held inside. (E) Isofield contours at 100-fT intervals projected onto the skull to illustrate the area over which measurements were obtained. (F) Corresponding deduced locations of the current dipole for 22 sets of measurements, with the origin denoting the actual location of the dipole.

was repeated 22 times over a period of several days. A representative isofield contour map is shown in Fig. 2E in relationship to the skull. The accuracy in determining the location of the dipole was virtually the same (Fig. 2F) as for the sphere described earlier. All the deduced locations lie well within 3 mm of the actual location determined by computerized tomography scans.

**Auditory Evoked Responses.** The third study in this series assessed the accuracy of this procedure in locating an equivalent current dipole source within the human head. Three right-handed volunteers were studied by the same method as for the model skull, except that a circle on the scalp with a radius of about 5 cm with its center approximately 7 cm above the ear canal was digitally characterized for fitting the sphere model. Comparison with MRIs indicated that the thickness of the skull was uniform to within about 20% over this area, so the scalp characterization would yield the same locations for the center of the sphere as the curvature of the inner surface of the skull. Tone burst stimuli with a frequency of about 1 kHz and duration of 400 ms were presented with a random interstimulus interval uniformly distributed within the range of 1.0 to 3.4 s. Stimuli were provided to the right ear through airline style plastic earphones at an intensity of about 70 dB SPL. For each position 100 responses were averaged. The entire recording procedure took 60 min to obtain measurements at 64 sensor positions over the scalp. In addition, MRI recordings were obtained. The coordinates of positions on the MRI slices were indexed to the head-based coordinate system by attaching markers to the skin when the images were recorded.

Fig. 3 shows representative isofield contours for one subject, displaying the two areas of strongest field. The mid-point of the pattern lies above the ear canal, which is expected for a source lying in auditory cortex. The dots in the MRI scans depict the deduced position of the neuronal source with respect to the three principal cross sections of the head, for slices that pass near the computed location. To within our uncertainty of 3 mm, the source lies within the cortical layer forming a portion of the floor of the Sylvian fissure. Fig. 4 B

and D shows isofield contours for two other subjects. Note that here also the midpoints lie approximately over the ear canal. The corresponding positions of the computed sources are shown in the coronal MRI slices, here enlarged in comparison with those in Fig. 3. Again, the sources lie within

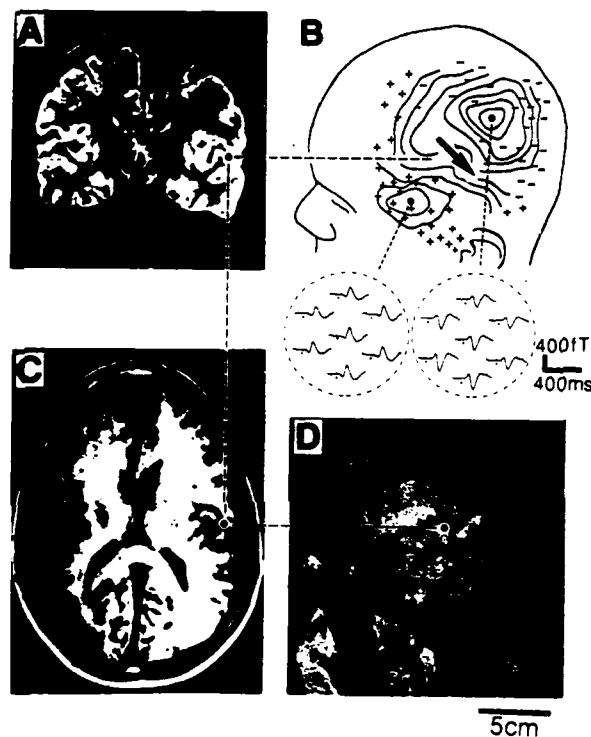


FIG. 3. (A, C, and D) MRI cross sections for subject WH that pass through the deduced location of the source for the 100-ms component of the auditory-evoked response (dots). (B) Positions of field measurements and isofield contours for the subject. Also shown are examples of the averaged time-series data obtained by the two seven-sensor dewars near the two-field extrema (100 responses).

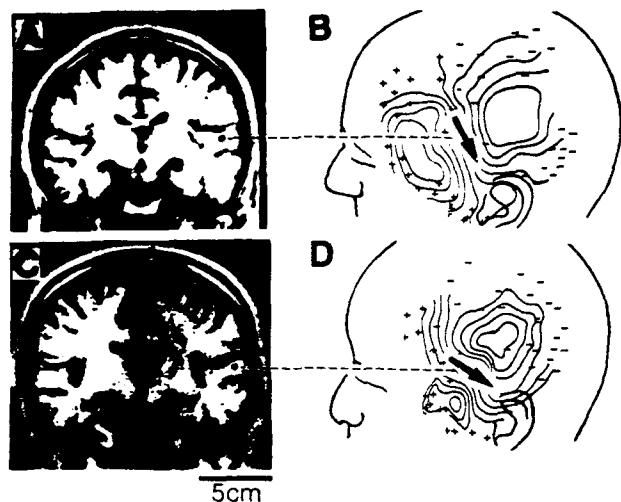


FIG. 4. (A and C) Portion of the MRI coronal cross sections that pass through the deduced locations of the source for the 100-ms component of the auditory-evoked response (dots), for subjects PF and TY, respectively. (B and D) Positions of field measurements and isofield contours for the subjects.

the cortex forming the floor of the Sylvian fissure. The agreement between the deduced locations and position of the floor of the Sylvian fissure is consistent with the accuracies previously obtained for measurements with the sphere and skull models. Dipole moments for the subjects ranged from 10 to 30 nA-m.

**Fixed Position Measurements.** The application of neuro-magnetic techniques to clinical diagnoses of neuronal disorders will depend very much on how quickly measurements can be carried out. To assess the ability of the present system to quickly characterize features of the tonotopic representation in human, where tones of higher frequency evoke activity deeper within the head, measurements were obtained with the dewars at fixed locations as close to the field extrema as possible. Tone bursts of 400 ms duration having frequencies of 0.75, 1.00, 1.25, and 1.50 kHz were presented to the right ear in random order. It was possible to fit the 14 recorded average amplitudes of the N100 magnetic component on the left hemisphere by a field pattern produced by a current dipole. The resulting uncertainty in lateral position was 4 mm and the uncertainty in depth was 3 mm. On 11 days the tonotopic sequence was determined over a single octave in frequency for one subject. These results are illustrated in Fig. 5. Excellent agreement is obtained with the tonotopic trends reported earlier (7-9). The precision of the results is

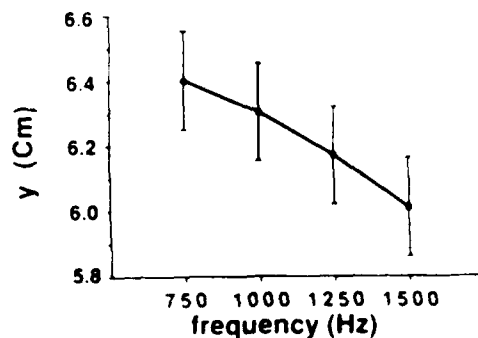


FIG. 5. Coordinates in y axis for the source of the 100-ms component of neuronal activity evoked by tone bursts of various frequencies. Bars give the standard error of the mean of the uncertainties (67% confidence levels) for the individual determinations of source locations on separate days.

also consistent with theoretical analyses for such a "fixed position" measurement (24, 25). The measurement time for locating a single source was about 20 min, although the setup time for the subject, including characterizing the scalp surface, was about 20 min.

**Adaptation.** In carrying out serial measurements on a subject it is essential to minimize adaptation within and across averages. Adaptation effects have long been known in studies of the auditory event-related potential. We employed a paradigm to investigate the phenomenon for both its intrinsic and methodological importance. A total of 700 tones of 1.0, 1.05, or 1.1 kHz were presented in random order, with the interstimulus interval varying randomly between 1.0 and 3.4 s. Separate averages for three subjects were obtained for the N100 amplitude of the first 350 responses and the last 350 responses, when the tone was preceded by the same tone and when preceded by a different tone. Fig. 6 illustrates the difference for the amplitude trends. Cortical neural activity decreases when a tone is preceded by an identical tone but less so when preceded by a different tone, provided there is a sufficient number of prior presentations of the same tone, not necessarily consecutive. Consequently there are short-term as well as long-term features in the response. There was no change in source location or orientation for adapted activity when compared with responses not preceded with the same tone stimulus. Thus each respective area of cortex responding to the particular tones shows this adaptation effect.

## DISCUSSION

The preceding results indicate that neuronal activity can be located with high accuracy within the human brain for field strengths at physiological levels, when the geometry of the cranium can be approximated by a spherical model. Accuracy in source location for both the sphere and skull models was consistently better than 3 mm for a current dipole source about 3 cm beneath the surface. Comparable precision, though perhaps not accuracy, may be expected in cases where the spherical model is less representative, as for fronto-temporal areas. In these instances, accuracy can be improved by interpreting the measurements through use of numerical models for the individual's cranium (22, 23).

Comparisons with MRIs of the individual subjects established that the neuronal activity giving rise to the 100-ms components of the auditory-evoked response for a tone burst lies in the floor of the Sylvian fissure, and the orientation of the current dipole is within  $10^\circ$  of being perpendicular to the surface of the cortex. This orientation is consistent with the neuronal currents giving rise to the field being the intracel-

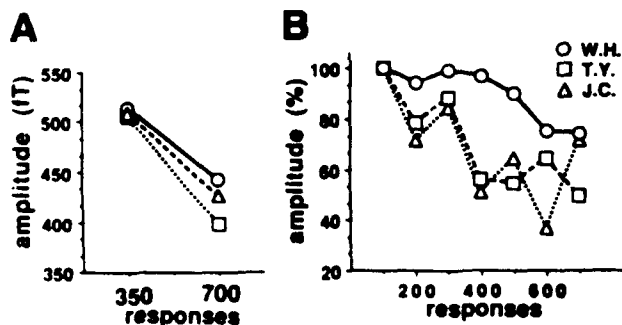


FIG. 6. (A) Response amplitude for the 100-ms magnetic component evoked by a tone burst stimulus when a tone is preceded by an identical tone (squares), different tone (circles), or either condition (triangles) for subject WH. Data represent an average of the first and last 350 responses. (B) Running average of relative response strengths when a tone is preceded by an identical one, for each of three subjects, averaged over 100 consecutive tone presentations.

ular currents within pyramidal cells, although we cannot rule out other possible sources within the cortex. The position of the source in relation to the ear canal indicates that this portion of cortex is Heschl's gyrus, the location of the auditory cortex. Thus we have established the reliability of the multisensor technique.

Rapid measurements are possible when the approximate locations of the field extrema are known and the two dewars are positioned over them. The possibility of extending this technique to studies of multidimensional functional representations of various modalities is especially attractive. For instance, in the human auditory system, an amplitopic map runs approximately at right angles to the tonotopic axis. Thus, with the "fixed position" paradigm, randomly presented stimuli at various intensities and frequencies can be utilized for a rapid diagnosis of normal or abnormal cortical activity with this truly noninvasive methodology. The prospects with larger arrays of sensors are profound.

While this research has been explicitly concerned with localization of neuronal activity, it is well to keep in mind that the magnitude of such activity is also obtained, as the equivalent current dipole moment. That is, localization provides an objective, quantitative measure of neuronal activity. Thus there is a real prospect that such quantitative measures may have value in diagnosing sensory disorders and disease states.

The adaptation described in this paper is an example where localization demonstrates that reduction in response field amplitude is not due to displacement or rotation of the source, corresponding to a shift of activity from one neuronal population to another, but to reduction in source strength. Adaptation is exhibited by neuronal activity in human auditory cortex with both short-term and long-term features. One significant point to be made is related to randomization of stimuli. For this procedure to be effective in reducing the influence of adaptation on neuromagnetic responses, several different stimuli must be interposed; or perhaps equivalently, more time must be permitted between the presentation of similar stimuli. It is worthwhile to consider whether a dishabituation phenomenon can be demonstrated in this context.

We thank Drs. Wayne Hostetler and Louis Comachia for their invaluable help, Mr. Patrick Fusco and Irene Martin for technical assistance, and Biomagnetic Technologies Inc. for their unfailing technical support during this period of instrumentation development. This work was supported in part by special funds from the New York University Medical Center, the Faculty of Arts and Sciences, Contracts F49620-85-K-0004 and F33615-85-D-0514 from the Air Force Office of Scientific Research, and Grant NS13742 from the National Institutes of Health.

This reprint is identical with the published manuscript except for a correction of field and current source directions.

- Ilmoniemi, R., Hari, R. & Reinkainen, K. (1984) *Electroencephalogr. Clin. Neurophysiol.* **58**, 467-473.
- Williamson, S. J., Pelizzone, M., Okada, Y., Kaufman, L., Crum, D. B. & Marsden, J. R. (1984) in *ICBC10: Proceedings of the Tenth International Cryogenic Engineering Conference*, eds. Collan, H., Berglund, P. & Krusius, M. (Butterworth, Guildford, UK), pp. 339-348.
- Romani, G. L., Leoni, R. & Salustri, C. (1985) in *SQUID '85: Superconducting Quantum Interference Devices*, eds. Hahlbohm, H. D. & Lübbig, H. (de Gruyter, Berlin), pp. 919-932.
- Knuutila, J., Ahlfors, S., Ahonen, A., Hällström, J., Kajola, M., Lounasmaa, O. V. & Vilkmann, V. (1987) *Rev. Sci. Instrum.* **58**, 2145-2156.
- Barth, D. S., Sutherling, W., Broffman, J. & Beatty, J. (1986) *Electroencephalogr. Clin. Neurophysiol.* **63**, 260-273.
- Hansen, J. S., Ko, H. W., Fisher, R. S. & Litt, B. (1988) *Phys. Med. Biol.* **33**, 105-111.
- Romani, G. L., Williamson, S. J. & Kaufman, L. (1982) *Science* **216**, 1339-1341.
- Romani, G. L., Williamson, S. J., Kaufman, L. & Brenner, D. (1982) *Exp. Brain Res.* **47**, 381-393.
- Pantew, C., Hoke, M., Lütkenhöner, B. & Lehnertz, K. (1988) in *Biomagnetism '87: Proceedings of the 6th International Conference*, eds. Atsumi, K., Katila, T., Williamson, S. J. & Ueno, S. (Tokyo Denki Univ. Press, Tokyo), pp. 146-149.
- Vaughan, H. G., Jr., & Ritter, W. (1970) *Electroencephalogr. Clin. Neurophysiol.* **28**, 360-367.
- Farrell, D. E., Tripp, J. H., Norgren, R. & Teyler, T. J. (1980) *Electroencephalogr. Clin. Neurophysiol.* **49**, 31-37.
- Elberling, C., Bak, C., Kofod, B., Lebech, J. & Saermark, K. (1980) *Scand. Audiol.* **9**, 185-190.
- Hari, R., Aittoniemi, K., Järvinen, M. L., Katila, T. & Varpula, T. (1980) *Exp. Brain Res.* **40**, 237-240.
- Tuomisto, T., Hari, R., Katila, T., Poutanen, T. & Varpula, T. (1983) *Il Nuovo Cimento* **2D**, 471-483.
- Sams, M., Hämäläinen, M. S., Antervo, A., Kaukoranta, E., Reinkainen, K. & Hari, R. (1985) *Electroencephalogr. Clin. Neurophysiol.* **67**, 254-266.
- Pelizzone, M., Williamson, S. J. & Kaufman, L. (1985) in *Biomagnetism: Applications and Theory*, eds. Weinberg, H., Stroink, G. & Katila, T. (Pergamon, New York), pp. 326-330.
- Arthur, D. L., Flynn, E. R. & Williamson, S. J. (1987) *Electroencephalogr. Clin. Neurophysiol. Supplement* **40**, 429-439.
- Barth, D. S., Sutherling, W., Engel, J. E., Jr., & Beatty, J. (1984) *Science* **223**, 293-296.
- Sutherling, W., Crandall, P. H., Cahan, L. D. & Barth, D. S. (1988) *Neurology* **38**, 778-786.
- Ricci, G. B., Romani, G. L., Salustri, C., Pizzella, V., Torrioli, G., Buonomo, S., Peresson, M. & Modena, I. (1987) *Electroencephalogr. Clin. Neurophysiol.* **66**, 358-368.
- Williamson, S. J. & Kaufman, L. (1987) in *Handbook of Electroencephalography and Clinical Neurophysiology*, eds. Gevins, A. & Rémond, A. (Elsevier, Amsterdam), Vol. 1 Revised, pp. 405-448.
- Hämäläinen, M. S. & Sarvas, J. (1988) in *Biomagnetism-88*, eds. Atsumi, K., Kotani, M., Ueno, S., Katila, T. & Williamson, S. J. (Denki Univ. Press, Tokyo), pp. 98-101.
- Hari, R. & Ilmoniemi, R. J. (1986) *CRC Crit. Rev. Biomed. Eng.* **14**, 93-126.
- Meijs, J. W. H., Bosch, F. G. C., Peters, M. J. & Lopes da Silva, F. H. (1987) *Electroencephalogr. Clin. Neurophysiol.* **66**, 286-298.
- Costa Ribeiro, P., Williamson, S. J. & Kaufman, L. (1988) *IEEE Trans. Biomed. Eng.* **35**, 551-560.

## CHANGES IN CORTICAL ACTIVITY WHEN SUBJECTS SCAN MEMORY FOR TONES

by L. Kaufman\*, S. Curtis\*, J.-Z. Wang\*\*, and S.J. Williamson\*\*

Departments of Psychology\* and Physics\*\*,  
and Center for Neural Science, New York University

### ABSTRACT

The magnetoencephalogram (MEG) was used to detect regional changes in spontaneous cortical activity accompanying short-term memory search. This method was chosen because magnetic fields are detectable only within a few centimeters of the projections of their sources onto the scalp. The specific hypothesis that auditory cortex is involved in scanning memory for tones was tested by sensing the field of the magnetic counterpart to N100 (N100m) which is known to originate in auditory cortex. N100m was measured at many different positions and the spontaneous cortical rhythms in the alpha bandwidth (8-12 Hz) were measured at the same places. These rhythms were found to be suppressed while subjects scanned memory for musical tones in a Sternberg paradigm. For three subjects, both the MEG suppression time (ST) and reaction time (RT) increased linearly with memory set size. The correlation between ST measured over the left hemisphere and set size was significant for two subjects but not significant for the third, and the slopes of the regression lines relating ST to set size were too shallow to be related to the time required to scan memory. However, the correlation between ST of the right hemisphere and set size was highly significant for all subjects, and the slopes of the regression lines were comparable to those relating RT to set size. The electroencephalogram (EEG) recorded with midline electrodes failed to reveal a significant relationship between suppression time and set size for 2 of the subjects, thus ruling out global alpha blockage and generalized arousal as the basis for the task-related suppression duration. The electric N100, measured at Cz, decreased significantly in amplitude with set size for 2 subjects, but it increased significantly in amplitude for the third subject. In contrast, RT increased with set size for all subjects. N100m measured over the right hemisphere was similar to the behavior of N100, while N100m measured over the left hemisphere showed little change in amplitude with set size, thus establishing an asymmetry in N100 between the hemispheres. Since N100 amplitude is normally larger when attention is paid to auditory stimuli, differential attention alone cannot account for the relation between ST and set size. Furthermore, the processing negativity, which may be superimposed on N100 in selective attention tasks, was not discernible for any set size. It was also found that ST prior to the button press was not correlated with RT. Hence, the covariation of set size with ST is not attributable to preparation for a motor response. In this experiment the sensors were placed where the field of N100m was approximately at its maximum value.

---

We thank Murray Glanzer, Larry Maloney, and Misha Pavel for their help and Arthur Kramer and Emanuel Donchin for valuable comments on an earlier version of the discussion of P300. This work was supported in part by AFOSR Grants Nos. AFOSR-90-0221 and F49620-88-K-0004 (L. Kaufman, Principal Investigator). Address reprint requests to: Lloyd Kaufman, Professor of Psychology and Neural Science, New York University, 6 Washington Place, NYC, NY 10003 USA.

Since many measures were made from somewhat different positions in these areas, it was possible to determine how N100m amplitude varied with sensor location over both hemispheres. These position-dependent changes in N100m amplitude were significantly correlated with corresponding position-dependent changes in percent suppression of the spontaneous MEG. Thus, auditory cortex contributes significantly to the spontaneous alpha activity suppressed during memory search. It is concluded that regional changes in cortical spontaneous activity are meaningfully related to ongoing memory scanning.

Earlier work on the relation between short-term memory and the N100 and P300 ERP components is reviewed in an Appendix. It is concluded that published conjectures on the relation between N100 and short-term memory are inconclusive, and neither P300 latency nor amplitude have been convincingly related to short-term memory scanning *per se*. These ERP components are complementary to the regional changes in spontaneous activity studied here, and reflect different facets of the processes involved in memory scanning.

**KEY WORDS:** Alpha, MEG, Local Suppression, Short-Term Memory, N100

## INTRODUCTION

In the classic Sternberg (1966) experiment a subject views or listens to a sequence of items ranging from 1 to as many as 7 in length. Then, two seconds later, is exposed to a "probe" item and asked to press one button if the probe had been a member of the memory set, and another if it had not. As Sternberg demonstrated, reaction time (RT) increases linearly with the size of the memory set being searched by subjects. Also, RT increases with set size at approximately the same rate for "new" probes (those that had not been members of the set) as for "old" probes (those that had been members of the set). Sternberg accounted for these results by postulating a serial and exhaustive search of short-term memory. This is predicated on the assumption that RTs of well-trained subjects who perform in a nearly error-free manner are not dissociated from the process of searching memory. Given this same assumption, we test the hypothesis that regional fluctuations in the brain's spontaneous activity accompany the scanning of short-term memory and reflect ongoing cognitive processes. The main advantage in adopting this approach to short-term memory is that many hundreds of papers have been devoted to the Sternberg paradigm, and the conditions under which its main effects occur are well understood. Despite criticisms of Sternberg's theory that memory search is both serial and exhaustive, his basic results are well established and documented. The basic assumption that RT is not dissociated from processing time is shared even by investigators who question the theory. Therefore, Sternberg's paradigm is extremely useful in psychophysiological investigations.

### Spontaneous Activity and Memory Scanning

The work of Mishkin (1982), Ungerleider and Mishkin (1982), and Ungerleider and Desimone (1986) indicate that many areas of neocortex, including the sensory projection areas, are involved in memory. This is reflected in a rough "schematic" or "circuit" representing the "anatomy of memory", in which the sensory area transmits information to hippocampus/amygdala, thence to the diencephalon, to the prefrontal cortex, to the basal forebrain, and then back to the sensory area. Although based on monkey, this map parallels that generated by the less complete data offered by human clinical cases. Behavioral evidence that short-term memory may be modality-specific (Murdoch and Walker, 1969) is consistent with this view, since it implies that working (short-term) memory involves sensory areas of neocortex. Similarly, some theorists suggest that the machinery of the visual system is actively involved in mental rotation - a form of imagery in which mental operations are performed on objects that may be present only in working memory (cf. Finke and Shepard, 1986; Kosslyn, 1983).

Direct evidence that different areas of neocortex are involved in short-term memory *per se* is difficult to find. Regional blood flow studies employing positron emission tomography (PET) reveal local differences in levels of cortical activity, depending upon the nature of mental tasks (cf. Petersen, Fox, Posner, Mintun, and Raichle, 1989). However, the coarse temporal resolution afforded by PET (~40 sec) proscribes identifying regions specifically involved in searching short-term memory. The experiment described in this paper was specifically designed to make use of the MEG in determining if neocortex is indeed active while subjects scan short-term memory.

A major assumption underlying the work described here is that regional differences in levels of brain activity occur during the performance of various mental tasks. This assumption is shared by PET blood flow studies, where different levels of blood flow are assumed to reflect different levels of brain activity (Petersen et al., 1989). It is also consistent with the work of Pfurtscheller (1988), Pfurtscheller and Aranibar (1978; 1979), and Klimesch, Pfurtscheller, and Mohl (1988) who found that power in the alpha band between 8 and 13 Hz showed a sharp reduction (*event related desynchronization*) subsequent to visual stimulation as well as voluntary motor acts. Their method is similar to one devised by Kaufman and Price (1967) to study modulation of high-frequency EEG by visual stimuli, and by Kaufman and Locker (1970) to study effects of attention on visual modulation of alpha activity. The only difference between these methods is that Kaufman et al. measured the variance around the average response remaining within the EEG after it was filtered, while Pfurtscheller et al. included the residual average response in their measures. The work of Pfurtscheller and his colleagues strongly suggests that regional changes in the level of the brain's spontaneous activity reflect ongoing cognitive processes. The main reason for using the MEG rather than the EEG is that the latter is often difficult to interpret. The intracranial sources of potential differences at the scalp may be a large distance away. By contrast, because the magnetic fields of neural sources fall off very sharply with distance, their maximum extracranial fields are detectable only over a relatively confined area at the scalp. In the case on cortical sources, sensors placed near field extrema are only a few centimeters away from the scalp projections of their sources. Ambiguity is reduced by the fact that the MEG is a truly monopolar measure, i.e., it does not need the equivalent of a "reference electrode", which contributes to the uncertainty about locations of sources of EEG phenomena.

To exploit this advantage of the MEG, Kaufman, Schwartz, Salustri, and Williamson (1990) measured the variance (power) about the event related field (ERF) within the alpha band of the MEG while subjects engaged in a mental imagery task. The subjects were presented with a memory set composed of 3 abstract polygons. Three seconds later, a fourth abstract polygon (the *probe*) was shown. Subjects then responded as instructed for either a *simple RT* condition or a *choice RT* condition. In the simple RT condition they pressed a button as soon as they saw the probe (without regard for whether it had been a member of the memory set). In the choice RT condition they pressed one button if it had been a member of the set or another button if it had not been a member of the set. Naturally, in the choice RT condition the reaction time (RT) was much longer than in the simple RT condition. The power in the alpha band (8-12 Hz) of the spontaneous MEG was markedly reduced after presentation of the probe, and this activity continued to be *suppressed* until the memory search task was completed. The duration of suppression of spontaneous alpha band activity was highly correlated with the RTs in both the simple and choice conditions. It was concluded that searching memory for visual forms is associated with a temporally commensurate reduction in spontaneous brain activity. The suppression across the parietal and occipital areas of the scalp was markedly enhanced over the midline. Again, because the extracranial field is close to the surface projection of its source, this indicates that the suppressed activity originates in the visual areas of the brain. A control condition involving the searching of memory for visually presented words (as opposed to nonsense forms) revealed no difference in the duration of suppression between simple and choice RT conditions when the MEG was recorded over the visual areas, although the simple task results in a dramatically shorter RT than the

choice, with the RTs being about the same for the corresponding simple and choice tasks involving the visual forms.

These results imply that visual cortex is actively engaged in searching visual memory. By extension, other regions of neocortex may be involved when scanning working memory for non-visual "items". Thus, the distribution of cortical activity following visual presentation of verbal stimuli could depend upon the nature of the task the subject is asked to perform in response to stimuli. For example, subjects could be asked to respond to words by forming mental images. In this case the visual areas could become active. However, if asked to respond to the same words by searching memory to find rhyming words, then speech areas could become more active.

Kaufman, Glanzer, Cycowicz and Williamson (1989) actually performed this experiment and found that when subjects form mental images of objects represented by words flashed on a screen, the pattern of the brain's extracranial magnetic field differed from the pattern associated with performing a verbal task using the same words. The two tasks (one involving mental imagery and the other involving rhyming) were equated for difficulty. More specifically, the occipital MEG in the 8-12 Hz band exhibited a period of suppression that began when the word was presented and had a duration that was significantly correlated with the time it took for subjects to report that they had completed forming the mental image. Although finding a rhyming word in memory took the same average amount of time, the duration of the suppression of the occipital MEG was much shorter, and was the same as that associated with flashed and passively viewed nonsense words. This suggested that forming a mental image involves the visual areas, but completing a verbal task involves still other portions of cortex. In subsequent work (Kaufman, Cycowicz, Glanzer, and Williamson, 1991) it was found that activity measured over the fronto-temporal area - particularly of the left hemisphere - exhibits a similar RT-related increase in suppression duration when the verbal task is performed, but not when the nonsense word was viewed passively. Therefore, as is the case for PET blood flow indicators, changes in patterns of spontaneous cortical activity do occur when subjects perform functionally different mental tasks, even when the tasks are initiated by similar sensory stimuli.

The foregoing considerations motivated this first full use of the Sternberg paradigm to study the relation between short-term memory scanning and the spontaneous activity of the brain. In this paper we describe an experiment designed to test the hypothesis that increases in RT with memory set size are reflected in the duration of local changes in level of spontaneous activity of neocortex. More specifically, we tested the hypothesis that spontaneous activity arising in auditory cortex is suppressed when subjects scan memory for previously heard musical tones, and this suppression is correlated with processing time as indicated by reaction time.

## METHOD

Two young adult female subjects (GK and FK) and one male (AM) subject listened to memory sets composed of one, three or five 200 msec long musical tones presented sequentially 300 msec apart and then, 2 sec later, to a probe tone. The probe had a 50% chance of being a member of the previously heard memory set. The task was to press one button if the probe had been a member of the memory set, and another button if it had not been a member of the set. Subjects were given 20 trials for each memory set, and this was repeated at least ten times over each hemisphere for each subject.

The musical tones were generated by an Amiga 1000 computer and presented via a loudspeaker placed at a porthole in the wall of a magnetically shielded room. The particular tones heard by the subjects were drawn from a pool of 16 musical notes ranging in pitch from 311.13 Hz to 739.99 Hz. All subjects were given as many practice sessions as they needed to insure that their performance accuracy was at least at the 95% level before embarking on the main experiment.

The subjects were placed on a kneeling stool inside the shielded room. With their foreheads and arms resting on padded supports, they listened to the stimuli and then, after presentation of the probe, depressed one of two buttons to indicate if the probe had been "old" or "new". The buttons were pressed with the right hand when neuromagnetic fields were recorded over the right hemisphere, and with the left hand when the fields were recorded over the left hemisphere. This was to prevent contamination of the recordings by activity of motor cortex in the hemisphere contralateral to the hand being used.

RT, which is the time between probe presentation and the button press, was measured while the subject's EEG and MEG were being recorded. For all subjects active electrodes were placed at Cz and Oz, and for the third subject (FK) at Pz and Fz as well. A reference electrode was placed on the right mastoid. The EEG was recorded with a Grass Model 12 Neurodata Acquisition System located inside the shielded room. The recording bandwidth was between .01 and 100 Hz with rolloffs at 6 dB/octave. The outputs of the Grass were applied to the data acquisition unit of a Hewlett Packard 9000-350 computer located outside the shielded room.

The MEG was recorded using a 5-channel neuromagnetometer, which is fully described elsewhere (Williamson, Pelizzone, Okada, Kaufman, Crum and Marsden, 1984). The 5 sensors are located within a fiberglass cryogenic vessel (dewar) where they are immersed in liquid helium. The detection coils of the sensors are second-order gradiometers 1.5 cm in diameter and 4 cm baseline. One coil is in the center of the tail section of the dewar and the other four arranged around it in a circular pattern, with 2 cm radius. The bottom of the tail section has a 9 cm radius of curvature, so that all five of the coils can be placed with axes nearly radial to the scalp. The lowest coil of each gradiometer is then 1.3 cm from the scalp, owing to the thickness of the dewar. With this geometry it is possible to measure the field normal to the scalp at five different places 2 cm apart.

In the main experiment no attempt was made to map the entire field distribution around the head. Earlier experiments (Curtis, Kaufman, and Williamson, 1988; Pelizzone, Williamson, Kaufman and Schafer, 1984) and extensive pilot work had already revealed the approximate locations of the field extrema associated with the N100m

component of the auditory evoked field. In the coordinates of the 10-20 System, one extremum over the left hemisphere is about 2 cm below the line connecting F7 and T3, and the other about 2 cm above T5, toward the vertex. Similarly, over the right hemisphere the extrema are below the line connecting F8 and T4, and above T6. In the experiment the neuromagnetometer was placed with its center pick-up coil about 2 cm above either T5 or T6 to insure that one of the coils would be at or near the field extremum. Thus, on alternate blocks of trials, the dewar was placed over the left and right hemispheres where it was certain that strong N100m responses would be recorded despite small changes in the positions of the pickup-coils from one block of trials to another.

The voltage outputs of the superconducting electronics of the neuromagnetometer are proportional to the field (in femtotesla (fT)) linking the pick-up coils. These outputs were first applied to analog filters set to pass activity between 0.1 and 50 Hz, and then to the same data acquisition unit of the 9000-350 computer as was used in recording the EEG data. Other inputs to the unit included the outputs of the two buttons used to record RT, and signals from the Amiga computer indicating time of presentation of memory set and probe tones, as well as whether the probe tone was new or old.

Subjects were presented with three sets of trials, corresponding to memory set sizes 1, 3 and 5, with the dewar over one hemisphere. After completion of the three sets, the dewar was moved to the opposite hemisphere. This was repeated until at least 10 complete blocks of trials were measured over each hemisphere. Throughout all of the blocks of trials, the EEG was recorded with midline electrodes insuring the accumulation of a large number of epochs for each set size.

After the EEG and MEG data were acquired, they were digitally filtered within four different passbands, to create four different records. The passbands were 1.0 to 40 Hz, 0.2 to 40 Hz, 8 to 12 Hz, and 16-24 Hz. These data were then averaged using the onset of the probe tone as the temporal reference signal. The epoch began between 6.5 and 4.5 sec prior to presentation of the probe, depending upon the size of the memory set, and terminated 4.5 sec after probe onset. A new memory set began 1 sec after the end of the epoch.

The 1-40 Hz record was used to compute the average response to the probe and to verify the presence of the N100 and N100m in the EEG and the MEG. The high-pass of 1 Hz was used to reduce the contribution of any low-frequency baseline shift commensurate in duration to the time needed to scan memory. Also, the amplitudes of the electric and magnetic N100 component were recorded as a function of set size for both the new and the old probes. To maximize the effect of any processing negativity on the amplitude of N100 and N100m, the same computation was performed using the 0.2 to 40 Hz bandpass.

The average response was also computed using the 8-12 Hz (alpha band) record, and the variance about that response was used as a measure of the power within the spontaneous alpha band activity of the MEG and the EEG. Plotting the smoothed alpha power shows how the level of this background activity varies with time and as a function of set size (Kaufman et al., 1990). An identical procedure was applied to the same data after it was bandpassed between 16 and 24 Hz, to capture any differential effects in the beta band of the EEG and MEG.

In determining how alpha power varies as a function of time, the averaging was performed with the onset of the probe as a reference trigger. To test the hypothesis that systematic changes in these plots may be due to a change in level of alpha accompanying readiness to make a motor response, the same activity was averaged backward using the button press rather than the probe as the reference trigger.

## RESULTS

### *Basic Behavioral Data:*

To insure that the electric and magnetic measures reflect the processes actually involved in performing the Sternberg task, we first examine the behavioral (RT) data and will then compare it with the physiological data. Figure 1 summarizes the way in which RT varied as a function of memory set size (MSZ). The regression lines relating RT to MSZ for old and new probes are shown for the three subjects. As in Sternberg's original experiments, the correlations are high and significant, implying a linear relationship between set size and RT. However, a *t* test on two independent samples for the differences between slopes for old and new items for each subject shows the differences between them to be highly significant (Hayes, 1981). The values of these slopes (in sec/item) are shown in Table 1. For all subjects the scan rate is faster for new probes than for old. Since the acoustic stimuli differed in some cases by more than an octave in pitch, on some "new" trials the probe was very different in apparent pitch from any member of the memory set. Hence, on those trials subjects could react solely to the relatively unique pitch of the new probe and assume that it had not been a member of the set. This seems to be a likely cause of the difference in slopes. Therefore, the slopes associated with the old probe are assumed to be more accurate indicators of memory scan rate than those associated with new probes. Averaging the slopes for old probes across subjects indicates that subjects scanned memory for tones at an average rate of about 138 msec/tone. Overall, the average scan rate for both old and new probes was 109 msec/item. We may now compare these data with those obtained using the MEG and the EEG.

### *Effects of Memory Scanning on the Electric N100 and the Magnetic N100m:*

For reasons considered in the Appendix to this paper, Picton, Campbell, Baribeau-Brown, and Proulx (1978) and Naatanen (1982, 1986) suggested that N100 and related ERP components may reflect short-term memory processes. Therefore, before turning to the effects of memory scanning on the spontaneous MEG, let us consider the N100 component of the ERP. As described earlier, the EEG was bandpassed between 1 and 40 Hz and between 0.2 and 40 Hz prior to averaging. This permitted the recovery of N100 at Cz with a bandwidth wide enough to insure detection of the processing negativity (0.2-40 Hz), and also with the processing negativity, if any, attenuated by the filter (1-40 Hz). Visual inspection of the resulting waveforms in the EEG failed to reveal any greater early negativity in the responses derived from the 0.2-40 Hz data. A sample N100 response filtered using the two bandwidths is shown at the bottom of Figure 2. N100 was essentially the same in the 1-40 Hz record as in the 0.2-40 Hz record and there was no obvious increase in baseline negativity superimposed on N100 in either case. This was true of responses obtained with all set sizes.

While 20 trials per set size were recorded in each block of trials, the electrodes were kept at the same positions from one block of trials to another. Consequently, it was possible to pool data for each set size across all blocks of trials, insuring a large enough N to compute reliable average ERPs. Figure 2 contains the actual average N100 waveforms from each set size for all three subjects, computed separately for old and new probes. Since there is no significant difference between N100 amplitudes for old and new trials, they were averaged, and the resulting overall N100 amplitudes are included in the graph shown in Figure 3. Clearly, as is also evident for both old and new trials in Figure 2, the amplitude of N100 diminished with set size for 2 subjects, while it increased significantly with set size for the third subject.

As we have seen, RT increased linearly and significantly with set size for all three subjects (Figure 1). However, the variation in N100 amplitude with set size is quite different from that of RT. First, the direction of its change in amplitude with set size differs significantly among the subjects while RT increases with set size for all subjects. It is notable that ANOVAs for each subject show that the differences in N100 amplitude over set size are highly significant and the agreement between the data for new and old probes (Figure 2) is evidence of the repeatability of the results. Also, unlike the RTs, the change in N100 amplitude with set size is non-linear for two of the subjects.

Similar results were obtained for N100m. Since five coils were placed at slightly different positions over each hemisphere and, on alternate blocks, switched from one hemisphere to the other, the outputs of the 5 channels over all blocks of trials were averaged for each hemisphere and each set size. While the pickup coils were at different locations, and these locations varied from one block to another, the locations of the coils were the same for all set sizes within each block. Hence, the variations in N100m with location were the same for all set sizes. The average amplitudes vary differently with set size over the two hemispheres.

The amplitude of N100 measured at the vertex is determined by sources in both hemispheres. However, any measure of N100m is due to the activity within the hemisphere over which the measurement is made. Therefore, the marked differences between N100m of the left and right hemispheres of all subjects demonstrate a previously unknown asymmetry in the responses of the two hemispheres to acoustic stimuli. The functional significance of this asymmetry, if any, is not known.

As shown in Figure 4, N100m measured over the right hemisphere of subjects AM and FK exhibits the same qualitative changes in amplitude as does N100, i.e., there is a monotonic reduction in N100m amplitude with set size for AM and FK. GK's right hemisphere shows an increase in N100m amplitude with set size, which is also what was found for N100.

Regardless of the hemisphere over which it is measured, N100m is not consistently related to RT, which is the putative indicator of memory scanning. Neither is N100. Nor do their latencies vary with set size. However, since both N100 and N100m are sensitive to levels of auditory attention, they may well reflect attentional components of the Sternberg task. Therefore, the reliable individual differences noted here could be due to differences in attentional strategies. This requires further study.

The failure of N100 and of N100m to show any clear relationship to the process of auditory memory scanning as reflected in the Sternberg procedure does not rule out the

participation of neurons of auditory cortex in this process. We now turn to the question of whether variations in levels of spontaneous activity of auditory cortex and adjacent regions reflect this process.

### *Effects of Memory Scanning on Spontaneous Activity*

The spontaneous MEG between 8 and 12 Hz was retrieved from the same recordings as those used to obtain N100m. The variance about the average response in this bandwidth was plotted at each point in time within the averaging epoch, and then the resulting records of fluctuation of variance (power) with respect to time were smoothed. Sample plots of data from the three subjects are shown in Figure 5. Unlike N100m, these were not obtained by averaging the outputs of the five sensors. Rather, they are average power plots ( $N=20$ ) obtained from a single sensor for responses at each set size. The zero point along the x-axis indicates the time at which the probe stimulus was presented. Note the drop in field power which occurs near this point in time and persists for some time afterwards. In fact, as is evident in the sample traces shown in Figure 5, the time between presentation of the probe and recovery from suppression (*suppression time* (ST)) tends to increase with memory set size (MSZ). Therefore, to determine if this apparent increase in ST is reliably related to MSZ, the duration of ST in each power plot was divided into two parts. The first part (ST-) is the time between the onset of the probe and the onset of suppression. A positive value refers to the case where the suppression began prior to actual probe presentation. A negative value refers to the time between probe onset and later occurring suppression onset. We tested the hypothesis that ST- is correlated with RT for each subject. We also tested the hypothesis that time between the presentation of the probe and the termination of suppression (ST+) is positively correlated with RT. Since it is known that RT is correlated with MSZ, then a positive correlation would show that suppression is correlated with the time to scan memory and make a response. This was done separately for new and old probes so that only 10 epochs were used to compute the "old" and "new" power for each set size over all blocks of trials.

When the old and new items are compared with RT separately, the correlations are weak and largely not significant. However, when the old and new data are combined, the correlations become highly significant. The regression lines for the combined data are shown in Figure 6. The resulting coefficients of correlation relating ST+ to RT are:  $r=0.64$  ( $p=.0015$ ),  $0.43$  ( $p=.03$ ), and  $0.63$  ( $p=.0006$ ) for subjects AM, GK and FK, respectively. For subjects AM and GK the correlations relating ST- to RT are not statistically significant and the regression lines are essentially flat. However, for subject FK ST- is significantly correlated with RT ( $r=-0.59$ ,  $p=.0014$ ). Generally, FK's suppression starts well after presentation of the probe, but the interval between probe and suppression onset diminishes as RT increases. Therefore, FK's longer RTs could have been due to a delay in onset of processing. (RT is given by the Y-intercept of the RT versus MSZ regression functions of Figure 1, which shows that, overall, FK's RT was longer than that of the other two subjects.)

The strong positive correlations of ST+ with RT were obtained only by combining old and new data. While it suggests that ST+ is also highly correlated with MSZ, it is possible to directly examine the relation between ST+ and MSZ for both old and new trials.

Correlations between ST+ and MSZ were computed for old and new probes separately, and the slopes of these regression lines are presented in Table 2. Also, unlike the correlations with RT, the correlations of the ST+ data from old and new trials with MSZ are all highly significant. As shown in Table 2, a one-tailed *t* test (predicated on the hypothesis that the slope is lower for new than old probes) comparing the slopes of old and new regression lines show that they differ significantly for subject AM ( $p < 0.05$ ) and for FK ( $p < 0.01$ ). The slopes for new items are lower than for old for all subjects, as was found in the original RT data. Comparing the differences in slopes for old and new items for ST+ vs. MSZ and for RT vs. MSZ, they are 112 msec/item vs. 149 msec/item for AM, and 121 msec/item vs. 133 msec/item for GK. Most of the difference of about 25 msec/item could be accounted for by the criterion we adopted to determine the point in time at which the suppression "ended". However, subject FK's suppression time slope was almost a factor of 3 greater than the slope relating her RT to MSZ. Note however that for new probes the slope of her ST+ vs. MSZ regression line was only 189 msec. The ratio of old/new slopes for ST+ vs. MSZ is 1.82 and that for RT vs MSZ is 1.84 indicating that the faster scan rate for new items relative to old is about the same for both measures.

Figure 7 contains regression lines based on the combined new and old data. They indicate that the relationship between ST- and MSZ is inconsistent across subjects. It is to be noted that FK is the only subject in whom ST- is significantly correlated with MSZ, but the correlation coefficient ( $r = 0.04$ ) is so weak that it can be neglected.

At the present time we can only speculate as to why the slopes of the regression lines for FK relating ST+ to MSZ and to RT differ so dramatically from other subjects. While there is a strong positive correlation between ST+ and MSZ for FK as well as the other subjects, the greater slope for FK suggests that a serial search of short-term memory alone cannot explain her data, which are characterized by a constant percent increase in ST across set size. We also note that FK almost failed to meet our accuracy criterion and had to undergo many additional practice sessions before her performance was finally acceptable.

Since the MEG was recorded separately over the left and right hemispheres, it is possible to determine if the spontaneous activity of both hemispheres is affected in the same way during memory search. If suppression during memory search were a global effect of attention or arousal, one would expect the two hemispheres to respond in the same way to memory sets of different size. Alternatively, if regional changes in cortical activity reflect processes such as scanning memory for acoustic stimuli, then hemispheric differences are not unlikely. Unfortunately, if "old" and "new" trials are analyzed separately for each hemisphere, the sharply reduced sample size makes any conclusions too uncertain. However, the differences between old and new trials were shown to be of little consequence in analyzing the effects of set size on RT. Therefore, the data from old and new trials were combined and a sufficient numbers of trials was obtained to compute statistically reliable coefficients of correlation between suppression duration (ST+) and set size for each hemisphere (Figure 8). When measured over the left hemisphere the correlation coefficients for subjects AM, GK and FK respectively were 0.372 ( $p = .0035$ ), 0.301 ( $p = .48$ ), and 0.579 ( $p < .0001$ ). The slopes of these regression lines were 52, 28, and 256 msec/item, respectively. Over the right hemisphere the corresponding correlations were 0.769 ( $p < .0001$ ), 0.519 ( $p < .0001$ ), and 0.717 ( $p < .0001$ ) for AM, GK, and FK

respectively. Again, the slopes of these regression lines were 131, 174, and 364 msec/item for AM, GK, and FK, in that order. Based on these results, the right hemisphere appears to provide an index of memory scanning that is consistent with the classic RT data, while the left hemisphere does not. This result is consistent with the general belief that the right hemisphere predominates in processing musical stimuli (Springer and Deutsch, 1985). The scan rates for AM and GK are comparable to those predicated on their RT data. However, as pointed out previously, FK's data reflect a much longer scan rate than that reflected by her RT data. This suggests that suppression time in her case reflects processes in addition to memory scanning. As intimated previously, this asymmetry in suppression across hemispheres is strong evidence against the view that suppression of the MEG during memory search is simply global alpha blockage caused by generalized arousal or change in level of attention.

Let us now consider the EEG data. First, it was not possible to analyze the EEG data obtained from FK. In her case the suppression, when detectable, began at about the same time as in the MEG, but it rarely recovered prior to the end of the epoch for the two larger set sizes. In many cases it apparently extended from one epoch to the next. This was true for electrode positions Cz, Oz, and Pz and the data were even less useful from Fz. By contrast, the data recorded at Cz and Oz from subject AM were quite similar to those obtained from the same subject with the MEG. However, the Cz and Oz records obtained from subject GK failed to produce a significant correlation between ST+ and MSZ. These results also imply that the significant correlations between the MEG's ST+ and MSZ are not merely instances of global alpha blockage, perhaps due to covariation in generalized arousal and MSZ. For if global alpha blockage were the cause, then the EEG data from all of the subjects should have revealed the effect of MSZ on ST+, and it should have been detectable wherever alpha activity is observed. However, the results demonstrate that specific regions of cortex are selectively affected by memory search and that simple midline recordings are not suitable for studying effects of memory scanning on the brain's spontaneous activity. This difference between EEG and MEG is probably due to activity of distant cortical regions affecting the EEG. This is avoided in MEG recordings, where even subtle differences between the hemispheres become apparent. Of course, other electrode montages might reveal effects similar to those obtained with the MEG.

It might be argued that ST really reflects the time to prepare a motor response, and has nothing to do with mentally comparing the probe with memory set items. To investigate this idea we used the button press itself as the trigger for backward averaging and recomputed all of the variance plots to determine new values of ST- and ST+, where ST- refers to the suppression before the button press and ST+ the suppression after the button press. The hypothesis is that if ST- signifies preparation to make a motor act, then its duration should covary with RT. These correlations were not significant.

When the pre-button press ST- as computed above was compared with MSZ rather than RT, significance was achieved for two subjects. Subject GK's ST- was weakly but significantly correlated with MSZ ( $r=0.23$ ;  $p=.0053$ ). A somewhat stronger correlation was found for subject FK ( $r=0.39$ ;  $p<.0001$ ). For subject AM the suppression time prior to the button press (ST-) was not correlated significantly with MSZ ( $r=0.013$ ).

The 16-24 Hz (beta band) was processed in precisely the same way as was the alpha band activity. While suppression was observed in some sets of trials, it was not

consistently present, and when present it was seemingly unrelated to set size or RT. As Kaufman et al. (1990) found, the distribution of beta power about the scalp is largely independent of that of alpha power, suggesting different neuronal generators. It may be necessary to measure beta at many other places to determine if it is related to memory scanning in other cortical regions.

As indicated earlier, we found no systematic relationship across subjects between N100 or N100m and set size, thus ruling out a differential effect of auditory attention as the cause for findings. The fact that N100m was measured wherever the sensors measured the alpha band activity and its suppression also makes it possible to test the hypothesis that the auditory cortex contributes to the spontaneous activity suppressed by memory search. It is known that the source of N100m lies in auditory cortex (Hari et al., 1980; Elberling et al., 1980; Pantev et al., 1988; Yamamoto et al., 1988). Since the magnetic field sensors were all separated from each other by 2 cm, the amplitudes of the N100m component they sensed differed from each other. Furthermore, the coils were moved to slightly different positions from one block of trials to the next, which also caused a variation in N100m amplitude. Based on the theory that the neurons in auditory cortex that give rise to N100 are also spontaneously active and contribute to the fields we observed, it was hypothesized that position-dependent fluctuations in N100m amplitude would be reflected in the percent suppression detected on the same trials and at the same positions. Percent suppression is defined as the ratio of the mean power over a 1 sec interval 400 msec prior to presentation of the probe and the mean power within a 200 msec interval after the presentation of the probe stimulus. The hypothesis was confirmed as the position-dependent changes in N100m amplitude were found to be positively correlated with corresponding position-dependent changes in percent suppression of the spontaneous MEG. The coefficients of correlation between percent change in alpha and N100m amplitude are 0.31 ( $p=.0002$ ) for GK, 0.30 ( $p=.0003$ ) for FK, and 0.20 ( $p=.04$ ) for AM. The consistency of this relationship and the magnitudes of the correlations indicate that auditory cortex contributes substantially to the spontaneous activity suppressed during memory search. Nevertheless, this only accounts for a portion of the spatial variance in the suppression phenomenon, so areas of parietal and temporal cortex (other than auditory cortex) may also be involved in memory scanning. This too is a topic for further study.

## DISCUSSION

The main conclusions are quite clear. The level of MEG activity in the alpha band detected over the temporal and adjacent parietal areas of both hemispheres is sharply reduced when subjects scan short-term memory for previously heard tones. Fields associated with the magnetic counterpart to N100 (denoted N100m) are at their strongest in these same regions. While the suppression occurs bilaterally, the duration of suppression over the right hemisphere covaries significantly with the size of the memory set for all subjects. The covariation is not so good for the left hemisphere. This hemispheric asymmetry is evidence against a global alpha blockage explanation of the data. Since the equivalent current dipole source of N100m lies in auditory cortex, it is reasonable to assume that auditory cortex also contributes to the spontaneous activity that is suppressed during memory search. In view of the significant spatial covariation between the

amplitudes of N100m and the percent suppression of the MEG exhibited by all subjects in this experiment, it is concluded that auditory cortex contributes to the affected spontaneous activity. The failure to find the same suppression patterns in the EEG recorded at vertex and occipital electrodes is further proof that the suppression is of local cortical areas and not entirely a global effect, such as might occur because of generalized arousal. Otherwise the MEG and EEG would have yielded similar results. Also, while N100 detected at the vertex showed a statistically significant change in amplitude with set size, the direction of the change for one subject was in exact opposition to the direction of change for the other two. Yet the reaction times of all subjects increased reliably and linearly with size of the memory set, as did the duration of alpha suppression. Therefore, changes in N100 are not indicative of memory search *per se*, but may reflect effects of stimulation and early processing, including attention. Moreover, N100m recorded over the two hemispheres showed asymmetrical changes in amplitude with set size i.e., the right hemisphere exhibited the changes similar to those detected in N100 with a midline electrode. However, there was no relatively marked change in N100m measured over the left hemisphere, which is consistent with the predominance of the right hemisphere in attending to and processing musical tones. The fact that the right hemisphere's auditory cortex is also differentially affected by different memory set sizes, even though the effect is different across subjects, is further evidence that the neural source of N100m contributes to the spontaneous activity whose suppression tracks the RT data. Furthermore, it is consistent with the conjecture that N100 reflects early stages of cognitive processing preliminary to memory search, which is then revealed by changes in ongoing activity originating at least in part in the same cortical areas.

In the Appendix to this paper we review much of the pertinent literature on the ostensive roles of N100 and P300 in short-term memory. It is concluded that N100 is not a direct indicator of memory scanning, although it might well reflect neural processes related to echoic memory. We also review existing empirical data that are widely interpreted as showing that that P300 latency reflects short-term memory scanning (Gopher and Donchin, 1986; Bashore, 1987; Buchwald, 1987). A closer analysis reveals that, in the context of the Sternberg paradigm, P300 latency and amplitude are often dissociated from reaction time. In view of the basic assumption that in this task RT reflects processing time, it is difficult to establish that P300 latency or amplitude are direct indicators of memory scanning. A more suitable interpretation appears to be that P300, like N100, reflects other cognitive processes that happen to accompany or precede memory scanning. A contrary conclusion would require an alternative to Sternberg's theory - a theory in which reaction time is not closely tied to memory scanning even though subject accuracy is high. To our knowledge, no such alternative theory exists. Rather, existing alternatives deal with the issues of whether parallel processing (as well as or in lieu of serial processing) and self-terminating search (as opposed to exhaustive search) can underly the observed RT or related behavioral data, which nonetheless reflects processing time.

It is possible that some ERP components represent specific aspects of an overall memory scanning process. The timing and amplitudes of these components could be pertinent to memory scanning, but still be inconsistent with a more global measure, such as that provided by reaction time. However, no specific hypotheses have been offered as to the processes ostensibly signified by these components. The finding that a change in the brain's activity covaries with the more global measure of reaction time makes it possible

to infer that specific regions of neocortex are involved in the overall process. This does not cast any light on the deeper theoretical issues, but it makes it likely that the involved cortical regions can be identified and studied.

Finally, in this paper we emphasized an indirect approach to the problem of identifying the cortical regions affected by memory scanning. We relied on spatially correlated changes in spontaneous activity and the amplitude of an ERP component with its source in a known location. While this helped to establish that auditory cortex made a significant contribution, a more precise description of the cortical source is still possible, provided that the extracranial field is mapped completely from many positions at one time.

In a recent theoretical study, Kaufman, Kaufman, and Wang (1991) simulated a convoluted region of cortex populated by many dipoles having random moments. The net field pattern they produced at the surface of the spherical head model was computed using different sets of random dipole moments. This resulted in an ever-changing pattern, and invariant features could not be discerned in it. However, by averaging field power (as was done in this paper) rather than field, invariant features that depended upon the underlying cortical geometry (which constrains the possible field configurations) as well as levels of activity in different regions of the cortex did emerge. It was demonstrated in this simulation that it is possible to identify the location and depth of a region whose activity is locally incremented or decremented relative to a baseline of activity. Therefore, in principle it is possible to make use of cortical maps reflecting differences in levels of spontaneous activity as functional images similar to those generated by PET. In that case the spontaneous activity of incoherent sources may well serve as a valuable quantitative complement to ERPs in understanding how the brain's activity is related to cognition.

## APPENDIX

As stated in the body of this paper, the N100 component of the ERP may well represent early stages of the cognitive processing involved in short-term memory search, and that changes in levels of spontaneous activity that extend much farther in time appear to accompany the search process itself. Moreover, both phenomena arise in at least partly overlapping sets of neurons. Despite the likelihood of these complementary roles, we emphasized the role of spontaneous activity in short-term memory scanning and did not dwell extensively on the classic ERP components. In this Appendix we review some of the previous work relating the N100 and P300 components to short-term memory. This review was not included in the body of the paper because it would have distracted from the development of the main ideas and results. Since we would be remiss to ignore this work, this Appendix is provided. It will enable the reader to see the present paper in a broader context, and provide further justification for not dealing more explicitly with these components as indices of short-term memory scanning in the body of the paper.

*N100 and Short-Term Memory*

Picton, Campbell, Baribeau-Brown and Proulx (1978) and Naatanen (1982, 1986) suggested that N100 and related components may reflect short-term memory processes. N100 is thought to be composed of several superimposed components having origins in different portions of the brain, and possibly differing in functional significance (Naatanen and Picton, 1987). The variations in N100 associated with selective attention are described as being due to the *processing negativity* (Naatanen, 1982) or *negativity difference wave (Nd)* (Hansen and Hillyard, 1980) which is superimposed on N100. Nd is characterized as a negative shift in the baseline which may occur prior to N100 with a latency as short as 50 msec and extend for as long as about 500 msec. As compared with N100, Nd is a low-frequency phenomenon. The scalp distribution of Nd does not coincide precisely with that of N100, e.g., its later part is apparently more frontal. Typically, when subjects selectively attend to one "channel" (usually an auditory stimulus of particular pitch or one arriving from a particular spatial direction) the resulting N100 is of greater amplitude than that obtained when the channel is ignored. The difference between these two waveforms reveals the presence of Nd, which is widely interpreted as a separable ERP component which is temporally superimposed on N100, to create an apparent change in its amplitude. However, N100m, measured at the output of a high-pass filter (so that there is no residual Nd), also exhibits an effect of selective attention similar to that found for Nd (Curtis, Kaufman and Williamson, 1988). In fact, the amplitude of N100m may vary by as much as a factor of 2, depending upon whether or not the subject is paying attention to the acoustic stimulus. This is significant because it is known that the equivalent current dipole source of N100m is located in auditory cortex (Hari et al., 1980; Elberling et al. 1980; Pantev et al., 1988; Yamamoto et al., 1988). Furthermore, there is strong evidence to support the view that neurons in auditory cortex are also major contributors to the electrical N100 (Vaughan and Ritter, 1970), although other sources may contribute as well (Naatanen and Picton, 1987).

Noting that the increase in amplitude of N100 with interstimulus interval (ISI) may reflect a psychological refractory period, Picton et al. (1978) suggested that the refractory period may be a characteristic of the short-term storage system whenever it is activated by a sensory event. As evidence they show that when the ISI between similar stimuli is

small, the amplitude of N100 is also small. However, when the same stimuli are sufficiently dissimilar (in pitch) the amplitude of N100 is as large as when the ISI is made twice as long. Hence, measures of this ISI effect could well allow the characterization of this early modality-specific store.

While this is indeed a plausible hypothesis, alternative possibilities have not yet been ruled out. For example, the state of the subject's expectancy or arousal level may also change with ISI, and this could affect N100. Also, even if correct, the refractory period may be characteristic of sensory (echoic) store rather than of working short-term memory - a distinction that is sometimes made in the literature of cognitive psychology. In any event, there are as yet no conceptual links to connect the refractoriness identified by Picton and his colleagues to the process of searching short-term memory.

Naatanen (1982) suggested that the later-occurring portion of Nd is related to the rehearsing of features of the stimulus to which attention is being paid. He suggests that this rehearsal goes on in short-term memory. Again, beyond this conjecture no hypotheses are offered that connect this ostensible rehearsal to the operation of scanning short-term memory.

The mismatch negativity (MMN) of Naatanen, Simpson, and Loveless (1982) is another low-frequency component that partly overlaps N100 in time. It occurs in response to deviant stimuli, whether subjects are attending to them or not. Naatanen (1985; 1986) proposed that the MMN is a sign of a mismatch between an internal neural model of anticipated events and ongoing sensory inputs. Its earlier phases may be coincident with echoic store, and the later phases a sign of the comparison process itself. Since subjects performing the Sternberg task try to match recent sensory events with stored representations of prior events, Naatanen's conjecture may be taken to imply that the time required to complete the search task could be reflected in the MMN.

The results described in this paper fail to demonstrate any covariation of the MMN or Nd with set size or with RT. Therefore, whatever the roles of these phenomena in short-term memory, they are not revealed in the context of the Sternberg task. However, the amplitudes of N100 and of the right hemisphere's N100m do change with set size, albeit, inconsistently with RT since they change in different directions for different subjects. As we have seen, there is no clear way in which to relate this finding to short-term memory *per se*, although it may well reflect aspects of the task not dealt with in any existing theory.

### *P300 and Memory Scanning*

The full complexity of memory processes suggested by the distinctions between short-term and long-term memory, episodic, semantic and declarative memory, and declarative versus procedural memory, is barely if at all reflected in the ERP literature. Even so, it remains an open question as to how the various components of the ERP are related to the many facets of such processes. Yet P300 has sometimes been assumed to be a universal indicator of virtually all cognitive processes. Here we discuss the role of P300 in short-term memory scanning as revealed in the existing literature.

P300 is empirically related to stimulus evaluation time, which is considered distinct from the process of response selection and motor response time (Magliero, Bashore, Coles, and Donchin, 1984). Thus, P300 latency (evaluation time) may be dissociated

from RT in cognitive experiments where response selection varies independently of stimulus evaluation or perceptual processes (Isreal, Wickens, and Donchin, 1981). More generally, P300 is presumably related to the maintenance of the subject's internal model of the context of the environment (Donchin and Coles, 1988), and may even occur in the absence of an expected stimulus.

The rationale for experiments in which P300 is measured in the context of the Sternberg paradigm stems from the fact that P300 has been related to stimulus evaluation time (Kutas, McCarthy and Donchin, 1977), and the updating of memory (Donchin, 1975; 1981). In oddball experiments P300 is elicited when the event is classified by the subject as belonging to the category of rare events (McCarthy and Donchin, 1981; Magliero et al., 1984). This classification cannot be made before the stimulus is fully evaluated. If (and only if) RT signifies the completion of an evaluation of a stimulus, then P300 latency should covary with RT.

The foregoing makes P300 an ideal candidate for investigation as an indicator of memory search time. Assuming that high levels of accuracy are maintained, the latency of P300 should vary with the time required to determine if a probe had or had not been a member of the memory set. This hypothesis would be confirmed if P300 is a truly general indicator of all cognitive processes. However, if it should turn out that P300 represents the time to complete only some kinds of cognitive processes, then it might or might not reflect those involved in searching short-term memory.

There are some *a priori* reasons why P300 may not be an indicator of short-term memory scanning. For example, if its dominant neural generators should lie in the hippocampal formation (cf. Harrison and Buchwald, 1987; Okada, Kaufman and Williamson, 1983), then it is possible that it could be related to the transfer of information from short-term to long-term memory, but not to the scanning of short-term memory. This follows from the fact that bilateral damage to medial temporal cortex results in anterograde amnesia, which prevents patients from storing information in long-term memory, but it need not lead to deficits in short-term memory (cf. Squire, 1987). So it is not automatically given that P300 must unambiguously reflect short-term memory scanning. Even so, several reviewers have concluded that such a relationship has been demonstrated (Bashore, 1987; Buchwald, 1987; Gopher and Donchin, 1986).

Using acoustical stimuli, Gaillard and Lawson (1984) found no relationship between P300 latency and set size, but its amplitude did decrease with set size. Also, RT increased significantly with set size. By contrast, Gomer, Spicuzza and O'Donnell (1976), using visually displayed alphanumerics, did find an increase in P300 latency with set size. However, P300 latency increased with set size at the extraordinarily fast rate of 6 msec/item, while for RT the scan rate was only 14 msec/item, which alone is far short of the highest rate of 38 msec/item found in this type of task (Sternberg, 1966). The atypical RTs make it very difficult to evaluate this experiment. However, Marsh (1975) did find a substantial increase in P300 latency with set size in an experiment comparing older and younger subjects. These results are quite similar to those obtained in many of the subsequent studies reviewed below. Marsh used three set sizes composed of 1, 3, or 5 items and the RTs were quite typical of those reported in the psychological literature. That is, the scan rates reflected in the RT data were about 35 msec/item for the young subjects, and 31 msec/item for the older subjects, although the RTs of the older subjects were considerably longer than those of the young subjects. The slopes of the functions

relating P300 latency to set size were 18 msec/item for the young subjects and 22 msec/item for the older subjects. Although the average P300 latency was longer for the old subjects than for the young (the difference being about 60 msec), it did not reflect the large difference between the average RTs, which was about 358 msec.

Adams and Collins (1978) used visually presented digits in a Sternberg task where the set sizes ranged from 1 through 11 items. We disregard set sizes greater than 7 in this review, because the larger numbers of items lies outside the usual range of short-term memory, and the results are atypical. Over the range of from 1 to 7 items, P300 latency increased with set size. However, as in the Marsh experiment, the rate of increase was only 22 msec/item, a much faster rate than is indicated by Adams and Collins's RT data, which indicated an average scan rate of 38 msec/item. Adams and Collins sought to account for this discrepancy by adding the slopes of the regression functions relating both a 250 msec positivity (which we labeled "P300") and a 350 msec positivity (which gave results similar to "P300") to set size, but this does not appear to be a legitimate way in which to derive a net "latency". Adams and Collins found no correlated change in P300 amplitude with set size. In similar visual digit experiment Ford, Roth, Mohs, Hopkins, and Kopell (1979) found that while set size 1 was associated with the shortest latency, set sizes 2 and 3 had about the same latency, while set size 4 had the longest latency. Similar results were obtained in younger and older subjects, with the latter showing an overall increase in latency. Interestingly, Pfefferbaum (1980) obtained qualitatively similar results over the same set sizes for young subjects, but, for older subjects the latency of P300 increased for set sizes 1 and 2, and then decreased for set sizes 3 and 4. Despite an overall increase in P300 latency, Ford et al. older subject's data reflected a scan rate of about 29 msec/item. However, the scan rate reflected in their RT data was 55 msec/item. For younger subjects the scan rate given by RT was 35 msec/item, and the rate given by P300 about 27 msec/item. None of these P300 results appear to be well correlated with RT. In one interpretation the scan rate given by P300 reflects true cognitive processing, and the difference in the young and old RT data reflects differences in response selection. However, response complexity did not increase with set size, so the effect of aging should have been the addition of a constant to RT, which would only affect the Y-intercept of the regression function and not its slope. Ford, Mohs, Pfefferbaum, and Kopell (1981) conducted an experiment in which the quality of the stimulus was varied along with set size. Degrading the stimulus affected the intercept for both the RT and P300 functions, and the slope of the former was about double that of the latter. The data are inconsistent with any straightforward relation between P300 and memory search time as they suggest that degrading the stimulus affects processes both prior to and after P300.

Pratt, Michalewski, Patterson, and Starr (1989a,b,c) had younger and older subjects scan short-term memory for items composed of visually presented digits, and also acoustically presented digits, and musical tones. After averaging over subjects, Pratt et al. (1989a) identified an early-occurring P300 (referred to as P3a) which was strongest frontally (at Fz and Cz), and a later-occurring P300 (P3b) which was strongest at Pz. P3a (with a latency of about 350-400 msec) diminished in amplitude with set size, but did not change in latency. P3b (400-700 msec) increased in latency with set size. However, in the case of the visual and auditory digits, the latency increase with set size was at about half the rate of the increase in RT. More importantly, while RT increased with set size for musical tones, there was almost no change in latency for P3b. Moreover, as in the work

of Pfefferbaum and of Ford et al., in all conditions, there was a nonlinear relation between latency and set size. Thus, the latency of P3b for set sizes 3 and 5 did not differ significantly from each other, although both differed significantly from the latency associated with a set size of 1 digit. The failure to show a change in latency for musical tones despite an increase in RT with set size on the same trials is clearly at odds with the classic RT results. So for that matter is the nonlinearity in the variation in latency with set size. However, in some cases Pratt et al. accepted data with error rates as high as 20%, which is far greater than that accepted by Sternberg (1969), and this raises questions about whether cognitive processing time was truly represented by RT.

Pratt et al. (1989b) report that the RTs of their older subjects were generally longer than for the younger, but for both groups, RT was shorter for a set of 1 item than when the set size was 3 or 5 items. However, except for the visually presented digits, the latency of P3b was not delayed in the older subjects relative to the younger. Again, although RT results suggest a slowing of the search process in older subjects, this is not borne out in the latency results. P300 latency related to acoustically presented digits increased with set size at the same rates for both older and younger subjects. However, the set size effect for P300 did not occur at all for older subjects for either visually presented digits or musical tones, even though their RTs indicated an increase in time to scan memory as a function of set size. Therefore, RT and P300 are largely dissociated from each other in the work of Pratt et al.

Kramer, Schneider, Fisk, and Donchin (1986) observed considerable variability in their P300 data which they assumed was due to "response jitter". This jitter, which presumably caused P300 to shift in latency from trial-to-trial, made it difficult to evaluate the relation between set size and amplitude. In consequence, Kramer et al. employed a latency adjustment procedure to obtain less variability among the single trial P300s. Averaging amplitudes of latency-corrected single-trial measures of P300 both within and across subjects revealed a lower amplitude of P300 for set size 4 than for set size 1, where P300 was detected at Pz (not Cz or Fz as in Pratt et al.) and with an average peak latency of about 500 msec. This late P300 exhibited behavior similar to the P3a of Pratt et al., despite the difference in scalp location.

On average, the P300 latency, determined after jitter-correction, was longer for set size 4 than for set size 1. This latency difference diminished when the task was deliberately altered so that the subject's reactions would be more nearly automatic. This mirrored the reduction in difference between the RTs associated with the two set sizes.

With only two set sizes it is not possible to determine if the relation between P300 latency and set size is similar to the linear relation between RT and set size found by Sternberg. Therefore, it is particularly interesting that when they used 3 set sizes in a related experiment, Kramer and Strayer (1988), also found a nonlinear relationship between P300 latency and set size. the latency of P300 for set size 1 was shorter than for set sizes 3 and 4, which had the same latencies. Despite this, the RTs increased monotonically with the three set sizes of this experiment.

Strayer and Kramer (1990) examined the relationship between P300 amplitude and RT, but ignored the latency dimension. They found that P300 amplitude recorded at Pz, Cz and Fz varied with the degree of attention subjects devoted to the task relative to a different but concurrent task. this suggests that P300 amplitude may reflect the level of attention related to scanning different memory sets rather than the scanning of memory

*per se*. Clearly, controls for attentional demands due, perhaps, to rehearsal of memory sets of different sizes are needed.

Several other investigations of P300 and memory scanning are described in the literature. Some of these reported only on the results of using two set sizes, which is not sufficient to determine whether or not the resulting regression functions are linear. These are not discussed here as they would not be relevant to the matter at hand. Other studies, particularly those by Brookhuis and colleagues, are more elaborate than those based strictly on the Sternberg paradigm.

Brookhuis, Mulder, Mulder, Gloerich, van Dellen, van der Meer, and Ellermann (1981) and Brookhuis, Mulder, Mulder, and Gloerich (1983) combined a visual search task and a memory scanning task to investigate several interesting hypotheses. Memory sets consisted of 1 to 4 consonants displayed on a screen. Subsequently 1, 2, 3, or 4 consonants were displayed on the screen with nonconsonant positions filled by a dot mask. Subjects had to search the visual display of consonants to find stimuli and then had to decide if the stimuli had been members of the set. As many as 16 possible stimuli could be presented, 4 in the memory set and 4 in the display. Brookhuis et al. (1981) found that the slopes of the RT regression functions differed for old and new items, with the former being scanned at about 30 msec/item, and the latter at the rate of about 60 msec/item. This is consistent with self-terminating rather than exhaustive search (Schneider and Shiffrin, 1977). However, this difference failed to appear in the corresponding P300 data, where the scan rate was about 16 msec/item for both old and new items. This implies that RT reflects one kind of search, and P300 another (exhaustive). Furthermore, the absolute number of comparisons, whether they be made in memory or in visual search, were more important than were the nature of the comparisons being made. The authors offer several different and interesting hypotheses as to why these differences occur, but none of them are consistent with a simple division of processing into stimulus evaluation and response selection categories. Using a somewhat different paradigm Brookhuis et al. (1983) came to similar conclusions. By altering response probabilities they were able to demonstrate RT data reflecting a self-terminating memory search process. However, the P300 data were consistent with an exhaustive serial search process. While the RT results are consistent with the work of Schneider and Schiffrin, for some subjects there was a low correlation between the RT and P300 data, even after removal of outlier data. Brookhuis et al. suggest that this may be due to those subjects basing their responses only partly on a full evaluation of the stimuli.

As in many other studies reviewed above, Brookhuis et al. found P300 amplitude to diminish with load. They suggest that the confidence of the subjects in their decisions may vary with set size, and this results in the reduction in P300 amplitude. They also discuss alternative hypotheses, e.g., that of Isreal, Wickens and Donchin (1980) that the higher the amplitude of P300, the higher the available amount of processing capacity. This points to a major problem of interpretation, since the phenomenon of the change in P300 amplitude with set size could be due to any number of factors, and there are no hypotheses that link a change in amplitude to the process of memory-scanning *per se*.

Because of the ambiguity in the relationship between P300 and RT in the context of the Sternberg paradigm, we decided not to study this relationship in our experiment as we could not contribute more than has already been reported. We have no theory that could account for the dissociation of these measures in different age groups, nor can we

explain the widely observed nonlinearity of the relation between set size and P300. The work of Brookhuis et al. might ultimately shed some light on this issue, since they discuss alternative theories, but there is as yet no agreement as to the underlying processes that may be suitable for ERP studies. We leave the possibility open that P300 is not a ubiquitous measure, since it may not reflect all cognitive processes.

## REFERENCES

- Adams, N. and Collins, G.I. (1978) Late-components of the visual evoked potential to search in short-term memory. *Electroenceph. Clin. Neurophysiol.* 44, 147-156.
- Bashore, T.R. Jr. (1987) Age-related changes in mental processing revealed by analysis of event-related brain potentials. In Rohrbaugh, J.W., Parasuraman, R., and Johnson, R. Jr. (Eds.), *Event-Related Brain Potentials: Basic Issues and Applications*. New York, Oxford University Press, 242-278.
- Buchwald, J.S. (1987) Animal models of cognitive event-related potentials. In Rohrbaugh, J.W., Parasuraman, R., and Johnson, R. Jr. (Eds.), *Event-Related Brain Potentials: Basic Issues and Applications*. New York, Oxford University Press, 57-75.
- Curtis, S., Kaufman, L., and Williamson, S.J. (1988) Divided attention revisited: Selection based on location or pitch. In K. Atsumi, M. Kotani, S. Ueno, T. Katila, and S.J. Williamson (Eds.), *Biomagnetism '87*, Tokyo, Tokyo Denki University Press, 138-241.
- Donchin, E. (1975) On evoked potentials, cognition and memory. *Science.* 190, 1004-1005.
- Donchin, E. (1981) Surprise!...surprise? *Psychophysiology*, 18, 493-513.
- Donchin, E. and Coles, M. (1988) Is P300 a manifestation of context updating? *Behavioral and Brain Science*, 11:2, 355-425.
- Elberling, C., Bak, C., Kofoed, B., Lebech, J. and Saermark, K. (1980) Magnetic auditory response of the human brain. A preliminary report. *Scand. Audiol.* 9, 185-190.
- Ford, J.M., Roth, W.T., Mohs, R.C., Hopkins, W.F., and Kopell, B.S. (1979) Event related potentials recorded from young and old adults during a memory retrieval task. *Electroenceph. clin. Neurophysiol.* 47, 450-459.
- Ford, J.M., Mohs, R.C., Pfefferbaum, A., and Koppell, B.S. (1980) On the utility of P3 latency and RT for studying cognitive processes. In Kornhuber, H.H., Deecke, L. (Eds.) *Motivation, Motor and Sensory Processes of the Brain: Electrical Potentials, Behavior and Clinical Use. Progress in Brain Research*. Vol. 54. Elsevier/North Holland Biomedical Press, Amsterdam, 661-668.
- Gaillard, A.W.K. and Lawson, E.A. (1984) Evoked potentials to consonant-vowel syllables in a memory scanning task. *Ann. NY Acad. Sci.*, 425, 204-209.
- Gomer, F.E., Spicuzza, R.J., and O'Donnell, R. (1976) Evoked potential correlates of visual item recognition during memory-scanning tasks. *Physiol. Psychol.*, 4, 61-65.
- Gopher, D. and Donchin, E. (1986) Workload - An examination of the concept. In Boff,

K.R., Kaufman L. and Thomas J.P. (Eds.) *Handbook of Perception and Human Performance. Vol. II: Cognitive Processes and Performance*. New York, Wiley, 41-1 - 41-49.

Hansen, J.C. and Hillyard, S.A. (1980) Endogenous brain potentials associated with selective auditory attention. *Electroenceph. Clin. Neurophysiol.* 49, 277-290.

Hari, R., Aittoniemi, M.-L., Jarvinen, T., Katila, T. and Varpula, T. (1980) Auditory evoked transient and sustained magnetic fields of the human brain: Localization of neural generators. *Exp. Brain Res.*, 40, 237-240.

Harrison, J.B. and Buchwald, J.S. (1987) A cat model of the P300: Searching for generator substrates in the auditory cortex and medial septal areas. In R. Johnson, Jr., R. Parasuraman, and J.W. Rorbaugh (Eds.) *Current Trends in Event-related Potential Research (EEG Suppl. 40)*. Elsevier Science Publishers.

Hillyard, S.A., Hink, R.F., Schwent, V.I., and Picton, T.W., (1973) Electrical signs of selective attention in the human brain. *Science*, 182:177-180.

Isreal, J.B., Chesney, G.L. Wickens, C.D., and Donchin, E. (1980) P300 and tracking difficulty: Evidence for multiple resources in dual-task performance. *Psychophysiology*, 17, 259-273.

Kaufman, L. and Price, R. (1967). The detection of cortical spike activity at the human scalp. *IEEE Trans. Biomed. Eng., BME-14*, 84-90.

*Kaufman L. and Y. Locker, Y. (1970). Sensory modulation of the EEG. Proc. Amer. Psychol. Assoc., 75th Meeting*, 179-180.

Kaufman, L., Schwartz, B.J., Salustri, C., and Williamson, S.J. (1990) *J. Cog. Neurosci.* 2, 124-132.

Kaufman, L., Glanzer, M., Cycowicz, Y. and Williamson, S.J. (1989) Visualizing and rhyming cause differences in alpha suppression. In S.J. Williamson, M. Hoke, M. Kotani, and G. Stroink (Eds.), *Advances in Biomagnetism*, Plenum Press, New York (in press), pp. 241-244.

Kaufman, L., Cycowicz, Y., Glanzer, M. and Williamson, S.J. (1991) Verbal and imaging tasks have different effects on cortical activity. (In preparation).

Kaufman, L., Kaufman, J.H. and Wang, J.-Z. (1991) On cortical folds and neuromagnetic fields. *Electroenceph. clin. Neurophysiol.*

Klimesch, W., Pfurtscheller, G. and Mohl, W. (1988). Mapping and long-term memory: The temporal and topographical pattern of cortical activation. In: *Functional Brain Imaging*, G. Pfurtscheller and F.H. Lopes Da Silva, Eds. Hans Huber Publishers, Toronto, pp. 131-142.

- Kosslyn, S.N. (1983). *Ghosts in the Mind's Machine*. Norton, New York.
- Kramer, A., Schneider, W., Fisk, A., and Donchin, E. (1986) The effects of practice and task structure on components of the event-related brain potential. *Psychophysiol.* 23, 33-47.
- Kutas, M. McCarthy, G., and Donchin, E. (1977) Augmenting mental chronometry: The P300 as an index of stimulus evaluation time. *Science*, 197, 792-795.
- Kutas, M., and Donchin, E. (1978) Variations in the latency of P300 as a function of variations in semantic categorizations. In D. Otto (Ed.), *Multidisciplinary perspectives in event-related brain potential research*. EPA-600/9-77-043, Washington, D.C.: U.S. Government Printing Office, pp 198-201. 198-201.
- Magliero, A., Bashore, T., Coles, M.G.H., and Donchin, E. (1984) On the dependence of P300 latency on stimulus evaluation processes. *Psychophysiology*, 21(2), 171-186.
- Marsh, G.R. (1975) Age differences in evoked potential correlates of a memory scanning process. *Experimental Aging Research*, 1, 3-16.
- McCarthy, G. and Donchin, M. (1981) A metric for thought: A comparison of P300 latency and reaction time. *Science*, 211, 77-80.
- McCarthy, G. and Donchin, E. (1983) Chronometric analyses of human information processing. In Gaillard, A.W.K., and Ritter, W. (Eds.) *Tutorials in event-related potential research: Endogenous components*. *Advances in Psychology*, Vol. 10, G.E. Stelmach and P.A. Voon (Eds.) Amsterdam: North Holland Publishing Co., 251- 268.
- Mishkin, M. (1982) A memory system in the monkey. *Philos. Trans. R. Soc. Lond. B Biol. Sci.* 298, 85-95.
- Murdoch, B.B., Jr. and Walker, K.D. (1969) Modality effects in free recall. *Verbal Lrng. and Verbal Beh.*, 86, 665-676.
- Naatanen, R. (1982) Processing negativity: an evoked potential reflection of selective attention. *Psychol. Bull.*, 92, 605-640.
- Naatanen, R. (1985) Selective attention and stimulus processing: reflections in event-related potentials, magnetoencephalogram, and regional cerebral blood flow. In M.I. Posner and O.S.M. Marin (Eds.) *Attention and Performance*, Vol. XI, pp. 355-373, Hillsdale, NJ, Erlbaum.
- Naatanen, R. (1986) Neurophysiological basis of the echoic memory as suggested by event-related potentials, and magnetoencephalogram. In F. Klix and H. Hagendorf (Eds.), *Human memory and cognitive capabilities*, pp. 615-628, Amsterdam, Elsevier.
- Naatanen, R. and Picton, T. (1987) The N1 wave of the human electric and magnetic

response to sound: A review and an analysis of the component structure. *Psychophysiol.*, 84, 375-425.

Okada, Y.C., Kaufman, L. and Williamson, S.J. (1983) The hippocampal formation as a source of the slow endogenous potentials. *Electroenceph. clin. Neurophysiol.*, 55, 417-426.

Pantev, C., Hoke, M., Lehnertz, K., Lutkenhoner, B., Anogianakis, G., and Witowski, W. (1988) Tonotopic organization of the human auditory cortex revealed by transient auditory evoked magnetic fields. *Electroenceph. clin. Neurophysiol.* 69, 160-170.

Pelizzone, M., Williamson, S.J., Kaufman, L. and Schafer, K.L. (1984) Different sources of transient and steady state responses in human auditory cortex revealed by neuromagnetic fields. *Ann. New York Acad. Sci.*, 435, 570-571.

Petersen, S.E., Fox, P.T., Posner, M.I., Mintun, M. and Raichle, M.E. (1989) Positron emission tomographic studies of the processing of single words. *J. Cog. Neuroscience*, 2, 153-170.

Pfurtscheller, G. and Aranibar, A. (1977). Event-related cortical desynchronization detected by power measurements of scalp EEG. *Electroenceph. clin. Neurophysiol.* 42, 817-826.

Pfurtscheller, G. (1988). Mapping of event related desynchronization and type of derivation. *Ibid.* 70, 190-193.

Pfurtscheller, G., Steffan, J., and Maresch, H. (1988). ERD-mapping and functional topography - temporal and spatial aspects. (1988). In: *Functional Brain Imaging*. G. Pfurtscheller and F.H. Lopez da Silva, Eds., Hans Huber, Toronto, pp. 117-130.

Picton, T.W., Campbell, K.R., Baribeau-Brown, J. and Proulx, J.B. (1978) The neurophysiology of human attention: A tutorial review. In J. Requin (Ed.), *Attention and Performance VII*. Erlbaum, Hillsdale, N.J., pp. 429-467.

Pratt, H., Michalewski, H.J., Patterson, J.V., and Starr, A. (1989a) Brain potentials in a memory scanning task. I. Modality and task effects on potentials to the probes. *Electroenceph. clin. Neurophysiol.*, 72, 407-421.

Pratt, H., Michalewski, H.J., Patterson, J.V, and Starr, A. (1989b) Brain potentials in a memory-scanning task. II. Effects of aging on potentials to the probes. *Ibid.*, 72, 507-517.

Pratt, H., Michalewski, H.J., Patterson, J.V, and Starr, A. (1989c) Brain potentials in a memory scanning task. III. Potentials to the items being memorized. *Ibid.*, 73, 41-51.

Schneider, W. and Schiffrin, R.M. (1977) Controlled and automated human information processing I: detection, search, and attention. *Psychological Review*, 84, (1), 1-50.

- Squire, L.R. (1987) *Memory and Brain*, Oxford Univ. Press, New York.
- Starr, A. and Barrett, G. (1987) Disordered short-term memory in man and event-related potentials. *Brain*, 110, 935-959.
- Sternberg, S. (1966). High speed scanning in human memory. (1966) *Science*, 153, 652-654.
- Sternberg, S. (1969) Memory scanning: Mental processes revealed by reaction time experiments. *Amer. Scientist*, 57, 421-457.
- Strayer, D.L., and Kramer, A.F. (1990) Attentional requirements of automatic and controlled processing. *J. Exp. Psychol: Learning, Memory, and Cognition*. 16, 67-82.
- Ungerleider, L.G. and Desimone, R. (1986) Cortical connections of visual area MT in the macaque. *J. Comp. Neurol.* 248, 190-222.
- Ungerleider, L.G. and Mishkin, M. (1982) Two cortical visual systems. In D.J. Ingel, R.J.W. Mansfield, and M.A. Goodale (Eds.) *The Analysis of Visual Behavior*, MIT Press, Cambridge, MA. pp.,549-586.
- Vaughan, H.G., Jr., and Ritter, W. (1970) *Electroenceph. clin. Neurophysiol.* 28, 360-367.
- Williamson, S.J., Pelizzone, M., Okada, Y., Kaufman, L., Crum, D.B. and Marsden, J.R. (1984) In H. Collan, P. Berglund, and M. Krusius (Eds.), *Proc. 10th Intl. Cryogenic Engrng. Conf. - ICEC10*. Butterworth, Guilford, Surrey. 339-348.
- Yamamoto, T., Williamson, S.J., Kaufman, L., Nicholson, C., and Llinás, R. (1988) Magnetic localization of neuronal activity in the human brain. *Proc. Natl. Acad. Sci. USA*, 85, 8732-8736.

## FIGURE CAPTIONS

*Figure 1:* Reaction time (RT) versus memory set size (MSZ) for subjects AM, GK, and FK. RT vs. MSZ for old and new probe are plotted separately. Pearson product moment coefficients of correlation ( $r$ ) are presented in each graph.

*Figure 2:* Average N100 recorded at vertex for each of 3 subjects (AM, GK, and FK). The numerals associated with each trace represent the set size prior to the probe stimulus to each of the N100s. Responses to old and new probes are shown separately. Negativity is downward, and N100 peaks approximately 100 msec after 0.0 on the x-axis, which is the onset time of the probe. N100 amplitudes associated with old and new probes decrease as set size increases for AM and FK. However, for GK the N100 amplitudes increase with set size for both old and new probes. The bottom two traces are sample responses (subject FK) after digital filtering within two different passbands (0.2-40 Hz and 1.0-40 Hz). There is no discernible low-frequency component, e.g., baseline shift, within either passband. The same is true for all subjects and all set sizes.

*Figure 3:* Amplitude of N100 (averaged over old and new probes) as a function of MSZ for subjects AM, GK, and FK. While the amplitude of N100 changes monotonically with set size, it increases in amplitude for subject GK, and decreases for subjects AM and FK.

*Figure 4:* N100m amplitude (averaged over old and new probes) over: a) the right hemisphere and, b) the left hemisphere of each subject. When recorded over the right hemisphere N100m diminishes in amplitude with MSZ for AM and FK, and increases in amplitude for GK. N100m recorded over the left hemisphere has approximately the same amplitudes over set sizes for AM and FK, but diminishes in amplitude with set size for GK. However, the percent change in amplitude for GK is small as compared with the percent change in amplitude of the right hemisphere's N100m. There is no systematic relation to the RT vs. MSZ functions of Figure 1.

*Figure 5:* Sample graphs of changes in MEG power (variance) in the 8-12 Hz band as a function of time for 3 set sizes. The 0.0 point on the abscissa represents the time of presentation of the probe tone. The subsequent dip in power is shortest for MSZ=1, of intermediate duration for MSZ=3, and of longest duration for MSZ=5. Note the examples of early and late onset of suppression relative to time of probe presentation. Early onset or "anticipatory" suppression occurs prior to memory scanning.

*Figure 6:* Regression lines showing how suppression time (averaged over old and new trials) varies with RT for all 3 subjects. ST- graphs indicate the time between onset of suppression and probe presentation, with positive values indicating "anticipatory" suppression, and negative values suppression that begins after the probe presentation. ST+ is the time between onset of probe (0.0) and termination of suppression (see text).

*Figure 7:* Suppression time versus MSZ. Similar to Figure 6, but plotting MSZ instead of RT. ST+ is significantly correlated with MSZ for all 3 subjects.

*Figure 8:* Suppression time versus MSZ for: L) the left hemisphere and, R) the right

hemisphere. ST+ is significantly correlated with MSZ for all 3 subject's right hemisphere data, but, for only one subject (FK) in case of left hemisphere.

## TABLE LEGENDS

Table 1: Reaction time (RT) versus Memory Set Size (MSZ)

The slopes (in sec/item) of regression function relating RT to MSZ are given in Column 1 for RTs obtained with "old" probes and with "new" probes. Column 3 contains the Pearson product-moment coefficients of correlation between RT and MSZ for all subjects. All correlations are highly significant (Column 3). Column 4 contains the values of  $t$  resulting from comparing the slopes of the regression functions. The slopes of new and old probe regression functions all differ significantly, with  $p < .0001$ .

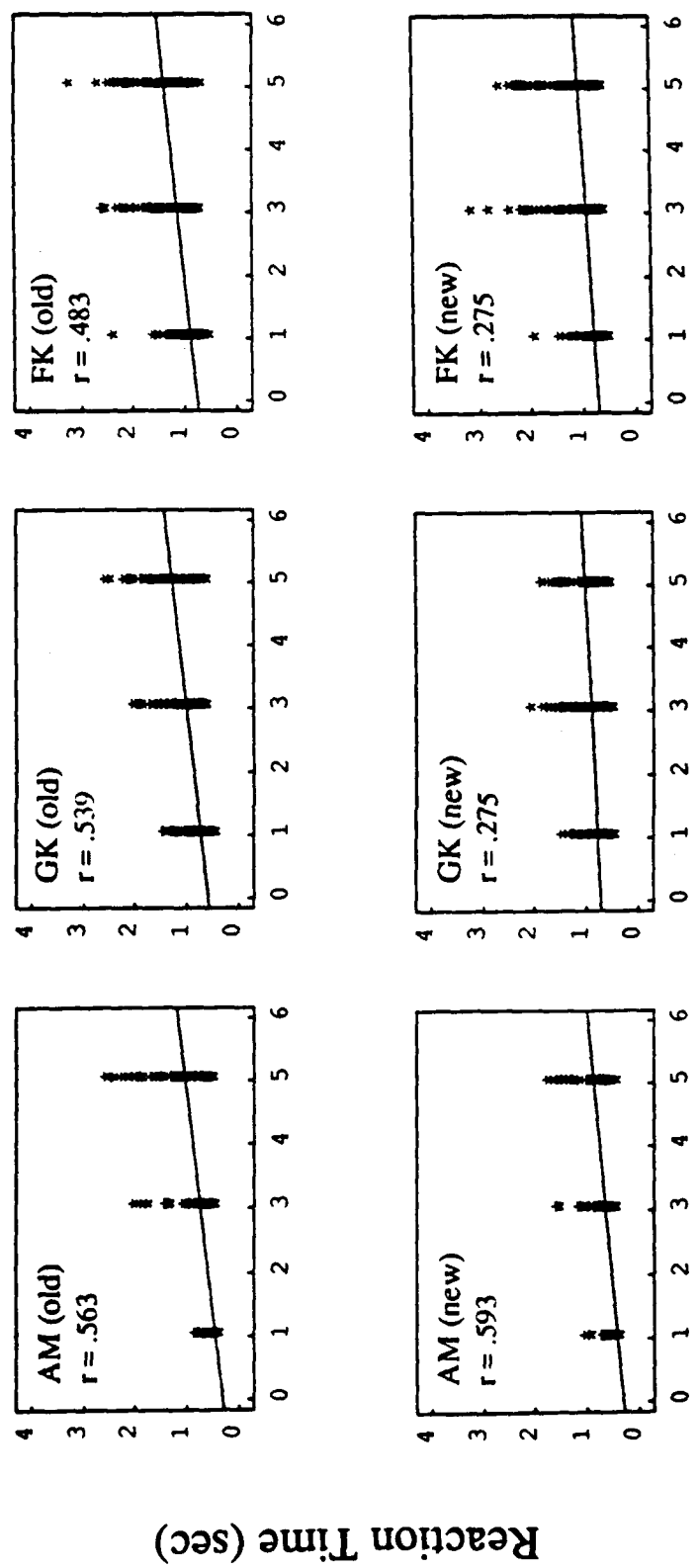
Reaction Time vs. Memory Set Size		slope	corr. coef.	sig. level	t-test	d.f.
AM	old	0.15	0.56	0.0001	25	376
	new	0.11	0.59	0.0001		
GK	old	0.13	0.54	0.0001	65	486
	new	0.06	0.28	0.0001		
FK	old	0.13	0.48	0.0001	115	1326
	new	0.07	0.28	0.0001		

Table 2: Suppression Time (ST) versus Memory Set Size (MSZ)

A) The slopes (in sec/item) of the regression functions relating suppression time between probe onset and offset of suppression (ST+) for old and new probes are given in the first column. The correlation coefficients are given in the second column, and their levels of significance are given in the third. All are statistically significant. The *t*-tests (fourth column) are for the significance of the differences between the slopes of the "old" and "new" regression functions. The difference between the "old" and "new" slopes reaches statistically significant levels of  $p < 0.05$  for subject AM and of  $p < 0.01$  for subject FK. For all three subjects, the slope is lower for new than for old trials, as in the RT data.

B) The same data as in A), but sorted by hemisphere over which recorded rather than new and old probes. The correlation between ST+ and MSZ, where ST+ is based on data recorded over the left hemisphere, fails to reach significance beyond chance for subject GK. While coefficients of correlation (Column 3) are significant with  $p < .003$  for subjects AM and FK, the slopes of the regression functions (Column 1) are low. Over the right hemisphere ST+ is significantly correlated with MSZ for all subjects. The *t*-tests of the significance of the differences between the slopes of the left and right hemisphere's regression functions are all very significant ( $p < .00001$ ) for all subjects.

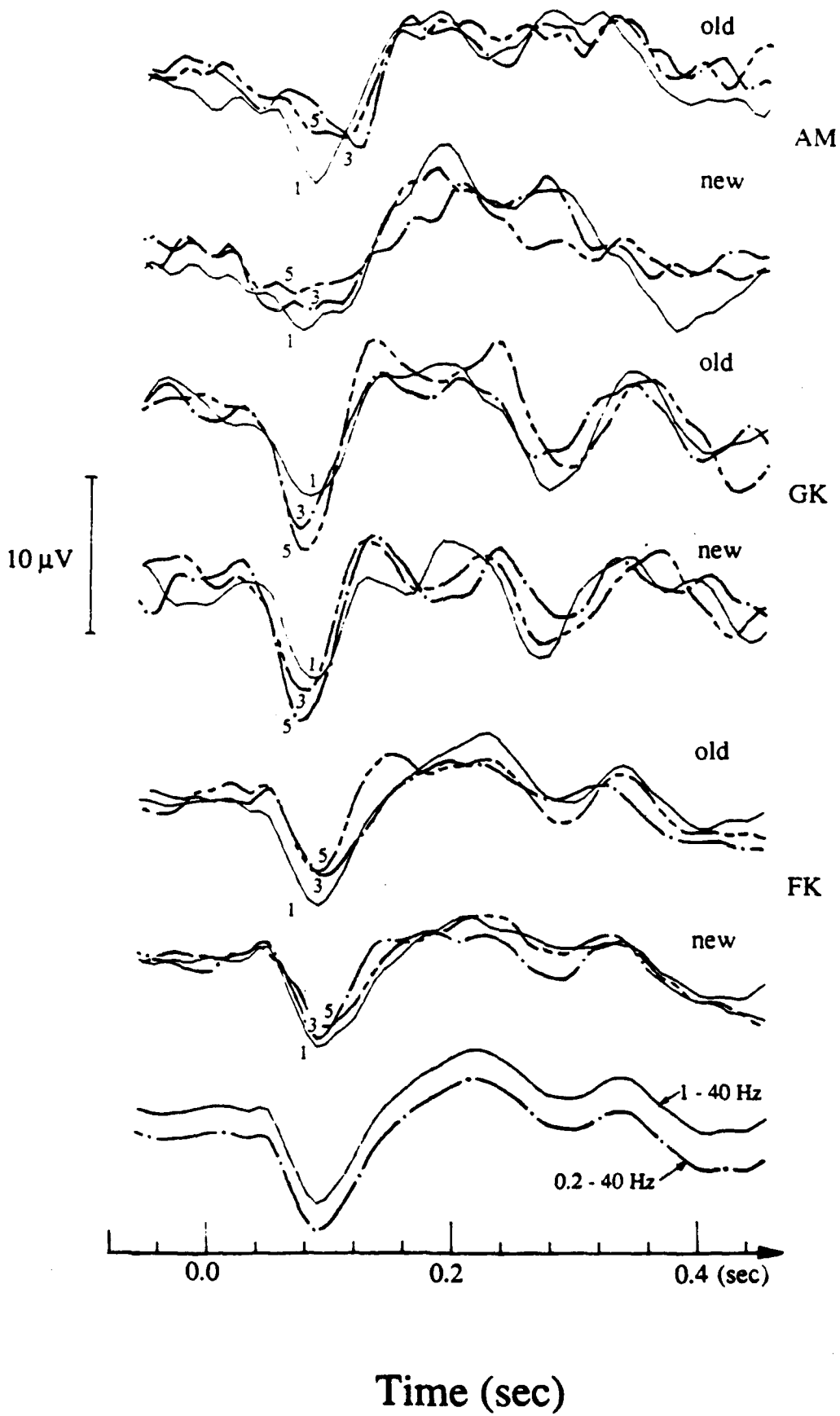
Suppression Time vs. Memory Set Size		slope	corr. coef.	sig. level	t-test	d.f.
AM (ST+)	old	0.11	0.47	0.0001	1.92	193
	new	0.06	0.33	0.001		
GK (ST+)	old	0.12	0.28	0.006	1.1	190
	new	0.07	0.32	0.001		
FK (ST+)	old	0.34	0.66	0.0001	3.35	279
	new	0.19	0.44	0.0001		
AM (ST+)	left	0.052	0.37	0.0035	23.2	100
	right	0.131	0.77	0.0001		
GK (ST+)	left	0.069	0.28	0.112	14.6	112
	right	0.174	0.52	0.0001		
FK (ST+)	left	0.256	0.58	0.0001	15.4	143
	right	0.362	0.72	0.0001		

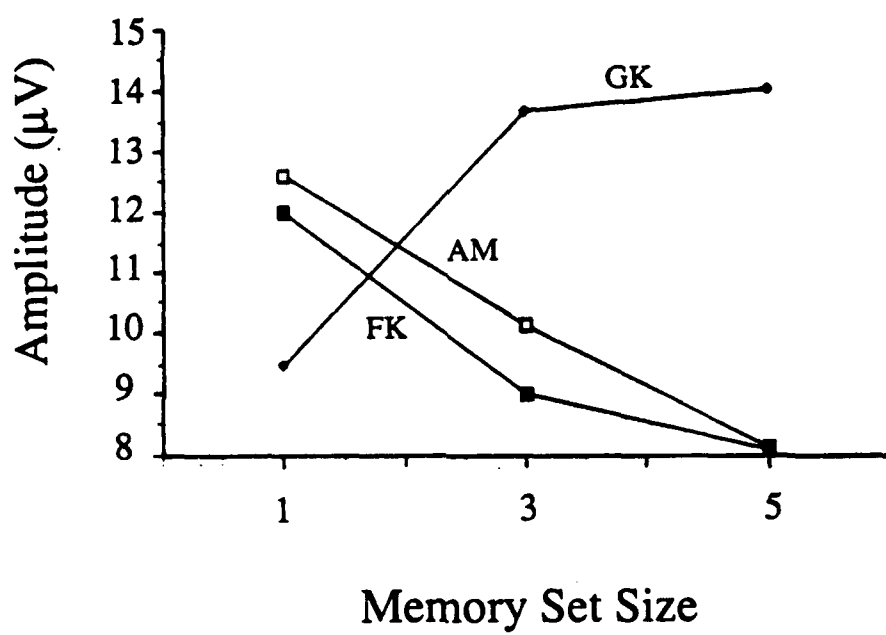


Memory Set Size

Figure 1

Response ( $\mu\text{V}$ )





Figure

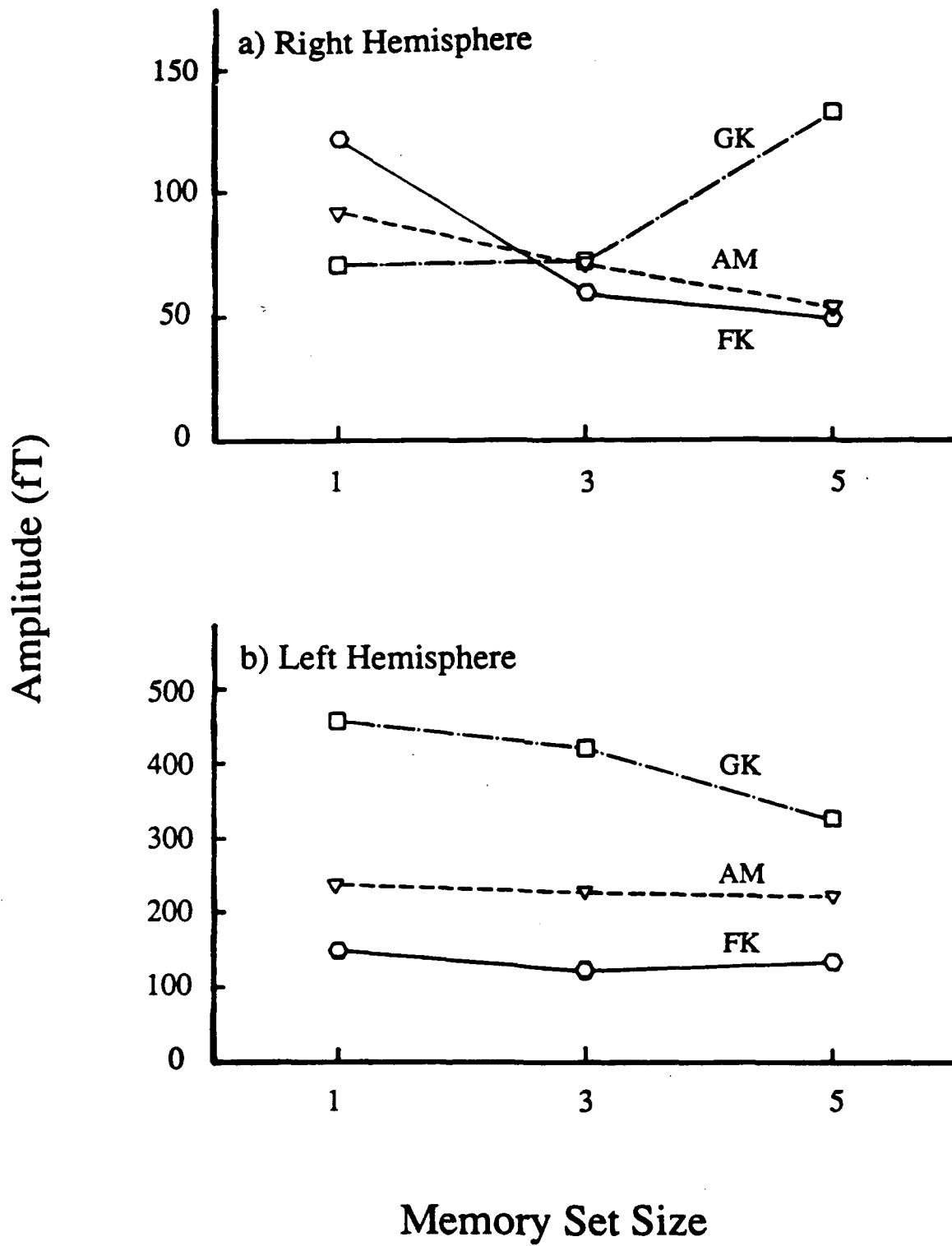
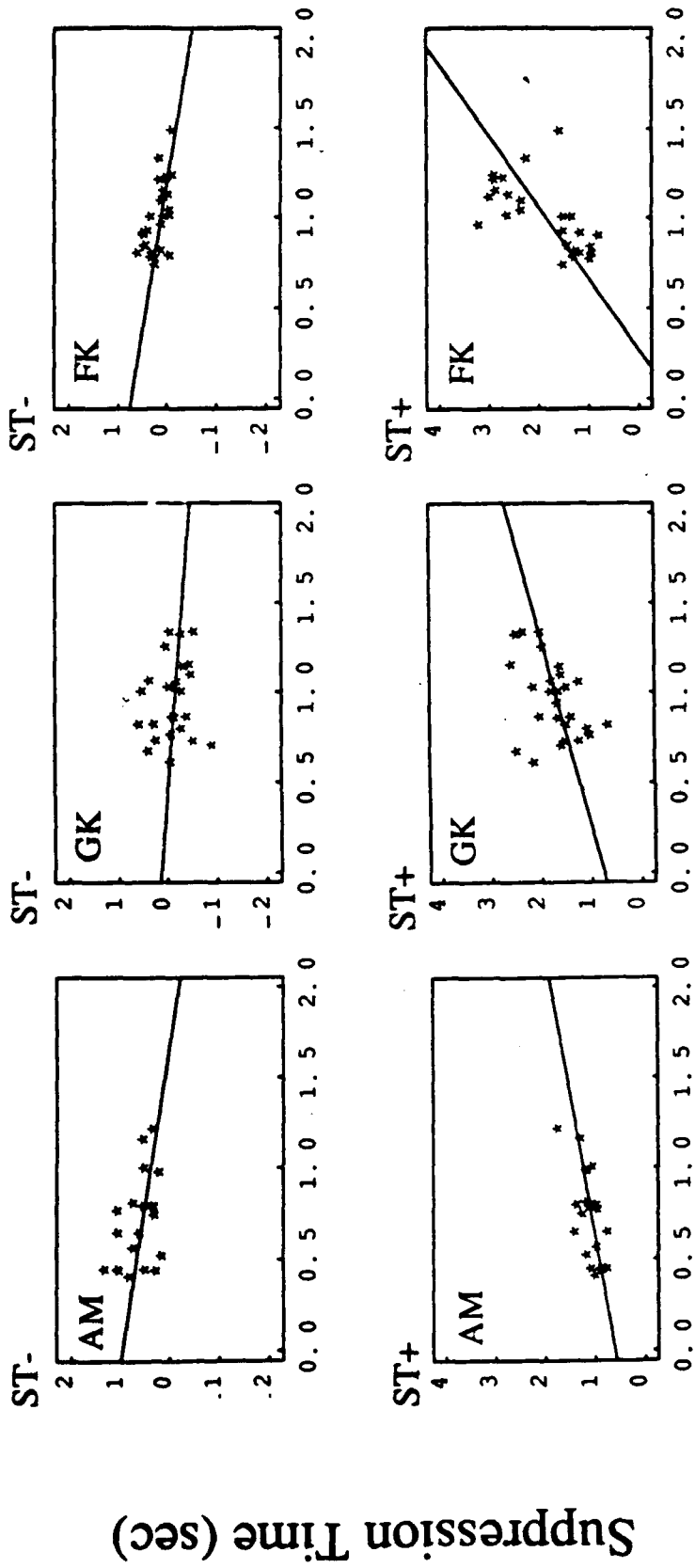
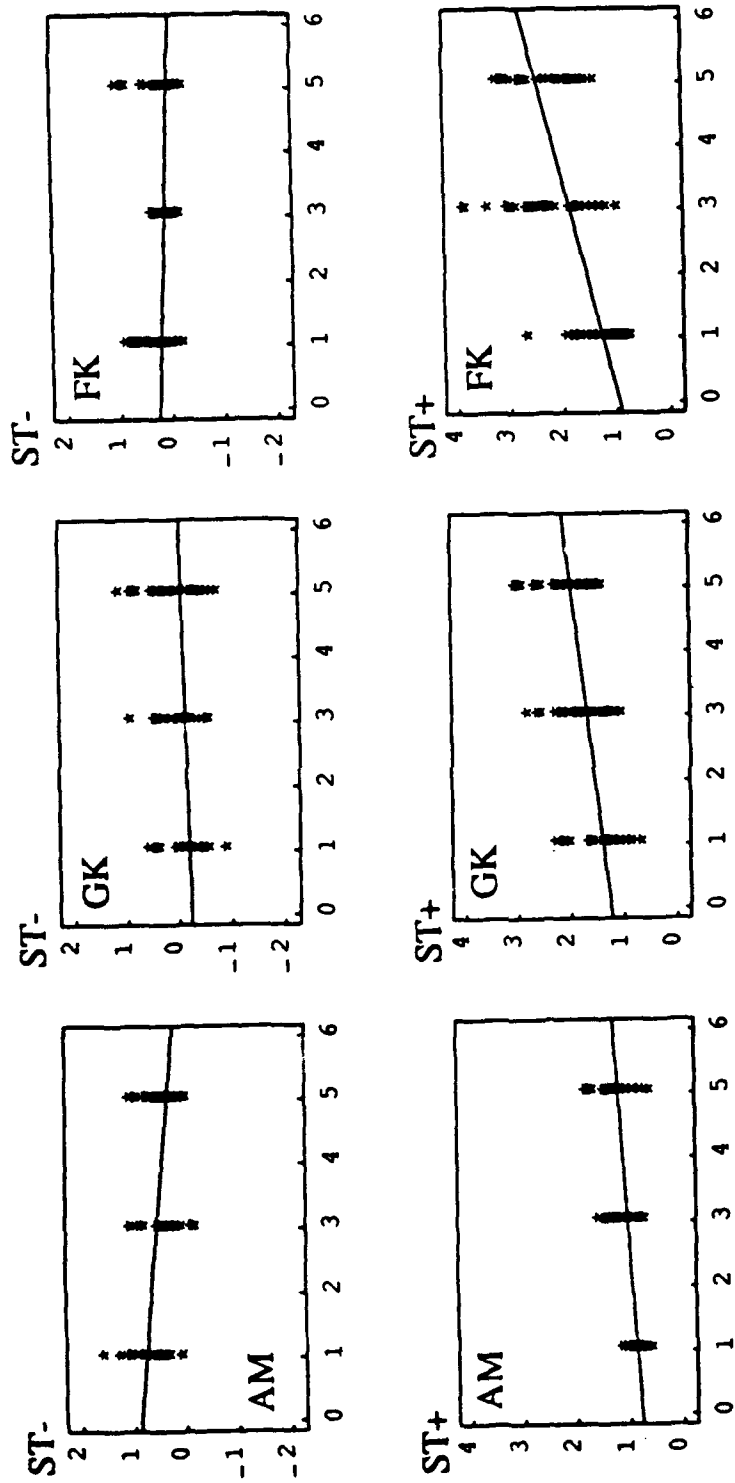


Figure 4



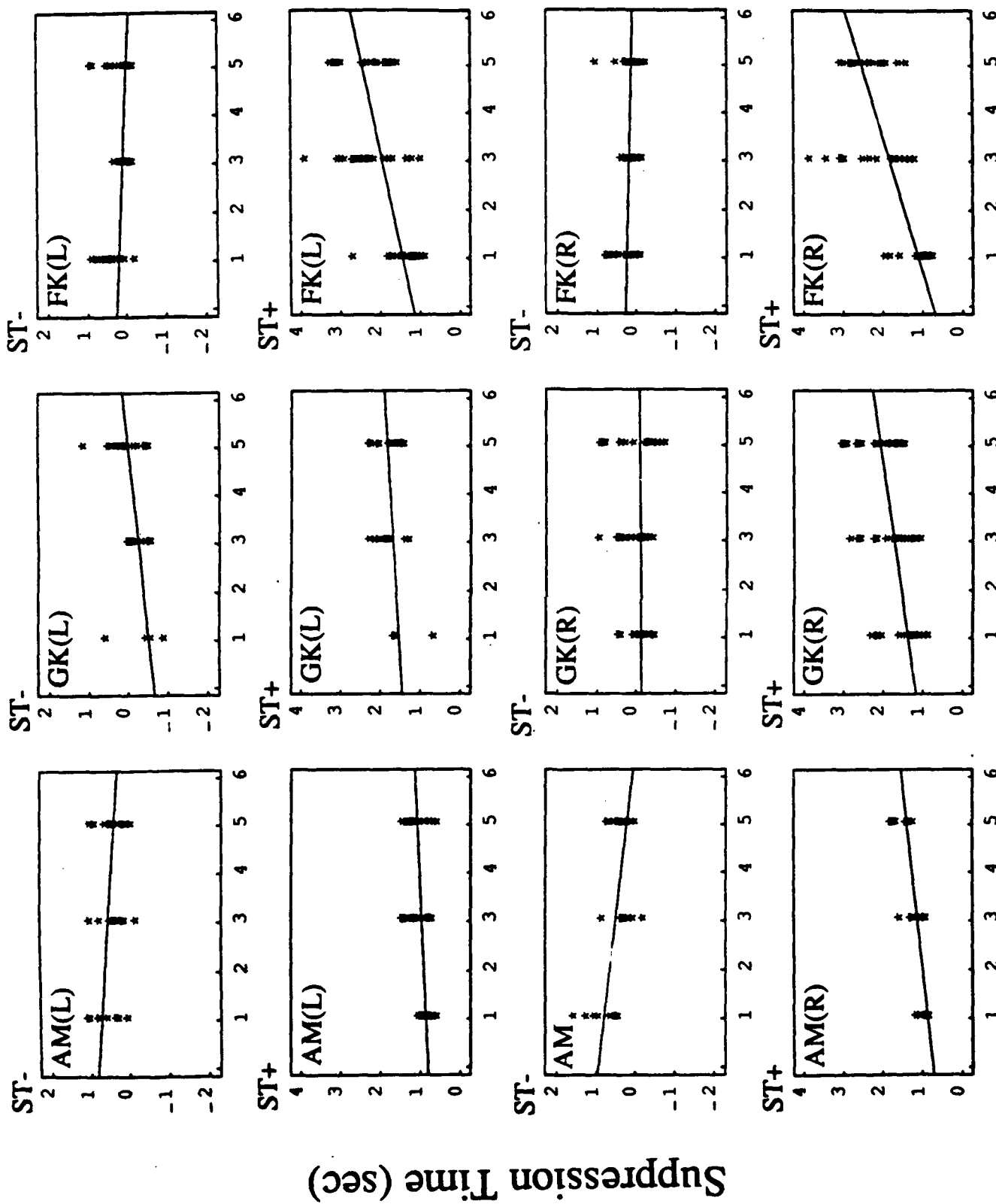
Reaction Time (sec)

Suppression Time (sec)



Memory Set Size

Figure 7



Memory Set Size